Mechanisms of Contextual Fear Memory Generalization

Dissertation

zur Erlangung des akademischen Grades

doctor rerum naturalium

(Dr. rer. nat.)

genehmigt durch die Fakultät für Naturwissenschaften

der Otto-von-Guericke-Universität Magdeburg

von Dr. med. Anne Albrecht

geb. am 31.01.1983 in Grimma

Gutachter: Prof. Dr. Oliver Stork

Privatdozent Dr. Carsten Wotjak

eingereicht am 25.09.12

verteidigt am 30.04.13

„Sicher ist, dass nichts sicher ist. Selbst das nicht."

- Joachim Ringelnatz

Summary

Dr. med. Anne Albrecht:

"Molecular mechanisms of contextual fear memory generalization"

Three models were applied to identify molecular factors involved in emotional relevant behavior. Combination of behavioral paradigms and gene expression analysis via laser capture microdissection and quantitative real time PCR highlighted the contribution of different hippocampal subregions to these processes.

Firstly, using classical fear conditioning to auditory cues and contextual stimuli, a pivotal role of neuropeptide Y (NPY) signaling in the dentate gyrus in determining contextual salience during auditory cued fear conditioning was revealed. Activation of NPY-positive interneurons in the hilus via immunhistochemically detected transcription factor P-CREB was found after cued but not contextual fear conditioning. Selective inhibition of CREB activation via conditional viral vectors in these interneurons resulted in increased contextual fear responses. Such contextual generalization was also observed when NPY signaling itself was pharmacologically blocked prior to cued fear conditioning.

Secondly, GABAergic factors like GAD65 and GABA A receptor subunits contributed to adaptive processes in response to juvenile stress in the ventral CA1 region in a model for posttraumatic stress disorder. Combined adult and juvenile stress omitted the correlation between marker genes for GABAergic and glutamatergic functioning, suggesting changes in the inhibitory/excitatory balance in the ventral CA1. These changes might also contribute to generalization towards the background context in auditory cued fear conditioning observed after juvenile stress in mice.

Fear memory reactivation applied as the third model induced such contextual generalization as well by retuning of the system after initial fear conditioning and exerted anxiolytic effects via corticosterone action in the ventral CA3 area.

All three models modulate anxiety and fear-related emotional behavior dependent on amygdalo-hippocampal interaction. Inhibitory signaling in different hippocampal subregions thereby regulates the balance between cue and contextual response in fear conditioning and contributes to contextual generalization. These findings are highly relevant for understanding (mal-) adaptation to fear-eliciting situations in anxiety disorders like posttraumatic stress disorder.

Summary - *Zusammenfassung*

Dr. med. Anne Albrecht:

"Molekulare Mechanismen kontextueller Generalisierung des Furchtgedächtnisses"

Die klassische Furchtkonditionierung ermöglicht die Untersuchung emotionaler Gedächtnisbildung. Besonders die Ausbildung eines sogenannten kontextuellen Furchtgedächtnisses, also die erlernte Assoziation zwischen einem furcht-induzierenden Stimulus wie einem Fußschock mit der Umgebung, in der dieser Fußschock erteilt wurde, wird durch die Interaktion zweier bedeutender Regionen des limbischen Systems, Amygdala und Hippokampus, geprägt.

Drei Modelle wurden von mir verwendet, um molekulare Faktoren zu bestimmen, die solch eine emotionale Gedächtnisbildung unterstützen und modulieren. Besonderes Augenmerk habe ich dabei auf die Funktion von inhibitorischen Interneuronen gelegt. Interneurone nutzen den Neurotransmitter GABA sowie zahlreichen Neuropeptide als Ko-Transmitter und gestalten lokale neuronale Netzwerke, die eine Informationsverarbeitung im Areal aber auch die Kommunikation zwischen verschiedenen Hirnregionen entscheidend bestimmen.

Im ersten Modell habe ich die Rolle bestimmter Interneuron- Subpopulationen bei der Konsolidierung des Furchtgedächtnis entweder auf einen Ton oder den Kontext verglichen. Per laser-gestützter Mikrodissektion wurden dazu Subregionen von Amygdala und Hippocampus in der Maus sechs Stunden nach Furchtkonditionierung isoliert und die Expressionsänderung ausgewählter Neuropeptide im Vergleich zu einer Kontrollgruppe durch quantitative real-time PCR verglichen.

Dabei zeigte sich eine Induktion von Neuropeptid Y (NPY) mRNA im Gyrus dentatus des Hippokampus nach ton- aber nicht kontext-assoziierter Furchtkonditionierung. Eine spezifische Aktivierung NPY-positiver Interneurone im Hilus des Gyrus dentatus nach Ton-assoziierter Furchtkonditionierung wurde durch den immunhistochemischen Nachweis von phosphoryliertem CREB, einem Transkriptionsfaktor, bestätigt. Mit Hilfe eines lokal injizierten konditionalen viralen Vektorsystems wurde eine solche CREB-Aktivierung durch Expression einer dominant-negativen CREB-Isoform in NPY-positiven Interneuronen des Hilus unterbunden. Dies führte zu einer Erhöhung der

kontextuellen, aber nicht ton-assoziierten Furchtantwort nach auditorischer Furchtkonditionierung. Eine solche Generalisierung wurde ebenfalls beobachtet, wenn die Transmitterfunktion von NPY selbst im Gyrus dentatus pharmakologisch blockiert wurde. Hierbei erhöhte die lokale Injektion eines NPY Y1 Rezeptor-Antagonisten die kontextuelle Furchtantwort, jedoch nur in einem auditorischen Furchtkonditionierungsparadigma und nicht wenn der Kontext selbst mit dem Fußschock assoziiert war. Dieser Effekt war außerdem nur bei Injektionen vor dem Furchtkonditionierungs-Training, nicht aber vor dem Abruf des Furchtgedächtnisses zu beobachten. Diese Ergebnisse weisen auf eine Bestimmung der kontextuellen Salienz in Balance zu einem eigentlich relevanten Ton hin, die durch NPY- abhängige Signalübertragung im Gyrus dentatus während der Akquisition und/ oder Konsolidierung des Furchtgedächtnisses moduliert wird.

Eine Ansteuerung dieser Interneuronen-Subpopulation wäre dabei mittels muscarinerger oder glutamaterger Neurotransmission möglich, denn die Analyse des Expressionsprofils in naiven Mäusen zeigte eine exklusive Anreicherung von mRNA für Rezeptoren des Kainat-Typs 2 (Grik2) sowie muscarinergic M1-Rezeptoren in NPY-positiven Interneuronen des Hilus im Vergleich zum restlichen Hilusgewebe bzw. hippokampalen NPY-positiven Neuronen außerhalb des Hilus.

Die Analyse der Expression sechs Stunden nach Furchtkonditionierung zeigte außerdem einen Anstieg von mRNA für das anxiolytische Neuropeptid Somatostatin im lateralen Kern der Amygdala, sowohl nach ton-assoziierter als auch nach kontextueller Furchtkonditionierung. Eine mögliche Involvierung von Somatostatin in Kodierung emotional bedeutsamer Ereignisse wurde unter Ausnutzung der Tatsache untersucht, dass die Somatostatin-Expression in der Amygdala einer zirkadianen Schwankung unterliegt. Tatsächlich erhöhte sich die Ängstlichkeit von Mäusen im sogenannten Licht-Dunkel-Test zu einem Zeitpunkt an dem die Peptid-Expression von Somatostatin gering war. In transgenen Mäusen, bei denen das kodierende Gen für Somatostatin ausgeschaltet wurde, war eine zirkadiane Regulierung von Angst-ähnlichem Verhalten nicht zu beobachten. Die konditionierte ton- oder kontext-assoziierte Furchtantwort wurde in diesen Experimenten jedoch weder vom Genotyp noch vom Zeitpunkt des Trainings beeinflusst, weshalb ich einen Beitrag von Somatostatin zur Kodierung emotionaler Salienz nicht bestätigen, aber auch nicht völlig ausschließen konnte.

In einem zweiten Model begann ich nun den Beitrag von Neuropeptiden und anderer Faktoren GABAerger Neurotransmission zu maladaptiven Prozessen emotionaler

Gedächtnisbildung zu untersuchen. Hierbei wurde das juvenile Stressmodell in Ratten in Zusammenarbeit mit Prof. Menahem Segal, Weizman- Institut, Israel, verwendet. Gestützt auf epidemiologische Daten wird davon ausgegangen, dass sich die Suszeptibilität für bestimmte Angsterkrankungen durch frühere Stresserfahrungen erhöht. Tatsächlich rufen intensive, psychologische Stresserlebnisse während der juvenilen Phase in Ratten und Mäusen Veränderungen von Ängstlichkeit und emotionalem Lernen bei erneutem Stress hervor, die mit Symptomen der Posttraumatischen Belastungsstörung (PTBS) im Menschen vergleichbar sind wie zum Beispiel eine generalisierte Furchtantwort. Außerdem wurden nach kombiniertem juvenilen und adulten Stress langanhaltende Veränderungen der Neuroplastizität in der Cornu ammonis (CA) 1-Region des ventralen Hippokampus im Vergleich zum dorsalen Teil in Ratten beschrieben, die auf eine erhöhte Erregbarkeit des ventralen Hippokampus hindeuten. Um Aufschluss über die molekulare Grundlage solcher Veränderungen zu erhalten, habe ich die Expression bestimmter GABAerger Faktoren in Schichten der ventralen und dorsalen CA1-Region mittels laser-gestützter Mikrodissketion und quantitativer real-time PCR untersucht. Es zeigten sich besonders im ventralen *Stratum radiatum* Veränderungen in der Expression des GABA-synthetisierenden Enzyms GAD65 und der GABA A-Rezeptoruntereinheiten α1 und α2 nach juvenilen, adulten Stress oder der Kombination aus beiden. Diese korrelierten teilweise mit der Expression von Corticosteron-Rezeptoren und könnten daher in der Tat direkt oder indirekt von der hippokampalen Corticosteronantwort abhängen. Weiterhin zeigte sich eine deutliche Korrelation zwischen der Expression das GABAergen Markers GAD65 und bestimmten Glutamat-Rezeptoruntereinheiten, die nach kombiniertem juvenilen und adulten Stress nicht mehr zu finden war. Dies deutet auf eine mögliche Verschiebung der Balance von exzitatorischer und inhibitorischer Neurotransmission in der ventralen CA1 im PTSB-Modell hin und könnte zur beobachteten erhöhten Erregbarkeit dieser Region beitragen.

Während juveniler Stress letztlich die Bildung eines emotionalen Gedächtnis durch veränderte Prädisposition und Adaption neuronaler Systeme beeinflusst, ist es auch möglich eine bereits etablierte Gedächtnisspur zu modulieren. Die Reaktivierung eines auditorischen Furchtgedächtnisses in Mäusen bildete hierbei das dritte von mir genutzte Modell. Während Furchtkonditionierung selbst zu langanhaltender Verminderung des Angst-ähnlichen Verhaltens und erhöhter mRNA-Expression für Corticosteron-Rezeptoren in der ventralen CA3-Region führte, waren diese molekularen

Veränderungen nach der Reaktivierung des Furchtgedächtnisses nicht mehr zu beobachten. Diese induzierte jedoch eine Erhöhung der Konzentration von Corticosteron im Blutplasma sowie eine kontextuelle Generalisierung der Furchtantwort bei gleichzeitig verminderter Ängstlichkeit. Lokale Applikation von Corticosteron in die ventrale CA3-Region konnte solch eine anxiolytische Reaktion verstärken. Reaktivierung ermöglicht also die „Rekalibrierung" stressabhängiger neuronaler Systeme, die zur Veränderung emotionalen Verhaltens führt.

In allen drei Modellen wurden molekulare Veränderungen in hippokampalen Subregionen in verschiedenen Verhaltensparadigmen beobachtet, die aufgrund ihrer hohen emotionalen Relevanz von einer Aktivierung der Amygdala abhängen. Die von mir erstellten Befunde weisen darauf hin, dass die Ausbildung und Modulierung emotionalen Gedächtnisses von inhibitorischer Neurotransmission im Hippokampus geprägt wird. Inhibitorische Neurotransmission im Gyrus dentatus sowie in den ventralen CA1 und CA3 Regionen steuert die Regulierung der Balance zwischen ton- und kontext-assoziierter Furcht und trägt dabei zu Phänomenen der kontextuellen Generalisierung während der auditorischen Furchtkonditionierung bei. Eine weitere Erforschung der hier identifizierten molekularen Faktoren würde dabei die Grundlage für die Entwicklung neuer therapeutischer Möglichkeiten für Angsterkrankungen wie PTBS bieten.

List of abbreviations

5HT2A	serotonine receptor type 2A
5HT2C	serotonine receptor type 2A
A	adenine
ACTH	adrenocorticotrophic hormone
Adra1d	α-adrenergic receptor type 1d
AMPA	α-amino-3-hydroxy-5-methyl-4-isoxazole proprionic acid
ANOVA	analysis of variance
AP	anterio - posterior axis
AS	adult stress
AutoLPC	automated laser pressure catapulting
AVP	vasopressin
BLA	basolateral amygdala
bp	base pairs
BSA	bovine serum albumine
C	cytosine
CA1	Cornu ammonis 1
CA3	cornu ammonis 3
CaMKIV	calcium/ calmodulin-dependent protein kinase type IV
cAMP	cyclic adenosine monophosphate
CCK	cholecystokinin
CCK-B	cholecystokinin receptor type 2 or B
cDNA	copy DNA
CeA	central amygdala
Chrm1	muscarinergic acetylcholin receptor type 1 (gene name M1)
Chrm2	muscarinergic acetylcholin receptor type 2 (gene name M2)
Chrm3	muscarinergic acetylcholin receptor type 3 (gene name M3)
Chrm4	muscarinergic acetylcholin receptor type 4 (gene name M4)
CR	conditioned response
CREB	cAMP response-element binding protein
CreERT2	cre recombinase – mutated human estrogen recepor fusion protein
CRH	corticotropin-releasing hormone
CS	conditioned stimulus

CT	Cycle threshold
CTL	control group
D1	dopamine receptor type 1
D2	dopamine receptor type 2
dB	decibel
DG	dentate Gyrus
DH	dorsal hippocampus
DMDC	dimethyl dicarbonate
DMSO	dimethyl sulfoxide
DMS-IV	diagnostic and statistical manual of mental disorders, fourth edition
DNA	Deoxyribonucleic acid
dNTP	desoxy-nucleotide
DV	dorso – ventral axis
EPM	elevated plus maze
EPSP	excitatory postsynaptic potential
ERK	extracellular-regulated kinase
FAM	6-carboxy-fluorescine
Fig.	Figure
FRET	Förster Resonance Energy Transfer
G	guanine
GABA	γ-aminobutyric acid
GABA A	GABA receptor type A
GABA B	GABA receptor type B
Gabra1	GABA A receptor subunit α 1 (gene name)
Gabra2	GABA A receptor subunit α 2 (gene name)
GAD	glutamic acid decarboxylase
$GAD65^{+/-}$	heterozygous GAD65 knock out
$GAD65^{-/-}$	homozygous GAD65 knock out
GAPDH	glycerinaldehyde-3-phosphate-dehydrogenase
GFP	green fluorescent protein
GR	glucocorticoid receptor
Gria1	ionotropic glutamate receptors, AMPA type, subunit 1 (gene name)
Gria2	ionotropic glutamate receptors, AMPA type, subunit 2 (gene name)
GRIK	G-protein coupled inwardly rectified potassium current

Grik1	ionotropic glutamate receptors, kainate-type, subunit 1 (gene name)
Grik2	ionotropic glutamate receptors, kainate-type, subunit 2 (gene name)
Grin1	ionotropic glutamate receptors, NMDA type, subunit 1 (gene name)
Grin2a	ionotropic glutamate receptors, NMDA type, subunit 2a (gene name)
Grin2b	ionotropic glutamate receptors, NMDA type, subunit 2b (gene name)
Grm4	metabotropic glutamate receptors, type 4
Grm5	metabotropic glutamate receptors, type 4
Grm7	metabotropic glutamate receptors, type 4
HA	hemagglutinine
HIPP	hilar perforant path-associated
HIV	human immune deficiency virus
HPA	hypothalamic-pituitary-adrenal
HUGO	human genome organization
IEG	immediate early gene
i.p.	intraperitoneal
IP_3	inositol 1,4,5-trisphosphate
IPSC	inhibitory postsynaptic currents
IPSP	inhibitory postsynaptic potential
ISI	inter-stimulus-interval
IUPHAR	international union of basic and clinical pharmacology
JS	juvenile stress
JSAS	combined juvenile and adult stress
KA	kainate
LA	lateral amygdala
LCDV	large denso core vesicle
LCM	laser capture microdissection
L/D	light-dark avoidance
LTP	long term potentiation
M1	muscarinergic acetylcholin receptor type 1
MAPK	mitogen-activated protein kinase
MGB	minor groove binder
mGluR	metabotropic glutamate receptor
ML	medial – lateral axis
MOPP	molecular layer perforant path-associated

MR	mineralocorticoid receptor
mRNA	messenger RNA
N	number of animals/ samples used
NCAM	neural cell adhesion molecule
NFQ	non-fluorescent quencher
NMDA	N-methyl-D-aspartate
NPY	neuropeptide Y
NR	no reactivation group
Nr3c1	nuclear receptor subfamily 3, group C, member 1 (gene name for GR)
Nr3c2	nuclear receptor subfamily 3, group C, member 2 (gene name for MR)
O-LM	*stratum oriens – stratum lacunosum moleculare*
PBS	phosphate-buffered saline
PCR	polymerase chain reaction
P-CREB	CREB phosphorylated at Ser133
PEN	polyethylene naphthalate
PFA	paraformaldehyde
PFC	prefrontal cortex
PGK	phosphoglycerate kinase
PKA	cAMP-dependent protein kinase
PLC	phospholipase C
PLL	poly-L-lysine
PLSD	protected least significant difference
PTSD	posttraumatic stress disorder
PVN	paraventricular nucleus
qPCR	quantitative real time PCR
R	reactivation group
REM	rapid eye movement
RNA	ribonucleic acid
RNAse	ribonuclease
rpm	rounds per minute
RQ	relative quantification value
SEM	standard error of mean
SIN-LTR	self-inactivated long terminal repeat
SO	*stratum oriens*

SP	*stratum pyramidale*
SPL	sound pressure level
SR	*stratum radiatum*
SSRI	selective serotonine re-uptake inhibitor
SST	somatostatin
$SST^{-/-}$	somatostatin knock out
$SST^{+/+}$	somatostatin wildtype
SST R2	somatostatin receptor type 2
T	Thymine
Tab.	Table
T_m	melting temperature
UNG	Uracil-N-glycosylase
US	Unconditioned stimulus
VH	ventral hippocampus
VTA	ventral tegmental area
Y1	NPY receptor type 1
Y2	NPY receptor type 2
Y5	NPY receptor type 5

1. Introduction

1.1 Emotional memory

“ … without memory we are capable of nothing but simple reflexes and stereotyped behaviors.” (Okano et al., 2000).

For the survival of an individual it is fundamental to adapt its behavior to new situations. For that, new skills and knowledge has to be acquired, a process called learning. However, behavioral changes cannot be achieved without remembering such experience. Although some information is gone within minutes, so-called short-term memory, other facts and events are remembered for hours, days or even years. For establishing such long-term memory mental processes of acquisition, consolidation and retrieval of new information and skills are essential. The newly acquired information is encoded in certain brain areas and then stabilized and stored away - a process called consolidation - , but then needs to be activated and accessible again - what is called retrieval of a memory trace (Dudai, 2004).

Different memory systems are characterized with distinct involvement of brain structures (Fig. 1-1). Here, the major classification is made between declarative and non-declarative memory, based on the level of consciousness during learning. For declarative memories, explicit learning occurs with a conscious recollection of facts and events. Events thereby can be remembered as complete episodes including references for time and place, e.g. autobiographical knowledge, while knowledge for single facts, objects and concepts is described as semantic memory. In contrast to that, neither the acquisition nor the recall of non-declarative memory directly depends on conscious processes. Therefore it is described as implicit and includes a heterogeneous group of learning forms, e.g. procedural learning of skills and habits, priming and habituation or sensitization. In addition, also associative learning in classical and operant conditioning paradigms occur implicitly (Squire & Zola, 1996).

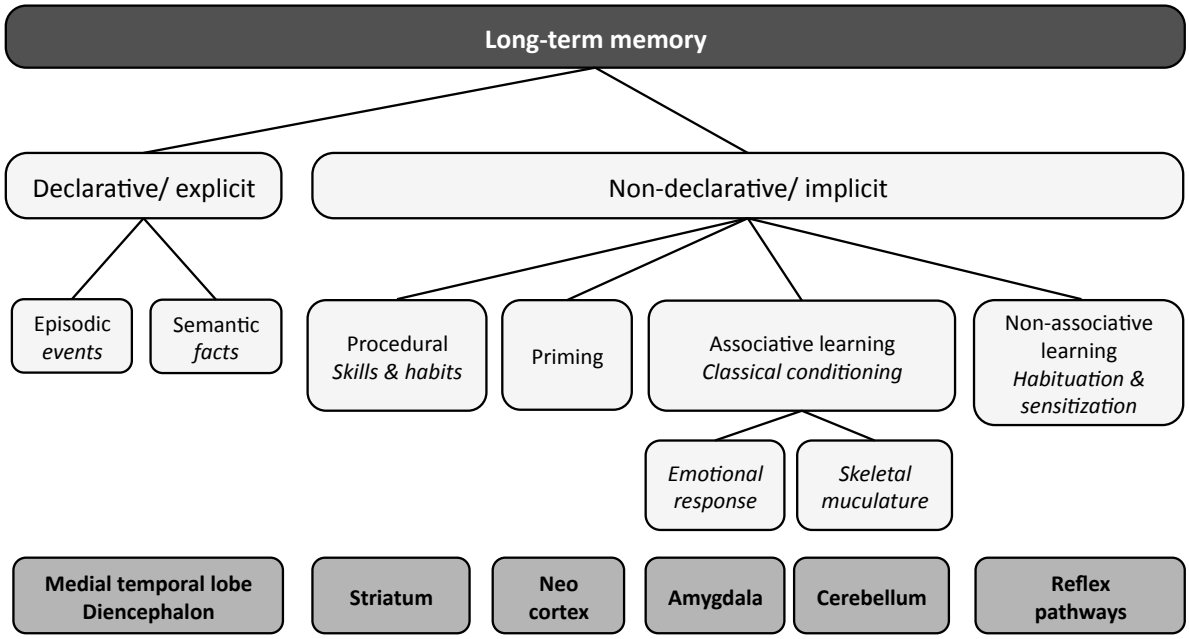

Fig. 1-1 Memory Systems. For long-term memory, especially in humans, different systems based on the perception of learning as conscious (explicit) or unconscious (implicit) process can be classified, involving different brain regions (bottom line). Adated from Squire & Zola, 1996.

However, during emotional memory formation, information about the emotional significance of an event, e.g. whether it is experienced as fearful, aversive or joyful is also acquired and stored. This can occur as an implicit process, while the memory for the event in which the emotion was experienced can be also explicit (LeDoux, 1993). Indeed, events experienced as loaded with emotions, e.g. the defense of a thesis, are actually very well remembered and often in an episodic-like fashion. That means, when remembering the event "defense of the thesis", a certain time and location can be assigned. Moreover, often multiple sensory inputs going along with the event, e.g. the smell and color of the room, the people in the room and their location within, the voice of the professors asking questions etc., are also well remembered. Thereby, a picture of the environment in which a certain event occurs is provided and builds a contextual framework. Upon re-exposure to such a context or parts of it, the whole memory for the event is recalled, e.g. when re-entering the room of the thesis defense.

Sometimes even situations or stimuli only distantly related to the original event can trigger recall of the memory. Such generalization of memory could then elicit inappropriate behavioral responses, that are disadvantageous or can even result in psychopathological states. Classical fear conditioning as a model allows for studying of emotional memory formation processes and generalization phenomena.

1.2 Classical fear conditioning as an animal model for emotional memory formation

In 1927, Ivan Petrowich Pavlow introduced the basis of classical conditioning by noticing a subject can form an association between previously not related events upon there mere coincidence. Thereby, a previously neutral stimulus can become effective in eliciting a certain behavior.

Such an associative learning process is also taking place in classical fear conditioning. Here, the individual learns an association between a neutral stimulus and an aversive event – an indispensable feature promoting survival, because the individual is now enabled to predict threatening events and avoid them before harm is done. Moreover, this paradigm bears a strong emotional component. The aversive event normally elicits a fear response, that will be now associated with certain stimuli as well as places, objects or people and a robust, lasting memory for this association is built up quickly (Maren, 2001).

1.2.1 The classical fear conditioning paradigm

Therefore, classical fear conditioning is a widely used paradigm to study memory and its modulation by emotional components in various species. In rodents, a previously neutral stimulus, such as a tone, and an aversive event, e.g. an electrical foot, are presented together. Prior to training, the footshock as the unconditioned stimulus (US) will evoke fear behavior. After training, the tone becomes the conditioned stimulus (CS) and is sufficient to elicit a fear response (conditioned response, CR; Maren, 2001; Schwartz et al., 2002). The conditioned response (Fig.1-2) is tested in a retrieval session by re-exposure of the animal to the CS. In rodents with a strong fear memory, high levels of defensive behavior are observed. Typical defensive behavior comprises of risk assessment (orientation towards the stimulus, alert watching with head movements and stretched attend), freezing (immobility except for respiratory movement) or flight responses, whereas the quality and quantity of the fear response is determined by the intensity of the training and the salience of the stimulus. Hence, risk assessment is often observed during a retrieval session and often followed by freezing, while flights can be counted only occasionally, especially following highly stressful training (Laxmi et al.,

2003; Albrecht et al., 2010). In addition, rats and mice display arousal of the autonomic nervous system and an elevation in stress hormones, reflecting again the intensity of the training (LeDoux, 2000).

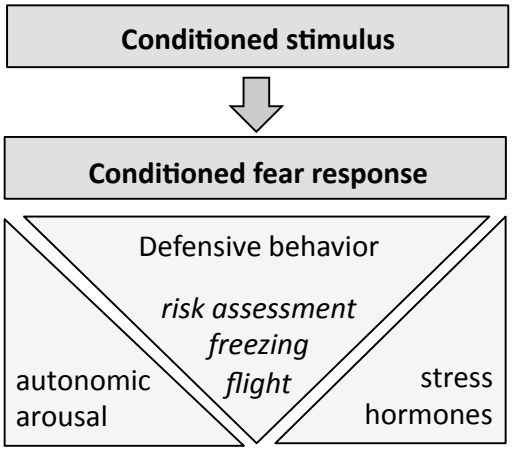

Fig.1-2 Components of the conditioned fear response. After classical fear conditioning training, the conditioned stimulus is sufficient to elicit a fear response, hence the conditioned response. Adapted from LeDoux, 2000; Laxmi et al., 2003.

Next to a tone as the conditioned stimulus, also an association to a cue with another modality can be trained e.g. a light flash or an odor. Even fear conditioning towards the environment in which the US occurred is possibly. This paradigm is called context conditioning. Here, the training environment, the so-called context, consists of multiple cues with different sensory modalities, e.g. the odor and the noises in the conditioning chamber, the texture of the floor and the color and form of the conditioning box. The animal now learns an association to such multiple cues and will show fear behavior upon re-exposure to the training context (Maren, 2001). Hence, in contrast to auditory-cued fear conditioning, no defined single cue is predicting the US but the whole environment. Therefore, the context is referred to being in the foreground.

Remarkably, auditory-cued fear conditioning is also taking place in the fear conditioning chamber, providing a context. But when a cue is presented in relation to the US, the cue will have a much higher predictive value for the occurrence of the CS than the context and will elicit a strong fear response upon re-exposure. Nevertheless, when the fear conditioned animal is re-exposed to the training context in absence of the CS, fear behavior is still observed, usually with lower freezing rates compared to the CS+ response. Therefore, the environment of auditory cued fear conditioning is referred to as the "background context" (Philips & LeDoux, 1994; Calandreau et al., 2005).

So-called unpaired fear conditioning is well illustrating the importance of the relationship between US, cue and context. In this paradigm, again an auditory cue is presented, but this time not in coincidence with the US. Therefore, the tone has no

predictive value for the occurrence of the US, but learning of environmental features will provide the animal with the relevant information. Therefore, foreground contextual fear conditioning is achieved with such a paradigm with a stronger fear response towards the context than the unpaired tone (Laxmi et al., 2003; Albrecht et al., 2010).

1.2.2 Salience determination and generalization

Background versus foreground fear conditioning demonstrates well that fear-associated stimuli can have a different predictive value for the US, thus determining the salience of a stimulus. Naturally, the stimulus predicting the occurrence of a US best will retrieve the highest attention from a subject and elicit the CR. This stimulus is then described as salient compared to other stimuli not relevant for predicting the US. Accordingly, the associative strength formed to a stimulus during the conditioning process is related to its salience, as described by the Rescorla-Wagner-model. Here, if compound stimuli are presented, an equal associative strength is formed only to equally salient stimuli. Moreover, using the CR as a read-out for such associative strength, only equally salient stimuli elicit an equal fear response (Rescorla, 1976; Schwartz et al., 2002).

However, a shift in stimulus salience can occur. For example, in auditory-cued fear conditioning a strong fear response occurs to a non-reinforced auditory stimulus (CS-) of another frequency than the originally conditioned tone (CS+) - a phenomenon termed generalization (Schwartz et al., 2002). While in this example generalization is described towards another stimulus with the same sensory modality, also intermodal shifts of saliency are described, e.g. from tone to visual cues (Schwartz et al., 2002), or even to the more complex fear conditioning environment. Such contextual generalization in an auditory-cued fear conditioning paradigm results then in increased freezing towards the background context. The context of the background is now assigned as a salient cue with high predictive value.

A systematical analysis of fear memory generalization by Laxmi and colleagues (2003) revealed a dependence of such contextual generalization on the intensity of the initial training. Overtraining, i.e. auditory cued fear conditioning with ten CS-US-pairings and high US intensities, results in increased fear response towards the background context in mice. The same was observed in rats after intensive training (Baldi et al., 2004). In a previous study I could identify the neural cell adhesion molecule (NCAM) as one

molecular factor contributing to contextual generalization of auditory-cued fear conditioning. Accordingly, mice deficient for NCAM display contextual memory deficits under highly stressful training conditions. Moreover, network synchronization between two regions highly relevant for fear memory formation, amygdala and hippocampus, is disturbed (Albrecht et al., 2010). This suggests a dependence of contextual generalization on the interplay between amygdala and hippocampus.

1.2.3 Brain regions involved in fear conditioning

Decades of genetic, pharmacological and lesion studies identified two critical regions for distinctly involved in fear conditioning – the amygdala and the hippocampus (Fig. 1-3).
The amygdala, named for its almond-shaped appearance, is a cluster of various subnuclei deep in the medial temporal lobe that differ in cytoarchitecture, molecular composure and anatomical connectivity (Pitkänen et al., 2000). For information processing during auditory cued, but also contextual fear conditioning, the lateral (LA), basolateral (BLA) and central (CeA) subnuclei of the amygdala are of great importance (LeDoux, 2000). Sensory input about the CS from thalamic and cortical areas on the one hand and nociceptive information about the US on the other hand are both directed to the LA, allowing for emotional stimulus association (Maren & Quirk, 2004). Such information is then further projected to the BLA and the CeA. In addition, the CeA itself receives nociceptive information and can modulate LA function via its reciprocal interconnections. The CeA is also the output structure of the amygdala, projecting to various areas in the brain stem, hypothalamus and periaqueductal grey, thereby generating the actual fear response (LeDoux, 2000).
In addition, the amygdala is closely interconnected with the hippocampus, in part also reciprocally and directly. The amygdala itself is capable of modulating activity in the hippocampus (Akirav & Richte-Levin, 2002) and the BLA is believed to receive information about the context from the hippocampus (Maren & Fanselow, 1995).
Whenever complex information is processed, the hippocampus is involved, i.e. when associations to a multimodal context has to be formed in contextual fear conditioning or when there is a temporal separation between US and CS in a traced fear conditioning paradigm (Philips & LeDoux, 1992; Maren, 2001; Rudy et al., 2004). The hippocampus is composed of two parts, the cornu ammonis (CA) and the cytoarchitecturally distinct

dentate gyrus (DG). The cornu ammonis can be further divided in three subunits, in which neurons and their neuritis are arranged in a highly organized pattern, forming different *strata* characterized by distinct neuron types and expression of molecular factors, *stratum oriens, pyramidale, radiatum and lacunosum-moleculare* respectively. Remarkably, the so-called pyramidal cells, located in the *stratum pyramidale*, are the principal excitatory cells of the hippocampus proper, while GABAergic interneurons are located mainly in the other strata (Watson et al, 2012). The dentate gyrus is also organized in different layers with granule cells representing the population of principal cells in this region. In the molecular layer of the dentate gyrus and in the hilus, GABAergic interneurons are located. Another type of excitatory neurons, the mossy cells, are also found in the hilus (Amaral et al., 2007). Information processing in the hippocampal subfields is traditionally believed to be mediated via excitatory neurotransmission along the trisynaptic pathway. Here, the dentate gyrus (DG) is the first station receiving inputs from the entorhinal cortex via the perforant pathway. The DG then relays information to the CA3 region via the mossy fibers. The CA3 pyramidal neurons send then projections to the CA1 area via the so-called Schaffer collaterals. However, one has to keep in mind that e.g. the entorhinal cortex has also connections to CA3 and CA1 directly and all subfields are closely interconnected, allowing for example for backpropagation of the CA3 to the DG (Yeckel & Berger, 1990; Scharfman, 2007).

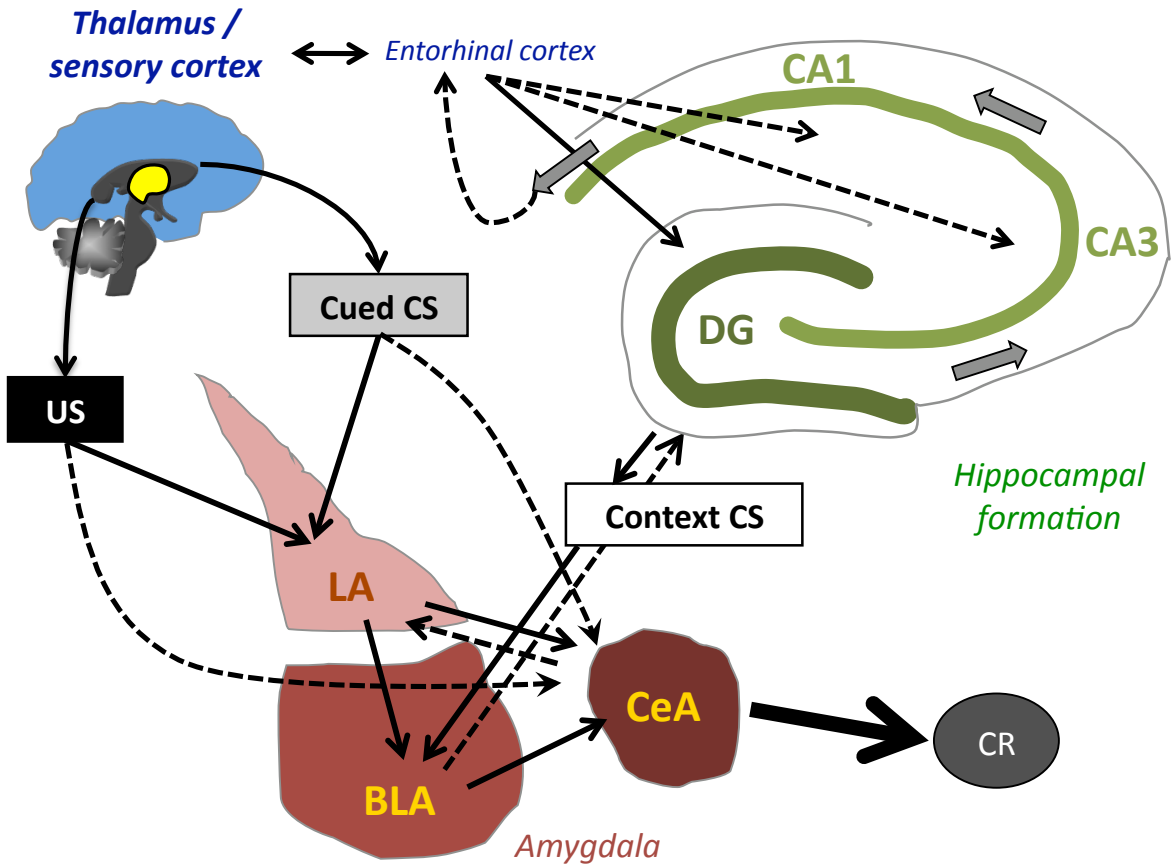

Fig.1-3 Fear conditioning circuit. Model for processing the unconditioned (US), cued and contextual conditioned stimulus (CS) in fear conditoning, mediating a conditoned fear response (CR). Stimulus information is processed in the lateral (LA), basolateral (BLA) and central nucleus of the amygdala (CeA), in interaction with cortical & thalamical areas. Infomation about the multimodal context is processed in subareas of the hippocampal formation, the dentate gyrus (DG) and the cornu ammonis (CA) subregions 1 and 3, and relayed to the BLA. Dashed lines display functional interactions. Adapted from Stoppel et al., 2006.

Lesion studies of the different subareas indicate an involvement of DG, CA3 and CA1 in contextual fear memory formation, while retrieval might require the DG and CA1 but not CA3 (Lee & Kesner, 2004). Although another study could not confirm the role of CA1 in contextual fear memory retrieval explicitly (Daumas et al., 2005), the general dependence of contextual fear memory on hippocampal function is evident.

Pharmacological manipulations and lesion studies in the last years pointed out a segregation of hippocampal function along its longitudinal axis. While the dorsal portion of the hippocampus (posterior part in humans) is believed to mediate spatial memory, the ventral hippocampus (anterior pole in humans) may be involved in affective and emotional processing (Moser & Moser, 1998). In this line, lesion of the ventral hippocampus reduced anxiety-like responses in different paradigms (Kjelstrup et al., 2002; Bannerman et al., 2004) and the structure also contributes to formation and

expression of contextual as well as auditory cued fear memory (Bannerman et al., 2004; Maren & Holt, 2004; Trivedi & Coover, 2004; Rudy & Matus-Amat, 2005). The functional differentiation is also reflected in diverse anatomical connectivity: The dorsal hippocampus together with the subiculum as its output structure is forming a network with the retrosplenial and anterior cingulate cortex as well as with the substantia nigra and the ventral tegmental area that are structures associated with locomotion and exploration. The ventral hippocampus is closely interconnected with the bed nuclei of stria terminalis, different amygdala subnuclei and the prefrontal cortex, which exert powerful control over emotional behavior (Fanselow & Dong, 2010). Furthermore, an indirect connection to the hypothalamus is established via bed nuclei of stria terminalis, the amygdala, the CeA respectively, and the ventral subiculum, thus allowing for control of neuroendocrin and autonomic activity. Thereby, the ventral hippocampus is able to control the individuals stress response by modulating the activity of relevant brain areas, the so-called hypothalamic-pituitary-adrenal (HPA) axis (Moser & Moser, 1998, Jacobson & Sapolsky, 1991). In turn, stress or increased levels of the stress hormone corticosterone differentially influence synaptic plasticity in the ventral versus the dorsal hippocampus. Long-lasting enhancement of synaptic transmission *in vivo* or *in vitro*, so-called long-term potentiation (LTP), is believed to model processes of memory formation (Kandel et al., 2000). LTP is increased in the ventral, but suppressed in the dorsal hippocampus after stress via differential activation of corticosterone receptors in both areas (Maggio & Segal, 2007). Thereby, excitability in the dorsal hippocampus is decreased by enhancing the inhibitory input via glucocorticoid receptor activation, while excitability in the ventral hippocampus is elevated be reduced influence of inhibitory currents via mineralocorticoid receptor activation (Maggio & Segal, 2009).

In addition, inhibitory interneurons determine also rhythmic activity patterns in the hippocampus, e.g. in the gamma (30-80 Hz) or theta frequency (4-12 Hz) range. Both rhythmical activity patterns can influence each other and are thought to link neuronal activity in the hippocampus with its interconnected areas (Buzsaki, 2001). They can be observed during exploration behavior or rapid eye movement (REM) sleep (Csicsvari et al., 1999), but occur also during encoding and retrieval of memory (Seidenbecher et al., 2003; Montgomery & Buzsaki, 2007). In this line, a synchronization of theta activity between the hippocampus and the amygdala is displayed after fear conditioning, in response to the conditioned cue and context respectively (Narayanan et al., 2007a).

Moreover, gamma oscillation in the ventral hippocampus is also associated with learned avoidance and anxiety–like behavior (Dzirasa et al., 2011; Lu et al., 2011).
Thus, the interplay between amygdala and different portions of the hippocampus is crucial for the formation of long-term fear memory on a systems perspective.

1.2.4 Amygdalo-hippocampal interaction

As stated above, the BLA serves as the entry site for contextual information processed in the hippocampus, but can itself modulate hippocampal function (Maren & Fanselow, 1995; Akirav & Richter-Levin, 2002; Maren, 2008). This indicates a strong dependence of especially contextual fear memory on amygdalo-hippocampal interaction. Indeed, lesions of the hippocampus, even the dorsal portion, on the one hand (Philips & LeDoux, 1994) or lesion of the BLA on the other hand (Calandreau et al., 2005) are both able to decrease fear memory to the background context.
States of emotional arousal have been demonstrated to increased BLA activity (Pelletier et al., 2005). Thereby, contextual generalization observed after overtraining (Laxmi et al., 2003; Baldi et al., 2004; Albrecht et al., 2010), might be induced by enhanced BLA activation and its subsequent stimulation of hippocampal activity. Indeed, a direct interaction of both structures is demonstrated in electrophysiological experiments. Here, stimulation of the BLA enhances LTP only in the DG, but not in the CA1 area of the hippocampus (Vouimba & Richter-Levin, 2005; Li & Richter-Levin, 2012). Such BLA modulation of DG activity is mediated via various neuromodulators, e.g. norepinephrine, and the stress hormones corticosterone (Akirav & Richter-Levin, 2002; Vouimba et al., 2007).
Taken together, such interaction between BLA and DG might be also involved in fear memory formation. Indeed, activation of the DG and BLA are observed after contextual fear conditioning, as indicated by expression of transcription factors (Stanciu et al., 2001; Kaouane et al., 2012).

1.2.5 Cellular plasticity mechanisms in fear conditioning

When an action potential travels along the axon of a neuron, voltage-sensitive calcium channels are opened, resulting in high intracellular calcium concentrations on the active zone of the synapse. Neurotransmitters are released from their storage vesicles in the presynpatic neuron and released in the synaptic cleft. At the postsynaptic neuron the small neurotransmitters bind to their specific receptors. Usually different subsets of receptors exist for each neurotransmitter that are either cation channels that open upon ligand binding (ionotropic receptor) or they are coupled to G-proteins and trigger an intracellular signaling cascade upon activation (metabotropic receptor). By this basic mechanism, neurons are enabled to communicate and whole brain areas can function as a network.

Glutamate is the neurotransmitter commonly used for excitation of postsynaptic neurons via its different receptor subtypes. Three different ionotropic receptors exist, named after their selective pharmacological agonists: N-methyl-D-aspartate (NMDA), α-amino-3-hydroxy-5-methyl-4-isoxazole propionic acid (AMPA) and kainite (KA). Each ionotropic receptor is composed of four heterogeneous subunits that are coded by single genes (Tab. 1-1; Brady & Siegel, 2012).

Tab. 1-1 Glutamate receptor subtypes. Naming of subunits according to the nomenclature of the international union of basic and clinical pharmacology (IUPHAR). Each subunit is coded by a single gene. The gene name is indicated in brackets according to the nomenclature of human genome organization (HUGO). Adapted from Collingridge et al., 2009, and Brady & Siegel, 2012.

Glutamate receptor subtypes					
ionotropic			metabotropic		
NMDA	**AMPA**	**Kainate**	**Group I**	**Group II**	**Group III**
GluN1 (*Grin1*) GluN2A (*Grin2a*) GluN2B (*Grin2b*) GluN2C (*Grin2c*) GluN2D (*Grin2d*) GluN3A (*Grin3a*) GluN3B (*Grin3b*)	GluR1 (*Gria1*) GluR2 (*Gria2*) GluR3 (*Gria3*) GluR4 (*Gria4*)	GluK1 (*Grik1*) GluK2 (*Grik2*) GluK3 (*Grik3*) GluK4 (*Grik4*) GluK5 (*Grik5*)	mGlu1 (*Grm1*) mGlu5 (*Grm5*)	mGlu2 (*Grm2*) mGlu3 (*Grm3*)	mGlu4 (*Grm4*) mGlu6 (*Grm6*) mGlu7 (*Grm7*) mGlu8 (*Grm8*)

The expression of those subunits in amygdalar and hippocampal subareas is regulated by stress (Rosa et al., 2001; Owen & Matthews, 2007; Hunter et al., 2009; Martisova et al., 2012). In addition, stress or stress hormones also modulate AMPA and NDMA receptor activity (Harvey & Shahid, 2012), hence highlighting the importance of ionotropic glutamatergic signaling in memory formation for emotional arousing events. Accordingly, specific antagonists for the different glutamate receptor types reveal a crucial contribution of NMDA and AMPA receptors to the various stages of fear memory. In summary, activation of both receptor subtypes in the amygdala appears crucial for the formation of fear memory, while only AMPA, but not NMDA receptors are involved in fear expression in this region (Walker & Davis, 2002). NMDA receptor activation in the hippocampus is also involved in contextual fear memory formation (Riaza Bermudo-Soriano et al., 2012). The role of the kainate receptor subtypes is less well understood, most likely because of the lack of specific pharmacological blockers that not modulate AMPA activity in addition. However, transgenic mice with disrupted expression of distinct kainite receptor subunits, provide a valuable tool for studying their contribution to sensory perception, learning and memory. In mice deficient for the GluR5 (= GluK1) subunit fear memory formation is intact (Ko et al., 2005), while in GluR6 (= GluK2) knock out mice auditory cued and contextual fear memory is impaired (Mulle et al., 1998; Ko et al., 2005).

On a cellular perspective, activation of NMDA, AMPA and at many synapses also KA receptors is required to establish an excitatory postsynaptic potential (EPSP). EPSPs are measured e.g. in neurons of the LA during fear memory formation and are characterized by a rapid depolarization of the membrane, caused by opening of AMPA receptors and subsequent influx of sodium ions. A slower, but lasting component of the EPSP is mediated by opening of NMDA receptors, allowing for temporal and spatial summation of multiple inputs. The ion channels of NMDA receptors are usually blocked by magnesium ions that are only removed when the postsynaptic membrane is depolarized sufficiently by stronger activation, e.g. when the particular LA neuron receives additional nociceptive input caused by the US. Then, the channel becomes permeable for sodium and potassium ions, but also calcium ions. An increase of intracellular calcium concentrations triggers further intracellular signaling cascades that are important components of synaptic consolidation processes (Brady & Siegel, 2012; Riaza Bermudo-Soriano et al., 2012).

During synaptic consolidation the interplay between neurons that have been activated together is facilitated lastingly. Such an enduring strengthening of synaptic connections is only achieved by a reorganization of the synapse, including changes in the cytoskeleton, rearrangement of neurotransmitter receptors and other synaptic proteins as well as modulation of extracellular matrix proteins around the synapse.

Therefore, synapses are not considered as stable, but changeable structures upon activation. This process referred as synaptic plasticity provides the basis for synaptic consolidation and establishing of a long-term memory trace, thus leading to system consolidation detected on a behavioral level of analysis (Dudai, 2004).

Long-term potentiation (LTP) is a widely accepted model for synaptic plasticity *in vitro* and *in vivo*, in which high frequency stimulation of afferent fibers induces a long-lasting enhancement of synaptic transmission. Indeed, a lot of the molecular events required for maintenance of LTP are also described during long-term fear memory formation (Schafe et al., 2001). In both processes, increase of intracellular calcium levels, mediated by NDMA receptors or voltage-gated calcium ion channels triggers signaling cascades that result in the induction of transcription of specific target genes.

In addition, intracellular signaling cascades are also initialized by metabotropic receptors. Upon ligand binding, G-proteins are activated which directly regulate different effector proteins. For glutamate, eight metabotropic glutamate receptors have been identified, which build up three different functional classes and trigger different intracellular signaling cascades (Tab. 1-1). Activation of group I metabotropic glutamate receptors (mGluRs) stimulates phospholipase C (PLC), which activates calcium ion channels via the second messenger inositol triphosphate (IP_3). Ligand binsing to group II and III mGluRs inhibits adenylate cyclase, resulting in reduced levels of the second messenger cyclic adenosine monophosphate (cAMP; Riedel et al., 1996). By that, metabotropic glutamate signaling also contributes to anxiety and fear memory formation (Riedel et al., 1996; Walker & Davis, 2002). Interestingly, anxiolytic properties of group II and III mGluRs in the amygdala or hippocampus appear to be mediated by neuropeptide Y (NPY; Wierońska et al., 2005; Smiałowska et al., 2007). NPY expression is regulated by the transcription factor cAMP response-element binding protein (CREB; Pandey et al., 2005).

CREB (Fig. 1-4) is the common target of the cAMP-dependent protein kinase (PKA) and the extracellular-regulated kinase (ERK)/ mitogen-activated protein kinase (MAPK) pathway, which are central elements for the formation of LTP and long-term memory

(Schafe et al., 2001). PKA is activated by enhanced levels of cAMP, while the ERK/ MAPK pathway is activated by cross-talk of intracellular signaling pathways and in response to other extracellular effectors, e.g. growth factors. PKA or interposed kinases then enter the nucleus and phosphorylate CREB. In addition, increased intracellular calcium concentration, mediated by IP_3, voltage gate calcium ion channels or ligand-gated ion channels (e.g. the NMDA receptor), activates the calcium/ calmodulin-depdendent protein kinase type IV (CaMKIV), which also phosphorylates CREB.

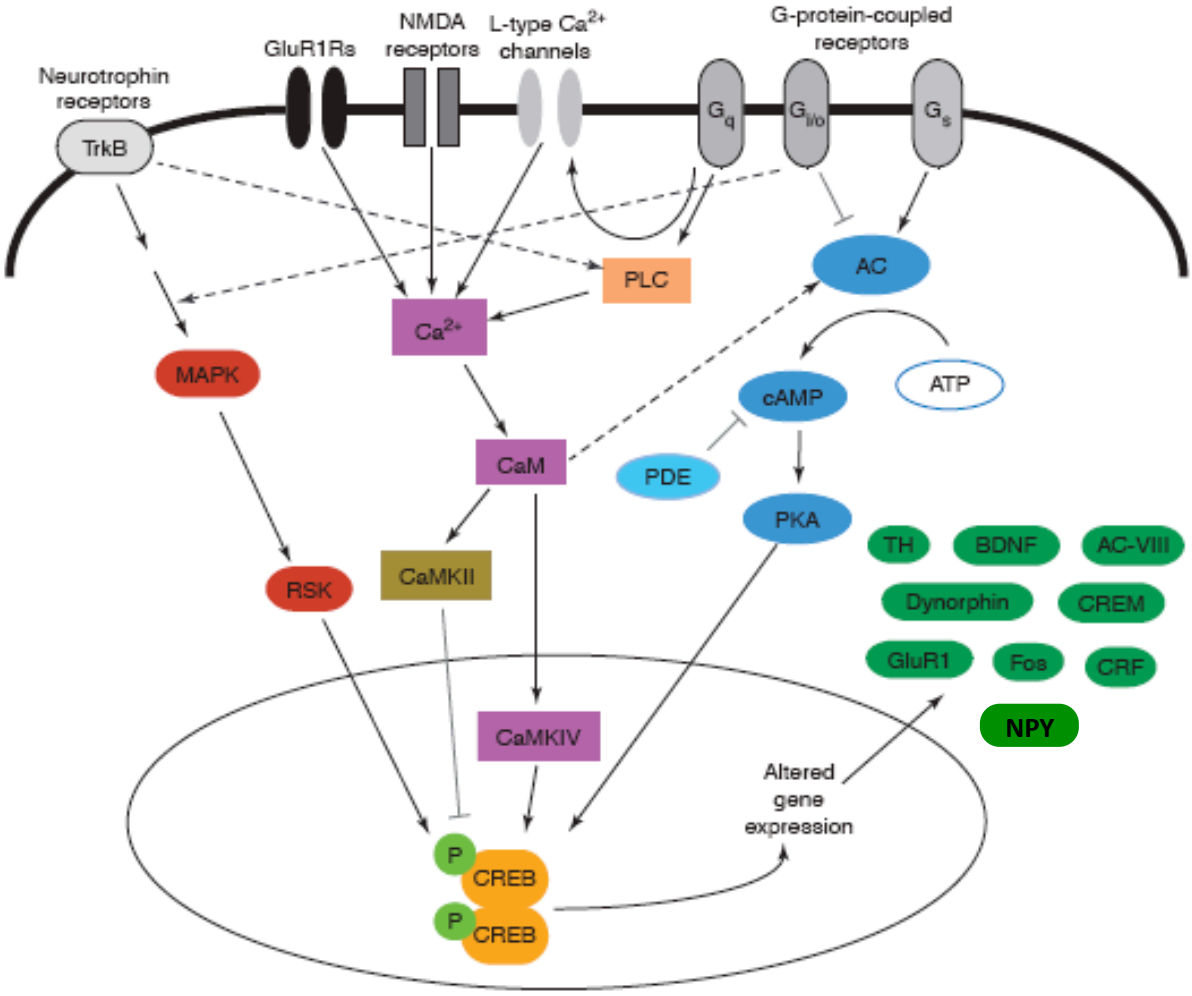

Fig.1-4 Intracellular signaling pathways leading to phosphorylation of CREB (see text for details). CREB then acts as an transcription factor, altering expression of various target gene, e.g. NPY. Adapted from Carlezon et al., 2008.

Together, phosphorylation of CREB occurring at seronine 133 finally allows for dimerization and binding to the cAMP-response element, a special DNA sequence at the promotor region of various target genes (Schafe et al., 2001; Carlezon et al., 2005). By

that, expression of several target genes is induced, including other transcription factors like c-Fos, enzymes for the synthesis of neurotransmitters (e.g. tyrosine hydroxylase), receptor subunits (e.g. GluR1) or neuropeptides (Carlezon et al., 2005).
During formation of fear memory phosphorylation of CREB is also observed in amygdala and hippocampus (Stanciu et al., 2001), indicating activation of neurons in these brain areas. Together with other transcription factors, e.g. c-Fos or c-Jun, CREB mediates fear conditioning-dependent expression changes in numerous target genes in a highly complex pattern. When comparing amygdala and hippocampus, time course and direction of the alterations or functional clusters of genes affected differ in part (Ressler et al., 2002; Mei et al., 2005; Ploski et al., 2010). Although functional consequences of such complex expression changes are not well understood, insights in molecular pathways involved in fear memory formation in the different brain areas would provide new entry points for the therapy of anxiety disorders (Mahan & Ressler, 2012).

1.2.6 Inhibitory systems and their modulation in fear conditioning

Activation of neurons by glutamatergic signaling is one of the core components of fear memory formation. For example, increased excitation is observed in the amygdala when a threatening stimulus occurs (Pelletier et al., 2005). But whenever stimuli not related to a threat arrive, excitation of amygdala subnuclei should be suppressed. In disorders characterized by heightened states of anxiety or fear and generalization of fear to inappropriate stimuli like phobia or posttraumatic stress disorder, the inhibition in the amygdala might be impaired (Möhler, 2012). Also, under non-pathological conditions, the activity of the amygdala subregions needs to be well balanced in order to allow reasonable fear memory formation (Makkar et al., 2010).
The molecule γ-amonibutyric acid (GABA) as the major inhibitory neurotransmitter ubiquitously used in the brain mediates such control of activity, often in concert with neuropeptide co-transmitters. Further modulation of inhibitory, but also excitatory signaling is achieved by the action of monoaminergic neurotransmitters like dopamine, norepinephrine, serotonin as well as acetylcholine in restricted brain areas

1.2.6.1 The GABAergic system in fear conditioning

The inhibitory neurotransmitter GABA is synthesized from glutamic acid by the enzyme glutamic acid decarboxylase (GAD). GAD is only expressed in neurons using GABA as a neurotransmitter, allowing its use as presynaptic marker of GABAergic neurons (Brady & Siegel, 2012). Two isoforms exists, named after their approximate molecular weight and derived from two different genes: GAD65 and GAD67. Both isoforms differ in their cellular localization and function. GAD65 is directly associated to the membranes when phosphorylated and is thought to preferentially synthesize GABA for vesicular release. GAD67 appear to be widely distributed in the cell and membrane association is only achieved indirectly by forming heteromers with GAD65. Therefore, GAD67 is believed to preferentially form cytoplasmatic GABA. Although both isoforms are basically expressed in interneurons, quantitative differences could reflect distinct functional properties. GAD67 accumulates in interneurons with a tonical firing pattern, while GAD65 is enriched in neurons with sparse firing upon synaptic input (Soghomonian & Martin, 1998), thus indicating different metabolic needs associated with GABA release modes. Moreover, chronic stress induces distinct expression patterns for GAD65 and 67 in hypothalamic and hippocampal subareas (Bowers et al., 1998), indicating a differential expression regulation. Mice deficient for GAD65 display increased anxiety (Kash et al., 1999) as well as an elevated, panic-like conditioned fear response that generalizes to non-reinforced stimuli (Stork et al., 2003; Bergado-Acosta et al., 2008).

GABA can bind to ionotropic GABA A or metabotropic GABA B receptors, both contributing to inhibitory postsynaptic potentials (IPSPs). The GABA A receptors are pentamers that usually contain α, β and ϒ subunits in different combinations (Tab. 1-2; e.g. α1β2γ2 as the major receptor subunit in the brain). Expression of the subunits differs between brain areas and is modulated by stress in amygdala and hippocampus (Orchinik et al., 1995; Jackobson-Pick et al., 2008; Poulter et al., 2010).

The pentamers build a chloride channel that causes a hyperpolarization upon opening and reduces the excitability of the neuron, thus mediating the fast component of the inhibitory postsynaptic potential (IPSP). However, especially in embryonic neuronal cells, the intracellular concentration for chloride ions is already increased. Opening of chloride ion channels results then in depolarization. Thus, the electrophysiological properties of the GABA A receptor depend also on the activity of chloride ion pumps in the neuron (Brady & Siegel, 2012).

The affinity of the receptor for GABA can be modulated by allosteric ligands, e.g. the GABA agonist muscimol, but also ethanol, benzodiazepines, volatile anaesthetics or neurosteroids. This substances have special binding sites apart from the GABA binding pocket, e.g. for benzodiazepines at the α subunit interface to β and γ subunits (Brambilla et al., 2003) and explain the sedative and anxiolytic effects of these substances

Tab. 1-2 Classes of GABA A receptor subunits. Naming of subunits according to the nomenclature of the international union of basic and clinical pharmacology (IUPHAR). Subunit is coded by different genes. The gene name is indicated in brackets according to the nomenclature of human genome organization (HUGO). Adapted from Collingridge et al., 2009.

GABA A receptor subunits							
α	**β**	**Υ**	**δ**	**ε**	**θ**	**π**	**ρ**
α1 (*Gabra1*) α2 (*Gabra2*) α3 (*Gabra3*) α4 (*Gabra4*) α5 (*Gabra5*) α6 (*Gabra6*)	β1 (*Gabrb1*) β2 (*Gabrb2*) β3 (*Gabrb3*)	Υ1 (*Gabrg1*) Υ2 (*Gabrg2*) Υ3 (*Gabrg3*)	(*Gabrd*)	(*Gabre*)	(*Gabrq*)	(*Gabrp*)	ρ1 (*Gabrr1*) ρ2 (*Gabrr2*) ρ3 (*Gabrr3*)

The metabotropic GABA B receptor mediates the slow component of the IPSP via modulation of the second messengers cAMP and IP_3 and subsequent activation of certain potassium ion channels. Initially, localization of GABA B receptors was described at the presynaptic site, where they modulate neurotransmitter release (Brambilla et al., 2003; Brady & Siegel, 2012).

In patients with anxiety disorders and depression a reduction of GABAergic neurotransmission and deficits in GABA A function is observed. Accordingly, mice deficient for different GABA A receptor subunits or GABA B receptors display also anxiety- and depression-like behavior (Möhler, 2012). In order to allow for fear memory formation and appropriate adaptive responses, excitation and inhibition needs to be well balanced. Pharmacological and genetic studies provide evidence that for acquisition and consolidation of fear memory a transient downregulation of inhibitory neurotransmission and GABA A receptor action in the amygdala is required. Accordingly, during retrieval of fear memory, activation of the amygdala is necessary, hence achieved also by reduced GABAergic neurotransmission (Makkar et al., 2010).

A well-balanced regulation of activity by GABAergic action is observed in the hippocampus as well. A highly specialized network of different types of GABAergic

interneurons is well described for the hippocampus. They inhibit hippocampal principal cells and communicate with each other. Such communication between different classes of interneurons occurs not only chemically via synaptic contacts, but also electrical via gab junctions. Together a large inhibitory network is formed that maintains oscillatory activity in the hippocampus, e.g. in the theta or gamma frequency range. Moreover, different classes of interneurons target distinct parts of the principle cells, i.e. its apical or proximate dendrite or the soma, allowing for a fine modulation of the signal propagated within a principle cell (Buzsáki, 2001).

The different interneuron subtypes can be classified by their physiological or morphological properties, but they are also characterized by expressing different calcium-binding proteins or neuropeptides.

1.2.6.2 Neuropeptides define classes of GABAergic interneurons and modulate fear and anxiety

Interneurons form local circuits that shape signal propagation. Especially in the hippocampus, interneurons were therefore initially classified according to their morphological appearance and their layer-specific synaptic inputs and axonal projections (Buzsáki, 2001; Maccaferri & Lacaille, 2003; Houser, 2007). Examples for that classification are basket cells and O-LM cells in the CA1 region (soma in the *stratum oriens*, axonal processes extending to *stratum lacunosum-moleculare*), however overlap exists between different description systems (e.g. horizontal cells are equivalent to O-LM neurons; Maccaferri & Lacaille, 2003). Using immunhistochemical tools, it became evident, that interneurons also differ in their neurochemical content, i.e. expressing different neuropeptides and calcium-binding proteins. Given the specific modulatory action of distinct neuropeptides, subsets of interneurons characterized by certain neuropeptides display also functional differences. However, the same neuropeptide can be expressed in morphological distinct neuron types (e.g. somatostatin in O-LM cells and bistartified cells of the stratum oriens), but morphologically similar interneurons can also express different, non-overlapping markers (e.g. parvalbumin and cholecystokinin in functionally different basket cells; Maccaferri & Lacaille, 2003). Furthermore, intracellular recordings are used to characterize interneurons, revealing differences in spike timing and integration of excitatory postsynaptic potentials. With this, networks of different interneurons exert powerful control over signal propagation in principal cells via feedback and feedforward inhibition. By that, caused by their oscillatory activity,

interneurons determine also hippocampal rhythmic activity (Buzsáki, 2001; Maccaferri & Lacaille, 2003).

GABAergic inhibition is also fundamental for the function of the dentate gyrus. Being the input structure of the hippocampus, the dentate gyrus has to "translate" the dense activity pattern coding incoming information from the entorhinal cortex into a sparse activity code in the hippocampal areas. Functionally, the dentate gyrus is enabled to encode multiple sensory inputs conjunctively and reduce interference between similar information, a process called pattern separation (e.g. during encoding of spatial memory; Acsády & Káli, 2007). Excitation from the entorhinal cortex reaches the hippocampus via the perforant path, but only the strongest inputs are shunted and propagated to dentate gyrus granule cells and further transferred to the CA3 area. This sparsification is mediated by strong inhibition via GABAergic neurons. The dentate gyrus granule cells therefore send axon collaterals to interneurons in the hilus. There, the cell bodies of so-called HIPP cells are located (hilar perforant path-associated cells). They send their axons to the outer two-thirds of the dentate molecular layer, where entorhinal inputs arrive, allowing for strong feedback inhibition of granule cell near their inputs. Other interneurons located in the molecular layer mediate a feedforward inhibition by modulating the incoming signals whenever activated by the perforant path (MOPP cells; molecuar layer perforant path- associated cells). Some interneurons are able to mediate feedforward and feedback inhibition, depending on their synaptic input, e.g. cells positive for parvalbumin (Houser, 2007). Dentate gyrus interneurons are characterized by specific expression of neuropeptides as well. Notably, HIPP cells express somatostatin (SST), which is often colocalized with NPY. Vice versa, the majority of all NPY-positive cells in the dentate gyrus are located in the hilus and display morphological characteristics of HIPP cells (Sperk et al., 2007).

Next to such network function in hippocampal subareas, interneurons share also signal propagation in the amygdala via local microcircuits and with specifity to neurochemical subtypes. For example, as described in the hippocampus, parvalbumin-positve interneurons can provide both, feedforward and feedback inhibition at the proximal dendrite of projection neurons (Ehrlich et al., 2009). A cluster analysis of electrophysiological distinct interneuron populations in the lateral amygdala demonstrated that some neuropeptides, e.g. cholcystokinin (CCK), are distributed among different functional classes, while for example SST is expressed more exclusively (Sosulina et al., 2010). However, other studies describe non-overlapping populations for

CCK and SST in the amygdala, while SST and NPY are also co-expressed in this brain area (McDonald, 1989). Overall, although different interneuron populations are defined by their content for neuropeptides that also display specific firing properties (Spampanato et al., 2011), their specific contribution to local microcircuits in the amygdala is less well understood than in the hippocampus and remains a topic of intensive research (Ehrlich et al., 2009).

On the behavioral level, evidence exist for a crucial involvement of neuropeptide signaling in amygdala and hippocampus for mediating fear and anxiety. NPY, SST and CCK are three neuropeptides that are expressed in amygdala and hippocampus and have been implicated in mediating fear and anxiety (Stoppel et al., 2006).

Anxiolytic, antidepressive, and anticonvulsive properties of NPY are described (Heilig, 2004) in accordance with its inhibitory actions in amygdala and hippocampus. The upregulation of NPY after stress observed in the dentate gyrus and the amygdala (Conrad & McEwen, 2000; Cui et al., 2008) is therefore believed to reflect adaptive responses. Indeed, when NPY signaling is impaired in the hippocampus via blockade of the Y1 receptor, anxiety and fear elicited by traumatic stress are enhanced (Cohen et al., 2012). Even in humans acute stress lead to increased levels of NPY and the stress hormone cortisol in the plasma, but elevated NPY levels are correlated with reduced subjective stress perception (Morgan et al., 2002). However, after chronic mild stress, an animal model for depression, NPY expression is decreased in the dentate gyrus (Sergeyev et al., 2004), further underlining the importance of NPY in mediating adaptive responses. Virally mediated overexpression of NPY in the amygdala confirmed anxiolytic properties of NPY that are mediated via the Y1 receptor (Primeaux et al., 2005). Conversely, knock out of NPY in transgenic mice increased anxiety, but had no effects on in hippocampus-dependent memory (Karl et al., 2008). In such mice fear memory towards a cue is increased. The same effect is also observed in Y1, but not Y2 deficient mice. Moreover, NPY and Y2 knock out mice show generalization of the cued fear memory towards a neutral stimulus of the same modality, which was not observed in the receptor deficient animals (Verma et al, 2012).

Together, NPY appears as a key player mediating adaptive responses to stress, thereby reducing anxiety and support determination of an appropriate threat in fear conditioning. In addition, earlier studies report increased spatial memory formation after NPY administration (Flood & Morley, 1989). However, virally mediated NPY overexpression in the hippocampus impaired long-term potentiation in the CA1 area of

the hippocampus and spatial discrimination memory, possibly mediated by reduced glutamatergic transmission (Sørensen et al., 2008).

NPY-positive interneurons can also express SST in the amygdala and the hippocampus (McDonald, 1989; Fu & van der Pol, 2007). Like NPY, SST has also anxiolytic properties (Yeung et al., 2011) and is expressed upon acute stress (Arancibia et al., 2001), most likely via increasing inhibition in the amygdala (Meis et al., 2005). The anxiolytic action is exerted via the SST receptor type 2 in the amygdala and the septum (Yeung & Treit, 2012). Knock out of this receptor leads to increased spatial discrimination learning, accompanied by enhanced glutamatergic transmission in the CA1 area of the hippocampus (Dutar et al., 2002). In mice deficient for SST, CA1 LTP is impaired (Kluge et al., 2008), suggesting involvement of other SST receptor subtypes in hippocampal function. In addition, contextual, but not cued fear memory was impaired in these animals.

While SST and NPY display some functional similarities in reducing anxiety-like behavior, CCK displays anxiogenic properties and CCK compounds are even able to induce panic attacks in humans (Rotzinger & Vaccarino, 2002; Wang et al., 2005). Remarkably, CCK is expressed cells diverse from SST/NPY-positive interneurons cells (McDonald, 1989; Mascagni & McDonald, 2003) and leads to increased cell excitability in the amygdala (Meis et al., 2007). The anxiogenic actions of CCK are mediated by the CCK receptor type 2 (or CCK-B; Wang et al., 2005). Accordingly, overexpression of this receptor increases anxiety-like behavior (Chen et al., 2006), while in mice deficient for CCK-B anxiety-like behavior is reduced. However, neither conditioned fear to the context nor to the cue was affected in CCK-B knock out mice (Raud et al., 2005), but injection of CCK-B antisense nucleotides in the lateral ventricle of rats reduced contextual conditioned fear (Tsutsumi et al., 2001). Furthermore, in the CCK-B overexpressing mice contextual fear conditioning was impaired, but when a strong training is engaged the freezing response is even enhanced towards to cue as well as the context (Chen et al., 2010), suggesting a modulatory role of CCK on fear memory dependent on stress intensity.

Overall, as demonstrated here with this few examples, neuropeptides display distinct cellular and behavioral functions by modulating glutamatergic and GABAergic neurotransmission in various brain areas. In addition to neuropeptidergic co-transmitters, monoaminergic and cholinergic neurotransmitters are also able to alter inhibitory and excitatory signaling and are therefore often referred as neuromodulators.

The impact of such neuromodulators on anxiety and fear memory is described in the following section.

1.2.6.3 Monoaminergic neuromodulation & acetylcholine

Acetylcholine, dopamine, norepinephrine and serotonin, are small molecules that are utilized as transmitters in various areas of the brain and the peripheral neuromuscular and neuroendocrine system. These molecules display all characteristics of classicial neurotransmitters, comparable to GABA and glutamate. However, they are not ubiquitously expressed, but only in specific nuclei of the brainstem and midbrain and give rise to long projections to various brain areas, including different parts of the cortex, striatum, hippocampus and amydala (see Tab. 1-3).

Tab. 1-3 Origin and projection of monoaminaergic and cholinergic neurotrasnmitters. Only the most relevant projections are summarized here (Kandel et al., 2000; Brady & Siegel, 2012).

	Origin	Projection
Acetylcholin	basal forebrain	amygdala, hippocampus, limbic cortices, neocortex
	tegmental nuclei	thalamus
Dopamine	substantia nigra & ventral tegmental area	caudate-putamen (*nigrostriatal pathway*)
		Amygdala, limbic cortices (*mesolimbic/ mesocortical pathway*)
	arcuate nucelur (hypothalamus)	pituitary gland
Norepinephrine	locus coeruleus	amygdala, hippocampus, limbic cortices, neocortex, cerebellum, spinal cord, hypothalamus,
Serotonine	dorsal and median raphe nuclei	amygdala, hippocampus, limbic cortices, neocortex, cerebellum, spinal cord, hypothalamus,

For each of these neurotransmitter different receptor subtypes exist, the great majority being metabotropic, i.e. coupled to G proteins. In general, like neuropeptides, these neurotransmitters are able to modulate GABAergic and glutamatergic signaling, however less is known about the molecular mechanism of all receptor subtypes. Functionally, monoaminergic neurotransmitters have been implicated in various brain functions linked to affective behaviors and psychiatric disorders, e.g. serotonin in depression (Kupfer et al., 2012), dopamine as a key player in reward and addiction

(Adinoff, 2004) and norepinephrine in mediating stress responses (Itoi & Sugimoto, 2010). Given their fundamental role in mediating affective behavior, often also in interplay with each other, such neuromodulators are well suited to regulate emotional memory formation.

Inactivation of their regions of origin via pharmacological or genetic tools provide insights in the contribution of the single transmitters to fear memory formation and anxiety. In the case of serotonin, neurotoxic lesion of the median raphe nucleus reduced contextual fear conditioning and fear potentiated startle (Borelli et al., 2005). However, mice with a more specific conditional ablation of central serotonergic neurons displayed enhanced contextual fear memory that was normalized by systemic serotonin application. In addition, these animals show reduced anxiety and also impaired spatial memory in a Morris water maze (Dai et al., 2008). This is in strong contrast to the widely noticed effect of selective serotonin re-uptake inhibitors (SSRIs), which elevate the level of synaptic serotonin and used successfully for the treatment of anxiety disorders. But as explained in the previous chapters of fear memory circuit, an increased contextual fear response could reflect enhanced amygdala modulation of hippocampal function, especially when spatial memory that depends on the hippocampus but not the amygdala is reduced in these animals. Indeed, long-term potentiation in the dentate gyrus is fascilitated by serotonergic action in the BLA via the 5HT2C serotonin receptor subtype (Abe et al., 2009a). In addition, pharmacological studies revealed that increased cued and contextual freezing is mediated by the 5HT2A receptor action during consolidation (Zhang et al., 2012).

Utilizing pharmacological tools, the role of the dopaminergic system in fear memory formation has been investigated. Increased dopamine release enhances conditioned fear in several studies, while blocking of the dopamine receptors D1 and D2 decreases the fear response in some, but not all studies (Pezze & Feldon, 2004). Although, D1 and D2 receptors can exert very different intracellular actions, they seem to contribute synergistically to the acquisition and expression of conditioned fear (Kamei et al., 1995; Fadok et al., 2009). The ventral tegmental area (VTA) gives rise to dopaminergic projections to the amygdala (Pezze & Feldon, 2004). In mice lacking the GluN1 subunit of the NDMA receptor in these neurons dopamine release is impaired. This results in decreased cue-dependent fear conditioning and increased anxiety (Zweifel, 2011), further highlighting the importance of mesolimbic dopaminergic projections in fear and anxiety. Moreover, lesion of the VTA evoked an impairment of long-term potentiation in

the dentate gyrus that was rescued by D1 and D2 stimulation in the BLA, suggesting also a modulatory role of dopamine on amygdalo-hippocampal interatction (Abe et al., 2009b).

A strong modulation of BLA activity during fear memory formation occurs also via norepinephrine. In general, pre- and posttraining administration of norepinephrin or its receptor agonists sufficiently enhanced emotional memory formation, while blocking of so-called β-adrenergic receptor subtypes reduced fear memory, even when the peripherally administered. In addition, studies in humans demonstrate that central brain action of norepinephrine receptors is required for these effects (van Stegeren, 2008). Since norepinephrine is released together with the stress hormone corticosterone in emotionally arousing situations, noreponephrine action is believed to determine emotional salience for an event by activating the amygdala. In this line, norepinephrine agonists applied directly to the BLA enhance fear memory, while antagonist and lesion of the amygdala occluded these effects on (McGaugh, 2004). Norepinephrine applied to the BLA also enhances long-term potentiation in the DG (Vouimba et al., 2007), suggesting modulation of amygdalo-hippocampal interaction by norepinephrin as well.

Together with norpepinephrine, modulation of DG-LTP also depends on acetylcholine-signaling via its muscarinergic receptors (Bergado et al., 2007). For acetylcholine two classes of receptors with distinct properties exist, nicotinergic and muscarinergic receptors respectively. Both have been implicated in fear conditioning. While few studies exist reporting involvement of nicotinergic signaling in fear memory retrieval, the role of muscarinergic signalin in fear memory formation is more comprehensively studied (Tinsley et al, 2004). Pharmacological blockers of muscarinergic receptors prior to fear conditioning consistently impair contextual fear conditioning when administered directly in the BLA or the hippocampus, while impairing effects on cued fear memory are reported only in some studies (Robinson et al., 2011). Such deficits in contextual fear memory might be mediated via the M1 subtype of muscarinergic receptors (Soares et al., 2006), but were not observed in mice deficient for M1 (Anagnostaras et al., 2003), further underlining side- and state-specific neuromodulatory action.

Together, all neuromodulators appear to contribute to fear memory formation via their action in amygdala and hippocampus. Moreover, they are well situated to mediate amygdalo-hippocampal interaction. Especially norepinephrin is identified as a key player in emotional salience determination. This function is exerted in concert with the

stress hormone corticosterone (McGaugh, 2004). The role of corticosterone in emotional memory formation and its regulation by the HPA axis is described in the following chapter.

1.2.7 Corticosterone in fear conditioning

Corticosterone, or its equivalent cortisol in humans, is systemically released from the cortex of the adrenal gland upon physiologically and psychologically stressful events. However, corticosterone plasma concentrations are maintained also at a certain level under basal conditions and these levels display a circadian rhythmicity. In C57BL/6 mice daily concentrations of corticosterone reach their peak at the beginning of the dark, hence active phase of the animals. They then quickly fall within the first hour sof the dark phase and are minimal at the beginning of the light, hence inactive phase (Dalm et al., 2005).

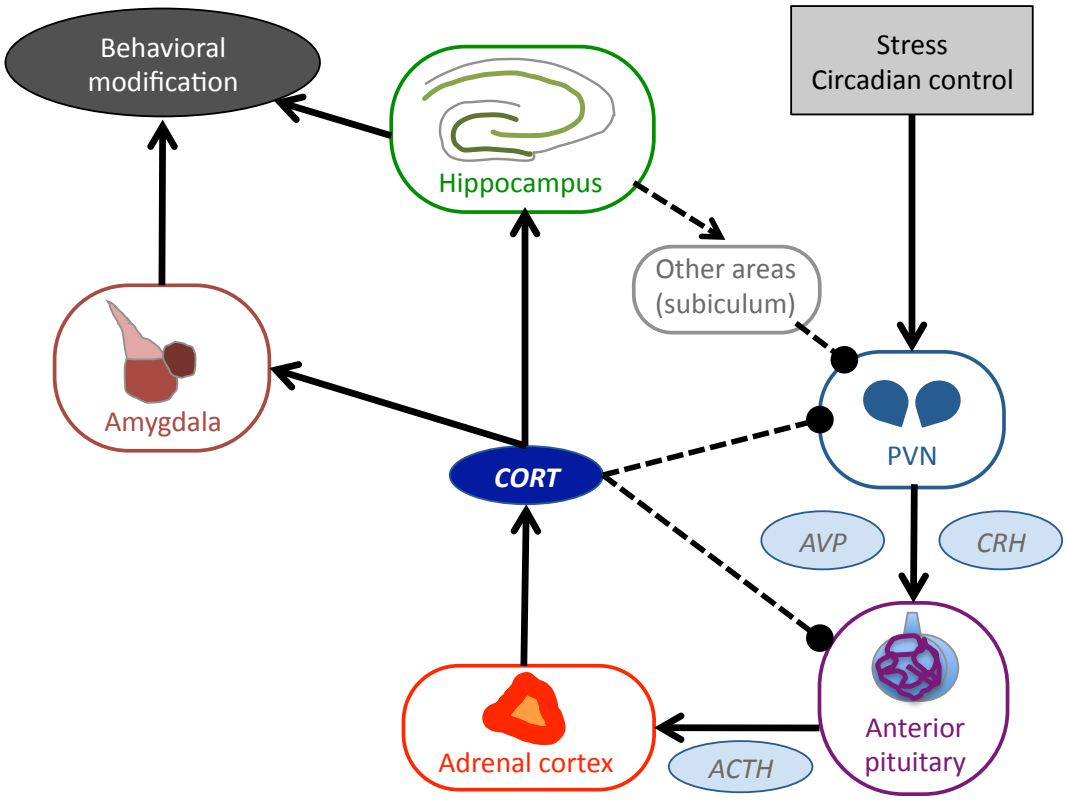

Fig.1-5 Activation and feedback inhibition of the hypothalamic-pituitary-adrenal (HPA) axis. ACTH – adrenocorticotrophic hormone; AVP – vasopressin; CORT – corticosterone; CRH – corticotropin releasing hormone; PVN - paraventricular nucleus of the hippothalamus; see text for details. Arrow heads incdicate activation, blunted end sinhibition; dashed lines indicateconnections of the feedback loop. Adapted from Kolber et al., 2008.

Levels of corticosterone under baseline conditions and after stimulation are tightly controlled by the activity of the hypothalamic-pituitary-adrenal (HPA) axis (Fig. 1-5). Neurons in the paraventricular nucleus (PVN) of the hypothalamus are activated by stress and under circadian control. They then release the neuropetides corticotropin-releasing hormone (CRH) and vasopressin (AVP) into the portal venous system of the pituitary gland. Here, adrenocorticotrophic hormone (ACTH) is secreted into the blood plasma, reaching thereby also the adrenal gland. There, corticosterone is released into the blood plasma. This sequential activation is inhibited via feedback mechanisms: Binding of corticosterone to glucocorticoid receptors (GR) at the different stations of the HPA axis will inhibit corticosterone release. GRs are also expressed in limbic areas like amygdala or hippocampus. Activation of the hippocampus by corticosterone inhibits PVN activity indirectly, e.g. via the ventral subiculum, thus integrating the hippocampus in feedback control of corticosterone release (Jacobson & Sapolsky, 1991; Kolber et al., 2008).

Corticosterone binds to two types of receptors. While GRs introduced above are expressed ubiquitously with particularly high concentrations in hypothalamical subnuclei, hippocampus and amygdala, expression of the mineralocorticoid receptor (MR) subtype is restricted to hippocampal and amygdala subareas, to the septum and some brainstem motor nuclei. The affinity of corticosterone to MR is believed to be around 10-fold higher than to GR, indicating activation of GR only with high corticosterone concentrations like after stressful events. However, the co-expression of both receptors in limbic areas indicates that an interplay of both may be required for the emotional memory formation. Both receptors directly control transcription of their target genes. Upon ligand binding, they dimerize and translocate to the nucleus were they act as nuclear transcription factors. In addition, rapid corticosterone effects are mediated via non-genomic mechanisms: MRs and GRs bound to the membrane can interact with G protein coupled receptors and intracellular signaling cascades, thereby modulating cell excitability within minutes after a stressor, e.g. via voltage-gated calcium channels (Kolber et al., 2008; Maggio & Segal, 2012).

In a large body of studies it became evident, that effects of corticosterone depend on the stage of fear memory. Posttraining administration of corticosterone consistently enhanced fear memory to cues and context via the concerted action with norepinephrine in the BLA described above (McGaugh, 2004). When corticosterone is applied before training only memory for emotional relevant stimuli is enhanced,

although high doses of corticosterone or intensive stressors rather impair memory (Schwabe et al., 2012). For hippocampal long-term potentiation (LTP), such an U-shaped relationship is reported as well, with high corticosterone doses reducing CA1-LTP while low to moderate doses enhancing it (Maggio & Segal, 2012). Interestingly, within the hippocampal formation there exists regional diversity for this relationship: While LTP is reduced in the dorsal hippocampus after stress or physiological concentrations of corticosterone, it is enhanced in the ventral hippocampus via a possibly non-genomic MR-mediated mechanism (Maggio & Segal, 2012), thus enhancing the excitability of the hippocampal part most relevant for emotional memory formation and anxiety.

In contrast to its memory promoting functions during the consolidation phase, corticosterone administration reduces the performance when memory is retrieved (Schwabe et al., 2012). In addition, corticosterone is able to alter an already established memory trace during retrieval, a process called reconsolidation (Cai et al., 2006; see also section 1.3.2). Together, this opens a therapeutic tool for reducing symptoms in patients with posttraumatic stress disorder, where consolidation of traumatic memories is already completed, but are still open to modulatory functions of corticosterone by reconsolidation processes (de Quervain, 2008).

1.2.8 Fear conditioning in modeling anxiety disorders: clinical implications

As stated in the beginning, anxiety and fear learning are fundamental tools for survival, allowing adaptation to stressful situations and avoidance of threats. Anxiety disorders develop when fear and anxiety is experienced excessively and in response to inappropriate stimuli beyond a sensible adaptive response. Anxiety disorders are the most often diagnosed type of mental illness with a life-time prevalence of nearly 30% (Garakani et al., 2006). Clinicians divide anxiety disorders in different categories with in part overlapping symptoms and high co-morbidity among each other (Tab. 1-4).

In the recent years, fear conditioning proved as tool for understanding the neurobiological basis of the “fear-based” anxiety disorders, panic disorder, phobia and posttraumatic stress disorder (PTSD) respectively (Garakani et al., 2006). Panic disorder is characterized by sudden attacks of extreme anxiety, together with the fear of losing control or dying, autonomic arousal and somatic symptoms (e.g. nausea, chest pain, numbness chills or hot flashes), lasting for minutes. Fear of new attacks induces

behavioral changes and can be associated with agoraphobia, leading to further avoidance of situations where quick escapes are impossible (e.g. large crowds, airplanes). Likewise, a panic attack can result from a specific phobia, i.e. elicited by a certain object or situation, for example exposure to spiders (arachnophobia) or narrow places (claustrophobia). Social anxiety disorder is a special case of social phobia, where intense fear occurs upon exposure to unfamiliar situations and persons, resulting in avoidance of situations that require social interaction and performance (Garakani et al, 2006). Together, the maladaptation to a stressful situation/ event leads in these disorders to an inappropriate fear response, resulting in avoidance of the situation that can be viewed as conditioned behavior.

Tab. 1-4 Classification of anxiety disorders according to Diagnostic and Statistical Manual of Mental Disorders, Fourth Edition: DSM-IV-TR®, 2000

Anxiety disorders (DMS-IV)
300.02 Generalized anxiety disorder
300.01 Panic disorder without agorophobia
300.21 Panic disorder with agoraphobia
300.22 Agoraphobia without history of panic diorder
300.29 Specific phobia
300.23 Social phobia (social anxiety disorder)
300.30 Obsessive-compulsive disorder
309.81 Posttraumatic stress disorder (PTSD)
308.30 Acute stress disorder
300.00 Anxiety disorder not otherwise specified

Such avoidance is also a core symptom of PTSD. This disorder is characterized as a maladaptive response to extreme stress. Such traumatic, life-threatening events comprise natural disasters, accidents, rape, assault or combat and it is assumed that 75% of the western population, e.g. in the USA, experience at least one of those events in their life time. Acute responses including hyperarousal and intrusive memories are observed frequently in the aftermath of a trauma, but decline within the first three months. However, a subset of trauma survivors will develop persistent symptoms that

indicate a failure for trauma recovery (< 10%; Breslau, 2009). These symptom clusters comprise re-experience of the traumatic event as intrusive memories and nightmares and avoidance of trauma reminders that lead to a generalized emotional and social withdrawal. PTSD patients display also lasting hyperarousal, characterized by insomnia, irritability, impaired concentration, hypervigiliance and increased startle response (Yehuda & LeDoux, 2007). Several risk factors have been identified that determine whether or not an individual will develop PTSD, e.g. the severity of the initial trauma, personality trait, social support or a history of childhood adversity (Yehuda & LeDoux, 2007). In addition, family and twin studies provided evidence for genetic risk factors, e.g. in genes affecting dopaminergic and serotonergic signaling (Sherin &Nemeroff, 2011).

A number of anatomical, neurochemical and neuroendocrine alterations are observed in patients with PTSD that can be related directly to the symptoms observed. Hypocortisolism and increased levels of corticotropin releasing hormone (CRH) indicate a dysregulation of the HPA axis. Together with increased levels in catecholamines, especially norepinephrine, this mediates increased arousal and autonomic activation. Moreover, activity of the GABAergic system and plasma concentrations of the anxiolytic neuropeptide NPY are reduced in PTSD patients (Sherin & Nemeroff, 2011), which favor a prolonged and increased stress response further. Alterations in inhibitory/ excitatory balance also influence appropriate determination of stimulus salience. While a hyperactivity of the amygdala is observed in PTSD patients, the activity and the volume of the hippocampus is reduced (Yehuda & LeDoux, 2007; Sherin &Nemeroff, 2011). Such a shift in the balance of amygdalo-hippocampal interaction can explain fear generalization to unrelated stimuli and the retrieval of episodic-like intrusive memories upon cues with a distant relation to the initial trauma (e.g. a loud noise bringing back the memory of combat situation in veterans with PTSD).

Therefore, insights in molecular events in amygdala and also hippocampus leading to formation of fear memory can provide new entry points for the treatment of PTSD (Mahan & Ressler, 2012). To date selective serotonine reuptake inhibitors (SSRIs) or behavioral therapy strategies (McNally, 2012) have been implicated in the therapy of PTSD alone or as combination of both (Hetrick et al., 2010). Nevertheless, PTSD appears difficult to treat and therefore new therapeutical strategies are required. Promising results were obtained in the treatment of traumatic memories in first studies using the modulatory functions of cortisol on fear memory retrieval (de Quervain, 2008).

Although fear conditioning can provide the basis for animal models of PTSD, it is clear that an emotional memory formed here is not necessarily a traumatic memory. Animal models have to face several validation criteria (see Siegmund & Wotjak, 2006), and several paradigms have been developed to induce PTSD-like symptoms in rats and mice (Stam, 2007). For example, some models engage reminders of the traumatic experience (Olson et al., 2011). Others classify their experimental animals into responsive or resilient towards traumatic stress (Cohen et al., 2012), allowing also for determination of resilience factors. The juvenile stress model of PTSD is based on the observation that childhood adversity increases the risk for developing PTSD upon later traumatic events (Tsoory & Richter-Levin, 2006).

Despite from modeling PTSD, procedures like juvenile stress and fear memory reactivation are powerful modulators of emotional fear memory formation in general and provide paradigms for studying shifts in amygdalo-hippocampal interaction. These aspects are described in the next chapter.

1.3 Balancing the fear: Rodent models for (mal-) adaptive fear memory formation

As stated above, PTSD is characterized by altered amygdalo-hippocampal interaction, favoring amygdala activation. Therefore, animal models of PTSD can be also used study shifts in the balance between amygdala and hippocampus.

1.3.1 Juvenile stress: A model for PTSD

Epidemiological data provide strong evidence for increased susceptibility to PTSD in individuals that experienced childhood adversity (Yehuda & LeDoux, 2007). From a neurobiological perspective, this suggests a two-step process in the pathogenesis of PTSD. A severe stress experience in young years might alter the brain systems involved in stress response. When a second hit occurs in adulthood, the altered system cannot respond appropriately, leading to the maladaptive responses described in PTSD. Gal Richter-Levin and co-workers translated this second hit process in an animal model that consists of combined stress experiences in juvenile stress and in adulthood.

In brief, rats are exposed to psychological stressors that are characterized as variable, intensive and uncontrollable (juvenile stress: JS). At their postnatal day 28 (P28), the young rats first undergo forced swimming for 15 min. On the next day, they receive three sessions of elevated platform stress (30 min each, 1 h intervals). Finally, at P30, the rats are restraint for 2 h. Later in their young adult life, at P60, the rats again experience stress (adult stress: AS). This can be a reminder of the stressor used in juvenility, e.g. forced swimming, or a stressful paradigm that allows for a behavioral read out in parallel. Here, during active avoidance learning in a shuttle box or fear conditioning, additional information about the impact of JS on emotional learning is gained.

Stress during juvenility increased anxiety-like behavior and startle response in adult rats, reminiscent of PTSD, along with reduced spatial learning in the Morris water maze (Avital et al., 2005). Importantly, enhanced anxiety-like behavior is not observed in young animals tested directly after JS, which display a hyperactive phenotype instead. Moreover, pre-test application of corticosterone further increased anxiety in adult rats and hyperactivity in juvenile rats (Jacobson-Pick & Richter-Levin, 2010). Moreover, JS remarkably decreased avoidance learning in a shuttle box. While animals that received

their first stressful experience in the shuttle box learned the task well, JS induced a shift from active learning to learned helplessness with animals showing no shuttling at all (Tsoory & Richter-Levin, 2006). Together, these results indicate altered responsiveness to stress and stress hormones induced by JS that has to develop over time, affecting the function of amygdala and hippocampus.

Single stressors either in juvenility or adulthood evoke a short-term increase on long-term potentiation in the ventral hippocampus, while it decreases in the dorsal hippocampus. Long-term depression is also altered, displaying an increase in the dorsal hippocampus, but a conversion to a slow-onset LTP in the ventral hippocampus. But when JS and AS are combined, such acute response to stress are transformed in long-lasting alteration of hippocampal excitability (Maggio & Segal, 2011). Since increased ventral hippocampal activity is assumed to depend on enhanced amygdala input, these findings further support the hypothesis of altered amygdalo-hippocampal interaction induced by juvenile stress. Indeed, JS stress induced also long-lasting alterations in GABA A receptor subunit expression in both brain areas (Jackobson-Pick et al., 2008), suggesting a contribution of the GABAergic system to the observed changes.

The juvenile stress model adapted for mice in our lab further underlined the modulation of amygdalo-hippocampal interaction by juvenile stress. Using auditory cued fear conditioning as adult stress, an enhanced contextual fear response was observed in only mice that had a history of JS (Iris Müller et al., unpublished observations).

Together the juvenile stress model allows for insights in altered emotional response to stressors and fear memory generalization phenomena that are related to PTSD on the one hand. On the other hand, understanding the neurochemical changes elicited by juvenile stress would provide further insights in mechanism of amygdalo-hippocampal interaction.

1.3.2 Fear memory reactivation

While juvenile stress provides one possibility to modulate neuroendocine and neurochemical systems in a way that presumably favors amygdala activation and therefore might increase amygdala input during initial formation of the fear memory trace, reactivation allows for modulation of already stored fear memory.

In Remarkably, during memory retrievala once consolidated fear memory is not only recalled, but becomes labile and can be modulation (Alberini, 2011; Rodrigues-Ortiz and Bermudez-Rattoni, 2007). This process, named reconsolidation, is dependent on *de novo* protein synthesis, as it is observed after reactivation of cued fear memories in the BLA (Nader et al., 2000). Moreover, although the hippocampus may not be the place for final storage of remote contextual fear memories, it is required their reconsolidation again in inducing transcription of target genes (Debiec et al., 2002; Myers & Davis, 2002).

The specific molecular events involved in consolidation and reconsolidation processes are not completely identical (Tronson & Taylor, 2006). For example, while ERK2 is required for both processes (Cestari et al., 2006), BDNF and the immediate early gene zif268 are thought to be uniquely recruited during consolidation or reconsolidation respectively (Lee et al., 2004). Other studies of IEG activation during consolidation vs. reconsolidation revealed that reconsolidation involves only a subset of molecules being regulated during consolidation (von Hertzen & Giese, 2005). CREB appears to be involved in reconsolidation as well (Mamiya et al., 2009): Disruption of CREB signaling reduced reactivated fear memory and reactivation of contextual fear memory CREB in amygdala subnuclei and in the CA1 and CA3 areas of the hippocampus.

Notably, prolonged or also repetitive re-exposure to the conditioned stimulus (CS) in absence of a threatening stimulus (US) will lead to a diminished fear response. During this process, called extinction, the individual learns that the CS is not longer associated with the US. Thereby, the original fear memory is not erased but rather inhibited by newly acquired, updated memory concerning the CS (Quirk et al., 2010). Extinction requires therefore also induction of transcription factors and subsequent protein synthesis. Among them, also CREB is activated, but in other brain areas than in reconsolidation: In extinction of contextual fear memory the prefrontal cortex (PFC) appears crucially involved while activation of hippocampal subareas is not observed (Mamiya et al., 2009).

In addition, the in part different molecular processed observed after consolidation and reconsolidation, might be induced by neurotransmitter systems that are also required for consolidation. In this line, blockade of noradrenergic transmission in the amygdala after reactivation reduced the fear memory, thus indicating disrupted reconsolidation (Debiec & LeDoux, 2006). In contrast, blocking of muscarinergic signaling in the amygdala affected only consolidation, but not reconsolidation processes, while the endocannabinoid system appeared to be involved in both processes (Bucherelli et al.,

2006). Next to neuromodulator signaling the GABAergic as well as the glutamatergic system is required for fear memory reconsolidation. Here, stimulation of GABA A receptors after contextual fear memory reactivation decreased the freezing response (Bustos et al., 2006), while application of NMDA receptor agonists enhanced freezing to the reactivated stimuli. Accordingly, blocking NMDA receptors during reconsolidation reduced freezing (Lee et al., 2006).

Corticosterone is not only able to modulate initial memory consolidation, but is also involved in reconsolidation processes. However, these show a state-dependency, since corticosterone application after fear memory reactivation reduced a subsequent fear response only after initially strong training. Moreover, blocking of GRs shortly after and corticosterone administration shortly before reactivation both reduced freezing as well in other studies (Cai et al., 2006; Jin et al., 2007).

Furthermore, reactivation is also used in modeling PTSD. Re-exposure to a stimulus initially associated to an intensive fear eliciting threats can thereby induce increased arousal and deficits in social interaction reminiscent of PTSD (Olson et al., 2011). In addition, reactivation of auditory cued fear memory also leads to increased freezing to the background context (Rehberg et al., 2011), indicating altered amygdalo-hippocampal balance that is also related to PTSD-like symptoms.

Although fear memory reactivation induced PTSD-relevant behavioral alterations, it provides a tool to modulate reconsolidation processes in a way that destabilizes the fear memory. Therefore, a better understanding of these processes will help to treat anxiety disorders in humans, e.g. by updating the reactivated memories with non-fearful information (Schiller et al., 2010).

1.4 Aim of the study

Emotional memory formation is an essential process allowing for adaptive responses and survival by prediction of threatening situations. Classical fear conditioning provides a tool for studying the formation of such fear memory. Here, the use of complex contextual stimuli as threat predictors is well balanced against more simple cues. To determine the salience of contextual information, amygdalo-hippocampal interaction is required that modulates the strength of the resulting contextual fear memory and disturbances in these processes are observed in anxiety disorders like posttraumatic stress disorder.

To date, molecular mechanisms contributing to the interaction of both structures are not well understood. However, the activity of amygdalar and hippocampal subareas is controlled by local inhibitory circuits. Therefore, I hypothesized that genes contributing to GABAergic signaling are prime molecular targets of amygdalo-hippocampal interaction.

Firstly, I aimed at the identification of inhibitory interneurons subpopulations that are activated during formation of fear memory with differential involvement of amygdala and hippocampus. To this end, I isolated subareas of the amygdala and hippocampus six hours after cued versus contextual fear conditioning via laser capture microdissection and analysed conditioning-induced expression changes of neuropeptide markers genes using quantitative real-time PCR. This initial screening revealed a putative function of NPY in determination of contextual salience via its action in the hippocampal dentate gyrus region. I confirmed a specific transcriptional activation of NPY-positive interneurons after cued versus contextual fear conditioning by immunhistochemical analysis od phosphorylted CREB. I hypothesized that the activation of NPY-positive interneurons in the hilus contributes to amygdalo-hippocampal interaction during fear memory formation and determines the behavioral response to the background context. To test this, I aimed to prevent the transcriptional activation of hilar NPY-positive interneurons via conditional virus-mediated expression of dominant-negative CREB. In the next step, I investigated the contribution of NPY signaling itself to these processes. For that, I locally applied pharmacological antagonists of NPY Y1 receptors, to the dentate gyrus before paired and unpaired auditory fear conditioning and used again the fear response to the background context as a behavioral read-out for hippocampal involvement.

As a second important result of the initial screening, somatostatin expression in the lateral amygdala appeared potentially involved in the determination of emotional salience. I began to test this hypothesis by investigating the effect of somatostatin expression differences on anxiety-like behavior and fear memory formation by taking advantage of circadian expression differences on the one hand and engaging mice deficient for somatostatin on the other hand.

In the second study, I aimed to identify molecular factors in the hippocampal CA1 regions that influence fear memory formation. To this end, I took advantage of the juvenile stress model of PTSD. Juvenile stress experiences alter the excitability of the ventral and dorsal CA1 region, thereby pre-defining hippocampal information processing in subsequent fear conditioning. In order to find molecular correlates of such lasting alterations, I screened for expression changes of target genes involved in GABAergic and glutamatergic signaling in laser capture microdissected sublayers of the CA1 after juvenile, adult stress or the combination of both.

Generalization towards the background context has been also described after fear memory reactivation via modulation of an already established fear memory trace. In the third study, to gain insights into the molecular mechanisms of fear memory reactivation, I firstly analyzed long-term consequences of reactivation compared to fear memory formation on the behavioral and endocrine level. Secondly, I began to investigate molecular changes in the CA3 region of the ventral hippocampus and thirdly I analyzed the relevance of the observed changes for the function of the ventral hippocampus on a behavioral level.

All three studies aimed at the identification of GABA-related molecular targets expressed in the hippocampus that can contribute to the generalization of background contextual fear memory.

2. Material & Methods

2.1 Animals

All mice used in these studies were housed in the animal facility of the Institute of Biology, Otto-von-Guericke University Magdeburg under standard laboratory conditions. The animals were kept in groups of two to six individuals in Macrolon cages (36.2 cm x 16 cm x 14.3 cm; Ebeco, Castrop-Rauxel, Germany) with standard bedding (Lignocel BK8/15, J. Rettenmaier & Söhne, Rosenberg, Germany) in an inverse 12 h light/ 12 h dark cycle (lights on automatically at 7:00 PM with a 30 min dawn phase). They had access to food, a standard pellet diet (Ssniff R/M-H V-1534, Ssniff Spezialdiäten, Soest, Germany), and water *ad libitum*. An air conditioning system kept room temperature constantly at 21°C and moisture at 50 % air.
5-7 d before experiments began, the mice were separated into single cages with the possibility of visual and acoustical contacting within each level of the rack. All experiments were conducted during the active phase of the animals, between 8:00 AM and 18:00 PM.

2.1.1 Animal welfare

Animal housing and experiments in these studies were conducted in accordance with the European and German regulations for animal experiments and approved by the Landesverwaltungsamt Saxony-Anhalt (AZ 2-441, 2-618, 2-887, 2-939).

2.1.2 Mouse lines used in the studies

2.1.2.1 C57BL/6 mice

C57BL/6 mice used in the different studies were either obtained at an age of seven weeks directly from Taconic (M&B Taconic, Berlin, Germany) or derived from breeding in the Institute of Biology, Otto-von-Guericke University Magdeburg. The breeding pairs were originally also obtained from Taconic. Their young pups were weaned at an age of four weeks and group housed until assignment for the different experiments. The

purchased C57BL/6 BomTac mice were allowed to habituate to the anima facility and the inverse light/ dark cycle for two weeks and were group-housed in this time. For experiments only male adult C57BL/6 mice were used (10-16 weeks of age).

2.1.2.2 SST deficient mice

SST deficient mice and their wildtype littermates descended from a mutant mouse line that carries a targeted disruption of the pre-prosomatostatin gene by inserting a neomycin-based selection cassette that deleted the last 30 bp of exons 1 and the first 39 bp of intron 1 ($SST^{-/-}$ mice; Zeyda et al., 2001). The SST mutant line was backcrossed to a C57BL/6 background for more than 12 generations. $SST^{-/-}$ mice and their wildtype littermates ($SST^{+/+}$) were obtained from heterozygous breeding pairs kept in the Institute of Biology, Otto-von-Guericke University Magdeburg. Young pups were weaned at an age of four weeks and raised in groups of 2-6 until assignment to the experiments. Genotypes were determined shortly after weaning by multiplex polymerase chain reaction on genomic DNA, as described previously (Kluge et al., 2008; see Appendix A1.1 for genotyping protocol). Only adult (> 10 weeks of age) male $SST^{-/-}$ and $SST^{+/+}$ mice were used in the experiments.

2.1.2.3 NPY-GFP mice

Heterozygous male NPY-GFP mice were obtained from the Jackson laboratories (Bar Harbor, Maine, USA; strain name: B6.FVB-Tg(Npy-hrGFP)1Lowl/J; stock number: 006417) and mated with C57BL/6 females in the animal facility of the Institute of Biology, Otto-von-Guericke University Magdeburg and breeding was continued by mating hemizygote mice with their wildtype littermates. The hemizygous mice express a humanized Renilla Green Fluorescent Protein (hrGFP) under the control of the mouse promotor for the neuropeptide Y (NPY) gene. The NPY-GFP transgene was produced by inserting the hrGFP sequence into the translational start site of the NPY gene with a bacterial artificial chromosome. Transgenic mice were backcrossed to a C57BL/6 background for more than eight generations (http://jaxmice.jax.org/strain/006417.html). All NPY-GFP mice used in experiments derived from the Institute's own breeding. Weaning and genotyping (see Appendix A1.2 for genotyping protocol) was done at an age of four weeks and animals were group-housed until assignment to experiments. Here, only adult (10-12 weeks of age) male mice carrying the NPY-GFP transgene were used. Since the GFP fluorescence pattern is

consistent with the expression of the NPY gene, the NPY-GFP mice were used for characterizing the NPY-positive interneurons in the hippocampus.

2.1.2.4 SST-CreERT2 mice

Heterozygous male SST-CreERT2 mice were obtained from the Jackson laboratories (Bar Harbor, Maine, USA; strain name: B6(Cg)-Ssttm1(cre/ERT2)Zjh/J; stock number: 010708 and mated with C57BL/6 females in the animal facility of the Institute of Biology, Otto-von-Guericke University Magdeburg and breeding was continued by mating heterozygous mice with their wildtype littermates. The heterozygous mice express a CreERT2 fusion protein under the promotor/ enhancer elements of the neuropeptide somatostatin. The CreERT2 fusion protein is composed of a cre recombinase fused to a triple mutated ligand binding domain of the human estrogen receptor. Estradiol as its natural ligand will therefore not bind at physiological concentrations, but the synthetic partial agonist tamoxifen. Only upon tamoxifen binding the CreERT2 fusion protein can translocate to the nucleus of the cell and the cre recombinase can be active whenever it is expressed under the SST promotor. Thereby, the tamoxifen-inducible Cre recombinase activity occurs specifically in SST-positive interneurons, although first reports describe a low induction efficiency (Taniguchi et al., 2011). In addition, induction of the SST-CreERT2 knock in homozygous animals would result in a knock out of SST (http://jaxmice.jax.org/strain/010708.html). All SST-CreERT2 mice used in experiments derived from the Institute's own breeding. Weaning and genotyping (see Appendix A1.3 for genotyping protocol) was done at an age of four weeks and animals were group-housed until assignment to experiments. Only the adult male mice carrying the SST-CreERT2 transgene heterozygously were used for inducible expression of lentiviral vectors in SST- and NPY-positive interneurons of the hilus.

2.1.3 Wistar rats

Gene expression in the ventral and dorsal hippocampus after juvenile and adult stress was assessed in male Wistar rats in cooperation with Professor Menahem Segal from the Department of Neurobiology of the Weizmann Institute, in Rehovot, Israel. Applying of stress protocols and brain preparations were conducted in Menahem Segals lab, while gene expression analysis was done by me in the Institute of Biology, Otto-von-Guericke

University Magdeburg. Therefore, Wistar rats were bred and kept at the animal facility of the Weizmann Institute under standard laboratory conditions.

2.2 Behavioral Analysis

Pavlovian fear conditioning is a well-established tool for studying processes of emotional memory formation. Here, in different studies the contribution of neuropeptides to fear memory formation, the involvement of different hippocampal regions as well as processes of fear memory reactivation were assessed.

2.2.1 Fear Conditioning

A standard protocol was engaged for fear conditioning training towards a specific cue, a tone, which is known to induce robust fear memory for the conditioned tone (CS+) and also to the environment in which the conditioning took place, the context (Laxmi et al., 2003; Albrecht et al., 2010).

All training and test sessions took place in a sound isolation cubicle containing a 16 cm x 32 cm x 20 cm acrylic glass arena with a grid floor, loudspeaker and ventilation fan (background noise 70 dB SPL, light intensity <10 lux ; TSE, Bad Homburg, Germany).

Prior to fear conditioning, all animals received four (twice per day, i.e. morning and afternoon) adaptation sessions. These sessions varied between experiments dependent on requirements of the single studies. Either, only adaptation to the conditioning context was performed (4 x 5 min context only sessions) or a neutral tone (CS-) was played during adaptation (2 min context, followed by 6 x 10 s CS- with 2.5 kHz, 85 dB and 20 s inter-stimulus-interval (ISI) each). On the consecutive day, fear conditioning training with the standard protocol took place: After 2 min exposure to the training context, animals received three footshocks (US: 0.4 mA for 1 s), each paired with a tone (CS+: 10 kHz for 10 s, 80 dB) and separated by 20 s ISI.

In studies were expression changes or activation of transcription factors after fear conditioning gene were assessed, animals were sacrificed at specific time points after training and tissue sample preparation took place.

In other studies, fear memory was assessed by re-exposure to the conditioned stimulus and the training context in a retrieval session at a specific time point after training.

Here, retrieval of the CS+ was done either in a neutral context (standard cage with bedding) or in the conditioned context. After 2 min context exposure, first the neutral CS- was presented (4x 10 s CS- with 2.5 kHz, 85 dB, 20 s ISI) to test for intramodal generalization of the fear memory, followed by re-presentations of the CS+ (4x 10 s CS+ with 10 kHz, 85 dB, 20 s ISI). Testing of contextual fear memory was conducted by re-exposure of the mice to the conditioning chamber for 2 min.
Finally, in a series of experiments long-term effects of such re-exposure to the context and the CS+ on the fear memory were investigated.

2.2.1.1 Cued versus contextual fear conditioning

Next to auditory cued fear conditioning to a specific tone, the CS+, conditioning to the context itself without additional tone presentation is possible. In one study, the effects of cued and contextual fear conditioning on the mRNA expression of different neuropeptides were assessed. Here, male adult C57BL/6 mice were randomly assigned to three training groups (naïve control, cued, contextual). Cued conditioning and naïve control groups were adapted to the fear conditioning apparatus during the first two experimental days in two daily sessions of 5 min each. The contextual training group was in the same manner exposed to a novel standard cage serving as neutral context. In the conditioning session, animals of the cued conditioning group received three CS (10 kHz tone, 85 dB SPL, for 10 s) / US (0.4 mA foot shock, for 1 s) pairings after two minutes habituation in the training context. The context group was exposed to three US (0.4 mA, 1 s), but no CS during training, whereas the naïve control group received three CS, but no US. Activity and defensive behavior were recorded during the entire training to individually confirm successful conditioning. Two minutes after the last US presentation animals were returned to their home cage.
For the analyses of expression changes in the mRNA of the neuropeptides Y (NPY), somatostatin (SST) and cholecystokinin (CCK) all mice were sacrificed six hours later, their brains taken out and snap frozen.
In a second study, the induction of transciption factors after cued versus contextual fear conditioning was investigated via immunhistochemistry. Therefore, animals were perfused with paraformaldehyde for tissue fixation at different time points after training: 10 min, 1 h, 3 h, 5 h, 9 h, 12 h and 24 h in pre-experiments as well as 1 h after training for quantification of CREB S-133 phosphorylation in NPY-positive interneurons of the Hilus.

2.2.1.2 Pharmacological intervention on fear conditioning

To interfere with activation of NPY-positive interneurons in the hilus of the dorsal dentate gyrus upon fear memory acquisition and consolidation, a blocker of the NPY receptor type 1, BIBP 3226, was applied directly to the dentate gyrus of male adult C57BL/6 mice, shortly before fear conditioning training or retrieval, as well as shortly before unpaired fear conditioning.

2.2.1.2.1 Canula implantation into dentate gyrus

To allow time-specific, local drug application with a minimum of disturbance of the mice *in vivo*, stable canulas were implanted bilaterally into the dentate gyrus of the dorsal hippocampus five to seven days before drug application took place.

After deep anaesthesia with Pentobarbital (50 mg/kg body weight intraperitoneally injected; Sigma-Aldrich, Seelze, Germany), the mouse head was fixed into a small animal stereotactic frame (World Precision Instruments, Berlin, Germany) and the scalp removed. After cleaning the skull with 0.2 % H_2O_2 and 0.9 % Saline, Bregma was identified and coordinates calculated (AP: -1.94; ML: ± 1.0 mm from Bregma) according to the mouse brain altas (Paxinos & Franklin, 2001). After drilling holes into the scull, a bilateral canula was lowered into the drill holes (DV: -1.4 mm from brain surface), consisting of two stainless steel canulas (length 3 mm; 26G; Plastics One, Roanoke, Va, USA), installed in a single plastic socket (5 mm length, 2 mm space between canulas). After applying a juweler's screw to the skull in a third drill hole, located right lateral to the canulas, the socket was fixed with dental cement (Hoffmann dental Manufaktur GmbH, Berlin, Germany) and covered with Paladur resin (Heraeus Kulzer GmbH, Wehrheim, Germany). The guide canula was closed with a dummy and the animals were allowed to recover for five to seven days before fear conditioning training or retrieval took place and the drug was administered.

2.2.1.2.2 Preparation of drugs

A 15 nmol/ µl stock solution of the NPY type Y1 receptor blocker BIBP 3226 (Tocris, Ellisville, Missouri, USA) was prepared in 0.9 % Saline and 1 % DMSO solution. Working solutions of 15 pmol/ µl and 1.5 pmol/ µl were prepared in 0.9 % saline and 1 % DMSO. As a control, only 0.9 % saline with 1 % DMSO was prepared. Stock solution was not

kept longer than one month at -20°C. All solutions were stored at -20°C and 4°C at the day of use.

2.2.1.2.3 Drug application

For application of BIBP 3226, mice received a brief inhalation anaesthesia with Isoflurane. The bilateral injection canulas (3.5 mm length; 33G; in a single socket; Plastic one/ Belani) was connected to a tubing system for bilateral canulas and connected to 10 µl glass syringes (Hamilton Bonaduz AG, Bonaduz, Switzerland). Injection canulas were preloaed with either 0.9 % saline/ 1 % DMSO or BIBP solution in two concentrations (15 and 1.5 pmol/ µl) and then plugged into the guide canula and fixed by a cap installed at the tubing system. The mouse was placed in a small cage without bedding and was allowed to awake out of the brief inhalation narcosis. 1 µl of the drug solution was then applied slowly via the tubing system at a rate of approximately 1 µl/ min. The internal canula was left plugged in for another five minutes. Then the animal was restraint briefly in the experimenters hands, the internal canula was removed and the guide canula closed with a dummy. Animals were placed back in there home cage until training or retrieval session, respectively, started.

2.2.1.2.4 Behavioral paradigms

All animals received four adaptation sessions on two days consisting of five minutes habituation to the conditioning context each. On the third day, all animals received standard cued fear conditioning (3x 9 s 10 kHz tone CS+/ 1 s 0.4 mA footshock US/ 20 s ISI). Fear memory testing started 24 h later.

In the first experiment, animals received either 1 µl saline, BIBP 1.5 pmol or BIBP 15 pmol 45 min before the training session. 24 h later contextual fear memory was tested by placing the animal back into the fear conditioning chamber. At 48 h after training, cued retrieval took place by re-exposing the animal to four neutral tones (CS-; 10 s 2.5 kHz, 85 dB, 20 s ISI), followed by four of the conditioned tones (CS+; 10 s 10 kHz, 85 dB, 20 s ISI), in a neutral context (clean standard cage with bedding).

In a second experiment, the effective dose of experiment one, 1.5 pmol BIBP 3226 in 1 µl vs. saline was administered 45 min before the contextual retrieval, i.e. 24 h after training. To determine effects of BIBP on cued retrieval, re-exposure the CS+ as well as a CS- was done immediately after contextual memory retrieval by just placing the mouse into a second fear conditioning apparatus containing the neutral context.

In a third experiment, the effective dose of experiment one, 1.5 pmol BIBP 3226 in 1 µl vs. saline was administered 45 min before unpaired fear conditioning. Here, the mice received footshocks and tones that were presented independently from each other. After 2 min in the conditioning chamber, three US (1 s, 0.4 mA; 29 s ISI) were presented, followed by another 2 min in the chamber until three tones were presented (CS_{up}: 10 s, 10 kHz, 85 dB each; 20 s ISI). The animals remained in the apparatus for another 2 min until they were brought back to their home cage. Fear memory to the context and to the CS+ as well as CS- was tested 24 h and 48 h later, respectively, as described above. Because of the unpaired presentation of US and tone, the animals received the same stimuli like in cued fear conditioning but built up a foreground contextual fear memory (Laxmi et al., 2003).

2.2.1.2.5 Validation of canula placement

To evaluate correct canula placement all animals received injection of 1 µl methylene blue (10 mg/ml in 0.9 % Saline/ 1 % DMSO) at a rate of 1 µl/ min as described above. 15 minutes after injection started, animals were sacrificed by cervical dislocation and brains removed from the skull. The brains were snap frozen in methylbutane cooled by liquid nitrogen.

Using a cryostat, 30 µm coronar sections of the dorsal hippocampus region were mounted on superfrost glass slides (Carl Roth, Karlsruhe, Germany). The first series of slices was mounted on native, pre-warmed super frost slides while a second series was mounted directly on pre-warmed super frost slides covered with 0.05 % Poly-L-Lysine. Directly after mounting, all sections were dried on a warming plate at 40°C. After final drying for 20 min at 40°C, sections of series one were embedded with Entellan (Merck, Darmstadt, Germany) and mounted by a glass cover slip (Carl Roth, Karlsruhe, Germany). Those slides were allowed to dry over night.

Sections of series two underwent a short staining protocol with cresyl violet acetate solution. In detail, sections were fixed with 70 % ethanol at -20°C for one minute. Then slides were transferred to a 1 % cresyl violet acetae solution, prepared in 50 % ethanol for one minute. For dehydration of the slices, slides were transferred to a 70 % ethanol solution and then to a 96 % ethanol solution, for two minutes each. Slices were dried at room temperature and then embedded with Entelan and mounted by a cover slip. Again, slides dried over night at room temperature.

Distribution of methylene blue as well as the position of the scar made by the stable guide canula was assessed by transmitted light microscopy at a 4x magnification.
Only animals with proper canula location in the dorsal dentate gyrus according to the mouse brain atlas (Paxinos & Franklin, 2001) were included in the analysis (Fig. 2-1).

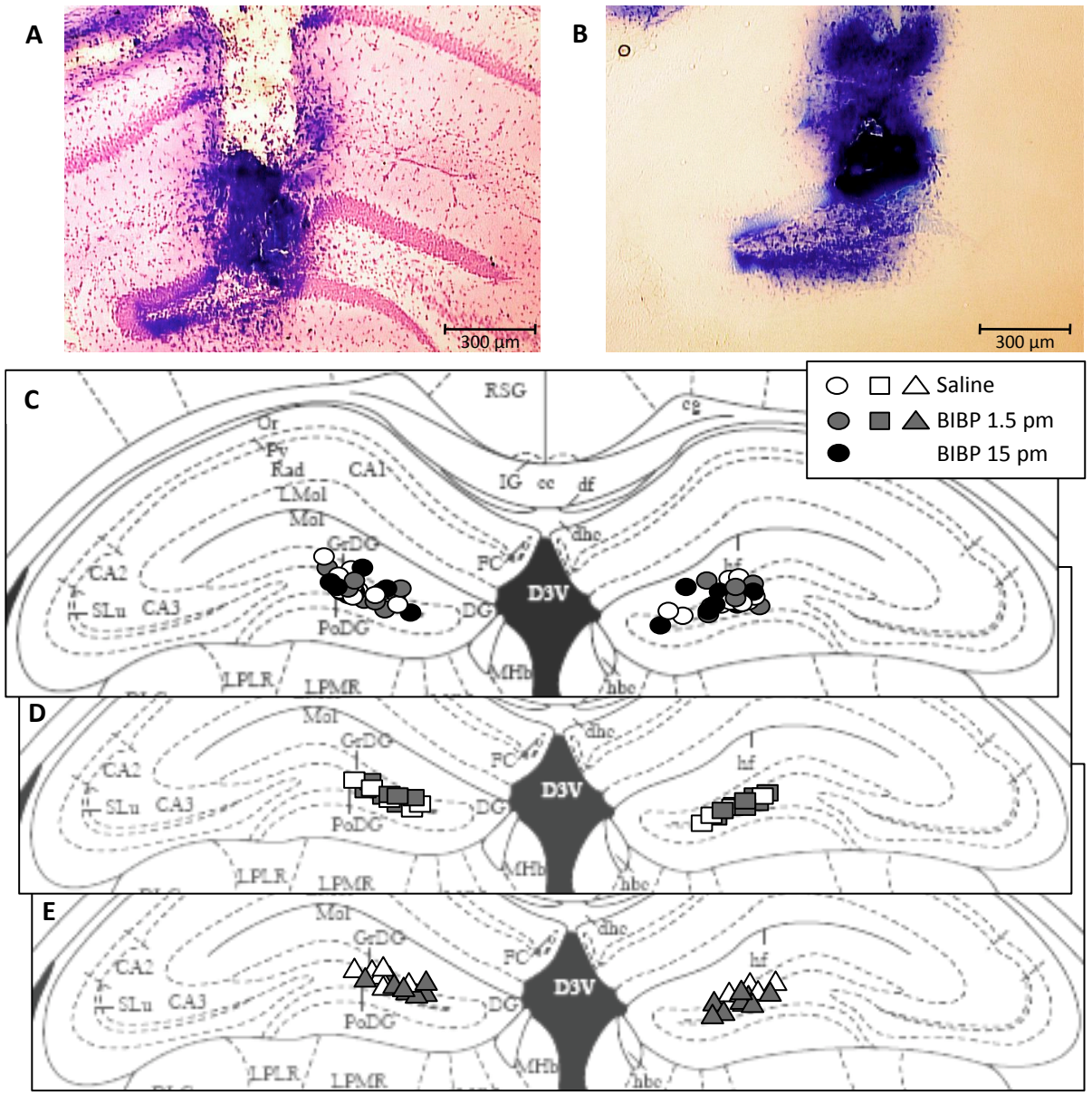

Fig. 2-1 Placement of bilateral stable canula in the dorsal dentate gyrus. Stable bilateral guide canulas were implanted in the dorsal dentate gyrus. To determine correct canula placement, 1 µl of methylene blue was injected in each side at the end of the experiment. The animals were sacrificed 15 min later and 30 µm sections were either stained with 1 % cresyl violet acetate solution (A) or remained native (B). Only animals with correct canula location were included in the analysis. Canula positions for those animals is depicted in C-E (C: Saline vs. BIBP 3226 1.5 pM vs. BIBP 15 pM 45 min pre-training; D: Saline vs. BIBP 3226 1.5 pM 45 min pre-retrieval; E: Saline vs. BIBP 3226 1.5 pM 45 min pre-training unpaired fear conditioning).

2.2.1.3 Viral knockdown of P-CREB in hilar interneurons before fear conditioning

To interfere with activation of P-CREB in NPY-positive interneurons of the hilus a conditional viral vector system was stereotactically delivered to the dorsal Hilus of a inducible cre recombinase transgenic mouse line. That allowed for specific expression of a dominant negative CREB isoform in hilar SST- and NPY-positive interneurons.

2.2.1.3.1 Viral vector system

2.2.1.3.1.1 CREB construct

The transcription factor CREB (cAMP-response element binding protein; Cre binding protein) is activated via phosphorylation at serine 133 by various kinases, e.g. PKA, PKC, and calmodulin kinases (CaMKs). P-CREB then binds to Cre elements in the promotor of different target genes, e.g. NPY (Pandey et al., 2005), and activates gene transcription (Silva et al., 1998).

In this study a mutant variant of human CREB protein was engaged that function as a dominant negative isoform and prevents CREB-mediated activation of gene transcription. The conditional viral vector for expression of a dominant negative isoform was prepared and provided by Dr. Bettina Müller in our lab. First, a CREB dominant-negative vector set was purchased from Clontech (Saint-Germain-en-Laye, France), containing three different vectors with different CREB coding sequences. Here, the pCMV-CREB133 Vector was used, that expresses a mutant variant of human CREB protein. Serine at position 133 is mutated to alanine, which prevents phosphorylation and thereby activation of CREB. CREB133 dimerizes and inactivate the endogenous wild-type CREB so that it can no longer function as transcription factor.

The CREB133 sequence was then cloned into a pCMV HA vector to obtain the sequence for HA CREB133 fusion protein. HA (hemagglutinine) then can serve as a tag to allow detection of the fusion protein, e.g. by immunhistochemical approaches. Finally, the HA CREB133 sequence was then cloned in a double-floxed vector, the pLL-dfRmFF which contains the sequence of mir30 and dsRed as a red fluorescent marker protein within two incompatible pairs of loxP sites. The mir30 and dsRed cassette was then removed and the HA CREB133 construct was induced in an inverted open reading frame position (see Fig. 2-2). This vector construct, pLL-dfHA CREB133, was then used as transfer plasmid for the production of lentiviral vectors. As a control vector, pLL-dfHA

was used, containing only the sequence for the HA tag protein, cloned in the double floxed system (exchange of mir30 and dsRed in the pLL-dfRmFF vector with HA).

Both constructs used in this study are called double floxed, because they contain two different loxP pairs that are incompatible. LoxP sites are specific 34 bp sequences where recombination of DNA sequences occurs, catalyzed by the bacteriophagic enzyme cre recombinase (Nagy, 2000). Depending on the placement of the loxP sites in the same or opposite orientation, the cre-recombinase can either mediate excision, translocation or inversion of the sequence that is flanked by the loxP sites (Nagy, 2000). In the constructs used here, the two different loxP sites both flank the target sequence in opposite reading directions, while the target sequence is orientated in an inverted open reading frame. Under presence of cre recombinase in the nucleus, inversion occurs of both loxP pairs, resulting in an irreversible inversion of the target sequence.

In this study these conditional, double floxed vectors are deliverd to cells via a lentiviral vector system, while the cre recombinase is provided by transgenic expression in the SST-CreERT2 mouse line.

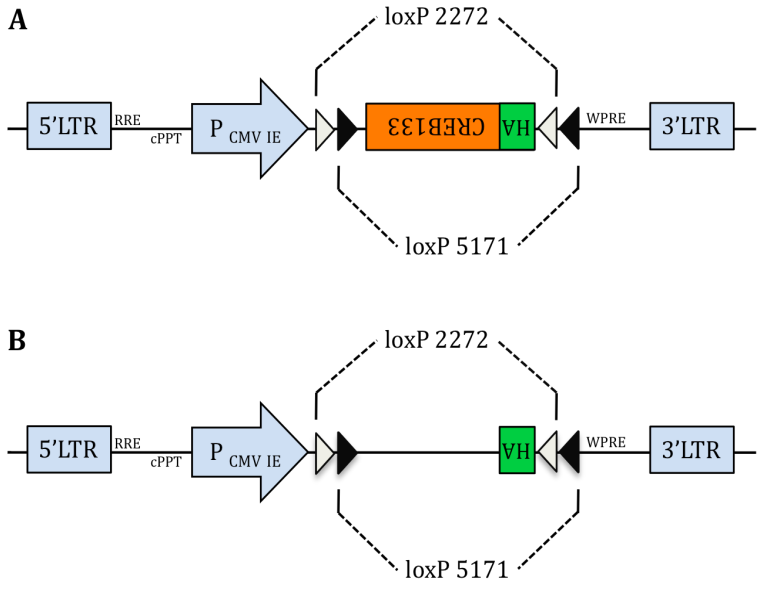

Fig. 2-2 Viral constructs used for expression of dominat negative CREB isoform. The constructs were delivered to the dorsal hilus of SST-CreERT2 transgenic mice via lentiviral vectors. After induction of nuclear cre recombinase activity by intraperitoneal injections of tamoxifen, irreversible inversion at both loxP pairs occured and the dominant negative CREB isoform is expressed together with hemagglutinine (HA) as tag protein under the strong cytomegalovirus (CMV) promotor (A). Some animals were transfected with the control vector (B) and expressed only HA in somatostatin-positive cells of the hilus.

2.2.1.3.1.2 Lentiviral vector system

The lentivirus belongs to the retroviridae family and is composed of RNA nucleotides packed in envelope proteins that mediate infection of the host cell while additional components are necessary for integration of the viral genetic information into the host genome. Lentiviral particles allow stable long-term expression of the target sequence

and transduce also non-dividing cells efficiently, because the virus shell can pass the nuclear membrane of the target cell. The nuclear translocation of the vector is further supported by the flap sequence. In order to produce lentiviral vector particles, the transfer vector has to contain self-inactivated long terminal repeats (SIN-LTRs) that allow for integration in the host genome and the Psi-sequence of the human immune deficiency virus (HIV), that serves as a signal sequence for packaging of the target RNA sequence into pseudovirus particles (http://openwetware.org/wiki/Griffin:Lentivirus_Technology).

As a control lentiviral vector, pLL-dfHA was used, containing only the sequence for the HA tag protein, cloned in the double floxed system (exchange of mir30 and dsRed in the pLL-dfRmFF vector with HA).

2.2.1.3.2 Acute stereotactical injection of viral vectors

To allow specific expression of the dominant negative CREB isoform and the control vector in SST/NPY (+) interneuron of the Hilus before fear conditioning, the conditional lentiviral vectors were delivered stereotactically to the Hilus of the dorsal hippocampus of SST-CreERT2 mice. Only adult male mice carrying heterozygously the CreERT2 transgene were used. These mice received a deep anaesthesia with Pentobarbital (50 mg/kg body weight intraperitoneally injected; Sigma-Aldrich, Seelze, Germany) and their head was fixed into a small animal stereotactic frame (World Precision Instruments, Berlin, Germany). After opening the scalp by an incision on the midline and cleaning of the skull with 0.2 % H_2O_2 and 0.9 % Saline, Bregma was identified and coordinates calculated (AP: -1.94; ML: ± 1.2 mm from Bregma) according to the mouse brain atlas (Paxinos & Franklin, 2001). After drilling holes into the scull, a stainless steel injection canula (33G; World Precision Instruments, Berlin, Germany) was lowered into the drill holes (DV: -1.8 mm from brain surface). The canula was mounted on a 10 µl NanoFil glass syringe (World Precision Instruments, Berlin, Germany) in which the virus solution was taken up. The syringe was fixed into a micropump (Ultra Micro Pump III; World Precision Instruments, Berlin, Germany) that was mounted directly to the stereotactic frame and connected to a control device. This allows for slow and exact application of small volumes. 1 µl of either the viral vector for the dominant negative CREB isoform, pLL-dfHA CREB133, or the empty control vector pLL-dfHA was injected at a rate of 0.1 µl/ min. After injection, the canula was left in place for another 10 min to prevent withdrawal of the virus solution in the injection channel. Then, the injection

canula was slowly retracted from the tissue. The canula and the syringe were then rinsed with sterile double-destilled water, fresh virus solution was taken up and the same viral vector was applied to the other hemisphere using the same approach.
After bilateral injection of the viral constructs, the skull was cleaned with sterile 0.9 % saline solution and the skin cut was closed with non-absorbable suture material (5-0/ PS-3, Perma-Hand silk, Ethicon GmbH, Norderstedt, Germany).
The animals were single housed after the surgery and allowed to recover for seven days before induction of the viral vectors with tamoxifen injections began.

2.2.1.3.3 Tamoxifen induction of cre recombinase action

The conditional lentiviral vectors for expression of the CREB dominant negative isoform as well as the control vector were delivered to the hilus of SST-CreERT2 mice. They express a CreERT2 fusion protein under the promotor/ enhancer elements of the neuropeptide somatostatin (Jackson laboratory, strain name: B6(Cg)-Ssttm1(cre/ERT2)Zjh/J; Taniguchi et al., 2011). The CreERT2 fusion protein is composed of a cre recombinase fused to a triple mutated ligand binding domain of the human estrogen receptor. Estradiol as its natural ligand will therefore not bind at physiological concentrations, but the synthetic partial agonist tamoxifen. Only upon tamoxifen binding, the CreERT2 fusion protein can translocate to the nucleus of the cell and the cre recombinase can be active and the dominant negative CREB isoform or the HA-tag as a control can be expressed.
In pre-experiments, expression of HA was determined by indirect immunflorescence staining virally transfected brain cells of SST-CreERT2 transgenic mice. Thereby tamoxifen injection protocol was developed that resulted in a sufficient expression of HA in hilar SST- and NPY-positive interneurons.
One week after surgery, mice received a daily injection of 2 mg tamoxifen (Sigma-Aldrich, Seelze, Germany) in 100 µl vehicle solution intraperitoneally, followed by 4 mg and 8 mg, respectively, on the two consecutive days.
Since Tamoxifen is not water soluble, the appropriate amount Tamoxifen was weight in and pre-solved 100 % ethanol. Then the final volume of the vehicle solution was adjusted with sterile sunflower oil (Kaufland, Neckarsulm, Germany; final concentration of ethanol: 10 %), resulting in 2 mg, 4 mg or 8 mg of tamoxifen in 100 µl vehicle solution. The different solutions were then sonicated for 2x 15 min, afterwards aliquoted and stored at -20°C until use.

Now, after administration of Tamoxifen, the cre recombinase-mediated expression of the HA CREB133 or HA sequence can take place in SST- and NPY-positive cells interneurons of the dorsal hilus.

2.2.1.3.4 Behavioral paradigm

The next two days after the last tamoxifen injection, all animals were handled two times daily for 2 min by the experimenter in the animal facility to avoid an association between experimenter and the injection pain.

On day 3 after the last injection, the auditory cued fear conditioning paradigm started. First, the mice received four adaptation sessions on two days (5 min habituation to the conditioning context). The following day, all animals were placed in the conditioning chamber for 2 min, then received standard cued fear conditioning (3x 9 s 10 kHz tone CS+/ 1 s 0.4 mA footshock US/ 20 s ISI) and remained in the conditioning apparatus for another 2 min. 24 h after training, fear memory to the background context was tested by placing the animal back into the fear conditioning chamber for 2 min. 48 h after training, retrieval of the cued fear memory was conducted by re-exposing the animal to four neutral tones (CS-; 10 s 2.5 kHz, 85 dB, 20 s ISI), followed by four of the conditioned tones (CS+; 10 s 10 kHz, 85 dB, 20 s ISI), in a neutral context (clean standard cage with bedding).

2.2.1.3.5 Analysis of virus expression

Within the next 24 h after the last retrieval session, all animals were perfused in order to assess correct local expression of the vectors. Both vectors, pLL-dfHA CREB133 and pLL-dfHA, contain the sequence for the HA-tag and will express HA in these cells, where the induction and recombination of the virally transmitted vectors are correct. The expression of HA in interneurons of the dorsal hilus was determined by indirect immunflourescence staining against the HA-tag in brain slices from all animals in the experiment. Only animals with expression of HA in the dorsal hilus according to the mouse brain atlas (Paxinos & Franklin) were included in the analysis of behavioral effects of dominant negative CREB expression on fear memory.

2.2.1.3.5.1 Special issues of sample preparation

After deep anesthesia Pentobarbital (50 mg/kg i.p.) a thoracal survey was prepared and the mouse was pre-perfused with 30 ml Tyrode buffer (+ 0.02 % Sodium Heparin Sulafte 25.000 I.E.), followed by perfusion with 100 ml 4 % paraformaldehyde (PFA) in phosphate-buffered saline (PBS) for fixation of tissue. The brains were removed from the skull, placed firstly in 4 % PFA in PBS for 3 h for postfixation and then in 30 % sucrose in PBS for the following 48 h for cryoprotection. Then, brains were snap frozen in methylbutane cooled by liquid nitrogen and stored at -20°C until 30 µm thick serial coronar sections of the dorsal hippocampus were prepared in a cryostate (chamber temperature -21°C, object temperature -19°C). Three adjoining sections per well were placed in a 24 well plate filled with 0.1 M PBS + 0.02 % sodium azid. The free-floating sections were stored at 4°C until indirect immunfluorescene staining against the HA-tag.

2.2.1.3.5.2 Immunhistochemical detection of HA-tag

From each animal 6 sections around the injections side (AP: - 2.46 mm to –1.06 mm from Bregma) were placed in a fresh 24-well plate (2 sections per well) and washed three times with 0.1 M PBS for 5 min each, gently tumbling. 500 µl of 5 % donkey normal serum, solved in 0.1 M PBS and 0.3 % Triton X (Sigma-Aldrich, Seelze, Germany), was applied to each well for 1 h at room temperature to block unspecific binding sites. Directly afterwards, the slices were incubated over night at 4°C with the first antibody against the HA-tag (Cell Signaling #3724, Frankfurt am Main, Germany; derived from rabbit) in a 1:300 dilution in 5 % donkey normal serum in 0.1 M PBS and 0.03 % Triton X (300 µl per well). Two slices remained in blocking solution and served as negative control for specific binding of the second antibody. On the next day, after three washing steps (0.1 M PBS for 5 min), the slices were incubated with the second antibody that detects immunoglobulin G heavy and light chains derived from rabbit (Alexa Fluor 488 donkey anti-rabbit; Life Technologies, Karlsruhe, Germany) in a 1:1000 dilution in 2 % bovine serum albumine (BSA; Carl Roth, Karlsruhe, Germany), solved in 0.1 M PBS and 0.03 % Triton X (300 µl per well, 1 h at room temperature). After removal of excess secondary antibody by washing the sections with 0.1 M PBS (3x 5 min each), the sections were mounted on a superfrost glass slide (Carl Roth, Karlsruhe, Germany), dried completely for 20 min at 40°C on a warming plate and then embedded in Entelan and cover slipped.

All sections were stored at 4°C until analysis of sections with an epifluorescence microscope.

Since the secondary antibody was coupled to the fluorochrome Alexa-Fluor 555 and is only adhering to epitops that bind to the HA-tag, the HA-tag can be visualized indirectly by detecting the fluorescence signal of Alexa Fluor 488 (absorption maximum at 495 nm/ emission maximum at 519 nm).

For all animals expression of HA was assessed qualitatively and only animals with positive cells in the dorsal hilus (Fig. 2-3) were included in the behavioral analysis.

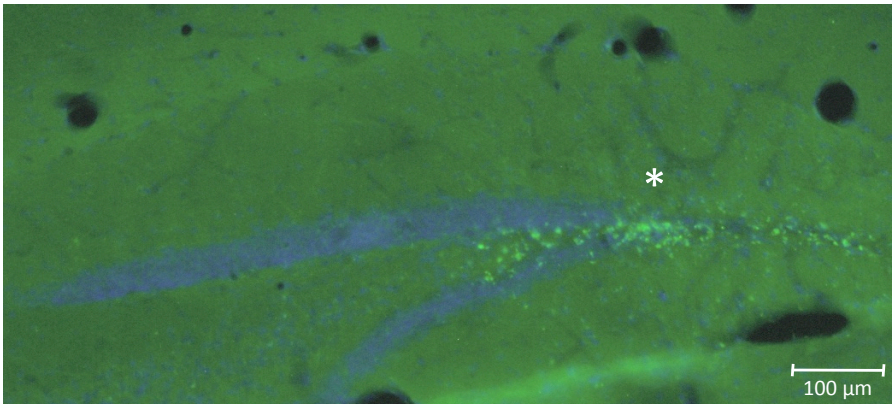

Fig. 2-3 Expression of viral constructs. Correct expression of the viral vector used for expression of the dominant negative isoform of CREB, HACREB133, and the control vector, HA, in the dorsal hilus were determined by indirect immunfluorescence staining using an antibody against the hemagglutinine (HA) tag. The HA-antibody is labelled by the secondary antibody Alexa 488 (green), indicating HA-expressing interneurons (*). The nuclear staining reagent DAPI (blue) was used to visualize cell bodies by nuclear labeling. Merged image, 10fold magnification of the dorsal hilus.

2.2.1.4 Circadian permutation in auditory cued fear conditioning

In one study circadian influences on fear memory formation were investigated, in $SST^{-/-}$ mice and their wildtype littermates respectively. The animals received first 4 adaptation sessions on 2 days, consisting of 2 min exposure to the conditioning context, followed by six exposures to a neutral tone (CS-: 2.5 kHz for 10 s, 85 dB; 20 s ISI). On the next day auditory cued fear conditioning training with the standard protocol took place, starting either at T1, 1 h after lights off (8:00 – 9:30 am) or at T7, 7 h after light off (14:00 – 15:30 pm). $SST^{-/-}$ and $SST^{+/+}$ mice were randomly assigned to those two groups. After 2 min exposure to the training context, animals received three footshocks (US: 0.4 mA for 1 s), each paired with a tone (CS+: 10 kHz for 10 s, 80 dB) and separated by 20 s ISI. Two days later fear memory to the auditory cued tone and the training context was

tested separately in two retrieval session for all animals at T1, starting 1 h after lights off. Retrieval of the auditory cue mice took place in a neutral context by re-exposed to four CS- (10 s each, 20 s ISI) and four CS+ (10 s each, 20 s ISI). One hour after the cue retrieval, the test animal was re-exposed to the training context for 2 min.

2.2.1.5 Reactivation of auditory cued fear conditioning

In one study the long-term effects of fear memory reactivation were studied. Male adult C57BL/6 mice received standard auditory cued fear conditioning (2 min exposure to the training context, followed by 3 tone- footshock- pairings (9 s CS+, 10 kHz, 80 dB; then 1 s US; 0.4 mA; 20 s ISI), followed by another 2 min in the conditioning chamber). Prior to the training session, all animals had received four (twice per day) adaptation sessions consisting of 2 min exposure to the conditioning context, followed by six exposures to a neutral tone (CS-: 2.5 kHz for 10 s, 80 dB; 20 s ISI). 24 h after training, fear memory was reactivated during a retrieval session by re-exposure to the training context alone for two minutes, followed by re-exposure to four CS- (10 s each, 20 s ISI) and four CS+ (10 s each, 20 s ISI). The long-term effect of this reactivation session on behavior was assessed 30 day later by repeating the retrieval session (2 min shock context, 4x CS- and 4x CS+ re-exposure). Additionaly, anxiety-like behavior was assessed in those animals in an elevated plus maze and corticosterone plasma levels were determined before and after the reactivated fear memory test. For evaluation of fear reactivation effects, the “reactivation group” (R) received the whole procedure, while two additional control groups were engaged. In the “no reactivation group” (NR) the reactivation session on day 4 was omitted; the “control group” (CTL) received only 3 tones (10 kHz, 10 s, 80 dB), but no foot shocks during the training session (Fig. 2-4).

In an additional experiment, additional animals from the R, NR and CTL group were used for determination of long-term expression effects on corticosterone receptors in the ventral hippocampus.

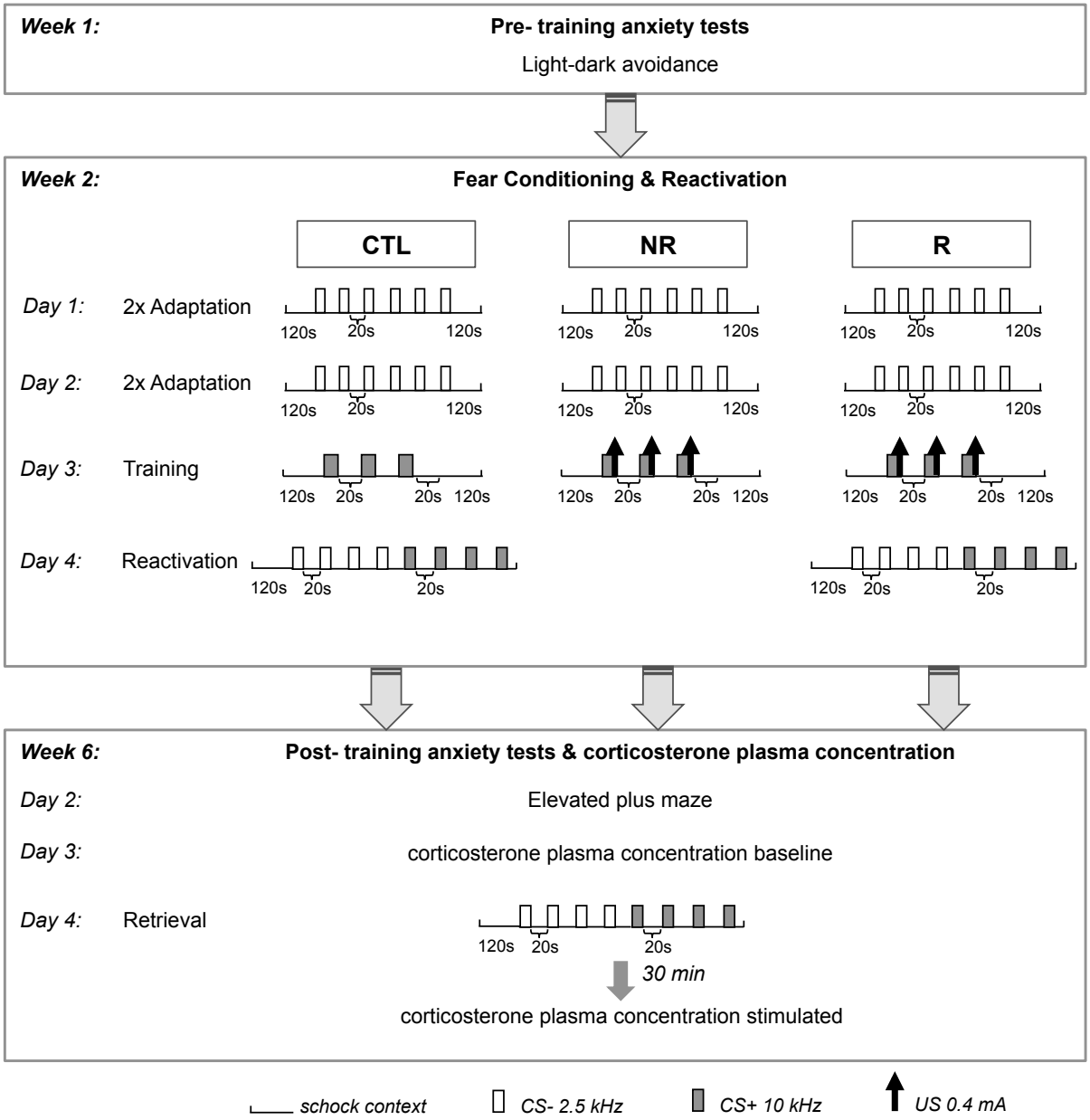

Fig. 2-4 Test schedule for assessing effects of fear memory reactivation. All animals underwent a six-week training and test schedule with evaluation of pre-training anxiety levels in week one and auditory cued fear conditioning and its re-activation in week two. In addition to this reactivation group (R), a non-reactivation group (NR) was engaged where the reactivation session was omitted and in the control group (CTL) only the tone without any footshock was presented during the training session. In all animals, long-term effects of fear memory re-activation were evaluated in week six, testing anxiety levels in the EPM, fear memory retrieval (involving a re-exposure to training context, CS- and CS+), and basal and retrieval induced corticosterone plasma concentration.

2.2.1.5.1 Pharmacological intervention after fear reactivation

To assess the corticosterone sensitivity of the fear memory reactivation effects on fear and anxiety, corticosterone was directly applied to the ventral hippocampus, a key region mediating these behaviors, of mice thirty days after fear memory reactivation.

2.2.1.5.1.1 Canula implantation into the ventral hippocampus

All animals underwent fear conditioning and fear re-activation (group R). In the third week after fear conditioning, guide canulas were stably implanted in the ventral hippocampus bilaterally. For that, in deep anaesthesia with Pentobarbital (50 mg/kg body weight intraperitoneally; Sigma-Aldrich, Seelze, Germany), the mouse was fixed into a small animal stereotactic frame (World Precision Instruments, Berlin, Germany). After removal of the scalp, the skull was cleaned with 0.2 % H_2O_2 and 0.9 % Saline, Bregma was identified, coordinates were calculated (AP: -3.08 mm; ML: ± 2.9 mm from Bregma) according to the mouse brain altas (Paxinos and Franklin, 2001), and holes were drilled. Guide canulas (26G, 5 mm length; Plastics One, Roanoke, Va, USA) were lowered into the drill holes in the right and left hemisphere (DV: -2.5 mm from brain surface) and a juweler's screw was installed in a third drill hole, located rostral and right parietal to the canulas. A socket was build with dental cement (Hoffmann dental Manufaktur GmbH, Berlin, Germany) and covered with Paladur resin (Heraeus Kulzer GmbH, Wehrheim, Germany). The guide canula was closed with a dummy and the animals were allowed to recover for five days.

2.2.1.5.1.2 Preparation of corticosterone

For final concentration of 10 ng corticosterone (Sigma Aldrich, Seelze, Germany) in an injection volume of 2 µl, the drug was first dissolved in 96 % ethanol. Then sterile double destilled water, a 9 % saline stock solution and DMSO was added resulting in final concentration of 10 % ethanol, 0.9 % saline and 1 % DMSO. The vehicle solution contained 10 % ethanol and 1 % DMSO in 0.9 % saline. Aliquots were prepared and stored at 4°C until use.

2.2.1.5.1.3 Local corticosterone application

All injections and behavioral tests started 6 h after beginning of dark phase (2.00 to 5:00 pm), were corticosterone plasma levels are low and anxiety levels in the elevated plus maze increased in fear memory re-activated animals. Four weeks after fear conditioning and its re-activation, animals received bilateral injections of either 10 ng cortcicosterone (N=9; solved in 10 % Ethanol/ 1 % DMSO/ 0.9 % Saline; Sigma Aldrich, Seelze, Germany) or vehicle solution (N=9; 10 % ethanol/ 1 % DMSO/ 0.9 % Saline) in each canula. Here, animals received a brief inhalation narcosis with isoflurane allowing plug in of the internal canulas (33G, 5+0.5 mm length; Plastics One, Roanoke, Va, USA) into the guide canula, followed by slow injection of 2 µl volume in each hemisphere. The internal canula was left plugged in for

another 1 min in the now awake and freely moving animal and then removed carefully. The mouse was then placed back in its home cage for 15 min.

2.2.1.5.1.4 Behavioral testing

15 min after injection of either corticosterone or vehicle solution, testing of anxiety-like behavior took place in an elevated plus maze (EPM) as describe below (see section 2.2.2.3). The, animals were placed back in their home cage for another 10 min, protected from light, and were then submitted to testing of re-activated fear memory as described above, re-exposing the mice to the conditioned context as well as a neutral and the conditioned auditory stimulus.

2.2.1.5.1.5 Validation of canula placement

To evaluate correct canula placement all animals received injection of 1 µl methylene blue (10 mg/ml in 0.9 % Saline/ 1 % DMSO) as described above. 30 min after injection animals were sacrificed by cervical dislocation and brains removed from the skull. The brains were snap frozen in methylbutane cooled by liquid nitrogen. 30 µm coronar sections of the dorsal hippocampus region were prepared with a cryostat, mounted on superfrost glass slides covered with 0.05 % Poly-L-Lysine (Carl Roth, Karlsruhe, Germany) and dried on a warming plate at 40°C for 20 min. One series of sections was directly embedded with Entellan (Merck, Darmstadt, Germany) and mounted by a glass cover slip (Carl Roth, Karlsruhe, Germany), while the second series of sections underwent a short staining protocol with cresyl violet acetate solution (Fixation with 70 % ethanol at -20°C for 1 min; 1 % cresyl violet acetae solution, prepared in 50 % ethanol for 1 min; dehydration with 70 % and 96 % ethanol solution, for 2 min each). Slices were dried at room temperature and then embedded with Entelan and mounted by a cover slip. Distribution of methylene blue as well as the position of the scar made by the stable guide canula was assessed by transmitted light microscopy at a 4x magnification in the native and cresyl violet-stained sections, respectively. Only animals with proper canula location in the ventral hippocampus according to the mouse brain atlas (Paxinos and Franklin, 2001) were included in the analysis (Fig. 2-5).

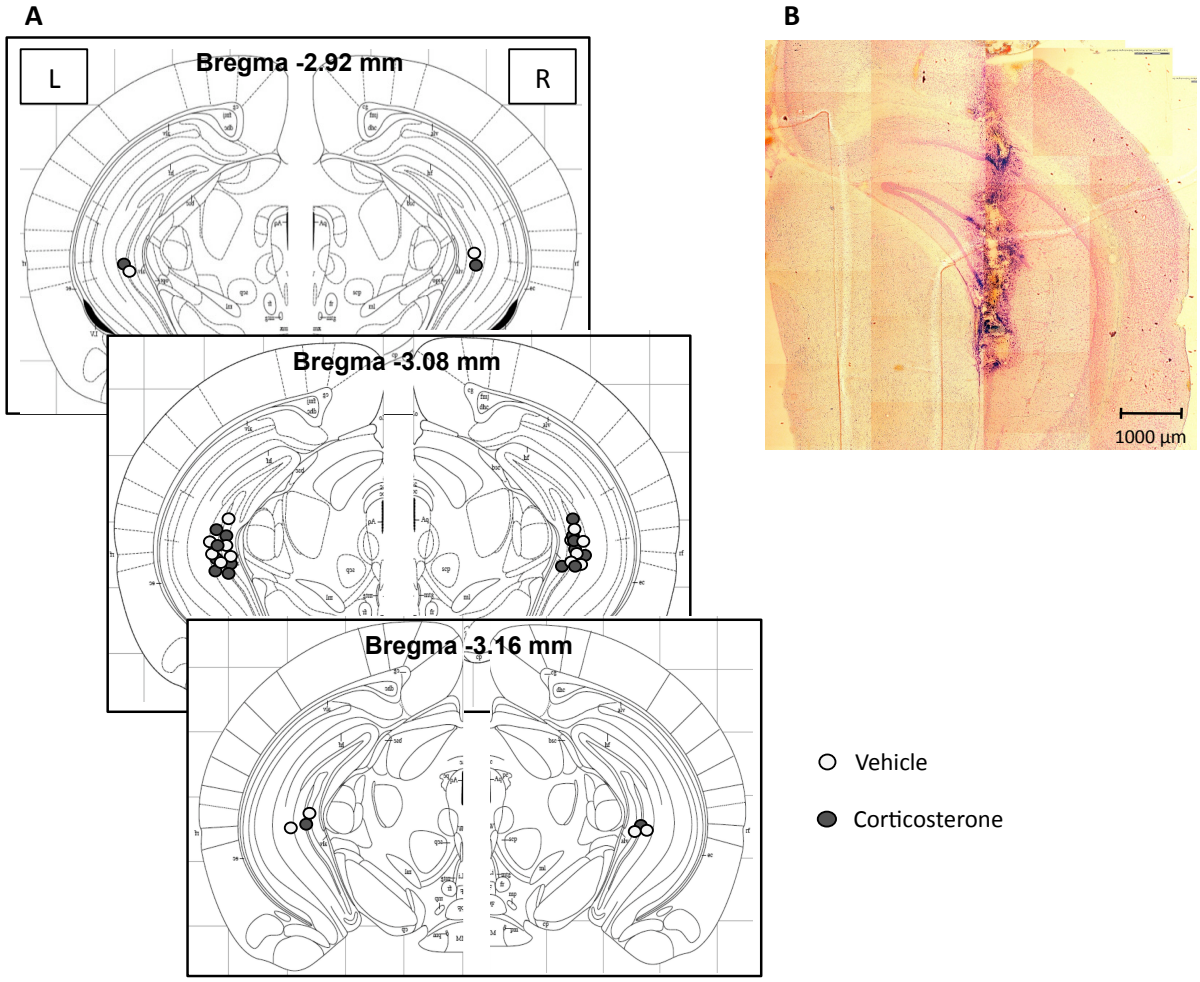

Fig. 2-5 Placement of stable canulas in the left and right ventral hippocampus. Stable guide canulas were implanted in the left and right ventral hippocampus. (A) Location of canula tipps in left and right ventral hippocampus of animals that had received either corticosterone or vehicle solution (modified from mouse brain atlas by Paxinos and Franklin, 2001). (B) Correct placement was assessed in cresyl violet stained brain sections of animals that had receive methylene blue injections under transmitted light microscopy (5fold magnification, composed image),

2.2.1.6 Data analysis

In the fear conditioning apparatus a photobeam detection system was installed that allowed online assessment of the animal's defensive behavior during posttraining and fear memory retrieval sessions. Duration of immobility periods < 1 s and number of activity bursts (< 20 cm/s) were detected automatically in the different phases of the retrieval sessions. The automatically gained immobility periods correlate well with observer rated freezing behavior while activity counts are negatively correlated with risk assessment behavior (Laxmi et al., 2003; Albrecht et al., 2010).

The freezing duration (in % of total time) was assessed separately for the different retrieval phases, namely re-exposure to the conditioning context as well as to the CS-

and CS+ (two minutes each, including 4 tone presentations for 10 s each and the adjacent 20 s ISI).

2.2.1.7 Statistics

The freezing durations (in % of total time) in different retrieval phases (context, CS- and CS+) were compared between the different training conditions, pharmacological treatment groups, virally infected animals as well as the genotypes engaged in the individual studies. For this, ANOVA was used for group comparisons and Fisher' s protected least significant difference test (PLSD) for *post hoc* analysis. To determine interactions between genotypes and training procedure, a multivariate ANOVA was engaged with pairwise comparison if required.

2.2.2 Anxiety testing

General activity and state anxiety levels were assessed in different conditions either before or after fear conditioning, depending on detailed design of the single experiments.

Basic principle of all anxiety tests presented here is the natural tendency of rodents to avoid conditions with heighten exposure to potential predators, i.e. open and well illuminated spaces. In steady conflict with the natural drive of rodents to explore new territory, animals with increased anxiety-like behavior tend to avoid exploration of potentially harmful environment, while less anxious animals show increased exploration of those.

2.2.2.1 Open field (OF)

Mice were placed in the center of a square arena made out of grey plastic (50 cm x 50 cm) and were allowed to explore the arena freely for 20 min. Animal's behavior was recorded online via the ANYMAZE video tracking system (Stoelting Co., Wood Dale, IL, USA). The distance covered during the test session was analyzed as a parameter for general activity, the time spent in the center of the open field (a rectangle 20 cm from sidewalls) as well as the number of entries to the center was determined to assess anxiety levels. Mice of both genotypes were randomly assigned to two groups either receiving the open field test in the morning or in an afternoon session.

2.2.2.2 Light-dark avoidance test (L/D test)

Animals were placed in the light compartment (100 lux, 19 cm x 21 cm) of the testing chamber (TSE, Bad Homburg, Germany). The brightly illuminated compartment was joined with a dim dark compartment (< 1 lux, 16.5 cm x 21 cm) by an opening (3.7 cm x 4 cm) in the wall's bottom center. During the five minutes session all mice were allowed to explore both compartments freely. Animal's location and activity (activity bursts > 20 cm/s) was detected online by a photo beam activity system. Increased activity and time spent in light compartment indicated decreased anxiety levels.

2.2.2.3 Elevated plus maze (EPM)

All animals were placed in the center of the maze and were allowed to explore the maze freely for 5 min at low light conditions (10 lux). The maze consisted two closed arms with 15 cm high plastic walls and two orthogonally positioned closed arms. Each arm was 35 cm long and 5 cm wide and elevated 110 cm above the floor. The position of the animal was assessed online by the ANYMAZE video tracking system (Stoelting Co., Wood Dale, IL, USA). The total arm entries, i.e. sum of entries to the open and to the closed arms, were assessed as parameters for overall activity, the % open arm entries were calculated to determine anxiety-like behavior (Rehberg et al., 2010).

2.2.2.4 Data analysis & Statistics

Parameters of general activity as well as entries to and time spent in different compartments of the different test apparatus were assessed automatically. Differences between treatment goups or genotypes were assessed with ANOVA and Fisher's PLSD for *post hoc* comparison. Interactions between genotype and treatment group was assessed by multivariate ANOVA with pairwise comparison if required.

2.2.3 The juvenile/ adult stress paradigm

To gain insights into mechanism of posttraumatic stress disorder (PTSD), Richter-Levin and co-workers (Avital & Richter-Levin, 2005; Tsoory & Richter-Levin, 2006) developed a rodent model consisting of intensive stress experience in juvenility, followed by a reminder stress in young adulthood. In one study, long-term expression changes of different GABA-related genes in the hippocampus after composite juvenile and adult

stress were investigated in co-operation with Menahem Segal and co-workers at the Weizmann Institute in Rehovot, Israel.

The stress protocols were applied to male Wistar rats in Menahem Segal's lab as described below. Prepared brains were then sent on dry ice for further analysis to Institute of Biology, Otto-von-Guericke-University Magdeburg, Germany.

2.2.3.1 Variable stress in juvenility

Young (P27-P29) male Wistar rats received three stressful experiences, once a day, between 9:00 and 11:00 am. On day one, all animals were placed in a water bucket filled with water, where they could not reach the bottom and confined to forced swimming for 15 minutes. On the second day, the same rats were placed on an elevated platform for 30 minutes. On day three, at an age of 29 days, juvenile rats were restraint in a container for 2 hours.

2.2.3.2 Adult stress

At the age of 60 days, young adult rats were confined to forced swimming again for 15 min in a water bucket. Afterwards, the rats were left undisturbed except for animal care for another 14 days until tissue preparation took place.

2.3 Determination of corticosterone plasma concentrations

Corticosterone concentrations in blood samples of mice were determined by Oitzl and co-workers as described previously (Dalm et al., 2008). Ca. 50 µl blood were collected from the tail of each mouse, using potassium-EDTA coated capillaries (Sarstedt AG & Co, Nümbrecht, Germany). Blood samples were collected within two minutes after the animal's removal from their home cage, fixing mice only at the tail and thereby minimizing restrain stress. Blood samples were immediately cooled on ice and centrifuged with 3000 x g at 4°C for 5 min. The plasma was stored at -80°C and sent to the lab of Melly Oitzl in the Leiden/Amsterdam Center for Drug Research, in Leiden, Netherlands, on dry ice. There, plasma corticosterone concentrations were analyzed with a commercially available 125I-corticosterone radio immunassay kit (MP Biomedicals Inc., New York, USA; sensitivity 3 ng/ml).

2.4 Preparation of tissue samples

2.4.1 Fresh frozen brain tissue

Fresh frozen brain tissue was used for gene expression analysis of specific brain areas via real time PCR. For that, animals were sacrificed via cervical dislocation. The skull was opened and brains removed immediately. Native brains at a whole were placed in a cup made out of aluminum foil and covered completely in Tissue-Tek® freezing compound (Sakura Finetek Europe, Zoetwerwoude, Netherlands). The cup was the placed in methylbutane (Fluka, Neu-Ulm, Germany) cooled by liquid nitrogen to -70°C. Snap frozen brains in Tissue-Tek® were stored at -80°C until further analysis.

2.4.2 Perfusion

In deep anesthesia by intraperitoneal injection of ketanest/ xylacine (100 µl i.p.; Sigma-Aldrich, Seelze, Germany), animals were fixed at a preparation board and abdominal survey was prepared. Under protection of the liver, two lateral thoracal incisions were made and the diaphragm opened. The sternum was dislocated and a thoracal survey achieved. An injection needle (26G) connected with tubing was inserted in the left ventrical of the animal's heart. Then, the right atrium was opened by a small incision and the animal's system was pre-perfused with Tyrode buffer containing 0.02 % heparine sodium sulfate (25.000 I.E.; B. Braun Melsungen AG, Melsungen, Germany) assisted by a roller pump set at a flow rate of 25 ml/ min. After pre-perfusion with ca. 50 ml Tyrode buffer, perfusion solution was exchanged to 4 % PFA in PBS for fixation of the tissue. Around 100 ml of PFA were injected, then the brain was removed from the skull and placed in fresh PFA at 4°C over night for postfixation. For cryo protection, brains were immersed in 30 % Sucrose solution in PBS at 4°C for 48 h.

Afterwards, brains were mounted on a small plate made of frozen Tissue-Tek® and placed in metylbutane cooled by liquid nitrogen. The snap frozen brains were placed in a 50 ml plastic tube containing water ice at the bottom to avoid drying of the tissue.

The frozen brains were stored at -20°C or at -80°C when isolation of RNA was planned from those samples. For the purpose of RNA preparation, perfusion was done with solution prepared under RNAse-minimized conditions.

2.4.3 Cryo sectioning

Sections of rat and mice brains were prepared with a cryostat (CM 1950, Leica, Nussloch, Germany). For sectioning of fresh frozen brain tissue the temperature of the cryostat chamber was set to -16°C while the object head was set to -14°C. PFA-fixed brain tissue was cut at a temperature of -21°C for the chamber and the object head, respectively. Upon requirement of the single studies either horizontal or coronar serial sections around the targeted areas were prepared.

When laser capture microdissection was planned, 20 µm thick sections were directly mounted on pre-warmed glass object slides covered by a PEN-membrane and coated with 0.05 % PLL under RNAse-free conditions. Object slides were placed on a warming plate, previously sterilized by 30 min UV light exposure, at 40°C after each section. Laser capture microdissection followed immediately after preparing sections, in part preceded by staining of sections with cresyl violet acetate.

If an immunhistochemical stainings followed, 30 µm sections from PFA-fixed brain tissue were cut and placed free floating in 0.1 M PBS, in which 0.02 % sodium azid was added to prevent growth of microorganisms in the solution. Sections were stored at 4°C upon further processing.

2.4.4 Laser capture microdissection

Laser capture microdissection (LCM) allows for ultra-pure isolation of tissue and cells on high-resolution level. A microscope offering transmitted light or epifluorescence was connected to a camera and a personal computer, recording microscopic live images and digital images. Regions of interests were defined on the obtained digital images and a software controlled laser beam cut along the defined area. By applying a laser pulse in the cut area, the tissue was catapulted into a capture device located above the slide. Thereby, the laser contacted the glass slide only on the sample-free side and for a very short time, allowing for contact- and contamination-free collection of samples with high spatial accuracy due to automated, software-controlled movement of the stage (Burgemeister, 2005; Bova et al., 2005).

2.4.4.1 Preparation of object slides

For LCM special glass object slides were used. They were covered by a 1.35 µm thick polyethylene naphthalate (PEN) membrane (Carl Zeiss, Jena, Germany; PALM Microlaser Systems Protocols) that facilitates laser cutting and catapulting of the tissue samples. To

increase the adherence of brain slices on the membrane, the PEN-membranes were first exposed to ultraviolet light for 30 min and then covered by 1 ml 0.05 % Poly-L-Lysine (PLL; Sigma-Aldrich, Seelze, Germany) solution for 30 min at room temperature. Excess PLL was removed washing the object slides in 200 ml double distilled water (3x 5 min, in a staining cuvette).

Expression analysis on the level of mRNA requires working under RNAse-minimzed conditions. To achieve this, the object slides were soaked in „RNAse Zap" spray (Life Technologies, Darmstadt, Germany) for 2 min at room temperature and were then washed in 200 ml double distilled water that has been treated with dimethyl-dicarbonate (DMDC) before (5x 5 min, room temperature). The slides were air-dried under a hood and stored in slide boxes treated with „RNAse Zap" spray.

2.5 Gene expression analysis

2.5.1 Gene expression analysis on tissue level

The mRNA expression of different target genes was assessed in tissue samples from different mouse and rat brain areas. In the first study, expression of neuropeptides in subregions of amygdala and hippocampus was assessed six hours after fear conditioning in mice. In the second study, expression changes of genes related to GABAergic and glutamatergic neuronal transmission were investigated in different layers of *cornu ammonis* (CA) 1 subregion of the rat's hippocampus in the juvenile stress model of PTSD. In the third study, long-term expression changes for corticosterone receptors after reactivation of fear memory were assessed in sublayers of the ventral hippocampal CA3 region.

Since gene expression analysis in those studies were conducted with different protocols for sample preparation, RNA isolation and reverse transcription, the sections are described separately for each experiment.

2.5.1.1 Expression of neuropetides 6 h after fear conditioning in mice

2.5.1.1.1 Special issues in sample preparation

Male adult C57BL/6 mice underwent after fear conditioning towards an auditory cue, the context or exposure to a tone only (naïve control group) as described above. Six

hours later the animals were killed by cervical dislocation and the brains were quickly removed from the skull. The brains were then embedded in Tissue-Tek® O.C.T. Compound (Sakura Finetek Europe, Zoeterwoude, NL), snap frozen in methylbutane cooled by liquid nitrogen and stored at -80°C for a maximum of 3 weeks. Before preparation of sections on a cryostat, the snap frozen brains were transferred from the -80°C freezer to a -20°C freezer for 30 min and than to the cryostat chamber (chamber temperature -16°C, object temperature -14°C). There, 20 µm thick coronal sections were cut at the level of amygdala and dorsal hippocampus (-2.3 mm to -1.06 mm from Bregma, according to mouse atlas by Paxinos & Franklin, 2001) and thaw mounted on the PLL-coated RNAse free membrane slides. After every section, the slides were placed on a warming plate at 40°C, hence minimizing RNAse activity by drying of sections.

2.5.1.1.2 Staining of sections

For identification of amygdalar and hippocampal subregions the brain sections a histological overview staining was required. Therefore, the sections were first fixed with 70 % ethanol cooled to -21°C for 1 min, a brief hematoxylin-eosin staining under RNAse-minimized conditions was performed. Here, the sections were first dipped into hematoxylin solution (Sigma-Aldrich, Seelze, Germany) for 2 min, then washed in 200 ml DMDC-treated double distilled water for 1 min and again for 3 min in a fresh cuvette with 200 ml DMDC-water. Then the sections were transferred to eosin staining reagent (Sigma-Aldrich, Seelze, Germany) for 1 min and dehydrated by bathing in an increasing ethanol series (50 % - 70 % - 96 % ethanol for 2 min each, prepared with DMDC-treated double-destilled water). Afterwards, the sections were air-dried and laser capture microdissection took place immediately after. To further minimize RNAse activity, all solutions were prepared and handled in baked glass ware (3 h at 180°C).

2.5.1.1.3 Laser capture microdissection and RNA isolation

Under the laser capture microscope the dentate gyrus (DG), CA1 and CA3 regions of the hippocampus as well as the lateral (LA), basolateral (BLA) and the central (CeA) nuclei of the amygdala were identified on eight to twelve sections of the left and right hemisphere, respectively (10fold magnification) and marked at the digital life image on the computer screen. All six regions were then microdissected and catapulted in a capture device with the AutoLPC mode (automated laser pressure catapulting modus, laser energy at 100 %; see Fig. 2-6). The capture device was the cap of a special 500 µl

collection tube (Carl Zeiss, Jena, Germany) containing 10 µl of sterile mineral oil for better adherence of the sample fragments.

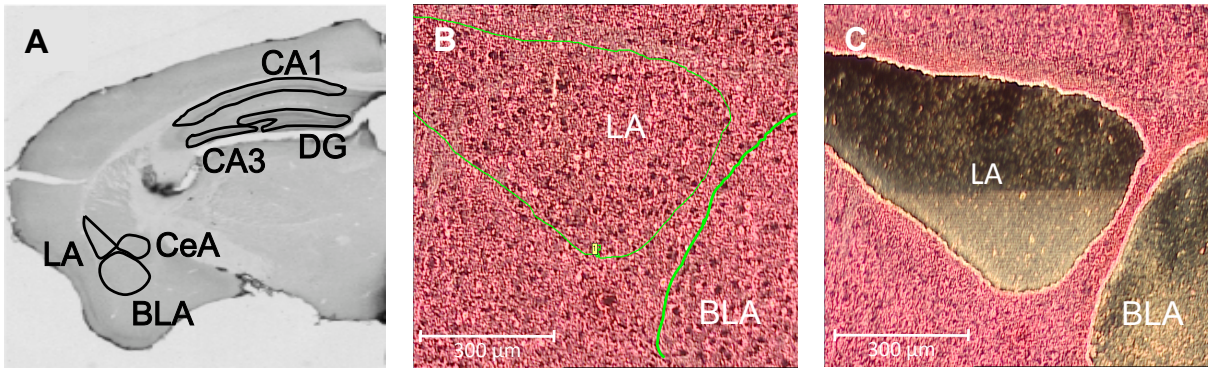

Fig. 2-6 Laser capture microdissection (LCM) of subregions of hippocampus and amygdala 6 h after fear conditioning. On 20 µm brain slices the lateral (LA), basolateral (BLA) and central (CeA) subnucleus of the amygdala as well as *cornu ammonis* (CA) 1 and CA3 and dentate gyrus (DG) of the dorsal hippocampus were identified (A). All slices underwent brief hematoxyline/ eosin staining, which allowed correct marking of the subareasat a 10fold magnification under the LCM microscope (B). The different subnuclei were then isolated by LCM (C).

Immediately after LCM, 50 µl ice-cold lysis buffer (from "Ambion Cells-to-cDNA II"-Kit, Life Technologies, Darmstadt, Germany) was added to the samples in the collection tube. The tube was inverted repeatedly and vortexed to solved tissue fragments from the cap and repeated pipetting fascilitated lysis of the tissue. The tube containing the sample was then incubated in a water bath at 75°C for 10 min to gain RNAse-inactivation. After cooling down on ice, 1 µl DNAse I (2 U/µl; from "Ambion Cells-to-cDNA II"-Kit, Life Technologies, Darmstadt, Germany) was added to the sample to allow for DNA digestion during incubation at 37°C for 30 min. The DNAse was then inactivated by incubation of samples in a water bath at 75°C for 5 min. The direct lysate containing the RNA was stored at -80°C for maximal four weeks until reverse transcription took place.

2.5.1.1.4 Reverse transcription

For first-strand synthesis of cDNA a two-step-approach according to the "Ambion Cells-to-cDNA II" Kit (Life Technologies, Darmstadt, Germany) was performed. In the first step, 5 µl of direct lysate containing the total RNA was mixed with 11 µl of reverse transcription mix 1 containing dNTPs and oligonucleotide primer and incubated at 70°C for 3 min in a thermocycler, enabling heat denaturation of secondary structures of the template RNA. After cooling on ice and subsequent brief centrifugation, the second step

proceeded by adding 4 µl of mix 2 containing the reverse transcription enzyme, buffer and RNAse inhibitor (see Tab. 2-1 for details; all reagents from "Ambion Cells-to-cDNA II"-Kit, Life Technologies, Darmstadt, Germany). The cDNA synthesis was conducted in 50 µl PCR tubes in a thermocycler at 42°C for 60 min followed by enzyme inactivation at 95°C for 10 min. The cDNA samples were stored at -20°C until real time PCR was performed.

Tab. 2-1 Master mix 1 & 2 for Reverse transcription reaction.

Mix 1:	5 µl	Lysate
	4 µl	dNTP Mix (2.5 mM each)
	2 µl	Oligo (dT)18 first strand primer (50 µM)
	5 µl	RNAse free water
Mix 2:	2 µl	10x RT-Buffer
	1 µl	M-MLV Reverse Transcriptase (100 U/µl)
	1 µl	RNase Inhibitor (10 U/µl)

2.5.1.2 Expression of GABAergic and glutamatergic genes after JSAS in rats

2.5.1.2.1 Special issues in sample preparation

14 days after the adult stress, comprising of forced swimming for 15 min, rats were killed by cervical dislocation. The brains were quickly removed from the skull and snap frozen in liquid nitrogen. The brains were then stored at -80°C until shipping to our facility and stored on dry ice for two days during shipping and immediately placed again at -80°C upon arrival. Before cutting of sections on a cryostat, the snap frozen brains were transferred from the -80°C freezer to a -20°C freezer for 30 min and than to the cryostat chamber (chamber temperature -16°C, object temperature -14°C). Prior to use, the chamber of the cryostat was sterilized by applying ultraviolet (UV) light for 30 min and only RNAse-free blades were used. Horizontal sections of 20 µm thickness were cut at the level of the dorsal (-4.1 until -4.5 mm from Bregma according to rat brain atlas, Paxinos & Watson, 1998) and ventral hippocampus (-6.3 until -6.8 mm from Bregma according to rat brain atlas, Paxinos & Watson, 1998) and thaw mounted on the PLL-coated RNAse free membrane slides. Between every mounting, the brain sections

on the object slide were allowed to dry on a warming plate at 40°C to minimize RNAse activity.

2.5.1.2.2 Staining of sections

To identify individual subregions a histological staining of the slices was necessary. Therefore, brain sections were first fixed with 70 % ethanol cooled to -21°C for 1 min and then a brief cresyl violet staining protocol was perfomed under RNAse- minimized conditions. Mounted sections were dipped into 1 % cresyl violet acetate (Sigma-Aldrich, Seelze, Germany) solved in 50 % ethanol for 1 min at 4°C, then washed and dehydrated in an increasing ethanol series (70 % - 96 % ethanol for 2 min each at 4°). All ethanol solutions were prepared with DMDC-treated double-destilled water in baked glass ware (3 h at 180°C) to further minimize RNAse activity. After staining, sections were dried on a warming plate for 2 min at 40°C and laser capture microdissection took place immediately.

2.5.1.2.3 Laser capture microdissection

Under microscopic view (LCM setup, 10fold magnification), *stratum oriens* (SO), *stratum pyramidale* (SP) and *stratum radiatum* (SR) of the *cornu ammonis* (CA) 1 were identified in the left and right hemisphere of four to five brain sections of the dorsal hippocampal region (DH) and six to eight sections of the ventral hippocampus (VH), respectively, and marked at the digital life image on the computer screen. While fragments of SO and SR layers were microdissected with the LineAutoLPC mode (automated laser pressure catapulting of the outline of a marked region, laser energy 70 %), the SP layer was microdissected with the AutoLPC mode (automated laser pressure catapulting modus, laser energy at 70 %) due to more densely packed cells (Fig. 2-7). Microdissected samples were collected in a capture device, the cap of a special 500 µl collection tube (Carl Zeiss, Jena, Germany) containing a adhesive membrane for restraining the tissue samples in the cap until lysis.

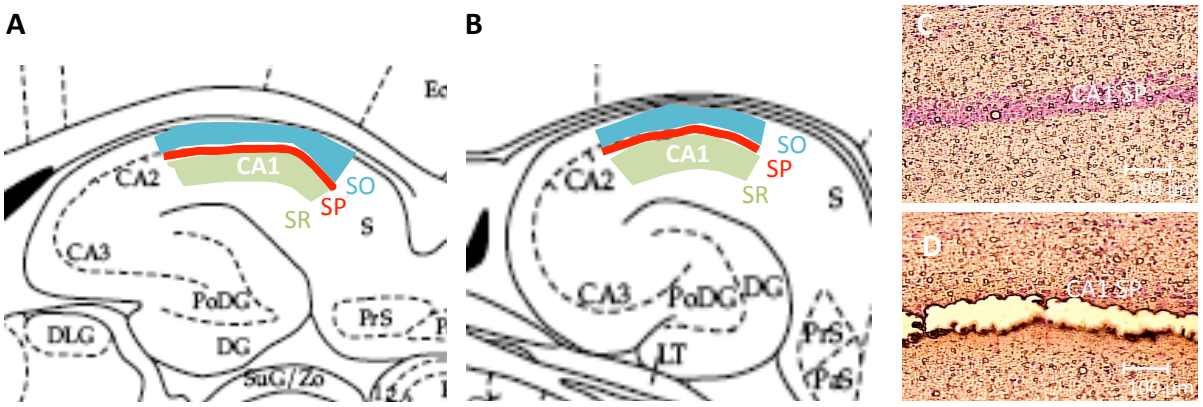

Fig. 2-7 Laser capture microdissection (LCM) of CA1 sublayers of the dorsal and ventral hippocampus after combined juvenile and adult stress. On 20 µm thick horizontal brain slices *stratum oriens* (SO), *stratum pyramidale* (SP) and *stratum radiatum* (SR) of the *cornu ammonis* (CA) 1 hippocampal subregion were identified, in the dorsal (A; sections starting at -4.1 mm from Bregma) and ventral hippocampus (B; sections starting at -6.82 mm from Bregma) respectively (modified from Paxinos & Watson, 1998, rat brain atlas). All slices underwent brief cresyl violet acetate staining, which allowed correct marking of the subareas at a 10fold magnification under the LCM microscope (C). The different sublayers were then isolated by LCM (D).

Lysis of samples was done by adding 350 µl RLT Plus lysis buffer (RNeasy Micro Plus kit, Qiagen, Hilden, Germany), prepared with 0.1 % ß-Mercaptoethanol (Serva, Heidelberg, Germany). The mixture was vortexed for 30 s up-side-down and then incubated on ice for 30 min, again up-side-down. Afterwards, the lysates were centrifuged at 13.400 rcf for 5 min at room temperature and then immediately frozen and stored at -80°C until RNA isolation was performed.

2.5.1.2.4 RNA isolation

RNA isolation of each sample was done via a spin column system specifically developed for purification of small amounts of RNA (up to 45 µg), the RNeasy Micro Kit (Qiagen, Hilden Germany). The lysates were thawed for 1 min at 37°C in a water bath before the isolation started. Genomic DNA was removed by transferring the thawed lysates to a special gDNA Eliminator column. After centrifugation (10.000 rpm for 30 s) genomic DNA should be removed from the lysates. To adjust binding conditions, 350 µl of 70 % ethanol, prepared with nucleotide-free water, was added to the flow through, containing the RNA. This mix was transferred the MiniElute spin columns and centrifuged 30 s at 10.400 rpm. Now, the RNA was bound to the membrane of the spin column and washed in three different steps. The first washing step was performed by adding 700 µl of RW1 buffer to the column and centrifugation for 30 s at 10.400 rpm, the second step by adding of 500 µl RPE buffer to the column and centrifugation for again 30 s at

10.400 rpm and the last washing step by adding 500 µl 80 % ethanol, prepared with nucleotide-free water, to the columns and centrifugation for 2 min at 10.400 rpm. After each washing step the flow through was discarded. After placing the spin column into a new collection tube, the membrane of the column was dried by 5 min centrifugation at full speed with the lids of the spin columns opened. Finally, the purified total RNA could be eluted from the membrane of the spin column by adding 14 µl of nucleotide-free water and centrifugation for 1 min at full speed after an additional incubation step (2 min at room temperature). The resulting 12 µl of eluate were stored at -80°C upon further use for reverse transcription.

2.5.1.2.5 Reverse transcription

For first-strand synthesis of cDNA the Sensiscript Reverse Transcription kit (Qiagen, Hilden, Germany), specifically designed for low amounts of RNA (< 50 ng) was used, providing the Sensiscript Reverse Transcriptase with its specific buffer, a dNTP mix (5 mM each) and nucelase-free water. First, a master mix (Tab. 2-2) was prepared, containing oligonucleotide $(dT)_{18}$ and random decamer primers (50 µM each; Ambion via Life Technologies, Darmstadt, Germany) as well as a RNAse inhibitor (SuperaseIN; 20 U/µl; Ambion via Life Technologies, Darmstadt, Germany). 16 µl of the master mix were distributed to 50 µl microfuge PCR tubes, kept on ice. The 4 µl of the individual RNA samples were added to the tubes, mixed by pipetting and centrifuged briefly. The cDNA synthesis was conducted in a thermocycler at 37°C for 60 min. A 1:5 dilution of the reverse transcription products in nuclease-free water was performed and the cDNA samples were stored at -20°C until further use for real time PCR.

Tab. 2-2 Master mix Sensiscript Reverse Transcription.

8 µl	RNAse- free water
2 µl	10x RT-Buffer
2 µl	dNTP Mix (2.5 mM each)
1 µl	Oligo $(dT)_{18}$ first strand primer (50 µM)
1 µl	Random Decamer first strand primer (50 µM)
1 µl	RNase Inhibitor (20 U/µl)
1 µl	Sensiscript Reverse Transcriptase

2.5.1.3 Expression of corticosterone receptors after fear memory reactivation in mice

2.5.1.3.1 Special issues in sample preparation

Adult male C57B/6 mice underwent either fear conditioning and its re-activation as described above (reactivation group, R; N=6 animals) or only fear conditioning without re-activation (non-reactivated group, NR; N=6). An additional control group (CTL; N=6) experienced only the tone. Thirty days later, all mice were killed by cervical dislocation, their brains were quickly removed from the skull, embedded in Tissue-Tek® O.C.T. Compound (Sakura Finetek Europe, Zoeterwoude, NL), snap frozen in methylbutane cooled by liquid nitrogen and stored at -80°C for a maximal one week. The brains were transferred to a -20°C freezer over night, then for 30 min to the cryostat chamber (chamber temperature -16°C, object temperature -14°C), before 20 µm thick horizontal sections at the level of the ventral hippocampus were prepared. Sections were thaw mounted on the PLL-coated RNAse free membrane slides and placed on a warming plate at 40°C for minimizing RNAse activity by drying of sections.

2.5.1.3.2 Staining of sections

For identification of brain subregions a brief cresyl violet acetate staining was performed under RNAse-minimized conditions as described above. Briefly, after fixation with 70 % ethanol (-21°C for 1 min) the mounted sections were stained with 1 % cresyl violet acetate (Sigma-Aldrich, Seelze, Germany; in 50 % ethanol; for 1 min at 4°C) and

dehydrated with 70 % and 96 % ethanol for 2 min each (4°C). Sections were then dried on a warming plate for 2 min at 40°C and laser capture microdissection took place immediately.

2.5.1.3.3 Laser capture microdissection

At the LCM microscope (5fold magnification), *stratum oriens* (SO), *stratum pyramidale* (SP) and *stratum radiatum* (SR) of the CA3 region were marked in the left and right hemisphere of eight to ten brain sections of ventral hippocampus at the digital life image on the computer screen. Fragments of SO and SR layers were microdissected with the LineAutoLPC mode (laser energy 80 %), the densly packed cells of the SP layer were microdissected with the AutoLPC mode (laser energy at 73 %). Microdissected samples were collected on the adhesive membrane of a special 500 µl collection tube cap (Carl Zeiss, Jena, Germany).

Lysis of samples was done witht the RNeasy Micro Plus kit (Qiagen, Hilden, Germany) as described above. Briefly 350 µl RLT Plus lysis buffer containing 0.1 % ß-Mercaptoethanol (Serva, Heidelberg, Germany) were added to the tube. After 30 s vortexing and 30 min incubation on ice up-side-down, lysates were centrifuged at 13.400 rcf for 5 min at room temperature and then immediately frozen and stored at -80°C until subsequent RNA isolation.

2.5.1.3.4 RNA isolation

Isolation of total RNA via a spin column system was conducted with the RNeasy Micro Plus kit (Qiagen, Hilden, Germany) according to manufacturer's instructions for laser capture microdissected samples as described above (see section 2.5.1.2.4), including steps for removal of genomic DNA.

2.5.1.3.5 Reverse transcription

First-strand synthesis of cDNA was performed with the Sensiscript Reverse Transcription kit (Qiagen, Hilden, Germany), specifically designed for low amounts of RNA (< 50 ng), under presence of 2.5 mM dNTPs, 50 µM Oligo (dT)18 and 50 µM random decamer first strand primers (both Ambion via Life Technologies, Darmstadt, Germany) as well as RNAse Inhibitor (SuperaseIN; 20 U/µl; Ambion via Life Technologies, Darmstadt, Germany) for 60 min at 37°C as described above (see section 2.5.1.2.5). A 1:5 dilution of cDNA samples

was prepared in nuclease-free double destilled water and stored at -20°C until determination of corticosterone receptor expression levels via quantitative PCR.

2.5.2 Gene expression analysis on the level of individual cells: NPY-positive interneurons

In this study the transcriptom of NPY-positive hippocampal interneurons was analysed by real-time PCR. The NPY-positive interneurons were identified in brain sections of NPY-GFP mice which express hrGFP under the promotor of NPY via fluorescence microscopy and isolated with laser capture microdissection. Then, the RNA was isolated, cDNA generated in a reverse transcription reaction and expression levels of genes of interest were analysed analyzed via real time PCR in NPY-positive interneurons of the hilus of the dorsal hippocampus versus the rest tissue of the hilus and versus other NPY-positive interneurons collected from other subregions of the dorsal hippocampus except the Hilus (e.g. dentate gyrus molecular layer; *strata lacunosum-moleculare, radiatum* and *oriens* of CA1 and CA3; Fig. 2-8).

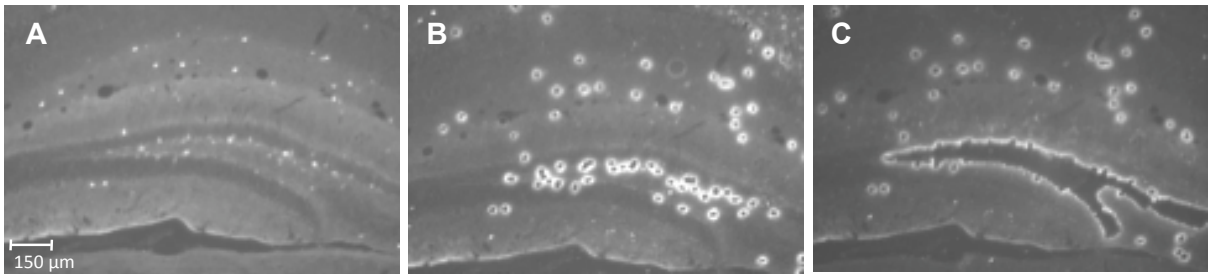

Fig. 2-8 Laser capture microdissection (LCM) of NPY-positive interneurons of the dorsal hippocampus. In 20 µm thick coronar slice from paraformaldehyde-fixed brain tissue of NPY-GFP transgenic mice the green fluorescent protein (GFP) was visualized with the epifluorescence mode of the LCM microscope, allowing for marking of NPY-positive interneurons (A; grey scale image). First, all NPY-positive interneurons of the dentate gyrus hilar region were isolated via LCM, then the NPY-positive interneurons from the other hippocampal subareas of the same slice (B). As a third sample, the rest of the hilus tissue was collected with LCM, i.e. all hilar NPY-negative cells (C). 5fold magnification.

2.5.2.1 Special issues in sample preparation

Naïve adult male NPY-GFP mice were perfused under RNAse-minimized conditions. Therefore, all solutions were prepared with DMDC-treated distilled water in baked glass ware (3 h at 180°C). All plastic ware was treated with "RNAse Zap" spray (Life Technologies, Darmstadt, Germany) and rinsed with DMDC-treated water before use.

Deeply anaesthetized mice were pre-perfused with 30 ml of ice-cold Tyrode buffer, containing 0.02 % heparine sodium sulfate (25.000 I.E.; B. Braun Melsungen AG, Melsung, Germany). Then, for tissue fixation perfusion was done with 100 ml ice-cold 4 % PFA in PBS. Brains were removed from the skull and kept at 4°C in 4 % PFA in RNAse-free for 24 h. For cryoprotection the brains were then transferred to a 30 % sucrose solution, prepared in DMDC-treated 0.1 M PBS, and incubated for 48 h at 4°C. Then, brains were snap frozen in methylbutane cooled by liquid nitrogen and were stored at -80°C.

One day before cutting of sections on a cryostat, the snap frozen brains were transferred to a -20°C freezer and than to the cryostat chamber for 30 min (chamber temperature -20°C, object temperature -19°C). Prior to use, the chamber of the cryostat was sterilized by applying ultraviolet (UV) light for 30 min and only RNAse-free blades were used. Coronar sections of 14 µm thickness were cut at the level of the dorsal hippocampus (-2.3 mm to -1.06 mm from Bregma according to the mouse brain atlas, Paxinos & Franklin, 2001) and thaw mounted on the PLL-coated RNAse free membrane slides. Between every mounting and in a final 5 min step, the brain sections on the object slide were allowed to dry on a warming plate at 40°C to minimize RNAse activity.

2.5.2.2 Laser capture microdissection

The dorsal hippocampus was directly visualized in the native, unfixed sections under the fluorescence mode of the LCM microscope (Filter set 10, excitation 450-490 nm/ emission 515-565 nm; 10fold magnification). Within this region, the magnification was set to 40fold and 50 µl 80 % ethanol, prepared with nuclease-free water, was applied directly on the slice to minimize background fluorescence. The GFP-marked cells of the hilus as one sample and of other hippocampal subregions in the slice as another control sample were then identified by their florescence signal as NPY-positive interneurons and marked at the digital life image on the computer screen. The outline of each single cell was cut by the laser via the CloseCut mode of the LCM set up (energy 53 %) and the cell was transferred into the adhesive cape of a special 0.5 ml capture device tube by applying Laser Pressure Catapulting (LPC; energy 78 %) to a dot in the middle of each cell. As another control sample, the remaining tissue of the hilus region after removal of all GFP-tagged cells was microdissected with the AutoLPC mode (automated laser pressure catapulting modus, laser energy at 78 %) and collected in the adhesive cap of the 0.5 ml capture device.

Directly after microdissection of each sample, sample lysis of the fixed tissue was performed using the RNeasy FFPE kit (Qiagen, Hilden, Germany). 150 ml PKD lyis buffer and 10 µl Proteinase K were added to the tube adjacent to the adhesive cap. After vortexing the tube up-side-down for 30 s, the tubes were incubated up-side-down at an incubator oven (SAUR Hybrid 2000) for 1 h at 55°C and then, after brief centrifugation, in an upright position over night. On the next day, each sample was placed in a water bath heated to 80°C for 15 min after being again vortexed and then centrifuged briefly to assure inactivation of the proteinase.

2.5.2.3 RNA isolation

Directly after the lysis and over night digestion RNA isolation was performed in each sample with the RNeasy FFPE kit from Qiagen (Hilden, Germany), designed for isolation of RNA from paraformaldehyd/ formaldehyd- fixed tissue samples.

After adding 320 µl of RPC buffer to each lysate for adjusting of binding conditions, genomic DNA was removed with a special gDNA eliminator spin column. Here, the samples were transferred to the columns and centrifuges for 30 s at 10.400 rpm. The flow trough contained the RNA that was now purified via a spin column system. To adjust binding conditions, 720 µl 100 % ethanol were added to each sample and thoroughly mixed. 700 µl of the sample were then transferred to the MinElute spin column and centrifuged for 30 s at 10.400 rpm. This step was repeated until the whole had passed the MinElute spin column. The RNA was now bound to the membrane of the spin column and washed two times with 500 µl RPE buffer by centrifugation for 30 s at 10.400 rpm. The spin columns were then placed in a new collection tube and the membrane was dryed by centrifugation for 5 min at full speed with the lids of the columns open. To elute the RNA from the membrane 14 µl nuclease-free water were applied directly to the membrane of the spin column. After incubation for 2 min at room temperature, the columns, placed in a new collection tube, were centrifuged for 1 min at full speed. The resulting 12 µl eluate containing the purified RNA were the stored at -80°C until further use for reverse transcription into cDNA.

2.5.2.4 Reverse transcription

For first-strand synthesis of cDNA the Sensiscript Reverse Transcription kit (Qiagen, Hilden, Germany) was used as described above. In short, 16 µl of the master mix (see

Tab. 2.2) containing oligonucleotide $(dT)_{18}$ and random decamer primers (50 µM each; Ambion via Life Technologies, Darmstadt, Germany) as well as a RNAse inhibitor (SuperaseIN; 20 U/µl; Ambion via Life Technologies, Darmstadt, Germany) were distributed to 50 µl microfuge PCR tubes, kept on ice. Then 4 µl of the individual RNA samples were added, mixed by pipetting and centrifuged briefly. The cDNA synthesis was conducted in a thermocycler at 37°C for 60 min. A 1:5 dilution of the reverse transcription products in nuclease-free water was performed and the cDNA samples were stored at -20°C until further use for real time PCR.

2.5.3 Quantitative real time Polymerase chain reaction (qPCR)

Gene expression was always assessed by quantitative real time polymerase chain reaction (qPCR) in cDNA samples prepared from RNA that has been isolated from specific areas of the rat or mouse brain after stress or fear conditioning, or that has been isolated from specific target cells

2.5.3.1 qPCR principle

The quantitative polymerase chain reaction (qPCR) was performed in an AbiPrism 7000 Sequence detection system (Life Technologies, Darmstadt, Germany) using TaqMan® reagents. With qPCR, specific amplification products can be detected via a fluorescence signal depending on FRET (Förster Resonance Energy Transfer). Here, fluorescence only occurs when a fluorescence dye is decoupled from a quencher on oligonucleotide substrates. The standard steps of a PCR with initial denaturation of DNA double strands at high temperature (94°C), annealing of the primer at lower temperatures (60°C) and extension of primer sequence according to the complementary binding of nucleotides to the template strand via a polymerase apply also for qPCR. However, the individual assay for each target gene contains the primer pair specific for the target sequence and an oligonucleotide probe, which is labeled by a fluorescence dye on the 5'-end contains a quencher on the 3'-end. At the beginning of the PCR reaction the quencher and fluorescence dye are in close proximity to each other, hence suppressing fluorescence emission. At 60°C, when the primers anneal to the target cDNA sequence, the probe is bound downstream to one of the primer. In the now following extension phase the polymerase elongates the primer according to the target sequence. Additionally, the polymerase possesses a 5'-nuclease activity that cleaves the probe sequence. Now the

reporter dye is dislocated from the quencher dye and a strong increase in fluorescence signal emission occurs. In addition, after removal of the probe from the target sequence the primer extension can continue undisturbed along the target sequence. With each PCR cycle, more reporter dye is unleashed and the fluorescence signal intensity increases proportional to the amount of amplicon, allowing for indirect quantification of cDNA input amounts. Thereby, a high number of cDNA at the beginning of the PCR will produce an increase of fluorescence significantly above background levels after relatively few PCR cycles (the so called cycle thresholt, CT) while low numbers of template will need more PCR cycles until the fluorescence signal reaches threshold level (VanGuilder et al., 2008).

2.5.3.2 General qPCR protocol

For all qPCRs pre-designed assays purchased from Life Technologies (TaqMan® Gene expression assays; Life Technologies, Darmstadt, Germany) were used for each target gene. The assays are based on TaqMan chemistry as described above and contain next to the gene-specific primer sequences the TaqMan MGB (minor groove-binder) probe with a non-fluorescent quencher (NFQ) and 6-carboxy-fluorescine (FAM) as a fluorescence dye (see Tab. 2-3a & b for overview of assay used in the different studies). In addition to the assay specific for the single target genes an assay for the housekeeping gene Glycerinaldehyde-3-phosphate-dehydrogenase (GAPDH; endogenous control; Life Technologies, Darmstadt, Germany) was used, designed either for mouse or rat (see Tab. 2-4). The GAPDH assays were labeled with a different fluorescence dye, VIC, and thereby allowed for determination of housekeeping and target gene expression within one multiplex PCR. Only in the first gene expression study, when expression levels of neuropeptides in subregions of amygdala and hippocampus were determined after fear conditioning, a singleplex PCR was engaged using a FAM-labeled assay for Phosphoglyceratkinase (PGK; see Tab. 2-4) as a housekeeping gene in distinct triplicates.

Tab. 2-3a Assays used for detection of the different target genes in mice. In one study, 6 h after fear conditioning neuropeptide gene expression levels were determined in subareas of hippocampus and amygdala. In another study, expression of different target genes was compared between NPY-positive cells in the hilus vs. NPY-negative cells in the hilus vs. NPY-positive cells in other hippocampal regions of mice. The assays used in both studies are listed here, all assys are labeled with the reporter dye FAM.

Target gene	Alias	Assay number	Probe exon location (nt)	Amplicon length (nt)
Gad2	GAD65	Mm00484623_m1	4 to 5	99
Gad1	GAD67	Mm00725661_s1	16	66
NPY	neuropeptide Y	Mm00445771_m1	2 to 3	65
SST	somatostatin	Mm00436671_m1	1 to 2	86
CCK	cholecystokinin	Mm00446170_m1	2 to 3	79
Grik1	glutamate receptor, ionotropic, kainate 1	Mm01150783_m1	7 to 8	67
Grik2	glutamate receptor, ionotropic, kainate 2	Mm01181235_m1	2 to 3	65
Grm4	glutamate receptor, metabotropic 4	Mm01306128_m1	7 to 8	62
Grm5	glutamate receptor, metabotropic 5	Mm01317978_m1	10 to 11	57
Grm7	glutamate receptor, metabotropic 7	Mm01189424_m1	8 to 9	80
5HT2C	serotonin receptor 2C	Mm00664865_m1	5 to 6	72
Adra1d	adrenergic receptor, alpha 1d	Mm01328600_m1	1 to 2	66
Drd2	dopamine receptor D2	Mm00438545_m1	7 to 8	62
Drd3	dopamine receptor D3	Mm00432889_m1	3 to 4	62
Chrm1	cholinergic receptor, muscarinic 1	Mm01231010_m1	2 to 3	75
Chrm2	cholinergic receptor, muscarinic 2	Mm01167087_m1	2 to 3	61
Chrm3	cholinergic receptor, muscarinic 3	Mm01338410_m1	2 to 3	66
Chrm4	cholinergic receptor, muscarinic 4	Mm00432514_s1	2	53
Nr3sc1	GR	Mm00433532_m1	1 to 2	68
Nr3sc2	MR	Mm01241593_m1	4 to 5	60
NCAM	NCAM	Mm00456815_m1	15 to 16	83

Tab. 2-3b Assays used for detection of the different target genes in rats. In one study, expression of GABAergic and glutamatergic target genes was determined in sublayers of the CA1 subregion of the dorsal and ventral hippocampus after juvenile and adult stress. The assays used in both studies are listed here, all assays are labeled with the reporter dye FAM.

Target gene	Alias	Assay number	Probe exon location (nt)	Amplicon length (nt)
Gad2	GAD65	Rn00561244_m1	4 to 5	79
Gad1	GAD67	Rn00566593_m1	5 to 6	107
Gabra1	GABA A receptor, alpha 1	Rn00788315_m1	6 to 7	75
Gabra2	GABA A receptor, alpha 2	Rn01413643_m1	7 to 8	123
NPY	neuropeptide Y	Rn00561681_m1	1 to 2	63
SST	somatostatin	Rn00561967_m1	1 to 2	117
Gria1	AMPA1	Rn00709588_m1	3 to 4	85
Gria2	AMPA2	Rn00691893_m1	3 to 4	65
Grin1	NMDAR1	Rn01436038_m1	3 to 4	68
Grin2a	NMDAR2A	Rn00561340_m1	3 to 4	59
Grin2b	NMDAR2B	Rn00680477_m1	3 to 4	79
Nr3sc1	GR	Rn00561369_m1	1 to 2	73
Nr3sc2	MR	Rn00565562_m1	4 to 5	79

Tab. 2-4 Assays used for detection of housekeeping genes in the different studies.

Target gene	Species	Assay/ part number	Reporter dye	Probe exon location (nt)	Amplicon length (nt)
PGK	mouse	Mm00435617_m1	FAM	5 to 6	137
GAPDH	mouse	4352339E	VIC	3	107
GAPDH	rat	4352338E	VIC	3	87

All further components needed for the PCR, dNTPs and AmpliTaq Gold DNA Polymerase in an optimized buffer, were provided by the TaqMan Gene Expression Master Mix (Life Technologies, Darmstadt, Germany). This master mix contained also AmpErase® uracil-N-glycosylase (UNG) that minimizes contamination by carryover PCR and the fluorescence dye ROX which serves as passive internal reference for the real time PCR instrument. All assays were run on the samples in triplicates with the reaction setup described in Tab. 2-5. In a singleplex qPCR, 0.5 µl water was used instead of the second assay.

Tab. 2-5 Reaction setup for qPCR.

Sample	2 µl	cDNA 1:5 dilution
Mix	5 µl	2x TaqMan ® Gene Expression Master Mix
	2 µl	H_2O
	0.5 µl	20x assay GAPDH (VIC-labeled)
	0.5 µl	20x assay target gene (FAM-labeled)

All qPCR runs were performed using the ABI Prism Step One real time PCR apparatus (Life Technologies, Darmstadt, Germany), which was connected to a personal computer, and controlled via the Step One v2 software package. All runs consisted of 50 cycles with 15 s at 95°C and 1 min at 60°C and were preceded by an initial 2 min step at 50°C for decontamination with UNG and initial denaturation at 95°C for 10 min.

2.5.3.3 Data Analysis, relative quantification and statistics

Using the Step One v2 Software (Life Technologies, Darmstadt, Germany) the mean cycle threshold (CT) values were determined for each triplicate assay. Relative quantification of expression levels for each target gene was conducted according to the ddCT method (Livak and Schmittgen, 2001). Therefore, the expression values of each target gene in each sample were normalized to the overall content of cDNA using GAPDH as an internal control which refers to the starting amount of cDNA. The so-called dCT value was determined by subtraction of the CT of GAPDH from the CT of the individual target gene for each triplicate sample, assisted by the software:

dCT (target gene) = (CT (target gene)) - (CT (GAPDH))

Then the mean value for each triplicate sample measurement was calculated from the dCT. If one value within the triplicate caused a high standard deviation, this value was omitted.

For determination of dCTs from a singleplex qPCR using the PGK as an internal control in one study, first the mean CT for each triplicate was calculated and the dCT was calculated from that value for each sample.

dCT (target gene) = (mean CT (target gene)) - (mean CT (PGK))

The dCT calculated for each sample was used for further statistical analysis.
For each target gene and each area, the group effect was determined with an one-way-ANOVA followed by *post hoc* Fisher's protected least significant difference (PLSD) test, evaluating either effects of different fear conditioning or stress protocols. The mean values based on the dCT as well as the standard error of mean of the single samples were determined for each treatment group and illustrated in a graph. It is important to note, that a small dCT resemble a high input amount of cDNA (early detection of the fluorescence signal) while genes with a low expression level would need more cycles until stable fluorescence signal is emitted an therefore show rather high dCT values.
For further illustration of expression differences between different treatment groups, relative quantification values can be determined in which the expression of a control group is set to 100 %. For that, first the ddCT value was calculated for each training group by normalizing the mean dCT of each treatment group to the mean dCT of the control group:

ddCT (treatment group) =
(mean dCT (treatment group)) - (mean dCT (control group))

Therewith, the reference is set to 0 with ddCT (control) = 0.

Since Real-time-PCR is based on an exponential function, the ddCT value for each treatment group was transformed in the Relative Quantification value (RQ), expressed in %:

$$RQ\ (\%) = 2^{-ddCT(\text{treatment group})} * 100$$

RQ now illustrates the relative expression of the target gene each treatment group for a specific area with RQ (control group) = 100 %.

Only in one study analyzing differences in expression profiles of NPY-positve interneurons of the hilus vs. other hippocampal NPY-positive interneurons vs. other

cells of the hilus, another approach was used. Here, the different samples compared derive from one animal. Therefore, it is appropriate to first set the expression levels of different target genes into relation to the expression of the housekeeping gene GAPDH and perform then the statistical analysis. The relative quantification (RQ) to GAPDH was performed as follows. The dCT for each sample was inserted in the relative quantification equation:

$$\text{RQ to GAPDH} = 2^{-\text{dCT(target gene)}}$$

Since the dCT is derived from normalization of expression values for the target gene by expression of GAPDH (dCT = CT (target gene) – CT (GPDH)), the expression level of GAPDH is 1 and expression of all target genes is expressed in relation to GAPDH.
For the different cell populations, the mean RQ to GAPDH was calculated for each group and compared with an ANOVA for cell group, followed by Fisher's protected least significant difference (PLSD) test for post-hoc analysis.

2.6 Immunhistochemistry

In this study activated transcription factors in NPY-positive interneurons of the dorsal hippocampus were detected. By using NPY-GFP mice that express GFP under the promotor of NPY, visualization of the interneurons by epifluorescence microscopy was possible. To assess activation of these interneurons after cued and contextual fear conditioning, an immunfluorescence staining of activated transcription factors was performed. In pre-experiments with a small number of animals a distinct, training-dependent activation of hilar NPY interneurons by phosphorylation of the transcription factor CREB at Ser133 was observed 1 h after fear conditioning.
This effect was quantified by using an indirect immunfluorescence method. Here, a specific primary antibody detected phosphorylation of CREB at Ser133 (P-CREB) specifically. A secondary antibody was used to label the primary antibody with a fluorochrome.

2.6.1 Special issues of sample preparation

For the immunhistochemical approaches perfusion of the NPY-GFP mice used here was necessary. One hour before perfusion the animals had received a fear conditioning training to either an auditory cue, the context or belonged to a naïve control group. Perfusion took place in deeply anesthetized mice with Tyrode buffer and 4 % PFA in PBS as described before. The brains postfixated in 4 % PFA in PBS over night and immersed in 30 % sucrose in PBS for the following 48 h for cryoprotection.

Afterwards, brains were snap frozen in methylbutane cooled by liquid nitrogen and stored at -20°C until sections were prepared in the cryostate (chamber temperature -21°C, object temperature -21°C). Coronar sections of 30 µm thickness were cut at the level of the dorsal hippocampus (-2.30 until -1.06 mm from Bregma; Paxinos & Franlin, 2001) and placed in 0.1 M PBS, containing 0.02 % sodium azid for protection against microorganism growth, in a 24-well plate with three adjoining sections per well. The free floating sections were stored at 4°C for further use in an immunfluorescene staining against P-CREB.

2.6.2 Immunhistochemical detection of phosphorylated CREB

2.6.2.1 Staining protocol

From each animal (n=6 per group) six sections at different levels of the dorsal hippocampus were placed in a fresh 24-well plate (2 sections per well) and were washed three times with 0.1 M PBS for 5 min each. During all washing and incubation steps, the plate was tumbled gently on a shaker and protected from light. Blocking of unspecific binding sites was done by applying 500 µl of 5 % donkey normal serum, solved in 0.1 M PBS and 0.3 % Triton X, per well for 1 h at room temperature. Then, the first antibody against CREB phosphorylated at Ser133 which was derived from rabbits (Cell Signaling #9191, Frankfurt am Main, Germany) was applied in a 1:250 dilution in 5 % donkey normal serum in 0.1 M PBS and 0.03 % Triton X (300 µl per well). To minimize unspecific binding of the antibody, incubation was done at 4°C over night. A negative control was included that contained slices only incubated in blocking solution to test for specific binding of the second antibody. On the next day, after three times washing of the sections with 0.1 M PBS for 5 min each, the second antibody was applied.

The second antibody, harvested in rabbits, detected immunoglobulin G heavy and light chains derived from donkeys and was coupled to the fluorochrome Alexa Fluor 555 (Life Technologies, Darmstadt, Germany). After centrifugation of precipitates in the secondary antibody aliquot (5 min at 5000 g), a 1:1000 dilution of the antibody was produced in 2 % BSA (Carl Roth, Karlsruhe, Germany), solved in 0.1 M PBS and 0.03 % Triton X and distributed to the sections (300 µl per well). After incubation for 1 h at room temperature, excess of secondary antibody that had not bound to the primary antibody, was removed by three washing steps with 0.1 M PBS for 5 min each. Staining of nucleus of individual cells, helping to confirm specificity of staining in the analysis later, was achieved by applying 4',6-diamidino-2-phenylindole dihydrochloride (DAPI; Life Technologies, Darmstadt, Germany) in a 300 nM solution (in 0.1 M PBS; 300 µl per well) to the sections for 5 min at room temperature. After three washing steps of the sections with 0.1 M PBS for 5 min each, 500 µl of a 10 % sodium thiosulfate solution (in 0.1 M PBS) was added for 30 min a room temperature to each well to reduce autofluorescence in the sections. After final washing (three times 5 min each with 0.1 M PBS), sections were transferred to a droplet of destilled water on a super frost glass slides and mounted on the slide under visual control in a binocular microscope. The sections were allowed to dry completely for 30 min at 40°C on a warming plate and were then embedded in Entellan (Merck, Darmstadt, Germany) and cover slipped. After air-drying of the slides at room temperature over night, the slides were stored at 4°C until analysis of sections with an epifluorescence microscope.

2.6.2.2 Microscopy and data analysis

Using the fluorescence modus of the LCM microscope, the fluorescence signal of hrGFP (emission maximum at 500 nm/ excitation maximum at 506 nm), expressed in NPY-positive interneurons, Alexa- Fluor 555 (excitation maximun at 555 nm/ emission maximum at 565 nm) bound to the primary antibody against CREB phosphorylated at Ser133 and DAPI (excitation maximum at 358 nm/ emission maximum at 461 nm) was detected in the Hilus of the left and right dorsal hippocampus of each section at a 40fold magnification. All GFP-postive and P-CREB S133 postitive cells were marked at the digital life image on the computer screen. With the help of the LCM software, each marked cell was counted as either GFP-, P-CREB- or double positive. These cell counts were collected in an Excel table and the mean cell number was calculated from the left and right hilus regions of all six sections per animal.

In the same fashion cell counting for NPY-, P-CREB- or double- labeled cells was conducted in the left and right CA1 *stratum oriens* (SO) region of each section and again the mean was calculated for all sections per animal (left and right hemisphere).

2.6.2.3 Statistics

Effects of the fear conditioning training (cue vs. context vs. naïve) on the mean number of NPY-positive and P-CREB- positive as well as double-labeled cells was assessed via an ANOVA and Fisher's protected least significant difference test (PLSD) for *post hoc* comparison for the Hilus and the CA1 SO region separately.

3. Results & Discussion

3.1 Model 1: Role of interneurons in amygdala and hippocampus in fear memory consolidation

3.1.1 Neuropeptide mRNA expression 6h after fear conditioning

3.1.1.1 Rationale

Systematic studies conducted in various laboratories over the last two decades have dissected the involvement of amygdala and hippocampus in particular aspects of fear memory, such as the acquisition and storage of stimulus-specific, contextual or temporal information (Maren et al., 2008). Recent work has now begun to resolve cellular circuits of these functions and the particular importance of GABAergic local circuit neurons (Ehrlich et al., 2009). These, typically GABAergic/peptidergic neurons control afferent circuitry and excitability of principle cells which are critically involved in short-term and long-term plasticity phenomena and their relation to circuit network activities in the gamma and theta frequency range. To understand their function in memory formation, it has to be considered that these interneurons comprise a vastly heterogenous population of cells with specific morphological, physiological and neurochemical features that are shaped by genetic, developmental and acute environmental influences. Recent evidence further suggests that local interneurons themselves underlie plastic changes in response to physiological activation, and thus might directly contribute to alterations in circuitry used for memory formation. In fact, prominent alterations have been observed on the molecular level concerning the GABAergic system in amygdala and hippocampus after fear conditioning (Ehrlich et al., 2009; Stoppel et al., 2006).

In this study, to further address the topography and population specificity of interneuron activation during fear memory formation, I used high-resolution gene expression analysis with laser capture microdissection and quantitative polymerase chain reaction (qPCR). I focused on populations of neuropeptide Y (NPY)- and somatostatin (SST)-positive interneurons in subregions of the amygdala (lateral (LA), basolateral (BLA) and central amygdala (CeA)) and hippocampal formation (dentate gyrus (DG), *stratum oriens* of *cornu ammonis* (CA)1 and CA3). Both peptides are highly enriched in these areas and specifically expressed in overlapping populations of γ-aminobutyric acid (GABA) containing interneurons (McDonald, 1989; Jinno & Kosaka,

2006). Moreover, activity-dependent expression of SST and NPY makes them suitable activity markers for their respective interneuron population (Conrad & McEwen, 2000; Arancibia et al., 2001), and both NPY and SST have been attributed with roles in development of fear and anxiety states (Viollet et al., 2000; Heilig, 2004) as well as fear memory formation (Kluge et al., 2008). Here, I identified NPY-positive interneurons in the hilus of the dentate gyrus as an interneuron population selectively activated following cued fear conditioning, hence dissociated from NPY and SST interneuron populations and from cholecystokinin (CCK)-positive cells in other hippocampal and amygdalar subareas.

3.1.1.2 Hippocampal & amygdalar expression changes in cued versus contextual fear conditioning

Expression patterns of the different neuropeptides were distinctly altered in subregions of hippocampus and amygdala 6h after contextual and cued fear conditioning, with an ANOVA revealing significant effects of peptide ($F(2,346)=219.782$; $p=0.000$), region ($F(5,346)=15.826$; $p=0.000$), peptide x region ($F(10,346)=28.925$; $p=0.000$) and region x training ($F(5,346)=1.27$; $p=0.041$). Compared to the naïve control group, cue and contextual fear conditioning differentially altered the expression levels of the neuropeptides (Fig. 3.1.1-1). *Post hoc* comparisons (Fisher's PLSD) revealed a significant change in NPY expression in the DG after cued but not contextual fear conditioning ($p=0.042$ cued vs. context). Calculations of the relative quantification value (RQ%) with expression in the naïve control group set to 100 % demonstrates a threefold increase of NPY mRNA expression after cued conditioning (308.93 %), but rather decreased NPY levels after contextual training (78.56 %). In contrast, SST expression was unchanged in the DG, and only a non-significant trend for reduction of SST expression was further observed in the CA1 region ($p=0.052$ cued vs. naive). However, SST was enhanced fivefold in the LA after cued (495.49 %; $p=0.018$ cued vs. naive) and threefold after contextual conditioning (300.93 %; n.s.). CCK expression, in turn, was significantly reduced in the CA1 after cued (33.95 %; $p = 0.043$ cued vs. naive), but only slightly after contextual conditioning (74.12 %, n.s.). However, contextual fear conditioning decreased CCK mRNA levels significantly in the BLA (46.48 %; $p = 0.022$ context vs. naive; $p = 0.044$ context vs. cued).

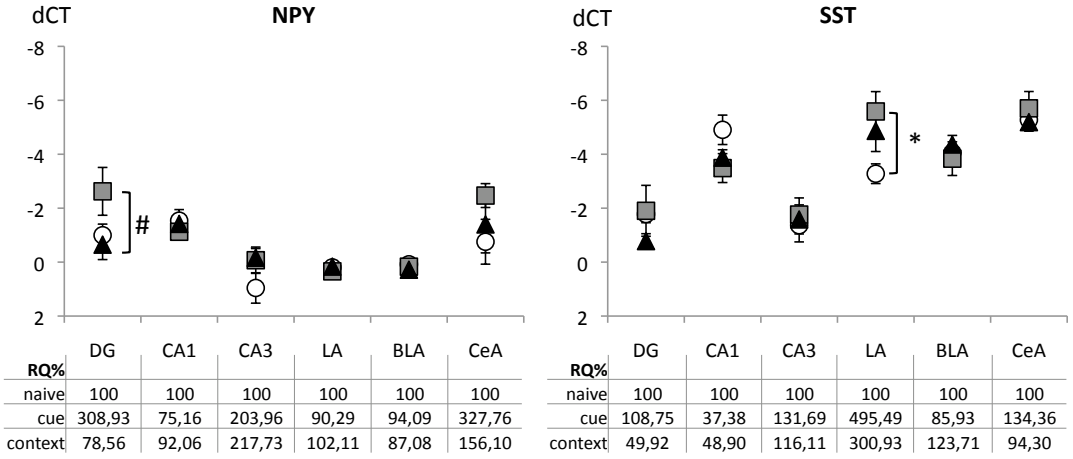

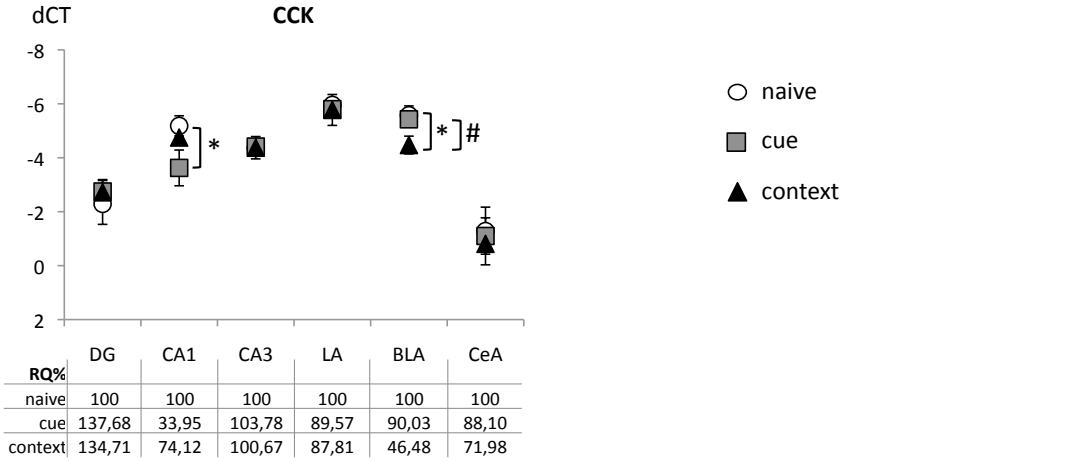

Fig. 3.1.1-1. Expression of neuropeptide Y (NPY), somatostatin (SST) and cholecystokinin (CCK) in subareas of hippocampus and amygdala six hours after fear conditioing. NPY shows a differential expression after auditory cued vs. contextual fear conditioing in the dentate gyrus (DG) of the hippocampus, while expression of SST is increased after both, cued and contextual conditioing in the lateral amygdala (LA). CCK expression is decreased in the *cornu ammonis* (CA) 1 region of the hippocampus after cued and in the basolateral amygdala (BLA) after contextual fear conditioing. No significant changes in neuropeptide expression are observed in the CA3 region of the hippocampus or in the central subnucleus of the amygdala (CeA). Graphs show the expression value normalized to the housekeeping gene (dCT) for each group as mean±SEM. Note that a higher dCT value indicates lower expression levels. For illustration of expression RQ% is depicted in the table below, showing relative expression compared to the naïve control group (expression set to 100%). * significant difference to naïve control group, $p < 0.05$; # significant difference cued vs. contextual fear conditioned groups, $p < 0.05$.

Local GABAergic interneurons in the amygdala and hippocampus are critically involved in fear memory formation. In this study, taking advantage of the neurochemical diversity of these cells, I began to investigate the topographic organization of memory-related interneuron activation in the amygdalo-hippocampal system via laser capture

microdissection and qPCR. The neuropetides NPY and SST are excellent targets for this analysis as they are 1) specific for certain, overlapping interneuron populations in both brain areas, 2) strongly regulated on the transcriptional level and 3) themselves involved in both mnemonic and affective neuronal functions (McDonald, 1989; Viollet et al., 2000; Heilig, 2004; Jinno & Kosaka, 2006). Indeed, previous observations have demonstrated expression regulation of NPY (Conrad & McEwen, 2000) and SST (Arancibia et al., 2001) in the amygdala and/ or hippocampus by physiological stress experience. As internal control, we included the anxiogenic peptide CCK, which is expressed in a distinct group of interneurons (McDonald, 1989) and in projection neurons in both areas (Handelmann et al., 1983; Mascagni & McDonald, 2003) and similarly responsive to acute stress (Giardino et al., 1999) to this analysis.

I found a distinct regulation of NPY, SST and CCK in different subregions of the amygdala dependent on the type of fear conditioning, either to the cue or to the context, six hours later.

Strikingly, cued but not contextual fear conditioning induced selectively NPY mRNA expression changes in the DG. *In situ* hybridization experiments done by Matthias Schulz in our department confirmed that this induction occurred exclusively in local interneurons without activation of granule cells in the DG (unpublished observations).

Anxiolytic, mnemotic and anticonvulsant functions of hippocampal NPY have been reported previously (Heilig, 2004; Primeaux et al., 2005; Sperk et al., 2007). In the hilus, NPY inhibits the glutamatergic transmission and the release of calcium in granule cells, thus preventing excess activity of granule cells (Sperk et al., 2007). Accordingly, NPY expression is also induced in the hilus following acute stress (Conrad & McEwen, 2000).

In this study, contextual conditioning entirely failed to induce NPY in the hilus. This observation is in agreement with the previously observed lack of hilar NPY induction by passive avoidance training (Krysiak et al., 2000), as both paradigms heavily rely on the function of the DG and CA3. During cued conditioning, in contrast, the successful stimulus-shock association reduces the salience of the context, which provides only "background" information (Rudy & Pugh, 1996; Albrecht et al., 2010). It is hence tempting to speculate that under these conditions differential amygdalar modulation of activity in hippocampal subareas (Vouimba & Richter-Levin, 2005) may be responsible for the observed selective expression change. In this line, an increase of NPY levels in the DG after cued conditioning may then dampen processing of contextual information.

Although NPY is expressed in a subpopulation of SST neurons in the hilus, the data obtained here suggest an entirely distinct activity-dependent regulation of both peptides. This might result from (a) the activation of different NPY-positive or -negative subpopulations of SST-positive interneurons and/or (b) transcriptional control by distinct extra- and intracellular signaling pathways. In fact, SST, unaltered in the dentate gyrus, showed a significant induction by both cued and contextual conditioning in the LA, where NPY in turn remained unchanged. Local interneurons in the LA receive input from cortical and thalamic fibers and exert profound control over the activity of LA projection neurons through feedforward and feeback inhibition (Szinyei et al., 2000). SST, through coupling of postsynaptic SST2 receptors with inwardly rectifying calcium channels, contributes to this inhibition (Meis et al., 2005). Activation of SST expression in the LA may thus reflect increased afferent input to this structure during fear conditioning. The relevance of this regulation to fear memory remains unclear, since null mutation and pharmacological depletion of SST affect hippocampus-dependent context conditioning as well as active and passive avoidance, but not the strongly LA-dependent cue conditioning (Schettini, 1991; Kluge et al., 2008). Blockade of the SST R2 receptor, which is the predominant postsynaptic factor in the amygdala, increases fear and anxiety (Yeung & Treit, 2012). It has also long been known that SST release in the amygdala can be induced by noradrenergic activation (Epelbaum et al., 1981), which in turn represents a mediator of the stress response during both cued and contextual fear conditioning (Roozendaal et al., 2006b). Hence, upregulation of SST function following fear conditioning might prevent the development of anxiety as seen after less predictable forms of stress.

Changes in expression of CCK mRNA, which based on the sheer quantity of expressing cells are likely to reflect alterations in projection neurons rather than interneurons, further confirmed the specificity of neuropeptide regulation after fear conditioning. CCK expression was unaffected in the DG or LA, but was reduced in the CA1 by cued and in the BLA by contextual training. The regulation of CCK in CA1 might again reflect a reduced hippocampal output during cued conditioning and could contribute to suppression contextual information in the presence of a distinct cue. As CCK in this region inhibits resting potassium conductance in local CA1 interneurons (Miller et al., 1997), it might in fact play an active role in this regulation. The reduction of CCK in BLA is particularly striking, as this structure is the primary target for hippocampal and entorhinal cortex afferences carrying contextual information into the amygdala (Maren

& Fanselow, 1995), and indicates a strong inhibitory component in this pathway. In fact, although CCK expression in the BLA is induced during anxiogenic stimulation with the inverse benzodiazepine agonist FG7142 (Pratt & Brett, 1995), its potential role in fear conditioning remains controversial. Along this line, the currently observed reduction of BLA CCK expression following context conditioning may best be interpreted as measure to generate stimulus specificity and/or to prevent over-excitation of anxiety-related neuronal circuits.

In summary, a highly region-specific and differential regulation of neuropeptide mRNA expression after cued and contextual fear conditioning was demonstrated. SST- and NPY-positive interneuron populations in the amygdala and hippocampus were identified that appear to contribute to specific aspects of fear memory formation. Both regions show intensive direct and indirect, partly reciprocal interconnectivity (Pitkänen et al., 2000) and a vivid interaction during fear memory formation and retrieval. In addition to the classical view of the amygdala as a mediator of simple CS-US association and the hippocampus providing information about spatial and temporal context, it has been demonstrated that, e.g. the ventral hippocampus is involved in both cued and contextual fear conditioning (Bast et al., 2001). Reciprocally, in auditory cued fear conditioning paradigms generalization of the fear response towards the background context can be observed (Rudy and Pugh, 1996) that increases with stimulus salience (Laxmi et al., 2003; Albrecht et al., 2010). This interplay appears to be mediated by the highly region-specific effects of the amygdala on neural plasticity in hippocampal substructures and a differential recruitment of the BLA in foreground and background context conditioning (Trifilieff et al., 2007), which cumulate in a competitive representation of cued and contextual feature representations in the amygdalo-hippocampal system (Rudy et al., 2004). In this line, the current observation of selective hilar NPY activation following cued conditioning might be a molecular correlate of this interaction. This is of particular functional relevance, as these interneurons are responsive to theta-rhythm frequency oscillations (Soltesz et al., 1993), which mediate amygdalo-hipocampal interactions and information processing during consolidation of both contextual and cued fear conditioning (Seidenbecher et al., 2003).

3.1.2 NPY in the hilus of the dentate gyrus – detector of contextual salience

3.1.2.1 Rationale

The analysis of neuropeptide gene expression after auditory cued and contextual fear conditioning in subregions of amygdala and hippocampus revealed a selective activation of NPY in the dentate gyrus (DG) after cued, but not contextual fear conditioning (see section 3.1.1). NPY is expressed in hilar interneurons of the DG and modulates glutamatergic transmission of granular cells (Sperk et al., 2007). The importance of the DG in pattern separation has long been noticed (Kesner, 2007) and several lesion studies emphasize the role of the DG in acquisition and in part also in consolidation of spatial memory (Lee & Kesner, 2004a; Ascády & Káli, 2007). Thereby, the DG is well suited for a role in the modulation of incoming contextual information during the formation of fear memory. In an auditory cued fear memory paradigm the animal acquires information about the environment in which the tone-footshock-pairing occurs, but this information is only in the background. The more salient information about the occurrence of the threatening footshock is provided by the tone. When the DG is lesioned via colchizin prior to auditory cued fear conditioning, only fear memory towards the background context is impaired, while freezing to the tone remains intact (Lee & Kesner, 2004b). The same result is also obtained when the perforant path input into the DG as well as the mossy fiber projection between DG and CA3 is pharmacologically impaired prior to auditory cued fear conditioning (Daumas et al., 2005). Training and retrieval of contextual fear memory activates several transcription factors, e.g. the immediate early gene (IEG) c-Fos in the DG (Skórzewska et al., 2006). Using optogentical tools, labeling of such c-Fos positive cells with a channelrhodopsin can be performed during contextual fear conditioning and indeed, stimulation of this cells by light activation of the channelrhodopsin during retrieval induces freezing specific to a habituated context (Liu et al., 2012). Interestingly, c-Fos induction in the hippocampus after contextual fear conditioning is no longer observed when the basolateral amygdala is inactivated (Huff et al., 2006). Thus, a contextual engram may be encoded in the DG but an additional, probably amygdala-dependent component is required for establishing an emotional memory trace, determining the salience of the context.

Within the DG, NPY or NPY-positve interneurons could contribute to such contextual salience determination, since NPY mRNA expression was differentially regulated after cued vs. contextual fear conditioning.

The increase of NPY mRNA levels after cued, but not foreground context conditioning indicates, firstly, that NPY-positive interneurons are activated during fear memory acquisition and consolidation. Such activation is also reflected in the posttrainining expression of transcription factors, e.g. IEGs like c-Fos (Skórzewska et al., 2006) or phosphorylation of the cAMP-response element binding protein (CREB; Silva et al., 1998), which are necessary for formation of long-term memory (Schafe et al, 2001). In this line, increased mRNA levels of NPY are then the result of general transcriptional activation during long-term fear memory formation.

Secondly, despite from a general activation of a NPY-positive interneuron subpopulation in the hilus, the observed NPY mRNA expression changes could reflect a crucial involvement of NPY signaling itself in contextual salience determination after fear conditioning.

In this study, I followed both lines of argumentation, investigating (1) the activation of NPY-positive interneurons after cued vs. contextual fear conditioning in the hilus and (2) the effects of blocked NPY-signaling in the DG during acquisition of auditory cued fear memory.

Independently, the question arises: What makes these NPY-positive hilar interneurons so special? Therefore, I (3) analyzed the expression profile of this cell population to determine distinct expression of receptors of selected neuronal signaling systems in NPY-positive cells in the hilus, but not the other hilar cells and also not in NPY-positive cells in other hippocampal subregions.

3.1.2.2 Differential activation of hilar NPY interneurons by cued versus contextual fear conditioning

3.1.2.2.1 Activation via CREB phosphorylation

During fear memory formation several transcription factors have been reported to be activated in amygdala and hippocampus shortly after fear conditioning training (Ahi et al., 2004; Huff et al., 2006), which then lead to expression changes in genes with various distinct functions, like cell structure, signaling, DNA/RNA regulation and metabolism/catabolism (Mei et al., 2005).

In this study I analyzed whether the activation of IEGs occurs also in NPY-positive interneurons in the hilus after fear conditioning to either an auditory cue or to the context in a differential manner. Mice, which express green fluorescent protein (GFP) under the promotor of NPY in a bacterial artificial chromosome (NPY-GFP mice) were fear conditioned to either a tone (three times CS+: 10 kHz, 85 dB, for 9 s; immediately followed by a footshock, US: 0.4 mA, for 1 s; 20 s ISI) or to the context (three times US only: footshock, 0.4 mA for 1 s; 29 s ISI). In addition, a control group naive to fear conditioning was engaged (three times CS+: 10 kHz, 85 dB, for 10 s; 20 s ISI). All animals were perfused with 4% PFA in deep anesthesia at different time points after training and brains were taken out. With indirect immunfluorescence the activation of different immediate early genes in naïve vs. cued vs. contextual conditioned animals was analyzed with specific antibodies. Double fluorescence for GFP and a secondary antibody emitting red fluorescent light upon stimulation labeling the immediate early gene of interest indicated activation of the NPY-positive cells. In an initial screening experiment specific antibodies against c-Fos, phosphorylated ERK1/2 at Thr204/Tyr202 and phosphorylated CREB at Ser133 served for determination of cell activation 10 min, 1 h, 3 h, 5 h, 9 h, 12 h and 24 h after fear conditioning to cue or context in the hilus of the dorsal hippocampus. In this pre-experiment, a distinct induction of CREB phosphorylation in the hilus one hour after cued, but to far lesser extend after contextual fear conditioning was obvious (Fig. 3.1.2-1).

Therefore, the study focused on quantification of phosphorylated CREB (P-CREB) in NPY-positive hilar interneurons one hour after the different training protocols. In total six animals of each group were analyzed and cell numbers were counted in six slices per animal at the same region from Bregma, providing mean cell numbers for each cell type, NPY-positive, P-CREB-positive and double-positive cells respectively, from 6 left and 6 right hili each.

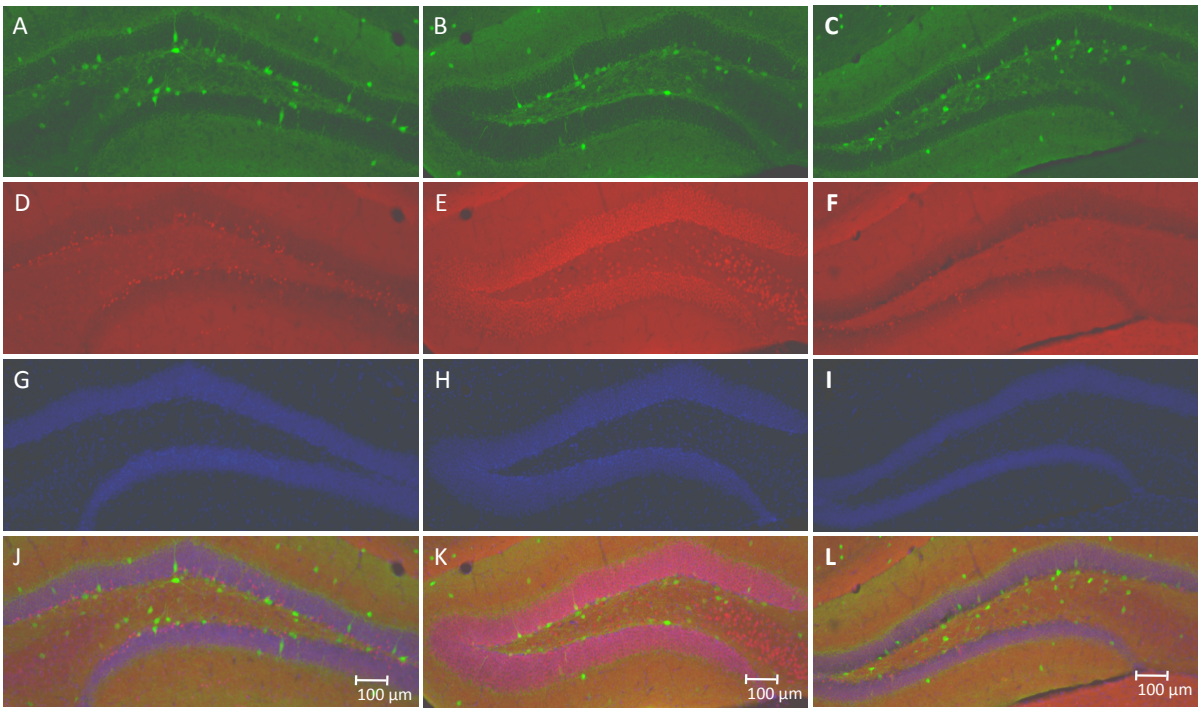

Fig. 3.1.2-1 Activation of NPY-positive interneurons by phosphoralated CREB (Ser133) one hour posttraining. Mice were either subjected to a naive control group (left column), to cued fear conditioing (middle column) or contextual fear conditioning (right column). (A-C) NPY-GFP mice were used to visualize NPY-positve interneuon. (D-F) Posttraining activation of neurons was determined by using a phospho-speciic antibody for CREB phosphorylation at Ser133, labeled with A555. (G-I) Nucelar staining with Dapi was used for visualization of cell bodies. (J-L) Merged image. Note the intense activation of granule cells but also hilar interneurons one hour after cued (K), but not contextual fear conditioning (L).

While the number of NPY-positive cells was not affected by the different training protocols one hour later (ANOVA for effect of treatment: $F(2,15)=0.717$; $p=0.504$) and also not the number of P-CREB-positive cells in the hilus (ANOVA for effect of treatment: $F(2,15)=0.813$; $p=0.462$), the training paradigm significantly influenced the number of double-labeled cells at this time point in the hilus (ANOVA for effect of treatment: $F(2,15)=21.769$; $p=0.000$). Fisher's LSD for *post hoc* comparison revealed that phosphorylation of CREB in NPY-positive hilar interneurons was significantly increased after auditory cued, but not contextual fear conditioning ($p=0.000$ cued vs. naïve; $p=0.001$ cued vs. contextual). This effect was specific for the hilus, since no effect of training paradigm was observed in numbers of labeled cells in the *stratum oriens* of the CA1, a region were no NPY mRNA expression effect was observed six hours after cued or contextual fear conditioning in the first study (Fig. 3.1.2–2; ANOVA for treatment in number of NPY-positive cells: $F(2,15)=2.697$; $p=0.100$; in number of P-CREB-positive cells: $F(2,15)=0.596$; p0.564; in number of double-positive cells: $F(2,15)=0.426$; $p=0.661$).

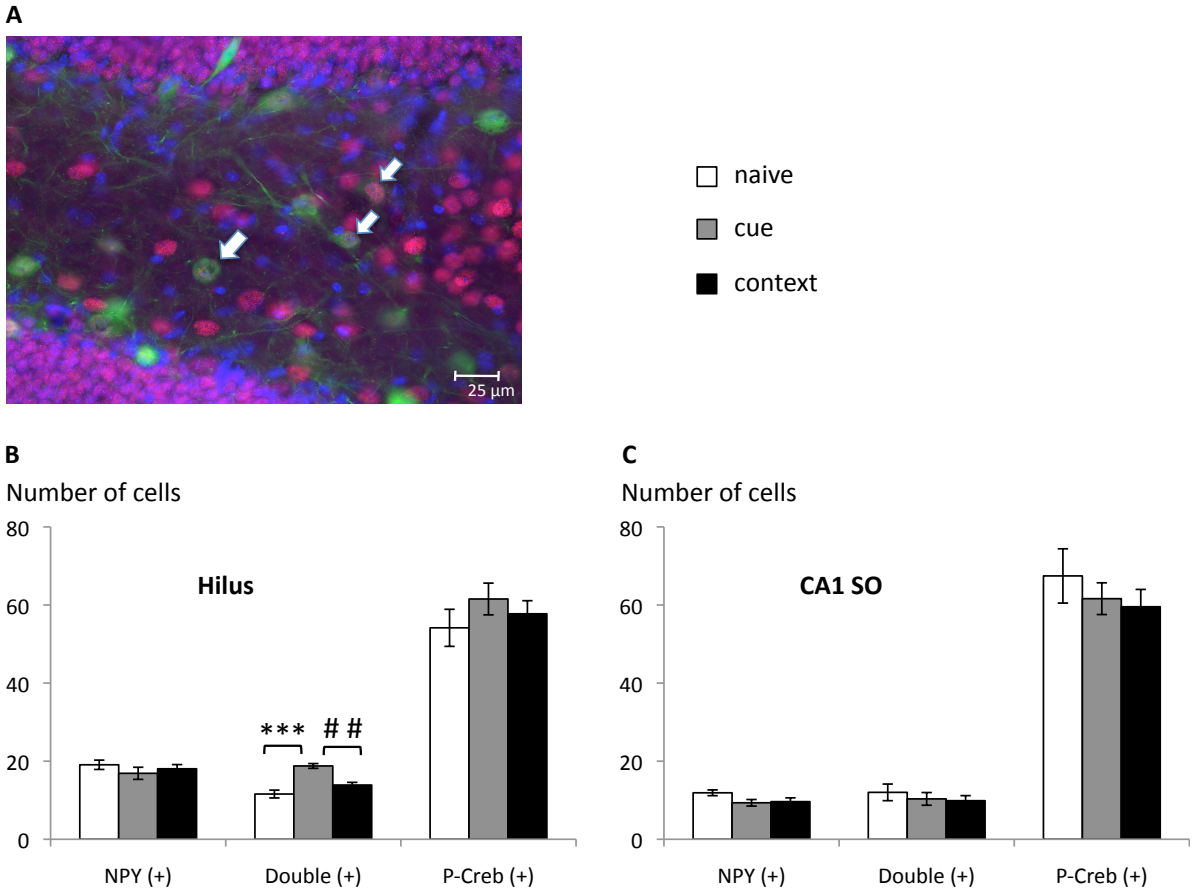

Fig. 3.1.2-2 The number of NPY-postive interneurons activated by P-CREB is increased after cued but not contextual fear conditioning. (A) Merged image, white arrows indicate NPY-expressing interneurons in the hilus (NPY-GFP, green) that also express CREB phosphorylated at Ser133 (P-CREB, red). Nuclear staining with Dapi (blue). (B) One hour after cued, but not contextual fear conditioning the number of NPY-postive interneurons activated by CREB (Double (+)) was increased, while neither the number of NPY-positive (NPY (+)) nor P-CREB-positive (P-CREB (+)) interneurons itself in the hilus were changed due to training. (C) In the *stratum oriens* (SO) layer of the *cornu ammonis* (CA) 1 region no specific induction of NPY-positive interneurons after cued or contextual fear conditioning was observed. Values are mean±SEM. *** significant difference cue vs. naive group, $p < 0.001$; # # significant difference cue vs. context group, $p < 0.01$.

CREB acts as a transcription factor by binding to the CREB responsive element (CRE), a specific DNA sequence in the promotor region of its target genes, and is activated by phosphorylation at the serine amino acid at position 133 via different kinases like calcium/calmodulin-depdendent protein kinase type IV (CaMKIV) or the cAMP-dependent protein kinase (PKA). CaMKIV is activated by rising intracellular calcium concentrations upon NMDA receptor stimulation or opening of L-type calcium channels, while PKA is activated when an agonist binds to a G-Protein coupled receptor leading to increase in cyclic AMP (Carlezon et al., 2005). In the hippocampus, only a strong activation of the cells leads to increases in P-CREB, thereby facilitating a rapid acquisition and formation of memory (Silva et al., 1998). Therefore, the data obtained in

this study demonstrate a specific activation of NPY-positive interneurons in the hilus after cued, but not contextual fear conditioning.

Increase of P-CREB after fear conditioning is indeed described for all hippocampal subregions and is restricted to certain time windows. After contextual fear conditioning for example, a rapid increase in P-CREB is already observed several minutes after the training, but also after a mere, non-associated context exposure or an immediate footshock, while a second wave of CREB phosphorylation (3 to 6 h later) occurs particularly in a group of animals that forms contextual fear memory (Stanciu et al., 2001), suggesting involvement of P-CREB in stress response and memory formation dissected by time. In addition, after cued and contextual fear conditioning comparable intracellular signaling cascades are engaged, with CREB phosphorylation occurring 1 h posttraining mediated by activation of the kinases PKA and PKC (Ahi et al., 2004). In this study, with the chosen 1 h posttraining time point for analysis, the increase in P-CREB in the hilar interneurons therefore most likely contributes to fear memory formation.

Indeed, there appears a rather direct connection between hippocampal P-CREB levels and the formation of long-term memory and long-term changes in synaptic plasticity. Overexpression of CREB in the hippocampus enhances long-term potentiation (LTP) in CA1 as well as spatial learning and contextual fear memory (Suzuki et al., 2011). However different constitutant and conditional CREB mutant mouse lines display only mild deficits in hippocampus-dependent learning and synaptic plasticity (Gass et al., 1998; Balschun et al., 2003). But using viral vectors for overexpression of a mutant dominant negative CREB form that cannot be activated by phosphorylation indeed disturbs long-term memory (Brightwell et al., 2005). In a rat model where contextual fear conditioning is impaired due to early sensimotor deprivation, this change is associated with decreased activation of CREB in the DG (Li et al., 2010). During LTP, P-CREB levels also increase in two2 waves in the DG, interestingly only after using a strong stimulation protocol (Schulz et al., 1999). Viral expression of a constitutively active form of CREB can even enhance LTP in the DG (Marchetti et al., 2011), but also contextual fear memory (Restivo et al., 2009).

In this study, an increase in P-CREB was observed also in dentate granule cells, although not analyzed quantitatively. Here, the focus instead was set on activation of interneurons by P-CREB. Indeed, activation of CREB in CA1 interneurons appears necessary for maintaining hippocampal LTP (Ran et al, 2012), suggesting that induction of gene transcription in interneurons alters the responsiveness of the local microcircuit

and thereby contributes to synaptic plasticity. In this line, the observed P-CREB increase in hilar, but not CA1 SO NPY-postive interneurons after cued conditioning indicates a role of this neuron population in the formation of long-term fear memory. Moreover, the lack of induction after contextual fear conditioning in these cells suggests a specific contribution of NPY-positive hilar interneurons to the determination of contextual salience, i.e. by actively "suppressing" contextual fear memory acquisition/ consolidation in a paradigm where the context is only in the background.

Accordingly, an impairment of CREB activation in these interneurons should interfere with the determination of contextual salience. So, when general transcriptional activation via CREB phosphorylation is not possible in NPY-positive interneurons of the hilus after cued fear conditioning training, the formation of long-term fear memory to the cue should be unimpaired. However, suppression of the contextual fear memory formation should become ineffective, resulting in enhanced contextual freezing. To test this hypothesis, a viral vector system was used that allowed for impaired CREB signaling by expression of a dominant negative isoform of P-CREB in a NPY-positive subpopulation of interneurons in the hilus.

3.1.2.1.2 Expression of dominant negative CREB isoform in hilar NPY-positive interneurons affects fear memory

To test whether impaired CREB signaling modulates the fear response to the background context, a viral vector for overexpression of a dominant negative form of CREB, CREB133, was injected locally in the hilus. Thereby, double-floxed viral constructs were engaged that allow for cell-type specific expression by using the SST-CreERT2 mouse line. These transgenic mice express cre recombinase only under the promotor of somatostatin. Furthermore, the cre recombinase is fused to a mutated ligand binding domain of the human estrogen receptor that is activated by the synthetic partial agonist tamoxifen, but not endogenous estradiol. Upon tamoxifen binding, the CreERT2 fusion protein translocates to the nucleus and the cre recombinase is active in SST expressing neurons. Because of the co-expression of SST and NPY in interneurons (Fu & van den Pol, 2007), expression of a dominant negative CREB isoform was achieved only on SST- and NPY-positive interneurons the hilus.

Viral constructs were stereotactically delivered to the hilus of the dorsal hippocampus. The pLL-dfHA CREB133 viral vector contained a double-floxed construct of the CREB133 and hemaglutinine (HA) sequences in an inverted open reading frame. HA

served as a tag for detection of the fusion protein after expression, while expression of the CREB133 construct resulted in a CREB isoform where serine at position 133 is mutated to alanine. Therefore, no phosphorylation took place at serine 133, hence preventing activation of CREB and CREB signaling was inhibited in neurons expressing HA CREB133. Upon activation of the cre recombinase by tamoxifen intraperitoneal injections, inversion occurred of both loxP pairs, resulting in irreversible inversion of the target sequence. By that, the HA CREB133 construct was expressed in the SST/ NPY-positive interneurons and CREB signaling was prevented in hilar NPY- positive interneurons. As a control, the pLL-dfHA construct was used, where only the tag HA was expressed in the target cells upon tamoxifen induction.

Tamoxifen induction was started one week after surgery by applying 2, 4 and 8 mg tamoxifen in 100 µl vehicle solution once a day on three consecutive days. One day after the last injection, the fear conditioning protocol started with eight adaptation sessions on four days, consisting of 6 min exposure to the conditioning context each. Since mice show increased levels of anxiety due to the surgery and injection procedure, the relatively high number of adaptation sessions was evaluated in pre-experiments to reach comparable pre- and posttraining activity levels to untreated animals (data not shown). A light-dark-avoidance test session was engaged after the sixth adaptation session. Here, no pre-training differences in anxiety-like behavior was observed, as indicated by % activity in light compartment (mean±SEM: 16.25±2.41% for HA vs. 12.25±1.15% for HA CREB133; Student's t-test (2-tailed): T(4)=-1.088; p=0.388), time spent in the light compartment (mean±SEM: 140.55±21.89 s for HA vs. 87.80±6.3 s for HA CREB133; Student's t-test (2-tailed): T(4)=-1.596; p=0.186) and number of transitions between the light and dark compartment (mean±SEM: 4.5±1.19 for HA vs. 5.0±1.0 for HA CREB133; Student's t-test (2-tailed): T(4)=-0.265; p=0.804). In addition, animals expressing either HA CREB133 or HA only in SST-positive hilar interneurons showed no difference in baseline activity in the last adaptation session (activity bursts >20 cm/s; mean±SEM: 91.25±31.83 for HA vs. 96.0±44.0 for HA CREB133; Student's t-test (2-tailed): T(4)=-1.081; p=0.341).

However, within one to four days after the last tamoxifen injection, some of the animals died. In total, from 13 animals expressing HA CREB133, nine died after tamoxifen injections, while only three of the mice expressing HA died. In addition, in both groups two animals were excluded from the analysis afterwards due to incorrect localization of HA expression bilaterally.

Finally, the remaining healthy HA CREB133 (N=2) and HA (N=4) expressing mice underwent standard auditory cued fear conditioning one day after the last adaptation session (2 min exposure to the context, followed by three CS+ (9 s 10 kHz, 80 dB) – US (1 s 0.4 mA) pairings, 20 s ISI, followed by 2 min context). 24 h later fear memory towards the conditioning context was assessed in a 2 min session, while fear memory to the CS+ (4x 10 s 10 kHz, 80 dB, 20 s ISI) and its generalization to a neutral CS- (4x 2.5 kHz, 80 dB, 20 s ISI) was tested 48 h later in a neutral context.

Here, mice expressing the dominant negative CREB isoform in hilar SST/NPY-positive interneurons demonstrated increased freezing to the background context (Fig. 3.1.2-3; Student's t-test (2-tailed): T(4)=3.701; p=0.021), while freezing to the conditioned tone, the CS+, was not significantly affected (Student's t-test (2-tailed): T(4)=2.078; p=0.106) in the animals tested. Moreover, HA CREB133 induced no generalization towards a neutral context (Student's t-test (2-tailed): T(4)=0.092; p=0.931) or towards a neutral tone (Student's t-test (2-tailed): T(4)=1.918; p=0.128).

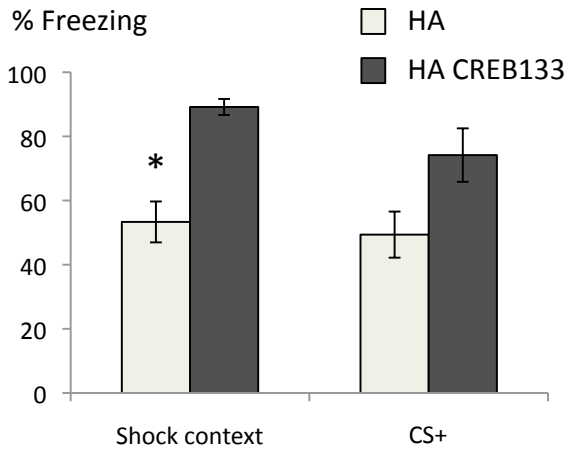

Fig. 3.1.2-3 Expression of a dominant negative CREB isoform in hilar NPY-positive interneurons resulted in contextual generalization. The dominant negative CREB construct HA CREB 133 was delivered via viral vectors to the hilus and expression was activated in SST/NPY-positive interneurons pre-training. Thus, freezing to the context was increased compared to animals expressing only the control vector HA, while the fear response to the CS+ was not significantly altered. Values are mean±SEM. * significant difference HA vs. HA CREB133, $p < 0.05$.

Although these results so far have to be interpreted with care due to the small number of animals successfully included in the behavioral analysis, CREB signaling in NPY-positive interneurons of the hilus during acquisition of cued fear memory might be indeed crucial for the determination of contextual salience. The observed contextual generalization was not related to changes in general anxiety as determined by the pre-training L/D test. Moreover, fear memory towards the CS+ was not impaired in animals with ineffective CREB activation. This supports findings from other animal models, where in mutant lines with reduced CREB gene dosage fear memory to the context is reduced (Gass et al., 1998), while expression of constitutively active CREB in the DG

enhances the contextual fear response (Restivo et al., 2009). However, a forebrain-specific expression of the dominant negative CREB isoform resulted in mild deficits in cued fear conditioning, with out changes in long-term potentiation in the basolateral amygdala or hippocampal CA1 region (Rammes et al., 2000).

To further confirm these finding presented here, more animals have to be included in the analysis. Strikingly, with the system used here a decreased survival of mice expressing the dominant negative CREB isoform in the hippocampus was observed. This could be related to adverse effects of the relatively high dose of tamoxifen. The high dose was necessary to sufficiently induce cre recombinase activity in the SST-positive interneurons, as reported by others (Taniguchi et al., 2011) and evaluated in pre-experiments (data not shown). As a partial agonist at the estrogen receptor, tamoxifen is used for the adjuvant therapy of mamma carcinoma. Frequently alterations in blood count including leukopenia and neutropenia as well as increased liver enzymes and levels of triglycerides in the plasma are observed. Fatal side effects are rarely seen in patients treated with tamoxifen, but they include stroke, pneumonia and hepatitis (see Fachinformation Tamoxistad 20/30 mg, January 2011). When used for the activation of cre recombinase in transgenic mice at a typical dose of 1 mg per day for five days, tamoxifen has no long-term effects on anxiety-like behavior, fear or spatial memory (Vogt et al., 2008). In this study now, an induction protocol using 2, 4 and 8 mg on three consecutive days was engaged. In some animals first weight loss and reduced mobility were observed and finally affected animals died within one to four days after the last injection. Similar side effects are observed in an inducible cre deleter mouse line also expressing the CreERT2 fusion protein, within five to 15 days after high tamoxifen doses (> 4,55 mg; http://www.taconic.com/ wmspage.cfm?parm1=4247). Thus, some of the death cases could be related to adverse side effects of tamoxifen. However, in mice expressing only the HA control vector, survival rate was much higher, indicating specific effects of the dominant negative CREB isoform. Studies from CREB deficient mice reveal that a total loss of all CREB isoforms is perinatally lethal (Rudolph et al., 1998), while no effects on general health are described for reduced expression of CREB or conditional CREB knock out (Gass et al., 1998; Balschun et al., 2003) or in transgenic mice expressing the dominant negative CREB isoform in the forebrain (Rammes et al., 2000). However, for the anterior cingulate cortex it was demonstrated that the viral mediated expression of the dominant negative CREB isoform induced apoptosis in pyramidal neurons (Ao et al., 2006). Therefore, it cannot be excluded that the expression of

dominant negative CREB in NPY-positive interneurons leads also to neurodegenration. Studies from NPY knock out mice show, that NPY is crucial in controlling epileptiform activity after kainite-induced seizures. Indeed, the survival rate of the knock out mice is dramatically reduced after kainite application (Baraban et al., 1997). However, it remains unclear whether hilar expression of the dominant negative CREB isoform leads to increased rate of spontaneous seizures. So far, it is reported that overall decreased level of CREB in a mutant mouse line even exert protective effects on the induction of epileptic seizures after pilocarpine administration (Zhu et al., 2012). Only in one mouse seizure-like behavior was observed directly after the last injection of tamoxifen that was finally lethal.

Together, impaired activation of CREB after cued fear conditioning in NPY-positive interneurons results in contextual generalization. Aversive side effects observed here need to be further evaluated. Both, specific effects on fear memory formation as well as adverse effects could be related to reduced expression of CRE-responsive target genes that are normally observed after CREB phosphorylation (Ploski et al., 2010). Among those CREB responsive genes is also NPY (Pandey et al., 2005). Interestingly, NPY itself appears to be a potent trigger for increasing CaMKIV or P-CREB levels (Zhang et al., 2010). The observed increase in NPY mRNA level six hours after training could be related to activation of CREB signaling one hour posttraining, but also NPY itself could contribute to the determination of contextual salience.

3.1.2.2.3 Effects of blocked NPY Y1 signaling

To test now if NPY itself is involved in contextual salience determination after fear conditioning, NPY signaling was pharmacologically blocked during acquisition of fear memory in the DG.

The cell bodies of NPY positive cells in the DG are mainly found in the in the hilus. They receive inputs from granule cells via mossy fiber collaterals, from perforant path terminals in the outer molecular layer of the DG and also from commissural-association fibers at the border between the outer and inner molecular layer of the DG. Most importantly, only 2% of the NPY-positive interneurons send projections to the contralateral hippocampus, whereas the majority of these interneurons build local microcircuits. Their terminals are found in the outer molecular layer, where they form synaptic contacts to dendritic shafts of granule cells. Because of this anatomical distribution, NPY belongs to the class of HIPP interneurons (hilar perforant path-

associated cells) that mediate feedback inhibition on granule cells near their excitatory inputs from the perforant path. These interneurons are also positive for the neuropeptide somatostatin (Houser, 2007; Sperk et al., 2007). Granule cells express the NPY receptor subtype Y1, which is able to reduce the depolarization-induced calcium influx in granule cells. By that, Y1 activation suppresses current in granule cells via voltage-dependent calcium channels (VDCC; Sperk et al., 2007). Moreover, Y1 is also expressed on hilar interneurons and can activate G-protein coupled inwardly rectifying potassium currents, although these effects are less well understood (Paredes et al., 2003). The Y1 receptor thereby appears to be the key player for NPY signaling in the DG compared to the other widely expressed NPY receptors, namely Y2 and Y5 (Sperk et al., 2007). The pharmacological compound BIBP 3226 acts as an antagonist on the Y1 receptor and has been used to study effects of NPY Y1-mediated signaling on anxiety-related behavior in rats and mice (Kask et al., 1998 & 1999; Redrobe et al., 2002; Primeaux et al., 2005; Cohen et al., 2012). For example, BIBP 3226 increased anxiety-like behavior in the open field in mice at a dose of 0.03 nm/ 2 µl administered intra-cerebro-ventricularly (i.v.c.; Redrobe et al., 2003). In this study, the effects of i.c.v. injections of BIBP 3226 at 3 and 0.03 nmol/2 µl on the fear memory response to the background context and the cue were assessed in pre-experiments. Here, again at a dose of 3 nmol/2 µl BIBP 3226 increased the contextual fear response in the background (data not shown). Since this effect could be mediated by blocking of Y1 signaling in the amygdala, the study was continued and broadened by using local injections of BIBP 3226 in the DG of mice that underwent cued fear conditioning.

For that, stable canulae were bilaterally implanted in the DG of the dorsal hippocampus of male adult C57/BL6 J mice. After one week for recovering, these animals were subjected to the standard cued fear conditioning protocol, receiving three CS+ (tones of 10 kHz, 85 dB, 9 s), immediately followed by the US (footshock of 0.4 mA, 1 s; ISI 20 s) after 4 adaptation sessions. 45 min before training, the animals received an injection of either 1 µl saline/ 1% DMSO (N=11) or the Y1 receptor blocker BIBP 2336 at either 1.5 (N=9) or 15 pmol (N=7) in each DG, thus blocking NPY signaling in the DG during acquisition of fear memory. The two different dosages were chosen based on the results from BIBP 3226 i.c.v injections in my pre-experiments and by others (Redrobe *et al*., 2003), where 0.03 nmol injected in 2 µl volume was effective. Therefore, the injection volume was reduced to 1 µl, resulting in a BIBP amount of 15 pmol. In addition, to avoid metabolic side effects due to high local dosages of BIBP compared to the vast

distribution possible for i.c.v. injections, an additional lower dosage of BIBP was engaged with 1.5 pm in 1 µl. For testing the effects of both BIBP 3226 dosages on long-term fear memory, the fear response towards the background context was tested 24 h later by re-exposing the animal for 2 min to the fear conditioning box again. The cue-specific fear memory was then tested 48 h after training by placing the animal in a neutral context and presenting four times an unconditioned neutral tone (CS-: 2.5 kHz, 85 dB, 10 s; 20 s ISI), followed by the conditioned tone (CS+: 10 kHz, 85 dB, 10 s; 20 s ISI).

Blocking Y1 receptors with BIBP 3226 before training increased the freezing response towards the context in which the training had occurred (ANOVA for drug effect: $F(2,24)=4.790$; $p=0.018$), while the fear response towards the CS+ was not altered (ANOVA for drug effect: $F(2,24)=0.302$; $p=0.742$). The effect of BIBP 3226 was dose-dependent since only the minor dose significantly increased contextual freezing ($p=0.005$ saline vs. BIBP 1.5 pmol, Fisher's LSD *post hoc* comparison; Fig. 3.1.2-4A). In addition, this effect was specific for the training context since no effect of drug treatment was observed in the neutral context ($F(2,24)=0.708$; $p=0.503$) and also no generalization of the conditioned fear response towards the neutral tone was observed (CS-; $F(2,24)=1.273$; $p=0.298$). Thereby, blocking NPY signaling via Y1 during auditory cued fear conditioning training, increases the fear memory towards the background context, suggesting a role of NPY in the DG in salience determination of contextual fear memory.

Another group of animals received injections of the effective BIBP 3226 dose in the DG bilaterally 45 min before the retrieval to the context (N=7 for BIBP 1.5 pmol in saline/1% DMSO; N=6 for saline/1% DMSO controls) to assess whether NPY signaling is specifically involved in fear memory formation. These animals were fear conditioned to the CS+ as described above and re-exposure to the conditioned context was done again 24 later and 45 min after the injections, respectively. To test for effects of pre-retrieval Y1 blockage also on cued fear memory, all animals underwent retrieval of the CS+ in a neutral context, preceded by CS- exposure, directly after the contextual retrieval and not 48 h after training, thus preventing repeated injections. Blocking NPY signaling in the DG before retrieval of conditioned fear memory had neither an effect on the freezing response towards the background context (Fig. 3.1.2-4B; ANOVA for drug effect: $F(1,11)=2.499$; $p=0.142$) nor towards the CS+ ($F(1,11)=0.004$; $p=0.952$). These results

demonstrate that NPY signaling determines contextual salience during acquisition and probably also consolidation, but not retrieval of fear memory.

To test whether NPY signaling in the DG is involved in acquisition/ consolidation of contextual fear memory *per se* or specifically in balancing contextual information against cued fear memory, additional groups of animals were engaged that received BIBP 3226 injections previous to unpaired fear conditioning. In this paradigm, a tone is also presented during training but independently from the footshock. Thereby, the animal learns an association between training context and US, while it receives all sensory information, i.e. the tones, like in the paired auditory cued paradigm used previously and the contextual information is used as the US-predicting cue in the foreground (Laxmi et al., 2003). After four adaptation sessions as described above, animals received on the training day either the effective dose of BIBP 3226 (N=8 for BIBP 1.5 pmol in saline/1% DMSO) or saline/1% DMSO as a control (N=6). 45 min later, all animals received unpaired fear conditioning. Here, after 2 min in the shock context, three US (0.4 mA, 1 s each; 29 s ISI) were presented. Separated by another 2 min break, three tones (CS_{up}; 10 kHz for 10 s; 20 s ISI) were then presented, followed by 2 min post-training exposure to the context. 24 h later contextual fear memory was tested by re-exposure to the fear conditioning box for 2 min, while 48 h post-training the fear response to the unpaired tone was assessed by placing the animal in a neutral context and presenting four times a neutral tone (CS-: 2.5 kHz, 85 dB, 10 s; 20 s ISI), followed by the tone presented in the training session (CS_{up}: 10 kHz, 85 dB, 10 s; 20 s ISI). Blocking Y1 before unpaired fear conditioning had no effect on contextual fear memory (Fig. 3.1.2-4C; ANOVA for drug effect: $F(1,12)=0.025$; $p=0.876$) or the fear response towards CS_{up} ($F(1,12)=0.007$; $p=0.933$). Blocking NPY signaling via Y1 in the DG had no effect on foreground contextual fear memory.

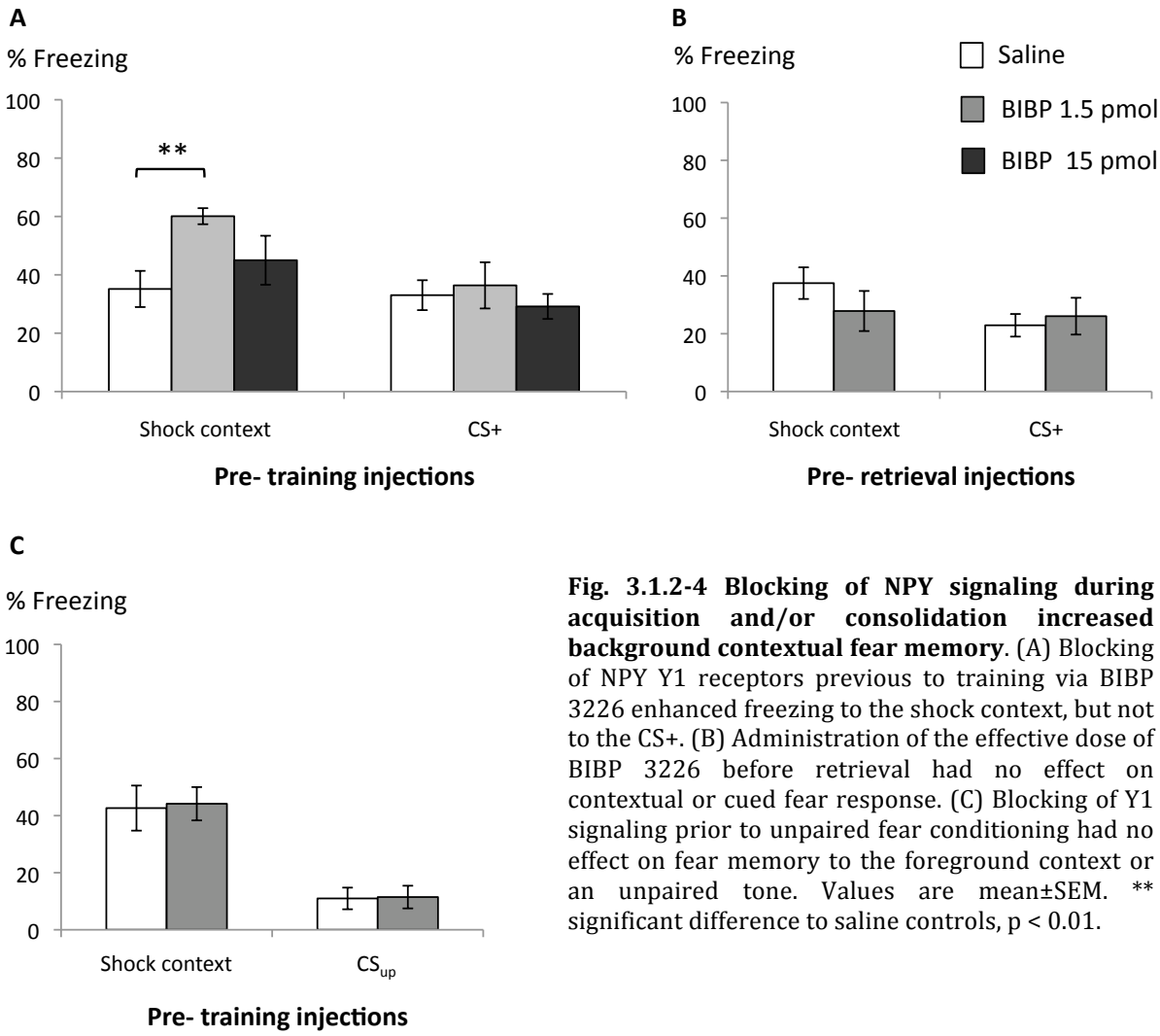

Fig. 3.1.2-4 Blocking of NPY signaling during acquisition and/or consolidation increased background contextual fear memory. (A) Blocking of NPY Y1 receptors previous to training via BIBP 3226 enhanced freezing to the shock context, but not to the CS+. (B) Administration of the effective dose of BIBP 3226 before retrieval had no effect on contextual or cued fear response. (C) Blocking of Y1 signaling prior to unpaired fear conditioning had no effect on fear memory to the foreground context or an unpaired tone. Values are mean±SEM. ** significant difference to saline controls, $p < 0.01$.

Together, these results demonstrate a significant involvement of NPY signaling in the determination of contextual salience during fear memory formation. Blocking of NPY signaling via its most important receptor Y1 in the DG results in increased response to the background context, while cue-specific memory is unaffected. This effect is also specific for fear memory acquisition and probably consolidation, but not for retrieval of the memory trace. Importantly, Y1 signaling modulates only contextual information in the background, in relation to a more salient cue, but not foreground contextual fear memory, e.g. in an unpaired training paradigm.

These findings are in line with the general role of the hippocampus in episodic memory formation (Acsády & Káli, 2007). The DG is thought to play a role in the conjunctive encoding of multiple sensory inputs that allow for pattern separation between spatial locations (Kesner, 2007). Computational models propose that the DG translates the dense activity patterns of the entorhinal cortex, which receives multimodal input from

various cortical areas, into a sparse activity pattern of the hippocampus. Therefore, only the DG granule cells with the strongest excitatory drive from the entorhinal cortex via the perforant path may transfer the information to the CA3 area and allow further processing. This code conversion is enabled by the unusually strong inhibition occurring in the DG, mediated by different subtypes of interneurons in the DG, like HIPP cells and basket cells (Acsády & Káli, 2007). HIPP cells are characterized by their anatomical appearance on the one hand, with cell bodies located in the hilus and axons sent to the outer two-thirds of the molecular layer, and by their expression of the neuropeptides NPY and SST on the other hand. In the molecular layer, they mediate feedback inhibition on the granule cells near their input from the perforant path (Houser, 2007).

During fear memory formation it has long been known that multimodal information about the environment in which the conditioning took place is processed by the hippocampus while information about the footshock and its association with a cue like a tone is processed via the amygdala (Phillips & LeDoux, 1992). The DG is the first station of hippocampal contextual information processing, receiving multimodal input from the entorhinal cortex via the perforant path. Lesion of the DG or impairment of its perforant path input before auditory cued fear conditioning in the DG therefore impairs fear memory to the contextual information in the background while cued fear memory remains intact (Lee & Kesner, 2004a; Daumas et al., 2009). In addition, training but also retrieval of foreground contextual fear memory leads to c-Fos activation in the DG (Skórzewska et al., 2006) and such c-Fos induction is also dependent on BLA inputs (Huff et al., 2006).

Blocking NPY signaling in the DG via its Y1 receptors, however, specifically affected contextual fear memory in the background but not in the foreground after unpaired fear conditioning. Therefore, NPY in the DG might contribute essentially to the determination of the contextual salience during auditory cued fear conditioning. Interestingly, freezing to the background context can be enhanced using intensive training protocols with increased numbers of tone-shock pairings and higher US intensity (Laxmi et al., 2003). This effect is thought to be mediated by increased amygdala activation and is not observed in animals with disturbed amygdalo-hippocampal interaction (Albrecht et al., 2010). The contextual aspects of fear memory are mediated via the BLA (Calandreau et al., 2005; Trifilieff et al., 2007) and recent studies also suggest an involvement of the DG in encoding of contextual information (Kaouane et al., 2012; Sauerhöfer et al., 2012). Evidence for a close interaction of both structures rises from electorphysiological

studies, where activation of the BLA is able to strengthen long-term potentiation (LTP) in the DG (Abe et al, 2001), but not in the CA1 (Vouimba & Richter-Levin, 2005; Li & Richter-Levin, 2012). Here, enhanced DG-LTP is only observed when BLA activation immediately before tetanization of the perforant path as the major DG input (Akirav & Richter-Levin, 1999) and intermediate, but not strong BLA stimulation protocols are engaged (Li & Richter-Levin, 2012). The modulation of LTP in the DG by BLA activation is mediated by corticosterone and norepinephrine actions in the BLA (Akirav & Richter-Levin, 2002; Vouimba et al., 2007). In parallel, noradrenergic neurotransmission in the BLA together with corticosterone are also able to increases fear memory formation in freely behaving animals (LaLumiere et al., 2003; Roozendaal et al., 2006a & 2006b).

Together, amygdalo-hippocampal interaction, more specifically between BLA and DG, may mediate the balance between context and cue salience with a stronger BLA activation leading to reinforcement of DG plasticity, thus favoring contextual fear memory formation. The results obtained here suggest, that NPY signaling in the DG may contribute to the modulation of the BLA input in the hippocampus, although future studies are required to prove this hypothesis.

NPY-positive interneurons, i.e. HIPP cells, exert powerful inhibitory control on granule cells in the DG, most likely via its receptor Y1 (Houser, 2007; Sperk et al., 2007). NPY interneurons from the hilus send their axons to the outer molecular layer of the DG, where Y1 is expressed on granule cell dendrites. So, activation of Y1 receptors on granule cells near their excitatory input from the entorhinal cortex allows for suppression of granule cell activity and therefore modulation of incoming information in the DG and its propagation along the hippocampal formation (Sperk et al., 2007).

After blockage of NPY signaling via Y1 in the DG the cue-context balance was shifted towards an enhanced contextual response. This suggests that activation of NPY Y1 signaling in a moderate auditory cued fear conditioning paradigm normally suppresses DG granule cell activation. Since no effect of Y1 blockage on foreground context memory was observed, NPY effects may depend on a modulation of DG inputs by the BLA and indeed, strong stimulation of the amygdala by kindling can induce the expression of NPY mRNA in the DG (Rosen et al., 1996).

Interestingly, Y1 is also expressed on hilar interneurons (Paredes et al., 2003) and Fu & van den Pol (2007) reported that more than half of the NPY-positive interneurons in the hilus can be excited rather than inhibited by GABA via GABA A receptors. Increased GABA release can then result in enhanced release of NPY and SST that inhibits granule

cell activity via pre- and postsynaptic mechanisms. An excitation of NPY-positive interneurons by GABA can then mediate a rapid synchronization of the overall output inhibition. Therefore, in addition to the proposed effects of Y1 on granule cell activity during the acquisition and consolidation of fear memory, additional modulation on the inhibitory circuits in the hilus via Y1 cannot be excluded, but they again would contribute to a strong feedback inhibition of granule cell activity. Moreover, also the NPY receptor Y2 is expressed in the DG and other subareas of the hippocampus and could additionally contribute to NPY-mediated inhibition of glutamate release in the DG *in vivo* (Silva et al., 2001).

Together, NPY Y1 signaling in the DG appears to be sufficient to mediate the determination of contextual salience in balance to a conditioned cue.

3.1.2.3 Transmitter systems for hilar NPY interneuron activation

As demonstrated in the first two parts of the study, NPY-positive interneurons in the hilus play a crucial role in the determination of contextual salience during formation of conditioned fear memory. Functionally, this interneuron population must be activated uniquely during fear conditioning by neurotransmitter systems that would then mediate for example an activation of transcription factors like P-CREB and/or initiate release of NPY in the DG. GABA and glutamate are the main inhibitory and excitatory neurotransmitters of the brain, but monoaminergic neuromodulators like serotonine, noradrenaline, dopamine and acetylcholine play an important role in shaping neurotransmission in various brain regions and are also active during fear conditioning (Kim & Jung, 2006; Stoppel et al., 2006).

To determine whether hilar NPY-positive interneurons are susceptible to respond to those neuromodulators uniquely, I analyzed the expression of distinct receptor subtypes from various neurotransmitter systems in this population. For that, male adult mice expressing GFP under the promotor of NPY in a bacterial artificial chromosome were used (NPY-GFP mice). Behavioral naïve, group- housed animals were perfused with 4% PFA under RNAse-minimized conditions. Via laser capture microdissection, the GFP-labeled NPY-positive cells of the hilus were isolated from several slices per animal (N=6 animals in total) and total RNA was isolated from this cell population. The remaining hilus tissue after removal of the GFP- labeled cells was isolated as well (N=6), serving as a control for expression profile of hilar non-NPY cells. In addition, in the same slices GFP-labeled cells were collected from other subregions of the hippocampus (*stratum*

radiatum and *stratum oriens* of CA1 and CA3, *stratum lacunosum-moleculare* of CA1 and molecular layer of DG) from each animal (N=6), allowing determination of local hilar NPY expression profiles. After reverse transcription of the total RNA into cDNA, the mRNA expression levels for the different target genes were then determined in 4-6 animals with real time PCR, using a relative quantification (RQ) towards the housekeeping gene GAPDH (expression level for GAPDH=1). Table 3.1.2-1 provides an overview about the genes analyzed and the specific expression pattern in NPY-positive interneurons.

Tab. 3.1.2-1 Overview of expression profile of hilar NPY-positive interneurons. The mRNA expression levels of receptors from different neurotransmitter systems (nomeclature according to human genome organization; HUGO) were assessed in cells expressing NPY in the hilus (NPY(+) hilus), compared to the remaining hilus tissue (NPY(-) hilus) and to NPY-positive cells in other hippocampal subareas (NPY(+) no hilus). All values are in relative quantification to the housekeeping gene (RQ to GAPDH with GAPDH expression level=1), mean±SEM. Significant changes with $p < 0.05$ are indicated by arrows.

	NPY(+) hilus	NPY(-) hilus	NPY(+) no hilus	Statistics	Significant difference of NPY(+) hilus	
	Mean±SEM	*Mean±SEM*	*Mean±SEM*	*ANOVA for cell type*	*to NPY(-) hilus*	*to NPY(+) no hilus*
GABAergic						
GAD65	0,3646±0,16899	0,2042±0,10682	0,5523±0,2935	F(2,15)= 1,206; p=0,327	=	=
GAD67	0,1802±0,02135	0,0463±0,00593	0,2103±0,0219	F(2,18)=25,094; p=0,000 ***	↑	=
NPY	0,2207±0,03691	0,0398±0,00326	0,2053±0,02961	F(2,18)=12,362; p=0,000 ***	↑	=
SST	0,0919±0,01549	0,0395±0,00469	0,0858±0,01506	F(2,21)= 5,029; p=0,016 *	↑	=
CCK	0,0315±0,00833	0,0482±0,0038	0,0482±0,00619	F(2,21)= 2,294; p=0,126	=	=
Glutamatergic						
Grik1	not detected	not detected	not detected			
Grik2	0,25±0,09128	0,0834±0,01647	0,0528±0,00971	F(2,21)= 3,886; p=0,037 *	↑	↑
Grm4	0,0006±0,00055	0,0026±0,00107	0,0031±0,00143	F(2,21)= 1,560; p=0,234	=	=
Grm5	0,0198±0,00264	0,0158±0,00175	0,0202±0,00469	F(2,19)= 0,533; p=0,596	=	=
Grm7	0,0695±0,02028	0,09±0,01233	0,0724±0,0241	F(2,21)= 0,322; p=0,728	=	=
Serotonergic						
5HT2C	not detected	not detected	not detected			
Adrenergic						
Adra1d	0,0452±0,0171	0,0513±0,00479	0,0448±0,00623	F(2,21)= 0,113; p=0,894	=	=
Dopaminergic						
Drd2	0,001±0,00086	0,0199±0,00171	0,0029±0,00216	F(2,18)=32,115; p=0,000 ***	↓	=
Drd3	not detected	not detected	not detected			
Muscarinergic						
Chrm1	0,0168±0,00429	0,0072±0,00108	0,01±0,0015	F(2,19)= 3,677; P=0,045 *	↑	=
Chrm2	0±0,00001	0,0043±0,00149	0,0133±0,00352	F(2,19)= 9,940; P=0,001 **	=	↓
Chrm3	0,0069±0,00331	0,0172±0,00315	0,0251±0,00642	F(2,18)= 4,017; P=0,036 *	=	↓
Chrm4	0,8653±0,00807	0,8807±0,00663	0,8587±0,00731	F(2,20)= 2,329; P=0,123	=	=
Glucocorticoid receptors						
Nr3c2	0,0474±0,00877	0,0487±0,00435	0,0588±0,0067	F(2,21)= 0,373; p=0,699	=	=
Nr3c1	0,0163±0,00727	0,0119±0,00147	0,0111±0,003	F(2,21)= 0,834; p=0,448	=	=
Cell adhesion molecule						
NCAM	0,1087±0,03678	0,1554±0,01773	0,0972±0,01659	F(2,18)= 0,95; p=0,402	=	=

In a first step, NPY mRNA levels were determined in the three populations. NPY expression was significantly increased in NPY-positive interneurons in the hilus and in the rest of the hippocampus (Fig. 3.1.2-5A; ANOVA for population: $F(2,18)=12.362$; $p=0.000$), but were low in remaining hilus tissue, thus proving specific expression of the marker GFP in NPY-positive cells in the used mouse strain. Moreover, the isolated GFP-tagged cells are enriched with GAD65 (Fig. 3.1.2-5B; $F(2,15)=1.206$; $p=0.327$) and, more pronounced, with GAD67 ($F(2,18)=25.094$; $p=0.000$) while GAD67 levels were low in hilus tissue after removal of GFP- labeled cells. As known from the literature, NPY-positive interneurons form a subpopulation of SST- positive interneurons (McDonald, 1989; Fu & van den Pol, 2007). Indeed, SST mRNA levels were enriched in NPY- positive cells in the hilus and other hippocampal subregions ($F(2,21)=5.029$; $p=0.016$). The mRNA expression levels of CCK, another neuropeptide localized in a distinct interneuron subpopulation, were low in all populations ($F(2,21)=2.2.94$; $p=0.126$).

Different subtypes of metabotropic glutamate receptors were expressed preferentially in all cell populations at comparable levels, but the ionotropic kainate receptor type 2 (Grik2) was expressed preferentially in NPY-positive interneurons of the hilus, but not in other hilar cell types. More strikingly, Grik2 mRNA expression levels were also significantly lower in NPY-positive cells of other hippocampal subregions ($F(2,21)=3,886$, $p=0.037$; Fig. 3.1.2-5C).

From all neuromodulator systems analyzed, the different muscarinergic receptor subtypes binding to acetylcholine displayed the most intriguing expression profile. The mRNA expression level of the muscarinergic receptor type 1 (Chrm1) was increased in NPY-positive cells of the hilus compared to other cell types in the hilus (Fig. 3.1.2-5D; $F(2,19)=3.677$; $p=0.045$), while the expression of the muscarinergic receptor types 2 and 3 (Chrm2 and Chrm3) were significantly lower in NPY- positive cells compared to other cell types in the hilus (Chrm2: $F(2,19)=9.940$; $p=0.001$; Chrm3: $F(2,18)=4.017$; $p=0.036$). No specific expression pattern was observed for the type 4 muscarinergic receptor (Chrm4: $F(2,20)=2.329$; $p=0.123$) and also for the alpha-adrenergic receptor type 1d (Adra1d: $F(2,21)=0.113$; $p=0.894$). The mRNA expression levels for the serotonergic receptor type 2C (5HT2C) and the dopaminergic receptor type 3 (Drd3) were too low for analysis. However, the dopaminergic receptor type 2 showed an interesting expression pattern with enriched mRNA levels in the hilus tissue after removal of all NPY- positive cells ($F(2,18)=32.115$; $p=0.000$), indicating susceptibility to dopaminergic modulation of hilar neurons other from NPY- positive cells.

In addition, expression for receptors for glucocorticoids, the mineralocorticoid (Nr3sc2) and glucocorticoid receptor subtype (Nr3sc1), was analyzed in the three different subpopulations, but no differential expression was observed (Nr3sc2: $F(2,21)=0.373$; $p=0.699$; Nr3sc1: $F(2,21)=0.834$; $p=0.448$). The neural cell adhesion molecule NCAM as a prominent member of extracellular proteins modulated by fear conditioning (Albrecht et al., 2010) showed no differential expression pattern ($F(2,18)=0.950$; $p=0.402$).

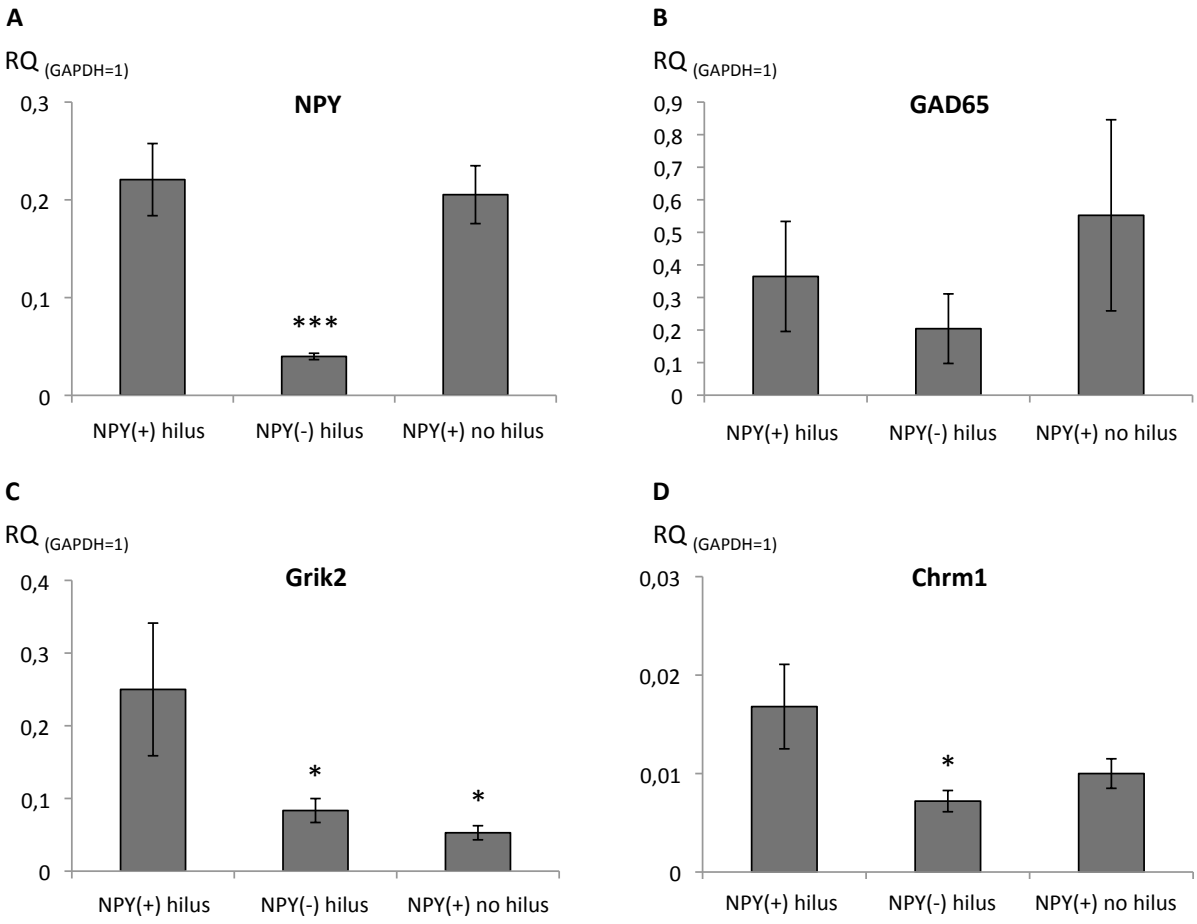

Fig. 3.1.2-5 Expression profile of NPY-positive interneurons in the hilus. (A) Determination of NPY mRNA levels confirmed the specificity of the approach, comparing mRNA expression levels in laser capture microdissected NPY-positive cells of the hilus (NPY(+) hilus) with the remaining hilus tissue (NPY(-) hilus) and NPY-positive cells in other hippocampal subareas (NPY(+) no hilus). (B) NPY-positive cells were indeed interneurons, but also other GABAergic interneuron subopulations exist in the hilus, as indicated by expression of GAD65 as a marker gene. (C) The ionotropic glutamate receptor from the kainate type, subunit 2 (Grik2), showed enriched expression in hilar interneurons. (D) The muscarinergic receptor type 1 (Chrm1) was preferentially expressed in NPY-positive hilar interneurons as well. All values relative quantification to housekeeping gene GAPDH (RQ to GAPDH with GAPDH expression=1), mean±SEM. * significant difference to NPY(+) Hilus, $p < 0.05$; *** $p < 0.001$.

In summary the expression analysis of NPY-positive interneurons first confirmed that the GFP-labeled cells analyzed here, are indeed a subpopulation of GABAergic interneurons that are also positive for the neuropeptide somatostatin, as it has been

described before (McDonald, 1989; Fu & van den Pol, 2007). Secondly, a distinct expression of the ionotropic glutamate receptor Grik2 and the muscarinergic acetylcholine receptor type 1 (Chrm1) in this interneuron population in the hilus was revealed. This may allow a specific triggering of hilar NPY interneurons during auditory cued fear memory formation leading to modulation of contextual salience.

Kainate receptors are ionotropic glutamate receptors combined of several different subunits (GluR5, 6 and 7, as well as KA1 and 2) that are expressed pre- and postsynaptically with a high density in the hippocampus (Kamiya, 2002). Expression of Grik2 (also known as GluR6) in hippocampal interneurons, at least of the CA1 region, has been described before and is thought to contribute to spontaneous and evoked inhibitory postsynaptic currents (IPSCs; Mulle et al., 2000). Moreover, firing rates of CA3 interneurons in the *stratum oriens* are also modulated by GluR6 and 7 and downregulated in rats with a chronic stimulation of the BLA and could contribute to changes in oscillatory activity of the hippocampus (Gisabelle et al., 2012). In general, Grik2 appears to be a possible target molecule for modulation of hippocampal activity via the BLA. Indeed, Grik2, but not Grik1 knock out mice display also reduced contextual and cued fear memory, most likely mediated by altered synaptic potentiation in the amygdala, although physiological properties of the hippocampus were not assessed in these animals (Ko et al., 2005). Chronic kainate application and its stimulation of kainate receptors evoke epiletic activity in the hippocampus and is therefore used as a well-established model to study this disease. Interestingly, in a chronic epileptic state a hyperinhibition of DG granule cells is observed (Sloviter et al., 2006) that is paralleled by increased levels of NPY and the NPY receptor Y2, which inhibit glutamate release and provide some level of control in the hyperexcited, epileptic hippocampus (Silva et al., 2005). In another mouse line deficient for Grik2, kainate-induced seizures are reduced and the induction of the immediate early gene c-Fos in the DG by kainate is prevented (Mulle et al, 1998), suggesting a prominent role of Grik2 in modulating excitability of the DG. Together, evidence exists for a modulation of DG signaling by Grik2, at least in part possible via interneuron circuits and in interplay with NPY. This highlights Grik2 as a possible candidate for modulation of NYP-positive interneuron signaling also during acquisition and/or consolidation of contextual fear memory balance in a cued fear conditioning paradigm.

Modulation of signaling in NPY-positive interneurons of the hilus could be also modulated by muscarinic neurotransmission. Projections using acetylcholine as

neurotransmitter arise from cell clusters in the basal forebrain, namely the *nucleus basalis magnocellularis* projecting to the frontal cortex and amygdala and the medial septal area projecting to the hippocampus. Acetylcholine can bind either to nicotinic or muscarinic receptors, which are both composed of different subunits and distinct in their pharmacological and signaling properties (Tinsley et al., 2004). Here, only the expression of the muscarinic receptor subunits, M1 to M4, in NPY-positive hilar interneurons was analyzed. Various pharmacological blocking experiments on the impact of the muscarinic system on fear memory formation have been made, e.g. using the antagonist scopolamine, with mixed but very interesting results. It appears that scopolamine is effective in blocking the acquisition of contextual fear memory, while effects on consolidation depend on the training protocol. Cued fear memory formation seems unaffected by pre- or posttraining scopolamine treatment (Tinsley et al., 2004; Robinson et al., 2011). Moreover, muscarinic blockade in the dorsal hippocampus is sufficient to impair contextual fear memory (Gale et al., 2001; Wallenstein & Vago, 2001) and depends mostly on the M1 receptor subunit (Soares et al., 2006). Interestingly, mice deficient for M1 display reduced freezing to a tone after fear conditioning (Miyakawa et al., 2001), while in another M1 knock out model no differences in cue freezing were described. However, these animals initially show even enhanced contextual freezing, but also increased forgetting of contextual fear 30 d posttraining (Anagnostaras et al., 2003). Reduced contextual freezing was also observed in mice deficient for the M3 subtype (Poulin et al., 2010), while M2 knock out mice displayed no differences in cued or contextual fear memory (Bainbridge et al., 2008).

M1 but not M2 or M4 receptors regulate the excitability of interneurons in the dentate gyrus by increasing the phasic inhibitory output and enhancing the activity of basket cells, thus promoting theta and gamma oscillation (Chiang et al., 2010). But also the activity on NPY- positive interneurons most likely depends on cholinergic input, since loss of it by septal deafferentation decreases NPY levels in the dentate gyrus and alters synaptic connectivity in the surviving NPY interneuron subpopulations (Milner et al., 1999). Together, the enrichment of M1 receptor subunits in the NPY-positive interneurons of the hilus on the one hand and the strong dependence of contextual fear memory acquisition/consolidation on this receptors on the other hand underlines further the importance of hilar NPY interneurons on contextual fear memory formation.

In contrast, the dopamine receptor D2 displayed a reduced expression in hilar NPY-positive interneurons, but not in others in the hippocampus. Experiments using

dopamine receptor type 1 and 2 (D1 and D2) agonists and antagonists suggested an involvement of D2 in the expression rather than consolidation of conditioned fear (de Oliveira et al., 2006). However, in mice deficient for D1 or D2 stabilization of fear memory is disturbed (Fadok et al. 2009). Reduced activation of dopaminergic neurons in transgenic mice impaires cued fear memory formation (Zweifel et al., 2012). Finally, stimulation of dopamine release by amphetamine in the hippocampus reduces freezing to the context, but not to the cue (White & Salinas, 2003). Therefore, a reduced responsiveness to dopamine in hilar NPY interneurons could contribute also to the regulation of cue/context balance.

All together, experiments targeting specifically M1 and Grik2 signaling in NPY interneurons of the hilus will reveal whether this candidate molecules have a striking impact on activity of these interneuron populations, on NPY release and signaling and on fear memory formation.

A disadvantage of pharmacological blocking experiments is, that the specific targeting of interneurons in the hippocampus is not possible. Both, M1 and also Grik2 are expressed at large also on granule cells, resulting in modulation of excitatory cell signaling when local blockers are administered. Using conditional viral vector systems, a specific knock down of M1 or Grik2 in NPY-positive interneurons in combination with local hilar application of the virus would be ideal. Then, it would be possible to assess the contribution of M1 and Grik2 signaling in NPY-positive hilar interneurons to the formation of a cue- and context-specific fear memory by celltype-specific pre-training knock down. In addition to the behavioral read out, such viral vector systems could be further used to study the impact of such a knock down on NPY expression and signaling (in combination with NPY receptor blockers) or the ability of NPY interneurons to be activated by CREB phosphorylation. Furthermore, it would be possible to study changes in physiological properties of feedback and feedforward inhibition in the dentate gyrus or synaptic transmission of NPY-positive interneurons themselves. In addition to gaining more insights in mechanism mediation cue/context balance during fear memory formation, valuable basic information about interaction of NPY with other neurotransmitter systems on local DG circuit function could be collected, with implications for disorders like epilepsy, Alzheimer's disease or anxiety disorders.

3.1.2.4 NPY-positive interneurons in the hilus as mediators of contextual balance in auditory cued fear conditioning: Discussion & conclusions

As demonstrated in the section before, NPY expression levels were increased six hours after cued but not contextual fear conditioning in the DG of the dorsal hippocampus. This suggested an involvement of either NPY-positive interneurons in the hilus or even NPY signaling itself in the determination of the cue-context balance after auditory cued fear conditioning. Both possibilities were investigated in this study.

First, by analyzing the induction of transcription factors in this cell population, a specific activation of NPY-positive interneurons by P-CREB in the hilus, but not in the CA1 SO was observed. This activation took place only after cued but not contextual fear conditioning and was functionally relevant for the determination of contextual fear memory. When P-CREB signaling was inhibited in these interneurons by expression of a dominant negative isoform of CREB in SST/NPY-positive interneurons in the hilus, increased freezing towards the environment of the conditioning occurred.

Second, by pharmacologically blocking NPY signaling prior to auditory cued fear conditioning, again such an increased contextual generalization was observed. Thus, not only the NPY-positive interneurons in the hilus, but NPY itself contributes to the determination of contextual salience. Moreover, NPY action in this process was specific for fear memory acquisition and/or consolidation, since blocking of NPY signaling before retrieval had no impact. In addition, NPY is not involved in formation of contextual fear memory *per se*, but in the balance of contextual fear memory in relation to a salient cue, as foreground contextual fear memory after unpaired fear conditioning was not affected by blocked NPY signaling as well.

Third, a specific targeting of NPY-positive interneurons in the DG is possible via glutamatergic inputs, activating Grik2 and via acetylcholinergic neurotransmission, activating M1 receptors.

Together, these findings further support the role of the DG in fear memory formation. Indeed, training and retrieval of contextual fear memory induce c-Fos in the DG (Skórzewska et al., 2006), although such transcriptional activation depends on amygdala inputs in the hippocampus (Huff et al., 2006). In this line, lesion of the DG or disturbed input to this structure impairs contextual fear memory in the background (Lee & Kesner, 2004a; Daumas et al., 2009).

Notably, despite the long proposed statement, that the amygdala mediates cued fear memory while only contextual fear memory involves the hippocampus (Philips and

LeDoux, 1992), this study further dissects the role of the hippocampus and the dorsal DG in cued fear memory formation in particular.

Thus, in addition to the well described anxiolytic action of NPY via the amygdala (Heilig, 2004; Primeaux et al. 2006), NPY in the DG appears to be necessary to actively suppress contextual encoding in association with the fear-eliciting stimulus to maintain low levels of contextual freezing to the insalient context. This is in line with recently described function of hippocampal NPY, where it normalized increased levels of fear and anxiety in an animal model of posttaumatic stress disorder (PTSD) via Y1 action (Cohen et al., 2012).

Together, hippocampal NPY function could provide a basis for new therapeutic strategies for the treatment of states of increased and generalized fear, as seen in anxiety disorders like phobia or PTSD.

3.1.3 Somatostatin in the lateral amygdala – detector of emotional salience?

3.1.3.1 Rationale

The marker gene for GABAergic interneurons, GAD65, shows circadian expression differences in the amygdala (Marlen Thiere, unpublished observations). Mice deficient for the GAD65 gene show changes in fear and anxiety related behavior dependent on the day time of testing (Dr. Jorge Bergado-Acosta, unpublished observations).

Question arises, whether the circadian regulation of fear and anxiety is mediated by certain interneuron populations in the amygdala.

Analysis of mRNA expression levels 6 h after fear conditioning revealed an increase of the neuropeptide somatostatin (SST) in the lateral subnucleus of the amygdala, regardless of conditioning to an auditory stimulus or to the training context. Moreover, SST mediates anxiolytic behavior responses via amygdala and septum (Yeung & Treit, 2012). A dynamic regulation of SST in different fear and anxiety-related paradigms could therefore also contribute to circadian differences in response to highly emotional experiences occur.

To check for circadian differences in SST levels, an Enzyme-linked Immunosorbent Assay (ELISA) was done by Bettina Müller on amygdala samples. Here, the basolateral complex of the amygdala, comprised of the basolateral and lateral subnucleus, was dissected manually at two different time points of the mouse active phase, at T1 (1h after lights off, 8.15-9.15 am with inverse 12 h light-dark-cycle) or at T7 (7h after lights off, 14.15 to 15.15 pm), respectively. There, a small, but significant increase in SST peptide levels was observed in amygdala samples prepared at T7 compared to T1 (see Appendix A.10 for details on methods and results).

To assess now whether SST expression influences fear and anxiety-related behavior, mice deficient for SST ($SST^{-/-}$) and their wildtype littermates ($SST^{+/+}$) underwent a battery of behavioral tests at T1 and T7, where SST expression is different in wildtype mice.

First, $SST^{-/-}$ and $SST^{+/+}$ mice were randomly assigned to the T1 and T7 test time points. General activity and anxiety-like behavior were assessed in an open field that all mice were allowed to explore freely in a 20 min test session at T1 (N for $SST^{+/+}$ =6; N for $SST^{-/-}$ =7) and T7 (N for $SST^{+/+}$ =8; N for $SST^{-/-}$ =7; due to technical problems in automated behavioral tracking one animal was excluded from analysis). One day after the open field tests, animals tested in the open field at T1 received a light-dark-avoidance (L/D) test

now at T7 and *vice versa* (T1: N for $SST^{+/+}$ =8 and N for $SST^{-/-}$ =6; T6: N for $SST^{+/+}$ =7 and N for $SST^{-/-}$ =7; due to technical problems in automated behavioral tracking one animal was excluded from analysis). Here, animals were placed in the light compartment that was joined with a dark compartment and were allowed to explore both compartments freely in a 5 min test session.

On day 3 the auditory cued fear conditioning paradigm started with four adaptation sessions (twice per day; 2 min exposure to the conditioning context, followed by six exposures to a neutral tone (CS-: 2.5 kHz for 10 s, 80 dB); 20 s ISI). On the consecutive day, paired auditory cued fear conditioning training took place (2 min exposure to the training context, followed by three tones (CS+: 10 kHz for 9 s, 80 dB) paired to footshocks (US: 0.4 mA for 1 s), 20 s ISI). Here, animals of both genotypes were randomly assigned to two groups, receiving the training either at T1 (N for $SST^{+/+}$ =7; N for $SST^{-/-}$ =7) or at T7 (N for $SST^{+/+}$ =8; N for $SST^{-/-}$ =7). Two days later fear memory to the auditory cued tone and the training context was tested separately for all animals in the morning. For retrieval of the auditory cue mice were placed in a neutral context (plexiglas standard cage with bedding) and received after 2 min in the context four CS- (10 s each, 20 s ISI) and four CS+ (10 s each, 20 s ISI). One hour after the cue retrieval, the test animal was re-exposed to the training context for 2 min.

3.1.3.2 Lack of circadian fluctuation of anxiety-like behavior in SST mutant mice

In the open field, a multifactorial ANOVA for genotype x time point of testing revealed significant effects of genotype ($F(1,24)=4.792$; $p=0.039$) on general activity of $SST^{-/-}$ mice and their wildtype littermates as indicated by the total distance walked in the 20 min open field test sessions (effect of time point: $F(1,24)=0.118$; $p=0.734$; interaction genotype x time point: $F(1,24)=2.159$; $p=0.155$). A direct comparison of the different time points demonstrated increased distance for $SST^{-/-}$ mice at T7 (Fig. 3.1.3-1A; $F(1,13)=10.982$, $p=0.006$), while no genotype difference was observed for T1 ($F(1,11)=0.172$; $p=0.686$). The time spent in the center of the open field as a measure for anxiety-like behavior was neither affected by genotype (Fig. 3.1.3-1B; $F(1,24)=0.172$; $p=0.682$) nor time point of testing ($F(1,24)=0.100$; $p=0.755$), nor the interaction of both factors ($F(1,24)=0.066$; $p=0.799$). This data indicates a moderate hyperactivity of $SST^{-/-}$ mice at T7.

In the light-dark-avoidance test, multifactorial ANOVA revealed significant effects for genotype ($F(1,24)=6.226$, $p=0.02$) and time point of testing ($F(1,24)=4.302$; $p=0.049$;

interaction genotype x time point: F(1,24)=1.563; p=0.223) on the distance walked in the light compartment. Distance in the light compartment was significantly enhanced at T7 in $SST^{+/+}$ mice (Fig. 3.1.3-1C; comparison of time points in $SST^{+/+}$ mice: F(1,13)=4.798), p=0.047), but not in $SST^{-/-}$ mice, resulting in a genotype specific effect at T6 (F(1,12)=9.403, p=0.01), but not T1 (F(1,12)=0.615; p=0.448). Next to such increased activity in wildtype but not SST deficient mice at T7, time spent in the light compartment was also enhanced at T7 in $SST^{+/+}$ mice (Fig. 3.1.3-1D; multifactorial ANOVA: effects of genotype (F(1,24)=6.148, p=0.021; but not time point of testing: F(1,24)=2.271; p=0.145; or interaction genotype x time point: F(1,24)=0.389; p=0.539), as this is further confirmed by paired comparison of genotypes for each time point (T7: F(1,12)=5.626; p=0.035; T1: F(1,12)=1.502; p=0.244).

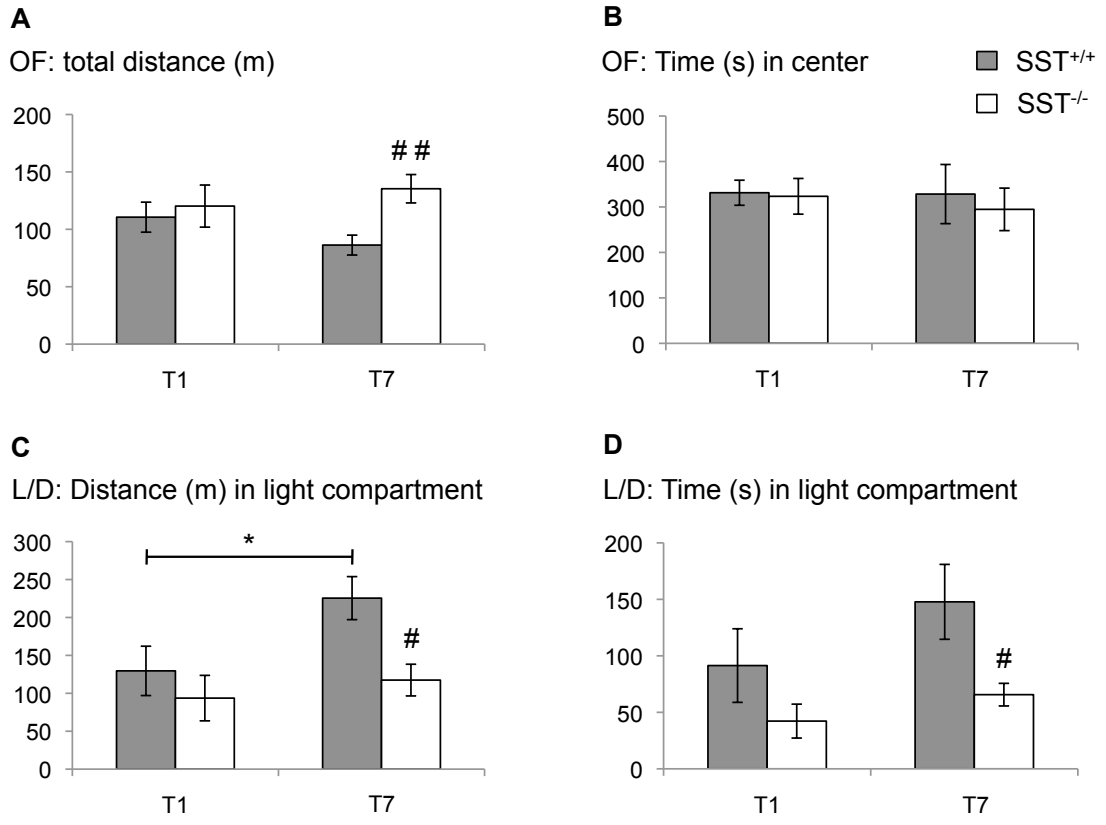

Fig. 3.1.3-1 Failed circadian fluctuation of the anxiety-like behavior in SST mutant mice. (A) $SST^{-/-}$ mice displayed hyperactivity at T7 as indicated by total distance walked in the open field. (B) Time spent in center did not differ between genotypes or time of testing. (C) However, in the light-dark avoidance (L/D) test, wildtype mice displayed increased locomotion in the light compartment at T7, while $SST^{-/-}$ mice showed no increase in activity. (D) Accordingly, time spent in the light compartment at T7 was increased in $SST^{+/+}$ but not in $SST^{-/-}$ mice, thus indicating a circadian modulation of anxiety-like behavior in the light-dark test that is not observed in SST deficient mice. Values are mean ± s.e.m. * Significant differences between time point of testing, p<0.05; #, significant differences between $SST^{-/-}$ and $SST^{+/+}$ mice, p < 0.05; ## p < 0.01.

Together, these data indicate a circadian modulation of anxiety-like behavior in wildtype mice with decreased anxiety in the second half of the dark phase. $SST^{-/-}$ mice did not display such a circadian modulation of anxiety-like behavior.

To date, several studies exist showing a rather weak circadian modulation of anxiety and overshadowed by other factors, for example the illumination conditions during the test or genetic background effects (Post et al., 2011; Bertoglio & Carobrez, 2002; Jones & King, 2001). In these studies, often anxiety-like behavior in the dark versus the light phase was tested instead of different time points in the active phase, the dark phase respectively. In this study now two time points at the beginning of the first and the second half of the active dark phase were compared. At these time points, I observed a differential response in anxiety-like behavior in the second half of the dark phase in naïve C57BL/6 mice also in other independent studies before (see also Fig. 3.3.3-3: increased activity in the light compartment in light-dark-avoidance test at T7 vs. T1). The same is also observed now in $SST^{+/+}$ mice with decreased anxiety in the light-dark-avoidance test at T7. However, anxiety-like behavior in the open field did not differ between time points of testing, suggesting again dependence on the test conditions.

Interestingly, such a circadian difference in anxiety-like behavior was not observed in $SST^{-/-}$ mice. In their initial screening by Zeyda et al. (2001), $SST^{-/-}$ displayed only insignificant trends towards reduced locomotor activity in the open field without any differences in center entries and a trend towards increased time spent in the dark compartment during a L/D test. However, here $SST^{-/-}$ mice even increased their locomotor activity in the open field, but only at T7. Therefore, the trends towards differences in OF and L/D test described by Zeyda et al. (2001), could depend on the time point of testing and a circadian profile in wildtype mice, since genotype-specific differences occurred only at T7. Interestingly, such differences appear to result from a circadian modulation of anxiety-like behavior in wildtypes that is abolished in $SST^{-/-}$ mice. This suggests an involvement of somatostatin in expression of anxiety-like behavior. Indeed, recent pharmacological studies (Yeung et al., 2011; Yeung & Treit, 2012) demonstrate a crucial involvement of SST in anxiety via activation of the SST type 2 receptor (SST R2) in the amygdala, but also in the septum.

Using Enzyme-linked Immunosorbent Assay (ELISA), SST peptide levels were assessed by Dr. Bettina Müller at T1 and T7 in the basolateral complex of the amygdala. SST peptide levels were increased at T7 compared to T1 in the amygdala. With respect to the pharmacological findings, increased levels of amygdalar SST could contribute to the

reduced anxiety-like behavior in wildtypes at this time point. In addition, no differences in anxiety were observed towards SST$^{-/-}$ mice at T1, despite their total lack of SST. This suggests, that anxiety responses are mediated by multiple factors and deficiency for SST can be partially compensated by other factors, e.g. expression of other anxiolytic neuropetides (e.g. NPY; Heilig, 2004) and/ or compensatory regulation of SST receptors (e.g. SST-R2; Viollet et al., 2000). Moreover, it was recently demonstrated for the hippocampus, that signaling factors of the Mitogen-activated phosphate kinase (MAPK) pathway show also a circadian regulated expression pattern (Eckel-Mahan et al., 2008) that could contribute to the modulation of the anxiety-like response as well (Wefers et al., 2012).

3.1.3.3 No influence of day time of training on auditory cued fear memory

Fear memory to the conditioned tone, the CS+, was not affected by the time point of auditory cued fear conditioning training (Fig. 3.1.3-2A; multifactorial ANOVA: $F(1,25)=1.663$; $p=0.209$), nor by the genotype ($F(1,25)=0.174$; $p=0.68$) or an interaction of both factors ($F1,25)=0,00$; $p=0.993$). Likewise, freezing to the context was neither affected by genotype (Fig. 3.1.3-2B; $F(1,25)=0.206$; $p=0.654$), different training time points ($F(1,25)=0.061$; $p=0.807$) nor the interaction of both factors ($F(1,25)=0.011$; $p=0.918$). In addition, no generalization to the neutral tone, CS-, was observed dependent on genotype ($F(1,25)=1.507$; $p=0.231$) or training time point ($F(1,25)=1.116$; $p=0.301$; interaction genotype x time point: $F(1,25)=0.001$; $p=0.977$).

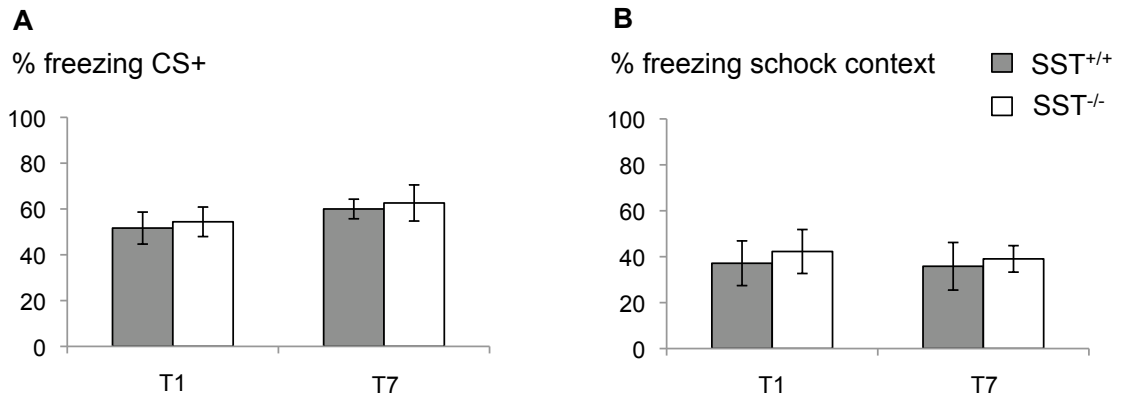

Fig. 3.1.3-2 No influence of day time of training on auditory cued fear memory. (A) Freezing towards the conditioned tone (CS+) did not differ between animals receiving auditory-cued fear conditioning training on different time points of the dark phase. (B) Freezing towards the context in which the training had taken place was not influenced by the time point of training. No deficits in either the fear response to the tone or to the shock context could be observed in SST$^{-/-}$ mice. Values are mean ± SEM.

These results indicate no circadian regulation of fear memory formation in wildtype mice of this line. In addition, $SST^{-/-}$ mice displayed no deficits in tone- or context-dependent fear response per se.

Previous studies report a strong influence of circadian factors and time of the day on memory formation in different species (Gerstner et al., 2009), suggesting "time-stamping" of episodic memory (O'Brien & Sutherland, 2007) and increased aversive memory when training is performed during the light, hence naturally inactive phase in mice and rats (Chaudhury & Colwell, 2002). In this study, using two training time points in the dark phase, no differences in contextual or cued fear memory were observed. In addition, whether the retrieval was done 48 h posttraining, at the same time of the day like the training or 42 h posttraining for the T7 group did not influence fear memory. This suggests also a reduced impact of "time-stamping", i.e. the contingency between day time of training and retrieval in the paradigm used here.

A previously observed deficit on contextual fear memory in $SST^{-/-}$ was not observed here. A disturbed acquisition of contextual fear memory is described in $SST^{-/-}$ mice after training with rather low US intensities (0.2 mA; Kluge et al., 2008), but not when using stronger US intensities (0.7 mA; Zeyda et al., 2001). This suggests an involvement of SST in fear memory formation in interplay with other factors that can be overcome by stronger training. In addition, altered expression and function of other molecular factors could compensate for the conventional knock out of the SST gene and mask effects of SST deficiency.

3.1.3.4 Somatostatin in the amygdala as a detector of emotional salience: Discussion & conclusions

Together, the data suggests a circadian modulation of anxiety-like behavior within the active phase of the mouse. Anxiety-like behavior was decreased at a time point when SST peptide levels were enhanced in the amygdala. Anxiolytic properties of SST are mediated by SST R2 activation in the amygdala (Yeung & Treit, 2012). Accordingly, in mice deficient for SST R2 the anxiety-like response in various behavioral tests is increased while exploratory behavior is inhibited in mildly aversive situations like the open field test (Viollet et al., 2000). SST is expressed in interneurons (Macagni et al., 2007), but its function in the amygdala on cellular level is not well understood. In the hippocampus, a morphologically distinct type of SST-positive interneurons is better studied. These so-called O-LM cells, receive local recurrent collaterals from pyramidal

neurons and take part in feedback inhibition, thereby also generating and controlling rhythmical hippocampal network activity (Maccaferri & Lacaille, 2003). Inhibition of pyramidal neurons by SST is described in the lateral amygdala as well, where activation of SST R2 results in hyperpolarization of pyramidal neurons via activation of inwardly rectifying potassium currents (GIRKs; Meis et al., 2005).

Inhibition of the amygdala would also affect the interaction with the hippocampus that is required for contextual fear memory formation. Indeed, in $SST^{-/-}$ mice acquisition of contextual fear memory was disturbed when a rather weak aversive stimulus was used (Kluge et al., 2008). However, with a more intensive training protocol used here, no such deficits were found, although the same training protocol induced expression of SST mRNA in the lateral amygdala (see section 3.1.1, Fig. 3.1.1-1).

Together, the disturbance of anxiety-like behavior in mild aversive test and of fear memory only after weak training in $SST^{-/-}$ mice suggests an involvement of amygdalar SST signaling dependent on the intensity of aversive stimuli. Indeed, a recent study demonstrated an activation of SST-positive interneurons in the BLA only after mild behavioral stress in the elevated plus maze test, while the activation was suppressed after exposure to ferret odor that elicits a strong fear response (Butler et al., 2012).

In this line, inhibitory actions of SST in the amygdala could prevent inappropriate overexcitation during processing of mildly aversive stimuli. Under conditions of stronger emotional salience like fear conditioning, a certain level of amygdala activation is required for robust fear memory formation. The observed induction of SST mRNA during the consolidation stage of cued and contextual fear memory could contribute also to these well-balanced processes in concert with other molecular factors. Hence, also the results obtained here cannot conclusively confirm its role in salience determination of aversive events, SST in the amygdala appears to be involved in processing of anxiety and fear related information. Further experiments and refined tools are required to confirm and reveal mechanisms of SST action in the amygdala in response to emotional stimuli.

3.2 Model 2: Role of interneurons in CA1 in a PTSD-model of juvenile stress

3.2.1 Rationale

Posttraumatic stress disorder (PTSD) is described as a maladaptation to a potentially threatening event, the so-called trauma, and is defined by core symptoms that persist over time, i.e. intrusive memories related to the trauma, emotional numbing and social withdrawal, avoidance and hyperarousal (Sherin & Nemeroff, 2011). Interestingly, only a subset of individuals that experience a trauma will develop these severe disturbances (< 10%; Breslau, 2009) and presumably the individual risk of developing PTSD is defined by genetic as well as environmental factors (Yehuda & LeDoux, 2007).

Based on epidemiological data reporting increased susceptibility to PTSD in individuals with childhood adversity in their personal history (Yehuda & LeDoux, 2007; Sherin & Nemeroff, 2011), an animal model for PTSD was developed by Gal Richter-Levin and co-workers consisting of combined stress experiences in juvenile and adult stages. In this behavioral model, rats are exposed to variable psychological stress during their juvenile phase (juvenile stress; JS). Here, intensive uncontrollable stressors are applied, namely forced swimming for 15 min at P28, elevated platform stress for three times 30 min (1 hour intervals) at P29 and restraint stress for 2 h at P30. In their young adult life, rats are again exposed to a stressful event (adult stress; AS) that can be either a reminder stress, e.g. again forced swimming for 15 min, or a more complex behavioral paradigm like active avoidance training in a shuttle box or fear conditioning. In the later, the impact of juvenile stress on learning can be analyzed and indeed a number of PTSD-related behavioral changes are described after combined JS and AS (JSAS). Next to increased anxiety in an open field and elevated plus maze, the JSAS animals show reduced active avoidance learning and instead a shift towards learned helplessness behavior in the shuttle box (Avital & Richter-Levin, 2005; Tsoory & Richter-Levin, 2006; Avital et al., 2006).

In mice, using auditory-cued fear conditioning as the second hit in adulthood (Iris Müller et al., unpublished observations), an increase of contextual fear memory after JSAS was observed. Thus, the combined stress enhances the salience of the multimodal contextual information that is usually in the background. Such a phenotype could also explain PTSD-related symptoms of intrusive memories triggered by cues that had been associated to the traumatic event despite being predictive for it.

On the level of hippocampal network function, Maggio & Segal (2011) could demonstrate differential changes in CA1 long-term potentation (LTP) in ventral vs. dorsal hippocampus that lasted for up to three weeks when rats underwent the JSAS paradigm previously, but were transient when only one stressor (either JS or AS) was applied. By that, LTP in the CA1 area of the dorsal hippocampus was lastingly decreased, whereas in the ventral CA1 region long-term depression (LTD) was shifted to LTP, resulting in enduring enhanced activity of the ventral hippocampus after combined stress. Such stress effects on hippopcampal network function are known to be mediated, at least in part by GABAergic interneurons (Maggio & Segal, 2009) and indeed, altered expression of different subunits of GABA A receptors is observed after juvenile stress (Jackobson-Pick et al., 2008). To gain insights in molecular mechanisms related to GABAergic interneuron functions, I investigated long-lasting changes in mRNA expression of molecules relevant for GABA function in the ventral and dorsal hippocampus in the JSAS PTSD model.

For this, young male Wistar rats (P27 to P29) received first variable stress (JS) as well as 15 min forced swimming in a water bucket at the age of 60 days (AS). The rats were left undisturbed except for animal care for another 14 days. Then, animals were sacrificed, brains were removed form the skull and snap frozen in liquid nitrogen. Next to animals receiving JSAS (N=6), animals of additional groups were exposed to only one stressful experience in juvenility (JS; N=6) or adulthood (AS; N=6). A control group (N=6) was handled only.

All brains were stored at -80°C. The behavioral part of this study was conducted by Menahem Segal ans co-workers at the Weizmann Institute, Rehovot, Israel. The brains were then shipped on dry ice to our lab where I performed cryosectioning and laser capture microdissection (LCM) of target areas.

From horizontal sections of the ventral and dorsal hippocampus sublayers of the CA1 region where isolated via LCM, *stratum oriens* (SO), *stratum pyramidale* (SP) and *stratum radiatum* (SR) respectively. After isolation and reverse transcription of total RNA, expression levels of different target genes relative to the housekeeping gene Glyceraldehyde 3-phosphate dehydrogenase (GAPDH) were assessed with quantitative real time PCR. The effect of the different treatment groups on target gene expression was analyzed via ANOVA for group for each gene in each subregion.

3.2.2 Long-term changes in gene expression in inhibitory and excitatory factors after JSAS

3.2.2.1 Long-term expression changes in GABAergic factors

Long-term effects, i.e. 14 d after JSAS, were analyzed on the expression of the GABAergic marker genes glutamate decarboxylase 65 and 67 (GAD65 and GAD67), as well as for GABA A receptor subunits α1 and α2 (Gabra1 and Gabra2, respectively) and the neuropeptides neuropeptide Y (NPY) and somatostatin (SST), which are expressed in subpopulations of GABAergic interneurons. Tab. 3.2-1 provides an overview of the observed changes (For F-values, see Appendix, A.11).

Tab. 3.2-1 Long-term mRNA expression changes after juvenile stress (JS), adult stress (AS) or the combination of both (JSAS) for selected GABAergic and glutamatergic marker genes in CA1 sublayers of the dorsal and ventral hippocampus. Changes may be driven by mineralocorticoid *(MR)* or glucocorticoid receptor *(GR)* expression changes as indicated by regression analysis (see Fig. 3.2-3). Significant increase/ decrease is indicated compared to control (#) or to JSAS (*), $p < 0.05$ each.

	DH CA1 SR	CA1 SP	CA1 SO	VH CA1 SR	CA1 SP	CA1 SO
GABAergic						
GAD65	=	=	=	↑ JS *, ↑ AS * *(GR)*	=	=
GAD67	=	=	=	=	=	=
Gabra1	=	=	=	↓ JSAS #	=	=
Gabra2	=	↑ JS #	=	=	↑ AS # *(MR)*	=
NPY	=	=	=	=	↓ AS #	=
SST	=	=	=	=	=	=
Glutamatergic						
Gria1		=			=	
Gria2		=			=	
Grin1		=			=	
Grin2a		=			↓ AS #	
Grin2b		=			=	

No changes were found in the mRNA expression of GAD67 and SST, while expression of NPY was decreased in the CA1 SP of the ventral hippocampus after single forced swim stress in adulthood (*post hoc* comparison with Fisher's PLSD: AS to JSAS: p=0.021; AS to

JS: p=0.016; AS to Control: p=0.007), but not after combined JSAS. In the same region, mRNA expression of Gabra2 was increased after single AS (to JSAS: p=0.009; to control: p=0.015). In addition increased expression of Gabra2 was also observed in CA1 SP of the dorsal hippocampus, but after JS only (to JSAS: p=0.025; to control: p=0.02).

An increase in mRNA expression of GAD65 was also observed after a single stress experience, either in juvenility or adulthood, in the ventral hippocampal CA1 SR subregion only (JS to JSAS: p=0.022; AS to JSAS: p=0.008), but were not observed when JS and AS occurred combined or in any other subregion of CA1 dorsal and ventral hippocampus (Fig. 3.2-1)

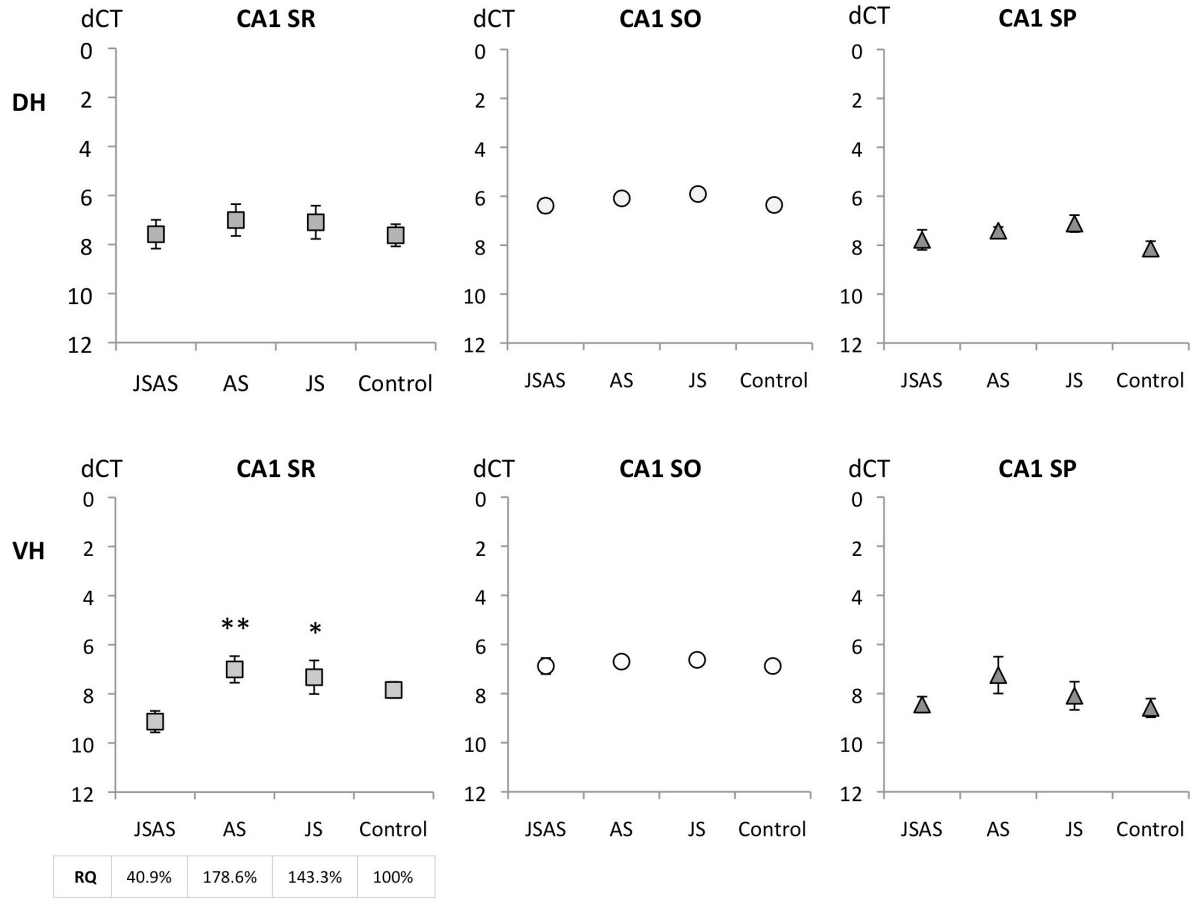

Fig. 3.2-1 mRNA expression of the GABA-synthezising enzyme GAD65 was increased after a single stress experience either in juvenility or adulthood in the *stratum radiatum* of the ventral hippocampus exclusively. Values in graphs dCT to GAPDH (mean±SEM); * significant difference to JSAS, p< 0.05; ** p<0.01

However, exclusively in the same region, CA1 SR VH, the mRNA expression of Gabra1 was reduced only when JS and AS were experienced in combination (JSAS to AS: p=0.028; to JS: p=0.013; to control: p=0.019; Fig. 3.2-2).

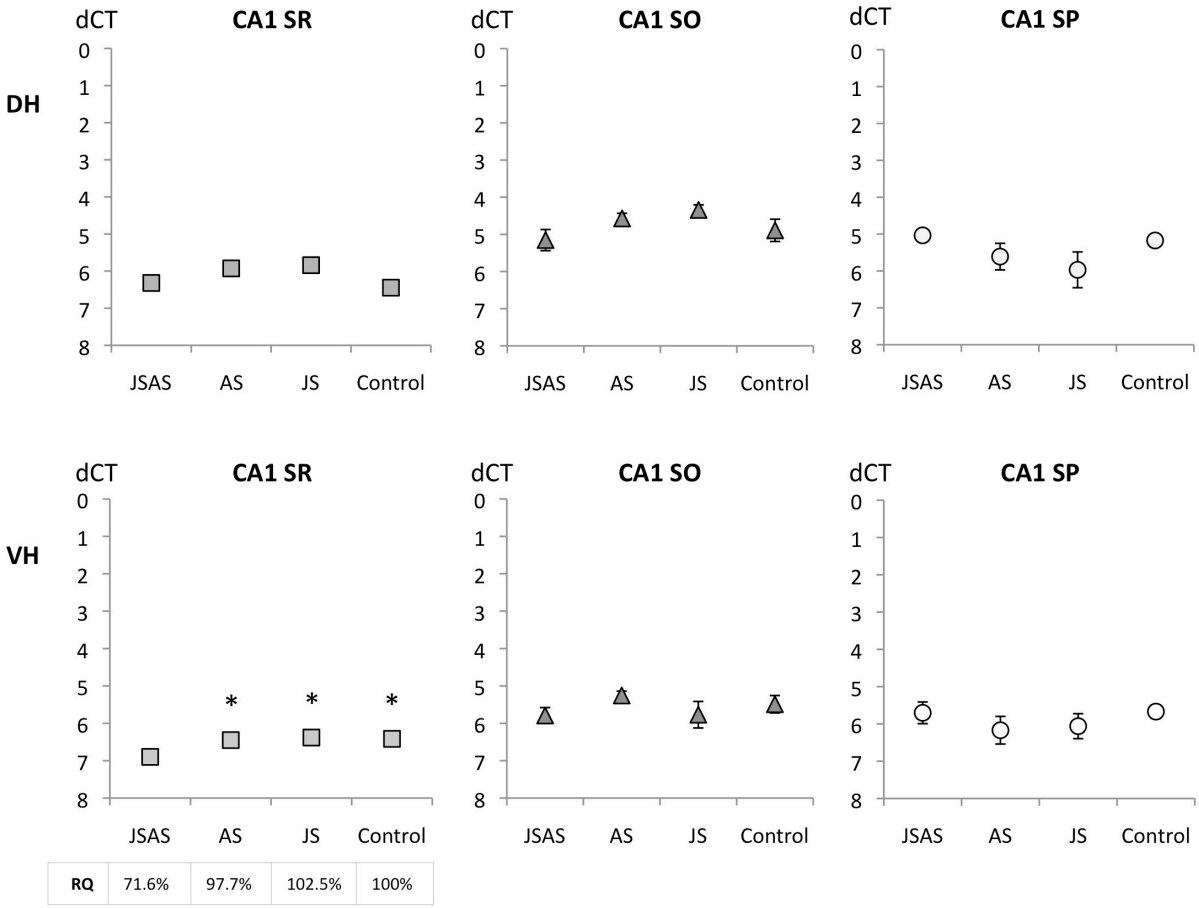

Fig. 3.2-2 The expression of Gabra1 (α1 subunit of GABA A receptor) was reduced only after combined juvenile and adult stress (JSAS) in *stratum radiatum* of the ventral hippocampus. Values in graphs dCT to GAPDH (mean±SEM); * significant difference to JSAS, p< 0.05; ** p<0.01

Together, distinct long-term expression changes of genes involved in GABAergic function were observed in the ventral hippocampus after juvenile and adult stress and after combined stress experience. On the presynaptic side, the mRNA of the GABA-synthesizing enzyme GAD65 was upregulated after juvenile or adult stress. Several studies could demonstrate that either acute or chronic stress is able to alter the expression of GAD65 in stress-relevant brain areas like hypothalamic subnuclei or the hippocampal subareas, like the DG (Bowers et al., 1998; Herman & Larson, 2001). Corticosterone administration as a hormonal mediator of the stress response affects also GAD65 expression in CA1 SO and SR sublayers, however, the observed reduction was only transient (Stone et al., 2001). In another set of experiments, chronic mild stress

was administered (for 6 weeks), which resulted in reduced GAD65 protein levels one month after the last stress. Interestingly, this was observed only in the ventral, but not the dorsal hippocampus and was paralleled by reduced GABA levels (Elizalde et al., 2010). A reduction in GABA levels can be achieved also by corticosterone application on hippocampal slices in vivo that can be reversed by both, GR and MR blockade (Martisova et al., 2012). Chronic corticosterone application however had no effect on GAD65 protein expression (Martisova et al., 2012). Together, the studies reviewed here found different effects of stress and corticosterone on GAD65 expression, dependent on the protocols engaged, levels of analysis (mRNA or protein) and expression detection methods. A high-resolution, but yet quantitative approach by combination of laser-capture microdissection and real time PCR was not used so far, meaning that expression changes in sublayers of the hippocampus are possibly missed in whole hippocampus preparations.

In this study, strikingly, no significant changes in GAD65 mRNA expression was observed when JS and AS were experienced combined, although severe alterations in ventral hippocampus excitability as well as on the behavioral level are described under this condition. If the lasting increase in GAD65 expression after a stressful experience contributes to PTSD susceptibility after a second hit occurs, a prevention of the GAD65 increase after single stress could have a rather protective effect on the development of PTSD-like symptoms. This hypothesis could be tested by e.g. viral knock down of GAD65 after juvenile stress in the CA1 SR of the ventral hippocampus specifically and administration of adult stress subsequently. After such a manipulation the lasting shift to LTP in the ventral hippocampus after JSAS or the behavioral alterations like increased anxiety or reduced active avoidance learning should be diminished.

A first support for this hypothesis comes from findings from Iris Müller from our lab. She engaged heterozygous GAD65 knock out ($GAD65^{+/-}$) mice in the combined JS and AS paradigm, that show a delayed maturation of the GABAergic system and reduced levels of GABA are described during juvenility and adolescence (Stork et al., 2000). After JSAS their wildtype littermates showed increase of contextual fear memory as a PTSD-related symptom. However, no such contextual generalization was observed in $GAD65^{+/-}$ mice after JSAS.

A complete knock out of the GAD65 gene ($GAD65^{-/-}$ mice) however results in increased anxiety (Kash et al., 1999) as well as altered conditioned fear behavior to a tone and the context with increased flight responses and intramodal generalization to a non-

conditioned tone stimulus (Stork et al., 2003; Bergado et al., 2008). Moreover, GAD65$^{-/-}$ mice show reduced postsynaptic inhibitory currents in the dorsal CA1 area (Tian et al., 1999), which are susceptible to modulation by the stress hormone corticosterone (Maggio & Segal, 2009) as well as reduced posttetanic potentiation and reduced paired pulse ratio (Tian et al., 1999), suggesting an altered function of excitatory and inhibitory synapses.

Thus, the development of the PTSD-like phenotype is dependent on a dynamic modulation of GAD65 expression during juvenility, when the first stressful experience occurs, and can contribute to the behavioral and electrophysiological alterations in the juvenile stress model of PTSD.

Next to the observed changes on presynaptic GABA-synthesis, an alteration of postsynaptic GABA A receptor subunit expression was also observed. Gabra2 mRNA expression was increased after single stress, either in juvenility or in adulthood, in the pyramidal layer of the dorsal or ventral hippocampus, respectively. The mRNA expression levels of Gabra1, however, were decreased after combined JSAS only, in the SR of the ventral hippocampus.

Changes in GABA A receptor subunit expression due to stress or to corticosterone in the hippocampus have been described in rats and mice (Orchinik et al., 1995; Matsumoto et al., 2007; Jacobson-Pick et al., 2008; Poulter et al., 2010), but again differ in protocols engaged, levels of analysis and expression detection methods. So revealed the analysis of expression on the protein level an increase of Gabra1 and Gabra2 in the whole hippocampus when mild stressors in juvenility where combined with mild behavioral stress in adulthood (Jackobson-Pick et al., 2008), while in this study differential effects on mRNA expression in hippocampal sublayers were observed. On the mRNA level, acute social stress elevates Gabra1 expression in the cortex, but no effects are found in the hippocampus (Kang et al., 1991), while chronic administration of corticosterone in doses observed also after stress decreases expression of Gabra1 and 2 in the DG but not the CA1 region of rats. In mice, on the other hand, chronic stress affects hippocampal Gabra1 or 2 expression only in a certain mouse strain (Poulter et al., 2010). In another chronic stress paradigm that has been described to evoke PTSD-like behavioral alterations, i.e. social isolation for more than four weeks, mRNA levels of Gabra1 and 2 were reduced in the hippocampus (Matsumoto et al., 2007).

Interestingly, not only can corticosterone affect GABA release (Martisova et al., 2012), Mikkelsen et al., (2008) suggested also a model how GABA via Gabra1 activation in

Hippocampus and mPFC, could modulate HPA axis activity via feedback on CRH neurons in the paraventricular nucleus of the hypothalamus Thereby, corticosterone and its release by stressful events can not only affect GABA A receptor subunit expression, but such changes itself can tune HPA axis response.

To test the functional relevance of the observed distinct changes in Gabra1 and Gabra2 expression the impact of either overexpression of Gabra1 in CA1 SR VH after JSAS or knock down of Gabra2 in CA1 SP DH after JS on PTSD-related electrophysiological and behavioral changes could be analyzed. Alternatively, it would be interesting to test whether a knock down of Gabra1 in animals that experienced only one stressor in juvenility would show alterations reminiscent of the PTSD-like phenotype.

3.2.2.2 GAD65 expression may be driven by glucocorticoid receptor changes

Since corticosteroids mediate many adaptive processes to stress and affect thereby behavior (Kaouane et al., 2012) and also cellular functions, especially in the hippocampus (Maggio & Segal, 2012), the mRNA expression levels of both corticosterone receptor subtypes, glucocorticoid receptors (GR) and mineralocorticoid receptors (MR), were also analyzed. Although no significant expression changes to JS, AS or the combination of both were detected, GR but not MR displayed expression profiles comparable to GAD65 in CA1 SR of the ventral hippocampus (Fig.3.2-3A, B). Therefore, regression analysis was performed using GAD65 dCT expression values as dependent variable of GR and MR dCTs. Indeed, expression of GAD65 was dependent on GR, but not on nor MR expression in this area (Fig. 3.2-3C), indicating a possible regulation of GAD65 expression by GR expression. An additional correlation analysis for dCTs of GAD65 and GR in CA1 SR VH for each treatment group revealed a strong association between mRNA expression of both factors after either JS (Pearson's correlation coefficient (2-tailed) r=0.978; p=0.001) or AS (r=0.959; p=0.002), but not after combined JSAS (r=0.491; p=0.322) or in controls (r=-0.729; p=0.1; Fig. 3.2-3D).

In addition, MR expression in ventral CA1 SP was associated with Gabra2 expression (see also Tab. 3.2-1).

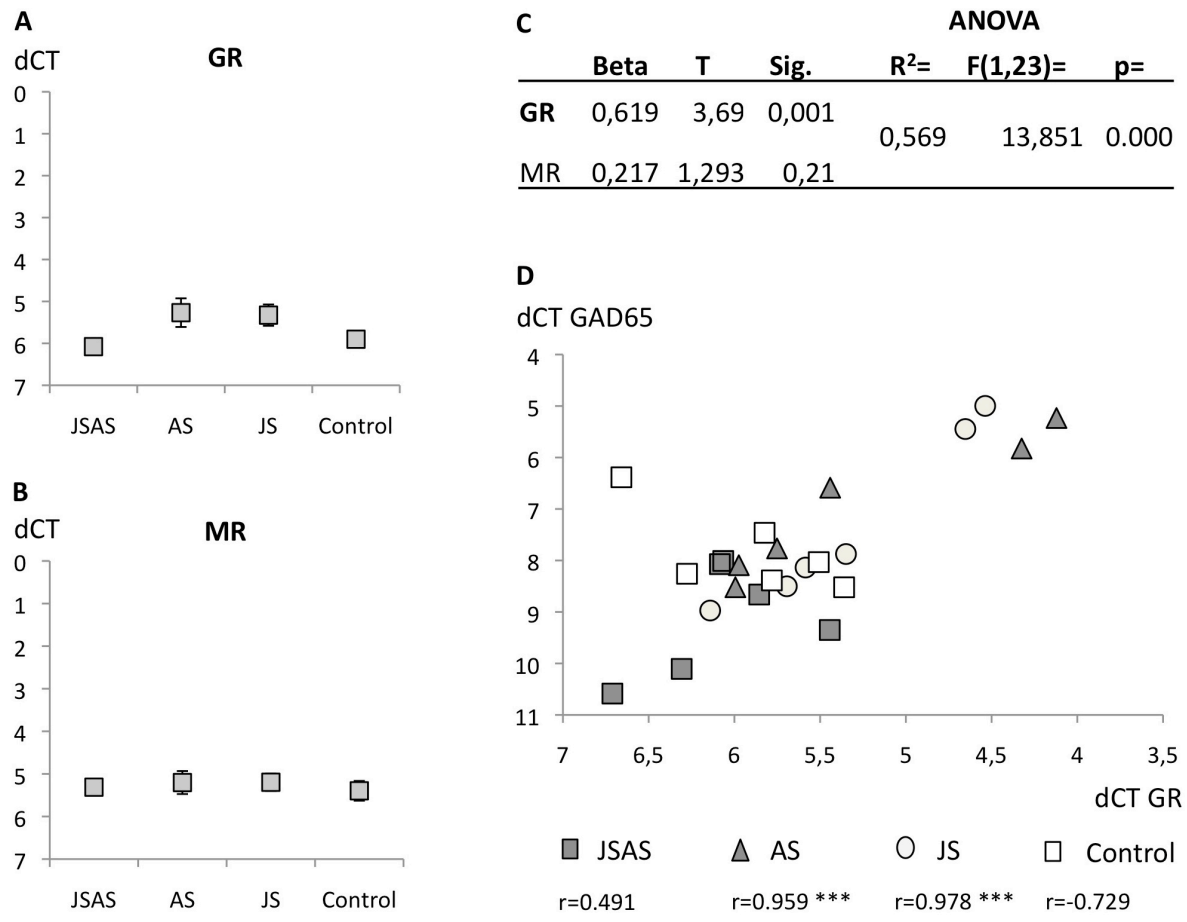

Fig.3.2-3 The Expression of GAD 65 in the *stratum radiatum* of the ventral hippocampus may be regulated by expression of glucocorticoid receptors (GR), but not mineralocortociod receptors (MR). (A) GR, but not (B) MR displayed comparable expression profiles to GAD65 after JSAS in CA1 SR VH. (C) Therefore, regression analysis was performed using GAD65 dCT expression values as dependent variable of GR and MR dCTs. Indeed, GAD65 expression was dependent on GR, but not MR expression in CA1 SR VH, suggesting possible expression regulation by GR. (D) Correlation analysis between dCTs of GAD65 and GR for each treatment group reveals a strong association between expression of both target genes after a single stress experience, either AS or JS, but not after combined JSAS. Values in graphs are mean dCT for each treatment group. Two-tailed Pearson's correlation coefficient (r) for each treatment group. *** significant correlation GR x GAD65, $p < 0.001$.

It has been reported that acute stressors modulated hippocampal GR and MR expression only transiently (Paskitti et al., 2000), while subchronic and chronic stress protocols had more lasting effects on GR and MR expression (Kitraki et al., 1999; Meyer et al., 2001; but see also Herman et al., 1999); in part also with a differential regulation in VH vs. DH (Romeo et al., 2007; Meyer et al., 2001). Moreover, as observed in another behavioral model of PTSD, single prolonged stress, administration of acute severe stress can have differential short- and long-term effects on GR mRNA expression, changing the relationship between GR and MR in hippocampal CA1 region lastingly (Liberzon et al., 1999).

The activation of glucocorticoid receptors can also trigger expression of different target genes (Datson et al., 2001; Morsink et al., 2007) either by direct action as a transcription factor or indirectly by induction of other transcription factors, e.g. NFKappaB (Djordjevic et al., 2009). By that, corticosterone release after stress can modulate the expression of target genes like GAD65 (Stone et al., 2001, Martisova et a., 2012).

3.2.2.3 Long-term expression changes in glutamatergic factors in association with GAD65 expression

On hippocampal network level inhibitory responses are always balanced against general excitability. Therefore, the expression of selected subunits of AMPA and NMDA glutamatergic receptors in the pyramidal cell layers of dorsal and ventral CA1 were also analyzed, namely Grin1, 2a and 2b (GluN1, GluN2A and GluN2B subunits of the NMDA receptor) as well as Gria1 and 2 (GluR1 and GluR2 subunits of the AMAP receptor; see Tab. 3.2-1 lower panel as well as Appendix A.11 for statistical details). Only a downregulation of Grin2a was observed after AS in CA1 SP VH (AS to JSAS: $p=0.027$; to JS: $p=0.004$; to control: $p=0.017$). To gain first insights in the balance between expression of excitatory and inhibitory factors a correlation analysis between GAD65 as a marker for GABAergic interneurons altered by stress and the selected glutamate receptor subunits was performed for each treatment group for CA1 SR VH. Strikingly, GAD65 was well correlated to the expression of Grin1, Grin2b as well as Gria1 and 2 after a single stress experience in either juvenility or adulthood but not after combination of both or in controls (Fig. 3.2-4 for examples). Thus, the loss of correlation in the JSAS group indicates a dysbalance of excitatory and inhibitory signaling in the ventral hippocampus.

Stressful experiences and corticosterone can influence also the expression of genes related to glutamatergic neurotransmission in the hippocampus, at least acutely and in certain time windows (Rosa et al., 2001; Owen & Matthews, 2007; Martisova et al., 2012). However, in this study long-term expression changes of selected NMDA and AMPA receptor subunits were not observed except for Grin2a after AS. Nevertheless, the expression profiles of the glutamatergic factors in the VH SR sublayer were well correlated with the expression of the interneuron marker GAD65 after a single stress experience either in juvenility or adulthood. After combined JSAS, this association was not longer observed, suggesting an alteration of excitation/inhibition balance in the ventral hippocampus driven by long-term changes of the inhibitory system.

	X GAD65
	■ JSAS
Gria1	r=-0,277; p=0,595
Gria2	r=-0,314; p=0,545
Grin1	r= 0,022; p=0,967
Grin2a	r=-0,037; p=0,944
Grin2b	r= 0,403; p=0,428
	▲ AS
Gria1	r= 0,889; p=0,018 *
Gria2	r= 0,834; p=0,039 *
Grin1	r= 0,880; p=0,021 *
Grin2a	r=-0,684; p=0,134
Grin2b	r= 0,861; p=0,028 *
	○ JS
Gria1	r= 0,985; p=0,000 ***
Gria2	r= 0,920; p=0,009 **
Grin1	r= 0,926; p=0,008 **
Grin2a	r= 0,976; p=0,001 **
Grin2b	r= 0,889; p=0,018 *
	□ Control
Gria1	r= 0,831; p=0,040 *
Gria2	r= 0,715; p=0,110
Grin1	r= 0,720; p=0,107
Grin2a	r= 0,819; p=0,046 *
Grin2b	r= 0,533; p=0,276

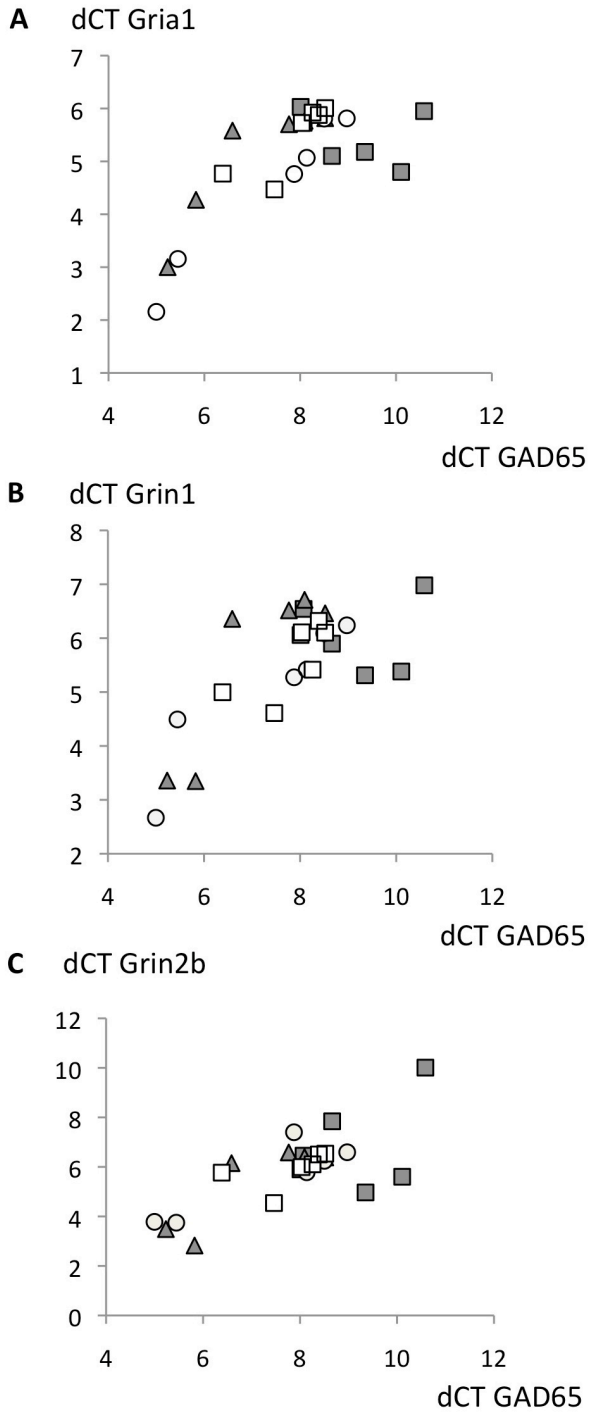

Fig. 3.2-4 Pearson's correlation (r) between the mRNA expression of GAD65, a marker for GABAergic interneurons, in CA1 SR and the expression of the AMPA receptor subunits GluR1 (Gria1) and GluR2 (Gria2) as well as the NMDA receptor subunits GluN1 (Grin 1), GluN2A (Grin2a) and GluN2B (Grin2b) in excitatory neurons of the CA1 SP subregion, in the ventral hippocampus respectively. After a single stress experience either in juvenility or adulthood expression profiles were well correlated. This correlation was lost in the JSAS group indicating a dysbalance of excitatory and inhibitory signaling in the ventral hippocampus. Correlagrams are shown for (A) Gria1 x GAD65, (B) Grin1 x GAD65 and (C) Grin2b x GAD65. All values in graphs are mean dCTs for each treatment group. * significant two-tailed Pearson correlation, $p < 0.05$; ** $p < 0.01$; *** $p < 0.001$

Such a dysbalance after JSAS could be tested by electrophysiological measures like the determination of conductance in patch-clamped neurons (e.g. Inhibitory post-synaptic current, IPSC; Maggio & Segal, 2009; LeRoux et al., 2006) in *ex vivo* preparations from stressed animals. However, pacth-clamp experiments are usually done in slice preparations from young animals, this approach could be technically difficult although straightforward. Alternatively, GABAergic transmission plays a key role in determination of hippocampal oscillatory activity at the theta and gamma frequency range (Colgin & Moser, 2010; Whittington & Traub, 2003). Theta activity in CA1 can be modulated by stress (Shors et al., 1997) and so far a reduced theta synchronization between amygdala and CA1 region was reported in GAD65 knock out mice (Bergado-Acosta et al., 2008). Therefore, it would be interesting to measure alterations of theta and gamma activity in the hippocampus of animals that underwent JSAS and examine the contribution of GAD65 and Gabra1 expression to such oscillatory activity.

3.2.3 Long-term expression changes after JSAS: Conclusions

Together, the data obtained in this study clearly indicate long-term gene expression changes after JS and AS or the combination of both in hippocampal CA1 subregions. Interestingly, the observed changes cumulate in the ventral hippocampus, namely in the SR sublayer. Here, GAD65 mRNA levels were increased after JS and AS, but not after the combination of both, while the expression of Gabra1 was decreased after JSAS. At least in part, some of the changes could be driven by GR expression.

Since Iris Müller observed contextual generalization after combined JSAS in wildtype, GAD65 and Gabra1 in the CA1 provide interesting molecular targets that could contribute to the shift in contextual salience after severe stress.

3.3 Model 3: Role of the ventral hippocampus in fear memory reactivation: interplay of anxiety and corticosterone

3.3.1 Rationale

Classical fear conditioning provides a well-established tool for studying the neurobiology of anxiety disorders like posttraumatic stress disorder (PTSD) or phobias in rodents (Siegmund & Wotjak, 2006; Stein & Matsunaga, 2006). In this paradigm the trained subject will form an associative memory between a previously neutral stimulus (e.g. a tone; conditioned stimulus, CS) and an aversive stimulus (a foot shock; unconditioned stimulus, US). Upon re-exposure to the CS or the training context the subject will then respond with fear in anticipation of the US. Moreover, fear memory is not simply retrieved, but the once consolidated memory trace becomes labile and susceptible to modulation again (Alberini, 2011; Rodriguez-Ortiz and Bermúdez-Rattoni, 2007). Such a process, called reconsolidation, may be engaged to destabilize fear memory in PTSD and phobia patients and update the reactivated memories with non-fearful information in specific therapeutic settings (Schiller et al., 2010). Otherwise, re-exposure to reminder cues have been also used to induce PTSD-like behavioral changes in rodents, indicated by alterations in anxiety-like behavior and stress responsiveness (Olson et al., 2011). As previous work in the lab demonstrates, a single re-exposure session of auditory cued fear memory results in increased freezing to the background context (Rehberg et al., 2011) and altered network activity in limbic areas (Narayanan et al., 2007b).

Fear memory formation and its reconsolidation depend also on the stress hormone corticosterone (McGaugh, 2000; Cai et al., 2008; Abrari et al., 2008). Interestingly, altered baseline corticosterone plasma levels or dysregulation of the hypothalamic-pituitary-adrenal (HPA) stress axis response upon stimulation are important features of various anxiety disorders, (Cameron & Nesse, 1988; Ströhle & Holsboer, 2003; Graeff et al., 2005; Yehuda, 2006; Meewisse et al., 2007; Vreeburg et al., 2010). Although the relation between cortisol in humans or corticosterone, its equivalent in rodents, and the formation of fear- and anxiety-related symptoms is complex and their neurobiological mechanisms are not well understood (Schwabe et al., 2011), empirical data propose even beneficial effects of elevated cortisol or cortisol agonists for the treatment of anxiety disorders (de Quervain, 2008; Soravia et al., 2006).

Therefore, studying the relationship between fear memory reactivation, anxiety and corticosterone could provide new insights in the neurobiological basis of anxiety disorders and lead to new therapeutical strategies.

The ventral hippocampus is thereby of special interest in this relationship. This structure is critically involved in anxiety and fear memory formation and expression (Bannerman et al., 2004; Trivedi and Coover, 2004). It possesses a close interconnection with amygdala and entorhinal cortex (Pitkänen et al., 2000) and interacts intimately with the HPA stress axis (Jacobson and Sapolsky, 1991), making the ventral hippocampus a prime target for stress and corticosterone signaling (Maggio & Segal, 2007; 2009).

In this study, long-term effects of fear memory reconsolidation were assessed on emotional behavior in mice and on ventral hippocampus function in relation to circulating corticosterone levels.

For that, male adult C57BL/6 mice went trough a six-week test schedule that was varied through five different experiments (see also Fig. 2-4): Pre-training anxiety levels were assessed in a 5 min light-dark-avoidance (L/D) test session. Then, mice received standard auditory cued fear conditioning with re-exposure to a set of four conditioned fear stimuli in their training context 24 h later. The long-term effects of such fear memory reactivation were tested four weeks later by assessing anxiety-like behavior on an elevated plus maze (EPM) to avoid effects of retesting in the L/D test. Corticosterone plasma concentrations before and 30 min after testing of the reactivated fear memory were measured. Reactivation was achieved by exposure to four conditioned fear stimuli in their training context. All tests were performed between 1.00 and 4.00 pm (except for experiment 4).

In experiment 1, the effects of fear memory reactivation on corticosterone plasma levels, anxiety and fear memory were assessed by comparing the “reactivation group” (R; N=7) receiving the full protocol to a “no reactivation group” (NR, N=8), receiving fear conditioning training only and a “control group” (CTL, N=8), receiving only tone stimuli but no foot shocks during training.

In experiment 2, kainate-induced gamma oscillation was assessed in animals of the groups R (N=7), NR (N=8) and CTL (N=6) 30 days after the initial training. The elctrophysiological experiments were conducted by Gürsel Caliskan, Institute of Neurophysiology, Charité Universitätsmedizin, Berlin. The results are presented in the Appendix, section A.12.

In experiment 3, mRNA expression of glucocorticoid (GR) and mineralocorticoid receptors (MR) were assessed in sublayers of the ventral hippocampal CA3 region, in the same groups (R: N=6; NR: N=6; CTL: N=6), again 30 days later.

In experiment 4 only the reactivation paradigm was employed, but two different time points for training, reactivation and test sessions were engaged and systematically varied, resulting in eight different groups (N=8 in each). Sessions took either place at time point 1 (T1) from 8.00 to 9.30 am, 1 hour after lights off when corticosterone is typically high in an inverse light-dark-cycle or at time point 6 (T6) from 1.00 to 3.00 pm, when corticosterone can be expected to be low (Dalm et al., 2005), allowing for variation of endogenous corticosterone levels through circadian fluctuations. EPM tests, blood sample collection and fear memory testing were done at daytimes corresponding to the individual retrieval test.

In experiment 5, again only mice with reactivation of fear memory were used to assess effects of corticosterone administered to the ventral hippocampus on fear memory and anxiety. In the third week after memory reactivation, guide canulae were implanted in the left and right ventral hippocampi through which either corticosterone (10 ng; N=9) or vehicle (N=9) was applied in the fourth week after fear conditioning. 15 min after drug infusion anxiety-like behavior was assessed in the EPM followed by fear memory retrieval 10 min later.

3.3.2 Fear conditioning and its reactivation induces long-lasting changes on behavior and corticosterone, accompanied by molecular changes in the ventral hippocampus

Fear conditioning and its reactivation led to long-term changes in corticosterone plasma levels, anxiety-like behavior and fear memory, as assessed in experiment 1.

Corticosterone plasma levels were enhanced even under baseline conditions after reactivation of conditioned fear (Fig. 3.3-1A; ANOVA for group: $F(2,20)=4.443$, $p=0.025$; Fisher's LSD *post hoc* comparison: $p=0.007$ to CTL), but not fear conditioning training alone ($p=0.119$ to CTL). Using fear memory retrieval as a stimulus, corticosterone plasma concentration were further increased 30 min later ($F(2,20)=15.924$; $p<0.001$), again only in group R ($p<0.001$ to CTL, $p<0.001$ to NR).

Anxiety-like behavior was comparable between groups in pre-training L/D test (activity in the light compartment: $F(2,20)=0.517$; $p=0.604$), However, four weeks after training, increased open arm entries in the EPM were observed in both groups, NR (Fig. 3.3-1B;

ANOVA for group: F(2,20)=4.86, p=0.019; Fisher's LSD *post hoc* comparison: p=0.03 to control) and R (p=0.008). At the same time indicators of general activity and closed arm entries did not differ between groups (total entries: F(2,20)=1.279, p=0.295; distance: F(2,20)=2.028, p=0.158; time active: F(2,20)=0.078, p=0.925; time immobile: F(2,20)=0.93, p=0.411; closed arm entries: F(2,20)=0.266, p=0.769), hence excluding hyperactivity or avoidance of the closed arms in these animals.

Fear memory reactivation however increased specifically the freezing response to the training context in the background, (Fig. 3.3-1C; ANOVA for group: F(2,20)=9.197, p=0.001) compared to the CTL group (p<0.001) and also to group NR (p=0.019). In contrast, no effect was observed concerning the freezing response to the neutral (CS-; F(2,20)=3.395, p=0.054) and the conditioned acoustic stimuli (CS+: F(2,20)=1.017, p=0.379).

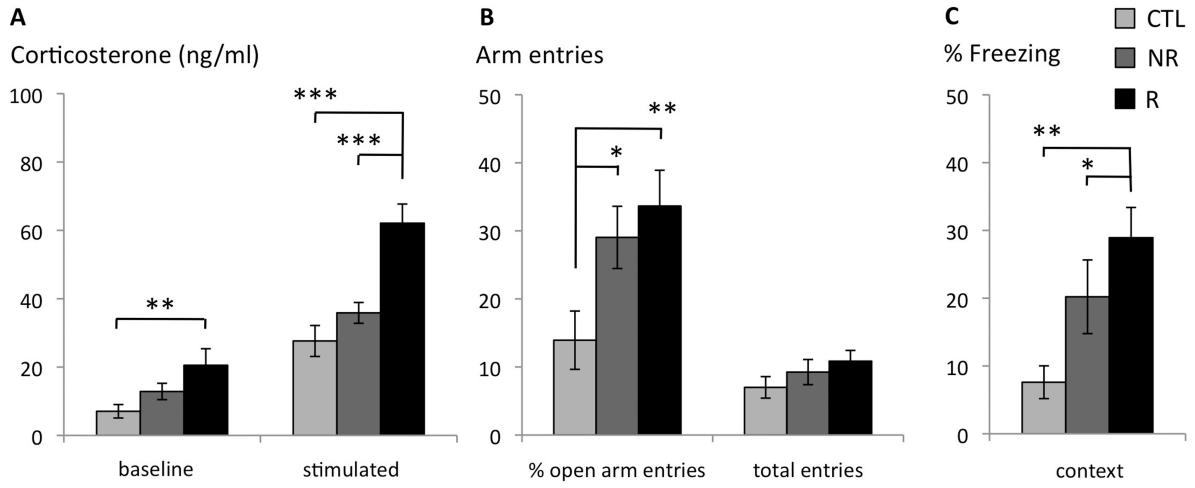

Fig. 3.3-1 Fear reactivation elicits long-lasting changes in corticosterone plasma concentration, anxiety and context fear memory. (A) Corticosterone plasma concentration (CORT) was increased after fear reactivation (R), even under unstimulated conditions. After fear memory testing, the increased corticosterone levels of group R are maintained at a high level. (B) Anxiety-like behavior in the EPM is reduced in group R, but also after fear conditioning alone (NR), compared to an unconditioned control group (CTL). The number of total entries to closed and open arms is not altered between groups, suggesting comparable levels of activity in all groups. (C) Fear reactivation increases freezing to the training context. Values are indicated as mean ± SEM * Significant difference between genotypes with p< 0.05; ** p < 0.01; *** p < 0.001.

Together, fear conditioning led to anxiolytic like changes in an elevated plus maze, regardless of its reactivation. But corticosterone plasma level and background context memory were enhanced specifically 30 d after fear memory reactivation.

Interestingly, in experiment 2, both after fear conditioning and its reactivation power of kainate-induced gamma oscillations in the CA3 area of ventral hippocampal slices was decreased. Development of gamma power was restored by application of high levels of

corticosterone to the slices prepared from NR group mice, but not from R group. Similar changes were also observed for auto-correlation analysis (see Appendix, A.12).

Fear conditioning and its reactivation induced long lasting changes in evoked ventral hippocampal rhythmic activity, with differential sensitivity to corticosterone.

In animals from the same treatment groups, mRNA levels of GR and MR were assessed in CA3 sublayers 30 d later (experiment 3). A three-way ANOVA for gene (GR/MR), *stratum* (*stratum radiatum* (SR)/ *stratum pyramidale* (SP)/ *stratum oriens* (SO)) and group (R/NR/CTL) revealed strong impact of each factor on expression levels (Fig. 3.3-2; gene: ($F(2,89)=22.347$, $p=0.000$; stratum: $F(2,89)=102.948$, $p=0.000$; group: $F(2,89)=5.344$, $p=0.006$). Moreover, expression differences between GR and MR were evident depending on different *strata* (interaction of *stratum* and gene: $F(2,89)=39.345$; $p=0.000$; *stratum* effect for GR: $F(2,45)=93.408$; $p=0.000$; for MR: $F(2,45)=13.208$; $p=0.000$). *Post hoc* comparison of the group effects revealed a significant downregulation of GR and MR in group NR (Fisher's LSD $p=0.005$ compared to CTL), but not in group R ($p=0.649$ compared to CTL; $p=0.018$ compared to NR). Together, GR and MR mRNA expression levels were reduced lastingly after fear conditioning, but not after its reactivation.

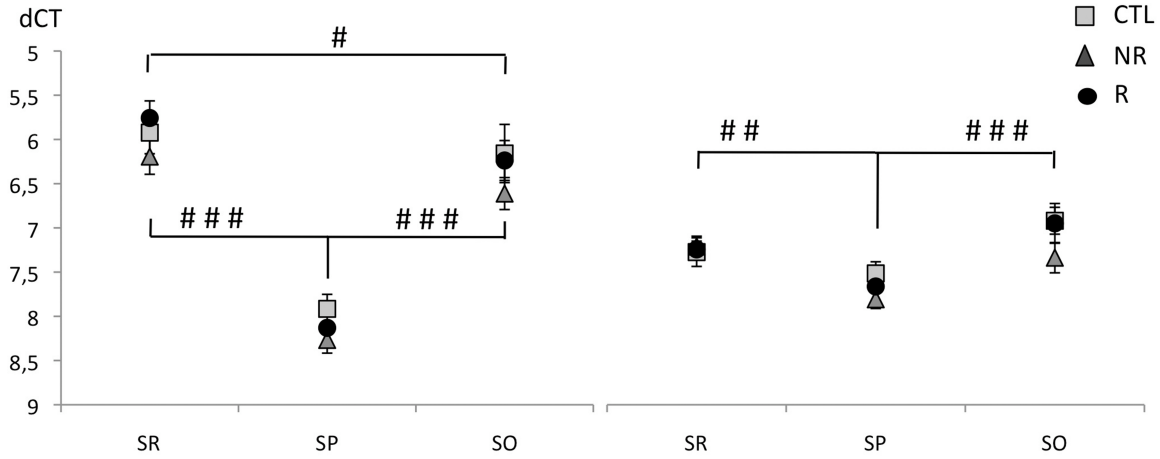

	GR			MR		
RQ%	**SR**	**SP**	**SO**	**SR**	**SP**	**SO**
C	100	100	100	100	100	100
NR*	82,89	78,37	73,05	104,46	81,63	74,86
R	112,16	86,17	94,65	102,13	90,28	97,97

Fig. 3.3-2: Expression of GR and MR mRNA is reduced in the ventral hippocampal CA3 after fear conditioning. Expression normalized to the internal control gene GAPDH (dCT values) revealed differential expression of GR and MR in *stratum radiatum* (SR), *stratum pyramidale* (SP) and *stratum oriens* (SO) of the ventral CA3 for all groups. The overall expression of both genes was reduced in group NR, but not in group R. Values are mean dCT±SEM. For quantitation of behaviorally induced expression changes refer to the table below the graph (relative quantification with CTL expression levels set to 100 %). * Significant difference between groups with $p < 0.05$; # significant difference between CA3 sublayers with $p < 0.05$; ## $p < 0.01$; ### $p<0.001$.

Together, auditory cued fear conditioning itself led to reduced anxiety-like behavior in the EPM four weeks later. In addition, in this NR group power of gamma oscillation was reduced in the CA3 area of the ventral hippocampus, but recovered after application of high doses of corticosterone. Furthermore, expression of the corticosterone receptors GR and MR was reduced in sublayers of the same area in fear conditioned animals. After reconsolidation, anxiolytic-like responses in the EPM were maintained, again associated with reduced ventral CA3 gamma power. However, the corticosterone sensitivity of ventral hippocampal network activity was reduced in animals of the R group and GR/MR expression reached again control levels. Moreover, fear memory reactivation induced a long-lasting elevation of corticosterone plasma levels as well as increased long-term fear memory to the background context.

This data suggests an association between ventral hippocampal network activity and anxiety-like behavior via corticosterone action that is modulated by fear conditioning and its reactivation. Indeed, the reduced anxiety-like behavior in the EPM observed here can be induced also by chronic mild stress (D'Aquila et al., 1994) or after highly aversive context conditioning (Laxmi et al., 2003; Radulovic et al., 1998). The ventral hippocampus appears to be crucially involved in such behavior, since lesion of this structure reduced anxiety-like responses in the EPM (Kjelstrup et al., 2002; Bannerman et al., 2004). In addition, acquisition and expression of auditory and contextually conditioned fear is also supported by the ventral hippocampus (Bannermann et al., 2004; Maren and Holt, 2004; Trivedi and Coover, 2004; Rudy and Matus-Amat, 2005). After fear conditioning and its reactivation, the power of kainate-induced gamma oscillations in slice preparations of the ventral hippocampus was reduced, thus reflecting changes in ventral hippocampal network activity that may be associated with reduced anxiety. Indeed, previous studies demonstrate an involvement of hippocampal gamma (30-80 Hz) oscillations with anxiety and avoidance behavior. Gamma oscillations emerge from rhythmic activity of GABAergic interneurons (Buszaki, 2001; Gloveli et al., 2005) and shape information flow in the hippocampus and interconnected limbic areas. Kainate-induced gamma oscillations reflect levels of this rhythmic activity *in vivo* and next to their role in encoding and retrieval of memory (Hajos and Paulsen, 2009; Montgomery and Buszaki, 2007), they have been associated with learned avoidance behavior (Lu et al., 2011) and the avoidance of open segments of a zero maze in Clock mutant mice (Dzirasa et al., 2011).

Neuronal activity of the ventral hippocampus is thereby modulated by corticosterone

(Maggio and Segal, 2007; 2009), while the hippocampus itself regulates the activity of the HPA axis in response to stress via corticosterone receptor activity (Jacobson and Sapolsky, 1991; Herman et al., 1995). However, corticosterone application alone in slices from control animals did not alter gamma power, in line with previous observations by Weiss et al. (2008), where corticosterone increased irregularity of frequency of carbachol-induced gamma oscillations, but had no effect on gamma peak power. Thus, considering the selective restoration of gamma power by application of corticosterone and the reduced expression of GR/ MR in association with unaltered corticosterone plasma levels, fear conditioning induced long lasting changes in corticosterone-sensitive functions in the ventral hippocampus. For the first time, such a tuning of ventral hippocampus network activity is now reported after fear conditioning and could be also related to altered GABAergic function, as observed after stress (Orchinik et al., 2001; Maggio and Segal, 2009).

But this tuning is further altered when fear memory is reactivated 24 h posttraining. During the reactivation session the animals are re-exposed to cues related to the initial fear conditioning. Re-exposure after intensive, traumatic fear conditioning can induce lasting alterations in arousal and social behavior that is related to PTSD in a subset of mice (Olson et al., 2011). However, previous work in the lab also demonstrated increased contextual freezing after a single memory re-activation session of the standard auditory-cued fear conditioning paradigm used also in this study (Rehberg et al., 2010). A generalization of contextual fear memory might be related to PTSD-like dysfunctions in identification of correct threat predictors as well (Kaouane et al., 2012). Alternatively, when tested weeks after the initial training, generalization of contextual fear memory could also result from forgetting of specific stimulus characteristics that lead to reduced discrimination of distinct contices (Sauerhöfer et al., 2012). In this study now, an auditory cued fear conditioning paradigm was used similar to the study by Rehberg et al. (2011), where the contextual fear response was increased 24 h after a single fear memory reactivation session. Here, the same effect was observed even four weeks later, suggesting that contextual generalization in this paradigm is specifically induced by reactivation.

Upon reactivation, a modification of fear memory occurs. This results either in a process called reconsolidation (e.g. following a single exposure) or in extinction of the fear memory (following repetitive exposures of the CS without US, leading to a diminished fear response, see Quirk et al., 2010 for review). Both processes open possibilities to

treat fear-related disorders by fear memory modulation (Quirk et al., 2010; Schiller et al., 2010). In this study, all mice were re-exposed to four non-reinforced CS+ in a single re-activation session. No differences in CS+ response between fear conditioned and reactivated animals were observed four weeks later and also previous data suggests the induction of fear memory reconsolidation but not extinction in this paradigm (Laxmi et al., 2003; Rehberg et al., 2010). During reconsolidation memory enters a labile phase that partly resembles the original memory consolidation and then is restored in a slightly modified form, allowing an update rather than a mere recapitulation of consolidation events (Alberini, 2011; Rodriguez-Ortiz and Bermúudez-Rattoni, 2007). In this line, protein synthesis dependent processes take place in key regions of the initial fear memory formation, e.g. in the basolateral amygdala (BLA; Debiec & LeDoux, 2006; Nader et al., 2000) or the hippocampus (Myers & Davis, 2002), although differences in molecular factors, transmitter systems and also in network activities are observed compared to consolidation itself (Tronson & Taylor, 2006; Narayanan et al., 2007b). However, like the primary fear development, also reconsolidation critically depends on glucocorticoid action (Wang et al, 2008; Blundell et al, 2011). Corticosterone administration shortly before initial training improves fear conditioning through activation of GR (McGaugh, 2004; Schwabe et al., 2012), while corticosterone administration before and inhibition of GR shortly after retrieval impairs reconsolidation of fear memory (Cai et al., 2006; Jin et al., 2007). Corticosterone action during the reconsolidation phase itself appears to depend on stress intensity, since post-retrieval application reduced freezing to the context only in animals trained with high but not with moderate shock intensity (Abrari et al., 2008).

Strikingly, also after fear memory reactivation animals displayed long-lasting reduction of anxiety-like behavior and gamma oscillation power in the ventral hippocampus. However, compared to mice with fear conditioning only, the corticosterone sensitivity of the network activity was reduced and GR and MR expression turned back to control levels. In addition, plasma corticosterone levels were lastingly enhanced after fear reactivation, both under baseline and stimulated conditions, suggesting a disturbed feedback inhibition of the HPA axis via the ventral hippocampus on the one hand. On the other hand, enhanced corticosterone levels could also compensate for the reduced corticosterone sensitivity in ventral hippocampal network activity and support the still maintained anxiolytic response. Thus, cellular changes induced in the ventral hippocampus upon fear memory reactivation may also exert protective effects against

potential structural and functional damage in the hippocampus, which is frequently observed after prolonged enhancement of corticosterone level (Conrad, 2006; Stranahan et al., 2008). Moreover, enhanced levels of corticosterone could also contribute to the observed contextual generalization, since corticosterone application to the dorsal hippocampus was reported to induce increased contextual fear memory before (Kaouane et al., 2012).

To now further investigate the impact of corticosterone on anxiety and fear memory behavior, fear reactivated animals were engaged and their endogenous corticosterone levels were further modulated by taking advantage circadian fluctuations on the one hand and direct local application to the ventral hippocampus on the other hand.

3.3.3 Anxiolytic properties of high corticosterone levels after fear memory reactivation

In experiment 4, circadian fluctuations of endogenous corticosterone plasma levels were used to vary endogenous corticosterone levels throughout fear memory formation and reactivation.

First of all, a circadian fluctuation of corticosterone plasma concentrations was maintained after fear reactivation, as we found high levels 1 h after the beginning of the dark phase (T1) and lower concentration 5 h later (T6), both under unstimulated conditions (Fig. 3.3-3A; ANOVA for time of testing: $F(1,47)=38.536$; $p<0.001$) and after fear memory retrieval (ANOVA: $F(1,47)=18.186$; $p<0.001$). Enhanced baseline levels occluded the stress induced response at T1 (repeated measure ANOVA with corticosterone concentration before and after stimulation $F(1,24)=3.961$; $p=0.058$), whereas a significant increase upon testing was detected at T6 ($F(1,23)=90,796$; $p<0.001$). No interaction was observed of testing time with training time (CORT baseline: $F(1,45)=2.280$, $p=0.138$; CORT stimulated: $F(1,45)=0.181$, $p=0.673$).

Anxiety-like behavior varied between time points of testing, dependent on reactivation. After fear memory reactivation, animals displayed more entries into the open arm of the EPM at T1 compared to T6 (Fig. 3.3-3B; ANOVA for time of testing: $F(1,47)=6.339$; $p=0.015$), without differences in general activity (number of total arm entries: $F(1,47)=1.74$; $p=0.194$; distance: $F(1,47)=1.226$; $p=0.274$; time active: $F(1,47)=0.242$; $p=0.625$). However, in the pre-training L/D test this pattern was inverse with activity (ANOVA for time of testing: $F(1,47)=10.504$; $p=0.002$) and time spent in the light compartment ($F(1,47)=10.032$; $p=0.003$) increased at T6 (Fig. 3.3-3C).

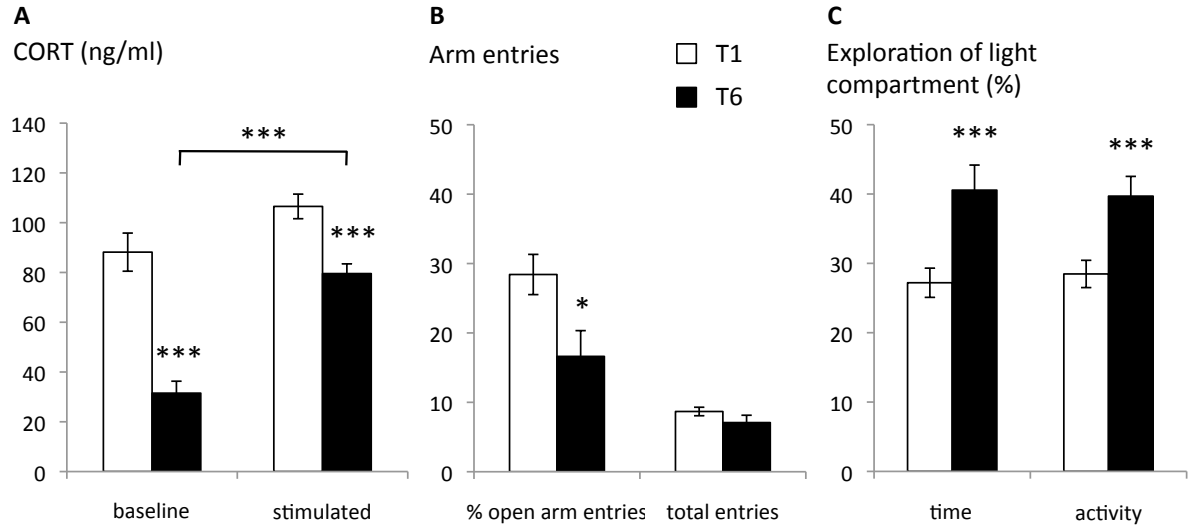

Fig. 3.3-3 Corticosterone plasma concentrations and anxiety depend on the daytime of testing in fear reactivated mice. (A) The circadian fluctuation in corticosterone plasma concentrations was maintained after fear reactivation and testing with heightened concentrations at T1 (1 h after beginning of dark phase). (B) In animals tested at T1 open arm exploration in the EPM was increased, compared to those tested at T6, indicating reduced anxiety (C) Anxiety-like behavior measured in the light-dark-avoidance test before training, however, showed the inverse pattern with reduced exploration of the light compartment at T1. Values are indicated as mean ± S.E.M. * Significant difference between groups with $p < 0.05$; ** $p < 0.01$; *** $p < 0.001$.

Fear memory to the background context was not affected by the time point of retrieval testing ($F(1,47)=3.836$; $p=0.056$), neither by the time of training ($F(1,47)=1.649$; $p=0.205$), nor by the time of reactivation ($F(1,47)=0.524$; $p=0.473$).

Strikingly, a relation between anxiety levels and corticosterone plasma levels were evident after fear memory reactivation. At T1, when corticosterone concentrations were high, anxiety levels in the EPM were low. A correlation analysis revealed positive correlation of percentage of open arm entries with basal corticosterone concentrations and over all time points (Pearson's correlation coefficient 0.267, $p=0.032$). Furthermore, a frequency analysis revealed strong inter-individual differences and overlapping distribution of unstimulated corticosterone plasma concentrations at T1 and T6 (Fig. 3.3-4A). Therefore, the data was reanalyzed with respect to basal corticosterone levels, independent from time point of testing. Groups were defined in relation to the median corticosterone concentration (57.81 ng/ml) four weeks after fear memory reactivation. By that, a high and a low post-reactivation corticosterone group derived, that differed almost fourfold in unstimulated corticosterone plasma concentrations (mean±SEM: 25.08±2.6 ng/ml in low vs. 94.34±6.42 ng/ml in high post-reactivation corticosterone; ANOVA: $F(1,47)=96.912$; $p<0.001$), but to lesser extend also after memory retrieval

(85.79±6.05 ng/ml in low vs. 100.55±3.89 ng/ml in high post-reactivation corticosterone; ANOVA: $F(1,47)=4.278$; $p<0.044$). While animals with low baseline levels of post-reactivation corticosterone showed a significant increase upon retrieval (Fig. 3.3-4B; Repeated measure ANOVA: $F(1,23)=156.523$; $p<0.001$), such responsiveness was not observed in animals with high baseline levels of post-reactivation corticosterone ($F(1,24)=0.870$; $p=0.360$).

The high post-reactivation corticosterone group showed decreased anxiety levels, indicated by increased open arm entries in the EPM (Fig. 3.3-4C; mean±SEM: 27.93 % vs. 17.4±3.79 %; ANOVA for group effect: $F(1,47)=4.65$; $p=0.036$).

Contextual fear memory generalization was differentially affected by the post-reactivation corticosterone group and the time point of reactivation (Fig. 3.3-4D; ANOVA; interaction group x time: $F(1,45)=4.264$; $p=0.045$). A within group comparison demonstrated decreased freezing in the low post-reactivation corticosterone group when fear memory had been reactivated at T1 (ANOVA for effect of retrieval time in low responders: $F(1,22)=5.986$; $p=0.023$), but not at T6 ($F(1,23)=0.068$; $p=0.796$). In the high post-reactivation corticosterone group in contrast, contextual freezing was high at T1 and T6 (paired comparison: ANOVA for corticosterone group effect at T1: $F(1,22)=8.876$, $p=0.007$; ANOVA for effects of reactivation time in high post-reactivation corticosterone group: $F(1,23)=0.288$; $p=0.597$).

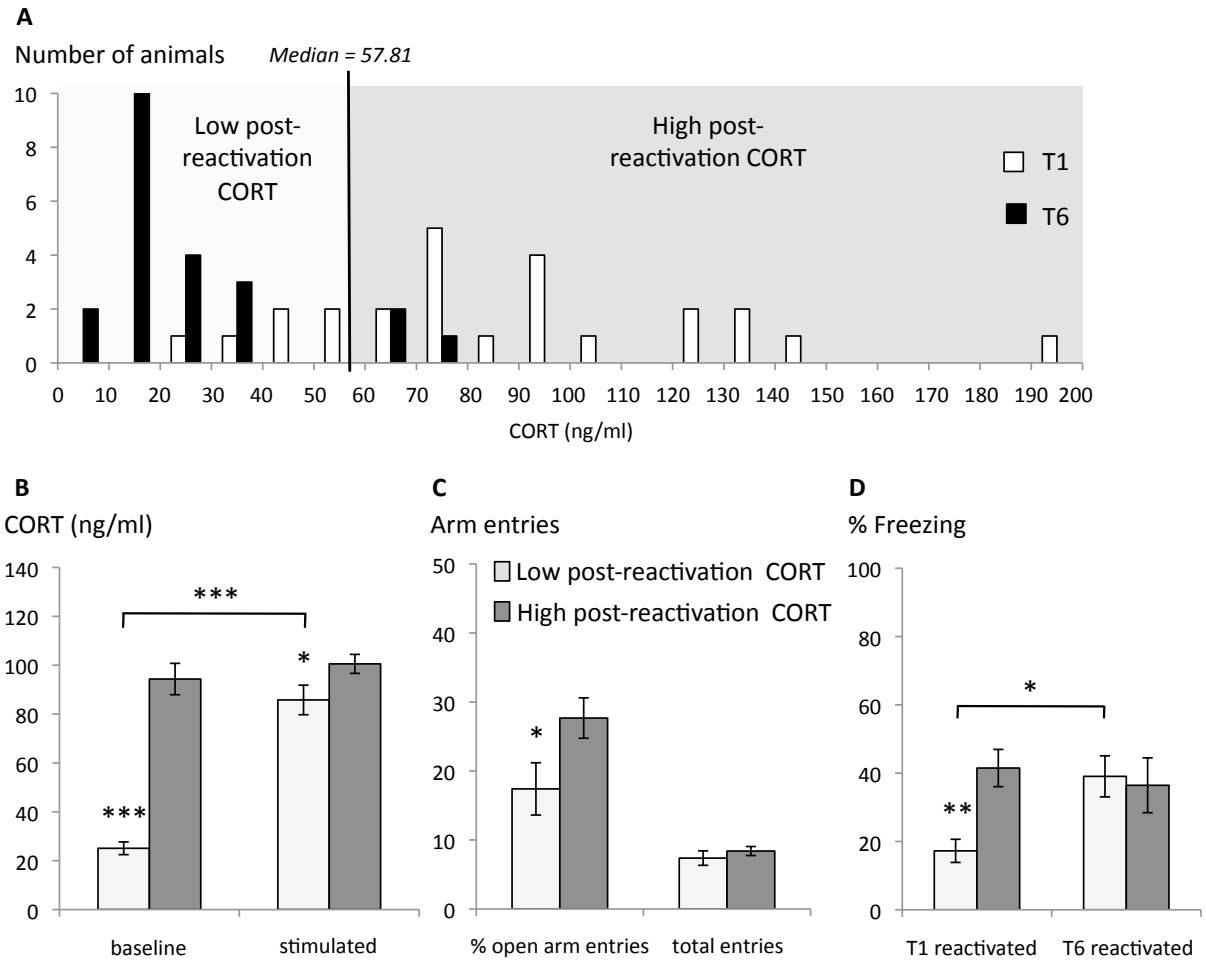

Fig. 3.3-4 High levels of post-reactivation corticosterone correspond with low anxiety but contextual generalization. (A) Histogram showing the distribution of individual basal corticosterone plasma concentration at one (T1) and six hours (T6) after lights off. Based on the median (57.81 ng/ml), mice were assigned to a low and a high post-reactivation corticosterone group. (B) The high post-reactivation corticosterone group shows near maximal plasma concentrations of corticosterone (CORT) under unstimulated conditions and fails to significantly increase upon fear memory retrieval. (C) The high post-reactivation corticosterone group shows reduced anxiety-like behavior in the elevated plus maze. (D) The low post-reactivation corticosterone group expresses reduced freezing towards the background context if fear reactivation is done at T1, indicating a state-specific memory effect. Values are indicated as mean ± SEM. * Significant difference between groups with * $p < 0.05$; ** $p < 0.01$; *** $p < 0.001$.

Together, fear memory reactivation resulted in inter-individual differences in HPA-axis activity and stimulus responsiveness that was correlated with post-reactivation anxiety-like behavior. Thus, elevated baseline corticosterone levels were associated with decreased anxiety, suggesting anxiolytic properties of corticosterone actions.

Since corticosterone responsiveness as well as molecular and network activity changes were observed in the ventral hippocampus, question arose whether such anxiolytic effects of corticosterone could be mediated directly and via the ventral hippocampus after fear memory reactivation. Therefore, in experiment 5, corticosterone was applied locally to the ventral hippocampus of fear reactivated mice at T6, i.e., in a period of low

endogenous corticosterone levels. Indeed, corticosterone injections directly into the ventral hippocampus increased the exploration of open arms in the EPM compared to vehicle injected controls (Fig. 3.3-5A; Student's t-test: $T(16)=3.153$; $p=0.006$), without affecting the total number of arm entries as a measure of general activity ($T(16)=0.487$; $p=0.633$). In contrast, the local corticosterone application had no effect on the freezing behavior displayed in the background context (Fig. 3.3-6B; $T(16)0.025$; $p=0.980$), or in response to a CS- ($T(16)=1.693$; $p=0.111$) or to the CS+ ($T(16)=1.210$; $p=0.244$).

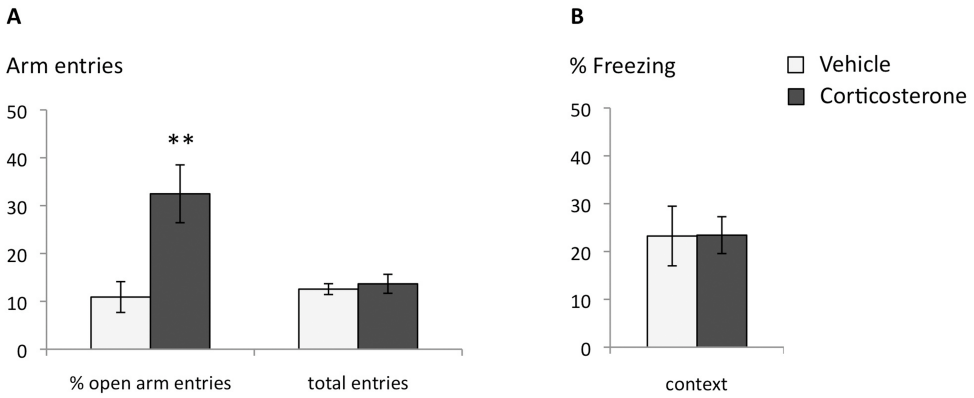

Fig. 3.3-5 Local administration of corticosterone to the ventral hippocampus decreases anxiety-like behavior in fear reactivated mice. (A) Corticosterone (10 ng) was injected into the ventral hippocampus of fear reactivated mice on T6, i.e. with low endogenous levels, leading to a reduced anxiety-like behavior in the elevated plus maze compared to vehicle-injected controls. (B) Local corticosterone application has no influence on background context generalization. Values are indicated as mean ± SEM. ** Significant difference between groups with $p < 0.01$.

Together, these experiments confirmed the association between reduced anxiety and increased corticosterone plasma levels in fear memory reactivated mice and revealed the ventral hippocampus as a key structure mediating this effect. By permutating the daytime of fear conditioning training, reactivation and testing four weeks later, different endogenous corticosterone plasma levels were achieved at the different stages of the paradigm by taking advantage of the circadian fluctuations in corticosterone plasma levels. In C57BL/6 mice, corticosterone plasma levels are usually high at the beginning of the dark phase, but decline within four to five hours (Dalm et al., 2005). This circadian pattern was still maintained after fear memory reactivation, allowing to assess the influence of different endogenous corticosterone levels also in the test phase four weeks later. There, high corticosterone concentrations at the beginning of the dark phase at T1, one hour after lights off, were associated with increased open arm entries in the EPM. When corticosterone levels were lower, at T6 five hours after beginning of the dark

phase, mice displayed less open arm entries. Remarkably, before fear conditioning and its reactivation, anxiety-like behavior was reduced at T6, suggesting a direct impact of fear memory reactivation on anxiety and its regulation by endogenous corticosterone.

Further analysis revealed large inter-individual differences of basal corticosterone concentrations that appeared to be only in part attributable to different test times. In fact, the re-analysis of the data based solely on basal corticosterone level revealed a strong negative correlation between corticosterone level and anxiety-like behavior after reactivation. Two groups of animals were distinguished after reactivation, displaying either low (< 57 ng/ml) or high corticosterone (> 57 ng/ml) concentrations. Interestingly, upon CS+ re-exposure, the high post-reactivation corticosterone group was not able to further enhance their corticosterone plasma level, while such stimulus-induced response of the HPA axis was still observed in the low post-reactivation group. Interestingly, animals with low individual corticosterone concentrations showed a differential contextual fear response that depended on the daytime of the reactivation. This suggests a state-dependent memory effect, that was not observed in the high post-reactivation group, were contextual fear memory was strong.

Circadian fluctuations as well as stress-induced alterations in corticosterone plasma concentrations are regulated by hippocampal feedback on the HPA axis (Jacobson and Sapolsky, 1991). In addition, the electrophysiological and molecular findings in non-reactivated and reactivated animals stated above, suggest a strong involvement of the ventral hippocampus in reactivation-induced effects on anxiety and fear memory. Therefore, to test the function of corticosterone in the ventral hippocampus directly, the hormone was applied locally in fear memory reactivated animals at T6, when endogenous corticosterone levels were low. This resulted in a profound increase in open arm exploration in the EPM, further confirming the anxiolytic action of corticosterone in fear reactivated animals and highlighting the involvement of the ventral hippocampus in these actions. Contextual fear memory was not affected by local corticosterone injections to the ventral hippocampus. However, as demonstrated by Kaouane et al. (2012), local injections to the dorsal hippocampus with the same dosage increased contextual fear memory. Thus, contextual generalization might be mediated by corticosterone action sites different from the ventral hippocampus, while this structure appears to be strongly involved in mediating anxiolysis.

3.3.4 Fear memory reactivation induces long-lasting increase of corticosterone, anxiolysis and modulates network activity in the ventral hippocampus: Conclusions & future perspectives

This study reports for the first time long lasting effects of fear conditioning and its reactivation, leading to anxiolysis, contextual fear memory generalization and increase in corticosterone plasma levels. These changes occurred in association with electrophysiological and molecular alterations in the ventral hippocampus, highlighting this structure as critical target for fear memory consolidation and reconsolidation processes. First, effects of fear conditioning and fear reactivation were dissected, suggesting altered tuning of ventral hippocampal molecular and physiological properties in both processes, contributing to anxiolytic behavioral responses. Secondly, it was demonstrated that such reduced anxiety-like behavior after fear reactivation was associated with increased corticosterone concentrations that exert their beneficial effects via the ventral hippocampus.

Although most studies report anxiogenic-like effects (e.g., Mitra and Sapolsky, 2008), anxiolytic actions of acute corticosterone application have been reported more then 30 years ago (File et al., 1979). In addition, evidence for beneficial effects of elevated glucocorticoid levels also derive from clinical studies. In patients with panic disorder, high cortical release during attacks is associated with a better outcome of exposure therapy (Siegmund et al., 2011). In phobic patients, fear symptoms are diminished when cortisol release is increased during exposure to the phobic stimulus. Accordingly, cortisone administration before such exposure decreases subjective feelings of fear (Soravia et al., 2006). And finally, in patients with PTSD daily administration of low dose cortisol reduced symptoms of traumatic memories (reliving, nightmares), long time after the initial trauma (de Quervain, 2008).

The results gathered here, suggest now that rhythmic network activities in the ventral hippocampus and their experience-dependent change might be critically involved in these processes. The detailed investigation of further molecular and physiological changes in the ventral hippocampus and its interacting structures may therefore provide valuable therapeutic tools for the treatment of anxiety disorders in future.

4. General discussion

During emotional memory formation a subject learns new behavioral responses that enable adaptation to new situations and promote its survival. These processes can be modeled in classical fear conditioning, where an association between a previously neutral stimuli and a fear-eliciting, threatening stimulus is learned. The correct determination of the threat-predicting stimuli is essential for adaption of the behavioral response and is disturbed in anxiety disorders.

Generalization is a process where the conditioned fear response broadens to neutral, non-reinforced stimuli, e.g. tones with a distinct frequency compared to the originally conditioned cue. Deficits in GABAergic signaling can contribute to such intramodal generalization, as observed in GAD65$^{-/-}$ mice (Bergado-Acosta et al., 2008).

However, generalization can also occur to stimuli with different sensory modality or even to the complex training environment. In auditory cued fear conditioning a tone predicts the threatening footshock, but naturally the training occurs in a certain environment, the context. In this line, cue and context can be viewed as two compound stimuli that are presented in parallel. As the Rescorla-Wagner model describes, the conditioned response is only equal to stimuli with the same associative strength (Rescorla, 1976). The conditioned fear response towards the context is normally lower than to the cue, indicating enhanced salience of the cue compared to the context in the background. Under certain conditions the fear response to the background context is enhanced, suggesting that the contextual information gained salience. This can be viewed as generalization towards the background context.

Two limbic brain regions are crucially involved in fear memory formation. The amygdala is activated in emotionally arousing situations and is believed to mediate the association between the threatening and neutral stimulus (Maren, 2001), while the hippocampus is required for processing of contextual information (Philips & LeDoux, 1992). In this line, the magnitude of contextual response might reflect a gradual involvement of hippocampal memory processing in interaction with the amygdala. Indeed, one condition where the fear response to the background context is enhanced is overtraining, i.e. fear conditioning with heightened stimulus intensities (Laxmi et al., 2003). In a previous study, I could identify the neural cell adhesion molecule (NCAM) as one component contributing to such interplay. Here, overtraining modulates NCAM

expression in the BLA. Furthermore, mice deficient for NCAM display disturbed network synchronization between amygdala and hippocampus in association with contextual memory deficits under highly stressful training conditions (Albrecht et al., 2010).

Overall, contextual generalization in auditory cued fear conditioning appears to be mediated by amygdalo-hippocampal interaction during the formation of fear memory. Information processing in both structures as well as their network activity is shaped by local inhibitory circuits that engage biochemically diverse interneuron subpopulations (Buzsaki, 2001; Ehrlich et al., 2009). However, underlying molecular mechanisms of amygdalo-hippocampal interaction that determines the balance between cue and contextual responses in fear memory are rarely studied.

As a first starting point, I studied the contribution of interneurons to the consolidation of cued and contextual fear memory in subregions of amygdala and hippocampus. Here, distinct region-specific patterns were revealed for the expression of neuropeptide markers. While somatostatin (SST) mRNA expression, determined by quantitative real-time PCR, was increased after both cued and contextual fear conditioning in the lateral amygdala, neuropeptide Y (NPY) expression was altered in the dentate gyrus of the hippocampus. Here, a differential activation was observed with increased levels of NPY after cued, but not contextual fear conditioning. NPY marks a population of interneurons in the hilus region of the dentate gyrus that mediates feedback inhibition (Sperk et al., 2007). Investigation of the activation of this interneuron population and NPY signaling itself in formation of fear memory suggested a determination of contextual salience via NPY. Thereby, NPY in the dentate gyrus suppresses acquisition and/or consolidation of contextual fear memory in presence of a more salient cue. When the context is in the background, inhibitory function of NPY in the dentate gyrus may prevent hippocampal information processing at its first station under moderate training conditions. Generalization towards the background context would then require a disinhibition of dentate gyrus signaling that would depend on the modulatory activity of the amygdala (Akirav & Richter-Levin, 2002).

The amygdala is activated during emotionally arousing events (Pelletier et al., 2005). The initial screening suggested a contribution of SST to the detection of emotional salience in the LA, independent of the stimulus. Circadian differences in anxiety-like behavior were associated to circadian expression changes in the amygdala. However, in transgenic mice with targeted ablation of SST deficits were only observed in a mildly aversive fear conditioning paradigm (Kluge et al., 2008) and anxiety tests. SST acts as an

inhibitory neuromodulator as well (Meis et al., 2005), suggesting a contribution to the prevention of amygdala "overexcitation" and appropriate adaptive responses. However, further experiments are required to determine the role of somatostatin in the amygdala for the detection of stressful, emotional highly relevant situations.

Together, the first study highlights the role of inhibitory signaling in the hippocampus, especially in the dentate gyrus, in determining cue/context balance in auditory cued fear conditioning. During contextual generalization this balance is shifted. Accordingly, altered GABAergic signaling in the hippocampus might mediate generalization phenomena.

Next to overtraining characterized by increased intrinsic stress related to the conditioning tasks, previous stress experiences not related to the learning task can alter the hippocampal signaling properties. This is described for juvenile stress that elicits contextual generalization of auditory cued fear memory in adulthood (Iris Müller et al., unpublished observations). Generalization as described for mice as well as increased anxiety and learned helplessness in active avoidance learning in rats (Tsoory & Richter-Levin, 2006) is related to maladaptive fear and anxiety symptoms in posttraumatic stress disorder (PTSD). Combined juvenile and adult stress is therefore used to model PTSD in rodents. Comprehensive work by Maggio & Segal (2011) further suggests that such altered emotional stimulus processing is mediated by changed hippocampal excitability. Especially the ability to produce CA1 LTP is enhanced lastingly in the ventral portion of the hippocampus (Maggio & Segal, 2011), a region crucially involved in emotional stimulus processing, fear and anxiety (Bannerman et al., 2004). As a potential molecular correlate, I found altered expression of GABAergic factors, primarily in the ventral CA1, after either juvenile or adult stress or the combination of both that were in part correlated to changes in corticosterone receptor expression. Specifically after combined juvenile and adult stress the correlation between marker genes for GABAergic and glutamatergic signaling was altered. Thereby, changes in the inhibitory/excitatory balance in the ventral CA1 could occur that contribute to the observed long-lasting increase in excitability. Increased levels of GAD65 were found after single, but not after combined stress. This could reflect system adaption for subsequent emotionally relevant stimuli. However, such "calibrating" might influence future information processing in the CA1. Upon subsequent fear conditioning altered GABAergic signaling in the ventral CA1 might promote encoding of contextual information, thereby generating generalization of contextual fear during auditory cued fear conditioning. In mice

deficient for GAD65 such an, adaptive molecular response after juvenile stress is occluded. Indeed, in these animals contextual generalization is not observed after juvenile stress (Iris Müller et al., unpublished observations).

GABAergic mechanism in the ventral CA1 defines the setting for information processing in subsequent fear conditioning and expression changes of pre- and postsynaptic factors may modulate amygdalo-hippocampal interaction as well.

However, even an already established fear memory trace can be altered via reconsolidation processes. Influences of fear memory reactivation on fear and anxiety were tested in the third model. Comparing fear conditioning and its reactivation revealed changes in anxiety and altered tuning of the ventral hippocampus, namely the CA3 region, thereby affecting its responsiveness to corticosterone and electrophysiological properties like gamma oscillation. Fear memory reactivation resulted in increased corticosterone plasma concentrations that evoked anxiolytic behavioral responses via the ventral hippocampus CA3 region. In addition, fear memory reactivation led to increased fear memory towards the background context, hence contextual generalization of auditory-cued fear memory. Although the contextual fear response was not altered by local corticosterone application to the ventral CA3, gamma oscillation and corticosterone responsiveness were altered in this region after reactivation. Thus GABAergic factors and neuropeptides in the ventral CA3 might also contribute to contextual generalization, although particular target genes altered by fear memory reactivation need to be evaluated in future studies.

4.1 Conclusions

With the three models applied, I was able to identify molecular factors involved in emotional relevant behaviors and I could highlight the contribution of different hippocampal subregions to these processes. NPY signaling in the dentate gyrus contributes to the balance between cued and contextual response. A generalization towards the context in auditory-cued fear conditioning occurs after severe stress experience in juvenility on the one hand and after reactivation of already established fear memory by reactivation on the other hand. The altered expression of pre- and postsynaptic GABAergic factors after juvenile and/or adult stress preset processing of newly incoming contextual information in the CA1, whereas fear memory reactivation

retuned the system and exerted anxiolytic effects via corticosterone action in the ventral CA3 area. Both resulted in a shift towards the contextual fear response, indicating enhanced amygdalo-hippocampal interaction.

Maladaptation to fear-eliciting situations and stimuli are core features of anxiety disorders like posttraumatic stress disorder. The generalization of trauma-related, fearful memory is one of the core features of PTSD. In this line, the identification of molecular factors contributing to appropriate salience determination and mechanisms of shifts in this balance would provide new therapeutic tools.

4.2 Future perspectives

Although the studies presented here provide new insights in amygdalo-hippocampal interaction and especially the contribution of different hippocampal subregions to emotional memory and behavior, they also raise several new questions.

While NPY signaling in the dentate gyrus indeed appears to suppress contextual fear memory, electrophysiological tools are required in future to determine inhibitory processes in the dentate gyrus during fear memory formation. Pharmacological and genetic manipulations could be used to study the contribution of NPY signaling to local microcircuit activity in the DG, e.g. by testing different feedforward and feedback inhibition protocols. Since contextual generalization appears to be an amygdala-dependent process (Rudy et al., 2004; Albrecht et al., 2010), hilar NPY signaling may be well suited to modulate amygdalar inputs in the DG during fear memory formation. Therefore, a further investigation of the amygdala impact on DG activity and NPY expression and action would provide valuable insights in the determination of contextual salience during fear conditioning. Moreover, a functional role of glutamatergic signaling via Grik2 and neuromodulation via M1 acetylcholin receptors in these processes needs to be assessed on the behavioral, electrophysiological and neurochemical level.

To assess the function of somatostatin in the amygdala in emotional salience detection, more specific molecular or pharmacological tools are required. Utilizing inducible conditional transgenic mice, compensatory mechanisms for SST deficiency that are expected in the conventional $SST^{-/-}$ mice could be circumvented. This could be realized by homozygous breeding of SST-CreERT2 mice, where an inducible knock down of SST

is possible by administration of tamoxifen. Moreover, effects of SST deficiency on fear memory acquisition, consolidation and retrieval could be investigated separately. Furthermore, to dissect the role of increased SST expression in the amygdala, local pharmacological manipulations, e.g. blockade of SST-R2 (Yeung & Treit, 2012) could be engaged in the different steps of fear formation. In addition local manipulation of SST by knock down or overexpression via viral vectors locally applied to amygdalar subnuclei would provide valuable insights towards the role of SST in fear and anxiety.

While the first study highlighted the involvement of interneuron function in amygdala and hippocampus, marked by two different neuropeptides, in fear memory formation, the second study aimed at the identification of molecular factors in the hippocampus that preset the conditions of fear memory formation by stress pre-experiences. Here, the juvenile stress model of PTSD was engaged and in future it will be essential to demonstrate the physiological and behavioral relevance of the observed gene expression changes for this model. The manipulation of GAD65 and Gabra1 expression levels with the help of viral vectors after single stress in juvenility could answer these still open questions. Then, knock down of GAD65 or overexpression of Gabra1 in the ventral CA1 SR, or the combination of both, after JS should have comparable effects to JSAS on PTSD-related anxiety and active avoidance behavior as well as on the pre-described lasting transition of LTD to LTP in the ventral hippocampus. Likewise, the impact of corticosterone or specifically ventral hippocampus GR activation on PTSD-related changes should be analyzed. Moreover, the breakdown of correlation between GAD65 and excitatory factor expression after JSAS provides an interesting starting point for studying the balance between inhibition and excitation in this PTSD model.

In the third study, the impact of reactivation of an already established fear memory trace was analyzed. The neuroendocrine, behavioral and electrophysiogical alterations observed after fear memory reactivation suggest adaptive changes in the ventral CA3 in genes relevant for GABAergic signaling and stress response. The identification of such target genes and the evaluation of their functional implication for the observed changes will be of great interest in future studies.

Together, these findings could open new therapeutic strategies for the treatment of states of increased and generalized fear, as seen in anxiety disorders like phobia or PTSD and highlight GABAergic signaling in hippocampal subregions as targets of action.

5. References

1. Abe K. (2001) Modulation of hippocampal long-term potentiation by the amygdala: a synaptic mechanism linking emotion and memory. Jpn J Pharmacol, 86(1): 18-22

2. Abe K, Fujimoto T, Akaishi T, Misawa M (2009a) Stimulation of basolateral amygdaloid serotonin 5-HT(2C) receptors promotes the induction of long-term potentiation in the dentate gyrus of anesthetized rats. Neurosci Lett, 451(1): 65-68.

3. Abe K, Fujimoto T, Akaishi T, Misawa M (2009b) Basolateral amygdala D1- and D2-dopaminergic system promotes the formation of long-term potentiation in the dentate gyrus of anesthetized rats. Prog Neuropsychopharmacol Biol Psychiatry, 33(3): 552-556.

4. Abrari K, Rashidy-Pour A, Semnanian S, Fathollahi Y (2008) Administration of corticosterone after memory reactivation disrupts subsequent retrieval of a contextual conditioned fear memory: dependence upon training intensity. Neurobiol Learn Mem 89: 178-184.

5. Acsády L, Káli S (2007) Models, structure, function: the transformation of cortical signals in the dentate gyrus. Prog Brain Res, 163: 577-599.

6. Adinoff B (2004) Neurobiologic processes in drug reward and addiction. Harv Rev Psychiatry, 12(6): 305-320.

7. Ahi J, Radulovic J, Spiess J (2004) The role of hippocampal signaling cascades in consolidation of fear memory. Behav Brain Res, 149(1): 17-31.

8. Akirav I, Richter-Levin G (1999) Biphasic modulation of hippocampal plasticity by behavioral stress and basolateral amygdala stimulation in the rat. J Neurosci, 19(23): 10530-10535.

9. Akirav I, Richter-Levin G (2002) Mechanisms of amygdala modulation of hippocampal plasticity. J Neurosci, 22: 9912-9921.

10. Alberini CM (2011) The role of reconsolidation and the dynamic process of long-term memory formation and storage. Front Behav Neurosci 5: 12.

11. Albrecht A, Bergado-Acosta JR, Pape HC, Stork O (2010) Role of the neural cell adhesion molecule (NCAM) in amygdalo-hippocampal interactions and salience determination of contextual fear memory. Int J Neuropsychopharmacol, 13(5): 661-674.

12. Amaral DG, Scharfman HE, Lavenex P (2007) The dentate gyrus: fundamental neuroanatomical organization (dentate gyrus for dummies). Prog Brain Res, 163: 3-22.

13. Anagnostaras SG, Murphy GG, Hamilton SE, Mitchell SL, Rahnama NP, Nathanson NM, Silva AJ (2003) Selective cognitive dysfunction in acetylcholine M1 muscarinic receptor mutant mice. Nat Neurosci, 6(1): 51-58.

14. Ao H, Ko SW, Zhuo M (2006) CREB activity maintains the survival of cingulate cortical pyramidal neurons in the adult mouse brain. Mol Pain, 2:15.

15. Arancibia S, Payet O, Givalois L, Tapia-Arancibia L (2001) Acute stress and dexamethasone rapidly increase hippocampal somatostatin synthesis and release from the dentate gyrus hilus. Hippocampus 11: 469-477.

16. Avital A, Richter-Levin G (2005) Exposure to juvenile stress exacerbates the behavioural consequences of exposure to stress in the adult rat. Int J Neuropsychopharmacol. 8: 163-173.

17. Avital A, Ram E, Maayan R, Weizman A, Richter-Levin G (2006) Effects of early-life stress on behavior and neurosteroid levels in the rat hypothalamus and entorhinal cortex. Brain Res Bull., 68(6): 419-424.

18. Bainbridge NK, Koselke LR, Jeon J, Bailey KR, Wess J, Crawley JN, Wrenn CC (2008) Learning and memory impairments in a congenic C57BL/6 strain of mice that lacks the M2 muscarinic acetylcholine receptor subtype. Behav Brain Res, 190(1): 50-58.

19. Baldi E, Lorenzini CA, Bucherelli C (2004) Footshock intensity and generalization in contextual and auditory-cued fear conditioning in the rat. Neurobiol Learn Mem, 81(3): 162-166.

20. Balschun D, Wolfer DP, Gass P, Mantamadiotis T, Welzl H, Schütz G, Frey JU, Lipp HP (2003) Does cAMP response element-binding protein have a pivotal role in hippocampal synaptic plasticity and hippocampus-dependent memory? J Neurosci, 23(15): 6304-6314.

21. Bannerman DM, Rawlins JN, McHugh SB, Deacon RM, Yee BK, Bast T, Zhang WN, Pothuizen HH, Feldon J (2004) Regional dissociations within the hippocampus--memory and anxiety. Neurosci Biobehav Rev, 28(3): 273-283.

22. Baraban SC, Hollopeter G, Erickson JC, Schwartzkroin PA, Palmiter RD (1997) Knock-out mice reveal a critical antiepileptic role for neuropeptide Y. J Neurosci, 17(23): 8927-8936.

23. Bast T, Zhang WN, Feldon J (2001) The ventral hippocampus and fear conditioning in rats. Different anterograde amnesias of fear after tetrodotoxin inactivation and infusion of the GABA(A) agonist muscimol. Exp Brain Res, 139(1): 39-52.

24. Bergado JA, Frey S, López J, Almaguer-Melian W, Frey JU (2007) Cholinergic afferents to the locus coeruleus and noradrenergic afferents to the medial septum mediate LTP-reinforcement in the dentate gyrus by stimulation of the amygdala. Neurobiol Learn Mem, 88(3): 331-341.

25. Bergado-Acosta JR, Sangha S, Narayanan RT, Obata K, Pape HC, Stork O (2008) Critical role of the 65-kDa isoform of glutamic acid decarboxylase in consolidation and generalization of Pavlovian fear memory. Learn Mem, 15(3): 163-171.

26. Bertoglio LJ, Carobrez AP (2002) Behavioral profile of rats submitted to session 1-session 2 in the elevated plus-maze during diurnal/nocturnal phases and under different illumination conditions. Behav Brain Res, 132(2): 135-143.

27. Blundell J, Blaiss CA, Lagace DC, Eisch AJ, Powell CM (2011) Block of glucocorticoid synthesis during re-activation inhibits extinction of an established fear memory. Neurobiol Learn Mem, 95: 453-460.

28. Borelli KG, Gárgaro AC, dos Santos JM, Brandão ML (2005) Effects of inactivation of serotonergic neurons of the median raphe nucleus on learning and performance of contextual fear conditioning. Neurosci Lett, 387(2): 105-110.

29. Bova GS, Eltoum IA, Kiernan JA, Siegal GP, Frost AR, Best CJ, Gillespie JW, Su GH, Emmert-Buck MR (2005) Optimal molecular profiling of tissue and tissue components: defining the best processing and microdissection methods for biomedical applications. Mol. Biotechnol., 29: 119-152.

30. Bowers G, Cullinan WE, Herman JP (1998) Region-specific regulation of glutamic acid decarboxylase (GAD) mRNA expression in central stress circuits. J Neurosci, 18(15): 5938-5947.

31. Brady ST, Siegel GJ (2012) Basic Neurochemistry. 8th Edition, p. 349-352, 368-369, 966-967. Academic Press. Waltham, MA, USA.

32. Brain SD, Cox HM (2006) Neuropeptides and their receptors: innovative science providing novel therapeutic targets. Br J Pharmacol, 147 Suppl 1: S202-11.

33. Brambilla P, Perez J, Barale F, Schettini G, Soares JC (2003) GABAergic dysfunction in mood disorders. Mol Psychiatry, 8(8): 721-737, 715.

34. Breslau N. (2009) The epidemiology of trauma, PTSD, and other posttrauma disorders. Trauma Violence Abuse, 10(3): 198-210.

35. Brightwell JJ, Smith CA, Countryman RA, Neve RL, Colombo PJ (2005) Hippocampal overexpression of mutant creb blocks long-term, but not short-term memory for a socially transmitted food preference. Learn Mem, 12(1): 12-17.

36. Bucherelli C, Baldi E, Mariottini C, Passani MB, Blandina P (2006) Aversive memory reactivation engages in the amygdala only some neurotransmitters involved in consolidation. Learn Mem, 13(4): 426-430.

37. Burgemeister R (2005) New aspects of laser microdissection in research and routine. J. Histochem. Cytochem., 53: 409-412.

38. Bustos SG, Maldonado H, Molina VA (2006) Midazolam disrupts fear memory reconsolidation. Neuroscience, 139(3): 831-842.

39. Butler RK, White LC, Frederick-Duus D, Kaigler KF, Fadel JR, Wilson MA (2012) Comparison of the activation of somatostatin- and neuropeptide Y-containing neuronal populations of the rat amygdala following two different anxiogenic stressors. Exp Neurol, Aug 17 [Epub ahead of print]

40. Buzsáki G (2001) Hippocampal GABAergic interneurons: a physiological perspective. Neurochem Res 26: 899-905.

41. Cai WH, Blundell J, Han J, Greene RW, Powell CM (2006) Postreactivation glucocorticoids impair recall of established fear memory. J Neurosci 26: 9560-9566.

42. Calandreau L, Desmedt A, Decorte L, Jaffard R (2005) A different recruitment of the lateral and basolateral amygdala promotes contextual or elemental conditioned association in Pavlovian fear conditioning. Learn Mem, 12: 383-388.

43. Cameron OG, Nesse RM (1988) Systemic hormonal and physiological abnormalities in anxiety disorders. Psychoneuroendocrinology, 13(4): 287-307.

44. Carlezon WA Jr, Duman RS, Nestler EJ (2005) The many faces of CREB. Trends Neurosci, 28(8): 436-445.

45. Chaudhury D, Colwell CS. (2002) Circadian modulation of learning and memory in fear-conditioned mice. Behav Brain Res, 133(1): 95-108.

46. Cestari V, Costanzi M, Castellano C, Rossi-Arnaud C (2006) A role for ERK2 in reconsolidation of fear memories in mice. Neurobiol Learn Mem, 86(2): 133-143.

47. Chen Q, Nakajima A, Meacham C, Tang YP (2006) Elevated cholecystokininergic tone constitutes an important molecular/neuronal mechanism for the expression of anxiety in the mouse. Proc Natl Acad Sci U S A, 103: 3881-3886.

48. Chen Q, Tang M, Mamiya T, Im HI, Xiong X, Joseph A, Tang YP (2010) Bi-directional effect of cholecystokinin receptor-2 overexpression on stress-triggered fear memory and anxiety in the mouse. PLoS One, 5(12): e15999.

49. Chiang PH, Yeh WC, Lee CT, Weng JY, Huang YY, Lien CC (2010) M(1)-like muscarinic acetylcholine receptors regulate fast-spiking interneuron excitability in rat dentate gyrus. Neuroscience, 169(1): 39-51.

50. Cohen H, Liu T, Kozlovsky N, Kaplan Z, Zohar J, Mathé AA (2012) The neuropeptide Y (NPY)-ergic system is associated with behavioral resilience to stress exposure in an animal model of post-traumatic stress disorder. Neuropsychopharmacology, 37(2): 350-363.

51. Colgin LL, Moser EI. (2010) Gamma oscillations in the hippocampus. Physiology (Bethesda), 25(5): 319-329.

52. Collingridge GL, Olsen RW, Peters J, Spedding M (2009) A nomenclature for ligand-gated ion channels. Neuropharmacology, 56(1):2-5

53. Conrad CD, McEwen BS (2000) Acute stress increases neuropeptide Y mRNA within the arcuate nucleus and hilus of the dentate gyrus. Brain Res Mol Brain Res, 79: 102-109.

54. Conrad CD (2006) What is the functional significance of chronic stress-induced CA3 dendritic retraction within the hippocampus? Behav Cogn Neurosci Rev, 5: 41-60.

55. Csicsvari J, Hirase H, Czurkó A, Mamiya A, Buzsáki G (1999) Oscillatory coupling of hippocampal pyramidal cells and interneurons in the behaving Rat. J Neurosci, 19(1): 274-287.

56. Cui H, Sakamoto H, Higashi S, Kawata M (2008) Effects of single-prolonged stress on neurons and their afferent inputs in the amygdala. Neuroscience, 152(3): 703-712.

57. Dai JX, Han HL, Tian M, Cao J, Xiu JB, Song NN, Huang Y, Xu TL, Ding YQ, Xu L (2008) Enhanced contextual fear memory in central serotonin-deficient mice. Proc Natl Acad Sci U S A, 105(33): 11981-11986.

58. Dalm S, Enthoven L, Meijer OC, van der Mark MH, Karssen AM, de Kloet ER et al (2005) Age-related changes in hypothalamic-pituitary-adrenal axis activity of male C57BL/6J mice. Neuroendocrinology 81: 372-380.

59. Dalm S, Brinks V, van der Mark MH, de Kloet ER, Oitzl MS (2008) Non-invasive stress-free application of glucocorticoid ligands in mice. J Neurosci Methods, 170(1): 77-84.

60. D'Aquila PS, Brain P, Willner P (1994) Effects of chronic mild stress on performance in behavioural tests relevant to anxiety and depression. Physiol Behav 56: 861-867.

61. Datson NA, van der Perk J, de Kloet ER, Vreugdenhil E. (2001) Identification of corticosteroid-responsive genes in rat hippocampus using serial analysis of gene expression. Eur J Neurosci., 14(4): 675-689.

62. Daumas S, Halley H, Francés B, Lassalle JM (2005) Encoding, consolidation, and retrieval of contextual memory: differential involvement of dorsal CA3 and CA1 hippocampal subregions. Learn Mem, 12: 375-382.

63. Debiec J, LeDoux JE, Nader K (2002) Cellular and systems reconsolidation in the hippocampus. Neuron, 36(3): 527-538.

64. Debiec J, LeDoux JE (2006) Noradrenergic signaling in the amygdala contributes to the reconsolidation of fear memory: treatment implications for PTSD. Ann N Y Acad Sci, 1071: 521-524.

65. de Oliveira AR, Reimer AE, Brandão ML (2006) Dopamine D2 receptor mechanisms in the expression of conditioned fear. Pharmacol Biochem Behav, 84(1): 102-11.

66. de Quervain DJ (2008) Glucocorticoid-induced reduction of traumatic memories: implications for the treatment of PTSD. Prog Brain Res 167: 239-247.

67. Diagnostic and Statistical Manual of Mental Disorders, Fourth Edition: DSM-IV-TR®, American psychiatric association, 2000.

68. Djordjevic A, Adzic M, Djordjevic J, Radojcic MB. (2009) Chronic social isolation is related to both upregulation of plasticity genes and initiation of proapoptotic signaling in Wistar rat hippocampus. J Neural Transm., 116(12): 1579-1589.

69. Doherty J, Dingledine R (1998) Differential regulation of synaptic inputs to dentate hilar border interneurons by metabotropic glutamate receptors. J Neurophysiol, 79(6): 2903-2910.

70. Dudai Y (2004) The neurobiology of consolidations, or, how stable is the engram? Annu Rev Psychol, 55: 51-86.

71. Dutar P, Vaillend C, Viollet C, Billard JM, Potier B, Carlo AS, Ungerer A, Epelbaum J (2002) Spatial learning and synaptic hippocampal plasticity in type 2 somatostatin receptor knock-out mice. Neuroscience 112: 455-466.

72. Dzirasa K, McGarity DL, Bhattacharya A, Kumar S, Takahashi JS, Dunson D et al (2011) Impaired limbic gamma oscillatory activity synchrony during anxiety-related behaviour in a genetic model mouse model of bipolar mania. J Neurosci 31: 6449-6456.

73. Eckel-Mahan KL, Phan T, Han S, Wang H, Chan GC, Scheiner ZS, Storm DR (2008) Circadian oscillation of hippocampal MAPK activity and cAmp: implications for memory persistence. Nat Neurosci, 11(9): 1074-1082.

74. Ehrlich I, Humeau Y, Grenier F, Ciocchi S, Herry C, Lüthi A (2009) Amygdala inhibitory circuits and the control of fear memory. Neuron, 62(6): 757-771.

75. Elizalde N, García-García AL, Totterdell S, Gendive N, Venzala E, Ramirez MJ, Del Rio J, Tordera RM. (2010) Sustained stress-induced changes in mice as a model for chronic depression. Psychopharmacology (Berl), 210(3): 393-406.

76. Epelbaum J, Tapia-Arancibia L, Kordon C (1981) Noradrenaline stimulates somatostatin release from incubated slices of the amygdala and the hypothalamic preoptic area. Brain Res, 215(1-2): 393-397.

77. Facharztinfomationen Tamoxistad 20/ 30 mg, Rote Liste Service GmbH, Berlin, Stand: January 2011

78. Fadok JP, Dickerson TM, Palmiter RD (2009) Dopamine is necessary for cue-dependent fear conditioning. J Neurosci, 29(36): 11089-11097.

79. Fanselow MS, Dong HW (2010) Are the dorsal and ventral hippocampus functionally distinct structures? Neuron, 65(1):7-19.

80. File SE, Vellucci SV, Wendlandt S (1979) Corticosterone -- an anxiogenic or an anxiolytic agent? J Pharm Pharmacol 31: 300-305.

81. Flood JF, Morley JE (1989) Dissociation of the effects of neuropeptide Y on feeding and memory: evidence for pre- and postsynaptic mediation. Peptides, 10(5): 963-966.

82. Fu LY, van den Pol AN (2007) GABA excitation in mouse hilar neuropeptide Y neurons. J Physiol, 579(Pt 2): 445-464.

83. Gale GD, Anagnostaras SG, Fanselow MS (2001) Cholinergic modulation of pavlovian fear conditioning: effects of intrahippocampal scopolamine infusion. Hippocampus, 11(4): 371-376.

84. Garakani A, Mathew SJ, Charney DS (2006) Neurobiology of anxiety disorders and implications for treatment. Mt Sinai J Med, 73(7): 941-949.

85. Gass P, Wolfer DP, Balschun D, Rudolph D, Frey U, Lipp HP, Schütz G (1998) Deficits in memory tasks of mice with CREB mutations depend on gene dosage. Learn Mem, 5(4-5): 274-288.

86. Gerstner JR, Lyons LC, Wright KP Jr, Loh DH, Rawashdeh O, Eckel-Mahan KL, Roman GW (2009) Cycling behavior and memory formation. J Neurosci, 29(41): 12824-12830.

87. Giardino L, Bettelli C, Pozza M, Calzà L (1999) Regulation of CCK mRNA expression in the rat brain by stress and treatment with sertraline, a selective serotonin re-uptake inhibitor. Brain Res., 824(2): 304-307.

88. Gisabella B, Bolshakov VY, Benes FM (2012) Kainate receptor-mediated modulation of hippocampal fast spiking interneurons in a rat model of schizophrenia. PLoS One, 7(3): e32483.

89. Gloveli T, Dugladze T, Rotstein HG, Traub RD, Monyer H, Heinemann U, Traub RD, Whittington MA, Buhl EH (2005) Orthogonal arrangement of rhythm-generating microcircuits in the hippocampus. Proc Natl Acad Sci U S A 102: 13295-13300

90. Graeff FG, Garcia-Leal C, Del-Ben CM, Guimarães FS (2005) Does the panic attack activate the hypothalamic-pituitary-adrenal axis? An Acad Bras Cienc 77(3): 477-491.

91. Hájos N, Paulsen O (2009) Network mechanisms of gamma oscillations in the CA3 region of the hippocampus. Neural Networks 22: 1113-1119.

92. Handelmann GE, Beinfeld MC, O'Donohue TL, Nelson JB, Brenneman DE (1983) Extra-hippocampal projections of CCK neurons of the hippocampus and subiculum. Peptides, 4(3): 331-334.

93. Harvey BH, Shahid M (2012) Metabotropic and ionotropic glutamate receptors as neurobiological targets in anxiety and stress-related disorders: focus on pharmacology and preclinical translational models. Pharmacol Biochem Behav, 100(4): 775-800.

94. Heilig M (2004) The NPY system in stress, anxiety and depression. Neuropeptides, 38: 213-224.

95. Herman JP, Cullinan WE, Morano MI, Akil H, Watson SJ (1995) Contribution of the ventral subiculum to inhibitory regulation of hypothalamo-pituitary-adrenocortical axis. J Neuroendocronol 7: 475-482.

96. Herman JP, Watson SJ, Spencer RL. (1999) Defense of adrenocorticosteroid receptor expression in rat hippocampus: effects of stress and strain. Endocrinology, 140(9): 3981-3991.

97. Herman JP, Larson BR. (2001) Differential regulation of forebrain glutamic acid decarboxylase mRNA expression by aging and stress. Brain Res., 912(1): 60-66.

98. Hetrick SE, Purcell R, Garner B, Parslow R (2010) Combined pharmacotherapy and psychological therapies for post traumatic stress disorder (PTSD). Cochrane Database Syst Rev, (7): CD007316.

99. Houser CR (2007) Interneurons of the dentate gyrus: an overview of cell types, terminal fields and neurochemical identity. Prog Brain Res, 163: 217-232.

100. Huff NC, Frank M, Wright-Hardesty K, Sprunger D, Matus-Amat P, Higgins E, Rudy JW (2006) Amygdala regulation of immediate-early gene expression in the hippocampus induced by contextual fear conditioning. J Neurosci, 26(5): 1616-1623.

101. Hunter RG, Bellani R, Bloss E, Costa A, McCarthy K, McEwen BS (2009) Regulation of kainate receptor subunit mRNA by stress and corticosteroids in the rat hippocampus. PLoS One, 4(1): e4328.

102. Itoi K, Sugimoto N (2010) The brainstem noradrenergic systems in stress, anxiety and depression. J Neuroendocrinol, 22(5): 355-361.

103. Jacobson L, Sapolsky R (1991) The role of the hippocampus in feedback regulation of the hypothalamic-pituitary-adrenocortical axis. Endocr Rev 12: 118-134.

104. Jacobson-Pick S, Elkobi A, Vander S, Rosenblum K, Richter-Levin G (2008) Juvenile stress-induced alteration of maturation of the GABAA receptor alpha subunit in the rat. Int J Neuropsychopharmacol, 11(7): 891-903.

105. Jacobson-Pick S, Richter-Levin G (2010) Differential impact of juvenile stress and corticosterone in juvenility and in adulthood, in male and female rats. Behav Brain Res., 214(2): 268-276.

106. Jin XC, Lu YF, Yang XF, Ma L, Li BM (2007) Glucocorticoid receptors in the basolateral nucleus of amygdala are required for postreactivation reconsolidation of auditory fear memory. Eur J Neurosci, 25(12): 3702-1372.

107. Jinno S, Kosaka T (2006) Cellular architecture of the mouse hippocampus: a quantitative aspect of chemically defined GABAergic neurons with stereology. Neurosci Res, 56: 229-245.

108. Jones N, King SM (2001) Influence of circadian phase and test illumination on pre-clinical models of anxiety. Physiol Behav, 72(1-2): 99-106.

109. Kamei H, Kameyama T, Nabeshima T (1995) Activation of both dopamine D1 and D2 receptors necessary for amelioration of conditioned fear stress. Eur J Pharmacol, 273(3): 229-233.

110. Kamiya H (2002) Kainate receptor-dependent presynaptic modulation and plasticity. Neurosci Res, 42: 1-6.

111. Kandel ER, Schwartz JH, Jessell TM (2000): Principles of neural science, 4th Edition. pp. 1259ff. McGraw-Hill. New York

112. Kang I, Thompson ML, Heller J, Miller LG. (1991) Persistent elevation in GABAA receptor subunit mRNAs following social stress. Brain Res Bull. 26(5): 809-812.

113. Kaouane N, Porte Y, Vallée M, Brayda-Bruno L, Mons N, Calandreau L, Marighetto A, Piazza PV, Desmedt A (2012) Glucocorticoids can induce PTSD-like memory impairments in mice. Science, 335(6075): 1510-1513.

114. Karl T, Duffy L, Herzog H (2008) Behavioural profile of a new mouse model for NPY deficiency. Eur J Neurosci, 28(1): 173-180.

115. Kash SF, Tecott LH, Hodge C, Baekkeskov S (1999) Increased anxiety and altered responses to anxiolytics in mice deficient in the 65-kDa isoform of glutamic acid decarboxylase. Proc Natl Acad Sci U S A, 96(4): 1698-1703.

116. Kask A, Rägo L, Harro J (1998) Anxiogenic-like effect of the NPY Y1 receptor antagonist BIBP3226 administered into the dorsal periaqueductal gray matter in rats. Regul Pept, 75-76: 255-262.

117. Kask A, Kivastik T, Rägo L, Harro J (1999) Neuropeptide Y Y1 receptor antagonist BIBP3226 produces conditioned place aversion in rats. Prog Neuropsychopharmacol Biol Psychiatry, 23(4): 705-711.

118. Kesner RP (2007) A behavioral analysis of dentate gyrus function. Prog Brain Res., 163: 567-576.

119. Kim JJ, Jung MW (2006) Neural circuits and mechanisms involved in Pavlovian fear conditioning: a critical review. Neurosci Biobehav Rev, 30(2): 188-202.

120. Kitraki E, Karandrea D, Kittas C. (1999) Long-lasting effects of stress on glucocorticoid receptor gene expression in the rat brain. Neuroendocrinology, 69(5): 331-338.

121. Kjelstrup KG, Tuvnes FA, Steffenach HA, Murison R, Moser EI, Moser MB (2002) Reduced fear expression after lesions of the ventral hippocampus. Proc Natl Acad Sci U S A 99: 10825-10830.

122. Kluge C, Stoppel C, Szinyei C, Stork O, Pape H (2008) Role of the somatostatin system in contextual fear memory and hippocampal synaptic plasticity. Learn Mem 15: 252-260.

123. Ko S, Zhao MG, Toyoda H, Qiu CS, Zhuo M (2005) Altered behavioral responses to noxious stimuli and fear in glutamate receptor 5 (GluR5)- or GluR6-deficient mice. J Neurosci, 25(4): 977-984.

124. Kolber BJ, Wieczorek L, Muglia LJ (2008) Hypothalamic-pituitary-adrenal axis dysregulation and behavioral analysis of mouse mutants with altered glucocorticoid or mineralocorticoid receptor function. Stress, (5): 321-338.

125. Krysiak R, Obuchowicz E, Herman ZS (2000) Conditioned fear-induced changes in neuropeptide Y-like immunoreactivity in rats: the effect of diazepam and buspirone. Neuropeptides, 34: 148-157.

126. Kupfer DJ, Frank E, Phillips ML (2012) Major depressive disorder: new clinical, neurobiological, and treatment perspectives. Lancet, 379(9820): 1045-1055.

127. LaLumiere RT, Buen TV, McGaugh JL (2003) Post-training intra-basolateral amygdala infusions of norepinephrine enhance consolidation of memory for contextual fear conditioning. J Neurosci, 23(17): 6754-6758.

128. Laxmi TR, Stork O, Pape H (2003) Generalisation of conditioned fear and its behavioural expression in mice. Behav Brain Res, 145: 89-98.

129. LeDoux JE (1993) Emotional memory systems in the brain. Behav Brain Res, 58(1-2): 69-79.

130. LeDoux JE (2000) Emotion circuits in the brain. Annu Rev Neurosci, 23: 155-184.

131. Lee I, Kesner RP (2004a) Encoding versus retrieval of spatial memory: double dissociation between the dentate gyrus and the perforant path inputs into CA3 in the dorsal hippocampus. Hippocampus, 14(1): 66-76.

132. Lee I, Kesner R (2004b) Differential contributions of dorsal hippocampal subregions to memory acquisition and retrieval in contextual fear-conditioning. Hippocampus, 14: 301-310.

133. Lee JL, Everitt BJ, Thomas KL (2004) Independent cellular processes for hippocampal memory consolidation and reconsolidation. Science, 304(5672): 839-843.

134. Lee JL, Milton AL, Everitt BJ (2006) Reconsolidation and extinction of conditioned fear: inhibition and potentiation. J Neurosci, 26(39): 10051-10056.

135. Le Roux N, Amar M, Baux G, Fossier P. (2006) Homeostatic control of the excitation-inhibition balance in cortical layer 5 pyramidal neurons. Eur J Neurosci, 24(12): 3507-3518.

136. Li F, Zhang YY, Jing XM, Yan CH, Shen XM (2010) Memory impairment in early sensorimotor deprived rats is associated with suppressed hippocampal neurogenesis and altered CREB signaling. Behav Brain Res, 207(2): 458-465.

137. Li Z, Richter-Levin G (2012) Stimulus intensity-dependent modulations of hippocampal long-term potentiation by basolateral amygdala priming. Front Cell Neurosci, 6: 21.

138. Liberzon I, López JF, Flagel SB, Vázquez DM, Young EA. (1999) Differential regulation of hippocampal glucocorticoid receptors mRNA and fast feedback: relevance to post-traumatic stress disorder. J Neuroendocrinol, 11(1): 11-17.

139. Liu X, Ramirez S, Pang PT, Puryear CB, Govindarajan A, Deisseroth K, Tonegawa S. (2012) Optogenetic stimulation of a hippocampal engram activates fear memory recall. Nature, 484(7394): 381-385.

140. Livak KJ, Schmittgen TD (2001) Analysis of relative gene expression data using real-time quantitative PCR and the 2(-Delta Delta C(T)) Method. Methods, 25: 402-408.

141. Lu CB, Jefferys JG, Toescu EC, Vreugdenhil M (2011) In vitro hippocampal gamma oscillation power as an index of in vivo CA3 gamma oscillation strength and spatial reference memory. Neurobiol Learn Mem 95: 221-230.

142. Maccaferri G, Lacaille JC (2003) Interneuron Diversity series: Hippocampal interneuron classifications--making things as simple as possible, not simpler. Trends Neurosci, 26(10): 564-571.

143. Maggio N, Segal M (2007) Striking variations in corticosteroid modulation of long-term potentiation along the septotemporal axis of the hippocampus. J Neurosci 27: 5757-5765.

144. Maggio N, Segal M (2009) Differential corticosteroid modulation of inhibitory synaptic currents in the dorsal and ventral hippocampus. J Neurosci 29: 2857-2866.

145. Maggio N, Segal M (2011) Persistent changes in ability to express long-term potentiation/depression in the rat hippocampus after juvenile/adult stress. Biol Psychiatry, 69: 748- 753

146. Maggio N, Segal M (2012) Steroid modulation of hippocampal plasticity: switching between cognitive and emotional memories. Front Cell Neurosci, 6:12.

147. Mahan AL, Ressler KJ (2012) Fear conditioning, synaptic plasticity and the amygdala: implications for posttraumatic stress disorder. Trends Neurosci, 35(1): 24-35.

148. Makkar SR, Zhang SQ, Cranney J (2010) Behavioral and neural analysis of GABA in the acquisition, consolidation, reconsolidation, and extinction of fear memory. Neuropsychopharmacology, 35(8): 1625-1652.

149. Mamiya N, Fukushima H, Suzuki A, Matsuyama Z, Homma S, Frankland PW, Kida S (2009) Brain region-specific gene expression activation required for reconsolidation and extinction of contextual fear memory. J Neurosci, 29(2): 402-413.

150. Marchetti C, Tafi E, Marie H (2011) Viral-mediated expression of a constitutively active form of cAMP response element binding protein in the dentate gyrus increases long term synaptic plasticity. Neuroscience, 190: 21-26.

151. Maren S, Fanselow MS (1995) Synaptic plasticity in the basolateral amygdala induced by hippocampal formation stimulation in vivo. J Neurosci, 15: 7548-7564.

152. Maren S (2001) Neurobiology of Pavlovian fear conditioning. Annu Rev Neurosci, 24: 897-931.

153. Maren S, Quirk G (2004) Neuronal signalling of fear memory. Nat Rev Neurosci, 5: 844-852.

154. Maren S, Holt WG (2004) Hippocampus and Pavlovian fear conditioning in rats: muscimol infusions into the ventral, but not dorsal, hippocampus impair the acquisition of conditional freezing to an auditory conditional stimulus. Behav Neurosci 118: 97-110.

155. Maren S (2008) Pavlovian fear conditioning as a behavioral assay for hippocampus and amygdala function: cautions and caveats. Eur J Neurosci, 28(8): 1661-1666.

156. Martisova E, Solas M, Horrillo I, Ortega JE, Meana JJ, Tordera RM, Ramírez MJ. (2012) Long lasting effects of early-life stress on glutamatergic/GABAergic circuitry in the rat hippocampus. Neuropharmacology, 62(5-6): 1944-1953

157. Mascagni F, McDonald AJ (2003) Immunohistochemical characterization of cholecystokinin containing neurons in the rat basolateral amygdala. Brain Research, 976: 171-184.

158. Matsumoto K, Puia G, Dong E, Pinna G. (2007) GABA(A) receptor neurotransmission dysfunction in a mouse model of social isolation-induced stress: possible insights into a non-serotonergic mechanism of action of SSRIs in mood and anxiety disorders. Stress 10(1): 3-12.

159. McDonald AJ (1989) Coexistence of somatostatin with neuropeptide Y, but not with cholecystokinin or vasoactive intestinal peptide, in neurons of the rat amygdala. Brain Research 500: 37-45.

160. McGaugh JL (2004) The amygdala modulates the consolidation of memories of emotionally arousing experiences. Annu Rev Neurosci, 27: 1-28.

161. McNally RJ (2012) Are we winning the war against posttraumatic stress disorder? Science, 336(6083): 872-874.

162. Meewisse ML, Reitsma JB, de Vries GJ, Gersons BP, Olff M. (2007) Cortisol and post-traumatic stress disorder in adults: systematic review and meta-analysis. Br J Psychiatry 191: 387-392.

163. Mei B, Li C, Dong S, Jiang CH, Wang H, Hu Y (2005) Distinct gene expression profiles in hippocampus and amygdala after fear conditioning. Brain Res Bull, 67(1-2): 1-12.

164. Meis S, Sosulina L, Schulz S, Höllt V, Pape H (2005) Mechanisms of somatostatin-evoked responses in neurons of the rat lateral amygdala. Eur J Neurosci 21: 755-762.

165. Meis S, Munsch T, Sosulina L, Pape HC (2007) Postsynaptic mechanisms underlying responsiveness of amygdaloid neurons to cholecystokinin are mediated by a transient receptor potential-like current. Mol Cell Neurosci, 35(2): 356-367.

166. Meyer U, van Kampen M, Isovich E, Flügge G, Fuchs E. (2001) Chronic psychosocial stress regulates the expression of both GR and MR mRNA in the hippocampal formation of tree shrews. Hippocampus, 11(3): 329-336.

167. Mikkelsen JD, Bundzikova J, Larsen MH, Hansen HH, Kiss A. (2008) GABA regulates the rat hypothalamic-pituitary-adrenocortical axis via different GABA-A receptor alpha-subtypes. Ann N Y Acad Sci. 1148: 384-392.

168. Miller KK, Hoffer A, Svoboda KR, Lupica CR (1997) Cholecystokinin increases GABA release by inhibiting a resting K+ conductance in hippocampal interneurons. J Neurosci, 17: 4994-5003.

169. Milner TA, Hammel JR, Ghorbani TT, Wiley RG, Pierce JP (1999) Septal cholinergic deafferentation of the dentate gyrus results in a loss of a subset of neuropeptide Y somata and an increase in synaptic area on remaining neuropeptide Y dendrites. Brain Res, 831(1-2): 322-336.

170. Mitra R, Sapolsky RM (2008) Acute corticosterone treatment is sufficient to induce anxiety and amygdaloid dendritic hypertrophy. Proc Natl Acad Sci U S A 105: 5573-5578

171. Miyakawa T, Yamada M, Duttaroy A, Wess J (2001) Hyperactivity and intact hippocampus-dependent learning in mice lacking the M1 muscarinic acetylcholine receptor. J Neurosci, 21(14): 5239-5250.

172. Möhler H (2012) The GABA system in anxiety and depression and its therapeutic potential. Neuropharmacology, 62(1): 42-53.

173. Montgomery SM, Buzsáki G (2007) Gamma oscillations dynamically couple CA3 and CA1 region during memory task performance. Proc Natl Acad Sci U S A 104: 14495-15000.

174. Morgan CA 3rd, Rasmusson AM, Wang S, Hoyt G, Hauger RL, Hazlett G (2002) Neuropeptide-Y, cortisol, and subjective distress in humans exposed to acute stress: replication and extension of previous report. Biol Psychiatry, 52(2): 136-142.

175. Morsink MC, Van Gemert NG, Steenbergen PJ, Joëls M, De Kloet ER, Datson NA. (2007) Rapid glucocorticoid effects on the expression of hippocampal neurotransmission-related genes. Brain Res., 1150: 14-20.

176. Moser MB, Moser EI (1998) Functional differentiation in the hippocampus. Hippocampus, 8(6): 608-619.

177. Mulle C, Sailer A, Pérez-Otaño I, Dickinson-Anson H, Castillo PE, Bureau I, Maron C, Gage FH, Mann JR, Bettler B, Heinemann SF (1998) Altered synaptic physiology and reduced susceptibility to kainate-induced seizures in GluR6-deficient mice. Nature, 392(6676): 601-605.

178. Mulle C, Sailer A, Swanson GT, Brana C, O'Gorman S, Bettler B, Heinemann SF (2000) Subunit composition of kainate receptors in hippocampal interneurons. Neuron, 28(2): 475-484.

179. Myers KM, Davis M. (2002) Systems- level reconsolidation: reengagement of the hippocampus with memory reactivation. Neuron 36(3): 340-343.

180. Nader K, Schafe GE, Le Doux JE (2000) Fear memories require protein synthesis in the amygdala for reconsolidation after retrieval. Nature 406(6797): 722-726.

181. Nagy A (2000) Cre Recombinase: The Universal Reagent for Genome Tailoring. Genesis, 26: 99-109.

182. Narayanan RT, Seidenbecher T, Kluge C, Bergado J, Stork O, Pape HC (2007a) Dissociated theta phase synchronization in amygdalo- hippocampal circuits during various stages of fear memory. Eur J Neurosci, 25(6): 1823-1831.

183. Narayanan RT, Seidenbecher T, Sangha S, Stork O, Pape HC (2007b) Theta resynchronization during reconsolidation of remote contextual fear memory. Neuroreport 18(11): 1107-1111.

184. O'Brien J, Sutherland RJ (2007) Evidence for episodic memory in a pavlovian conditioning procedure in rats. Hippocampus, 17(12): 1149-1152.

185. Okano H, Hirano T, Balaban E (2000) Learning and memory. Proc Natl Acad Sci U S A, 97(23): 12403-12404.

186. Olson VG, Rockett HR, Reh RK, Redila VA, Tran PM, Venkov HA, Defino MC, Hague C, Peskind ER, Szot P, Raskind MA (2011) The role of norepinephrine in differential response to stress in an animal model of posttraumatic stress disorder. Biol Psychiatry 70: 441-448.

187. Orchinik M, Weiland NG, McEwen BS (1995) Chronic exposure to stress levels of corticosterone alters GABAA receptor subunit mRNA levels in rat hippocampus. Brain Res Mol Brain Res, 34(1): 29-37.

188. Owen D, Matthews SG. (2007) Repeated maternal glucocorticoid treatment affects activity and hippocampal NMDA receptor expression in juvenile guinea pigs. J Physiol. 578: 249-257.

189. Pandey SC, Zhang H, Roy A, Xu T (2005) Deficits in amygdaloid cAMP-responsive element-binding protein signaling play a role in genetic predisposition to anxiety and alcoholism. J Clin Invest, 115(10): 2762-2773.

190. Paredes MF, Greenwood J, Baraban SC (2003) Neuropeptide Y modulates a G protein-coupled inwardly rectifying potassium current in the mouse hippocampus. Neurosci Lett, 340(1): 9-12.

191. Paskitti ME, McCreary BJ, Herman JP. (2000) Stress regulation of adrenocorticosteroid receptor gene transcription and mRNA expression in rat hippocampus: time-course analysis. Brain Res Mol Brain Res., 80(2): 142-152.

192. Paxinos G, Franklin KBJ (2001) The mouse brain in stereotaxic coordinates. 2nd edition, Academic Press, San Diego.

193. Paxinos G, Watson C (1998) The rat brain in stereotaxic coordinates. 4th edition, Academic Press, San Diego.

194. Pelletier JG, Likhtik E, Filali M, Paré D (2005) Lasting increases in basolateral amygdala activity after emotional arousal: implications for facilitated consolidation of emotional memories. Learn Mem, 12(2): 96-102.

195. Pezze MA, Feldon J (2004) Mesolimbic dopaminergic pathways in fear conditioning. Prog Neurobiol, 74(5): 301-320.

196. Phillips RG, LeDoux JE (1992) Differential contribution of amygdala and hippocampus to cued and contextual fear conditioning. Behav Neurosci, 106: 274-285.

197. Phillips RG, LeDoux JE (1994) Lesions of the dorsal hippocampal formation interfere with background but not foreground contextual fear conditioning. Learn Mem, 1: 34-44.

198. Pitkänen A, Pikkarainen M, Nurminen N, Ylinen A (2000) Reciprocal connections between the amygdala and the hippocampal formation, perirhinal cortex, and postrhinal cortex in rat. A review. Ann N Y Acad Sci, 911: 369-391.

199. Ploski JE, Park KW, Ping J, Monsey MS, Schafe GE (2010) Identification of plasticity-associated genes regulated by Pavlovian fear conditioning in the lateral amygdala. J Neurochem, 112(3): 636-650.

200. Post AM, Weyers P, Holzer P, Painsipp E, Pauli P, Wultsch T, Reif A, Lesch KP (2011) Gene-environment interaction influences anxiety-like behavior in ethologically based mouse models. Behav Brain Res, 218(1): 99-105.

201. Poulin B, Butcher A, McWilliams P, Bourgognon JM, Pawlak R, Kong KC, Bottrill A, Mistry S, Wess J, Rosethorne EM, Charlton SJ, Tobin AB (2010) The M3-muscarinic receptor regulates learning and memory in a receptor phosphorylation/arrestin-dependent manner. Proc Natl Acad Sci U S A, 107(20): 9440-9445.

202. Poulter MO, Du L, Zhurov V, Merali Z, Anisman H (2010) Plasticity of the GABA(A) receptor subunit cassette in response to stressors in reactive versus resilient mice. Neuroscience, 165(4): 1039-1051.

203. Pratt JA, Brett RR (1995) The benzodiazepine receptor inverse agonist FG 7142 induces cholecystokinin gene expression in rat brain. Neurosci Lett, 184: 197-200.

204. Primeaux SD, Wilson SP, Cusick MC, York DA, Wilson MA (2005) Effects of altered amygdalar neuropeptide Y expression on anxiety-related behaviors. Neuropsychopharmacology, 30: 1589-1597.

205. Quirk GJ, Paré D, Richardson R, Herry C, Monfils MH, Schiller D et al (2010) Erasing fear memories with extinction training. J Neurosci 30: 14993-14997.

206. Radulovic J, Kammermeier J, Spiess J (1998) Generalization of fear responses in C57BL/6N mice subjected to one-trial foreground contextual fear conditioning. Behav Brain Res 95: 179-189.

207. Rammes G, Steckler T, Kresse A, Schütz G, Zieglgänsberger W, Lutz B (2000) Synaptic plasticity in the basolateral amygdala in transgenic mice expressing dominant-negative cAMP response element-binding protein (CREB) in forebrain. Eur J Neurosci, 12(7): 2534-2546.

208. Ran I, Laplante I, Lacaille JC (2012) CREB-Dependent Transcriptional Control and Quantal Changes in Persistent Long-Term Potentiation in Hippocampal Interneurons. J Neurosci, 32(18): 6335-6350.

209. Raud S, Innos J, Abramov U, Reimets A, Koks S, Soosaar A, Matsui T, Vasar E (2005) Targeted invalidation of CCK2 receptor gene induces anxiolytic-like action in light-dark exploration, but not in fear conditioning test. Psychopharmacology (Berl), 181: 347-357.

210. Redrobe JP, Dumont Y, Fournier A, Quirion R (2002) The neuropeptide Y (NPY) Y1 receptor subtype mediates NPY-induced antidepressant-like activity in the mouse forced swimming test. Neuropsychopharmacology, 26(5): 615-624.

211. Rehberg K, Bergado-Acosta JR, Koch JC, Stork O (2010) Disruption of fear memory consolidation and reconsolidation by actin filament arrest in the basolateral amygdala. Neurobiol Learn Mem 94: 117-126.

212. Rescorla RA (1976) Stimulus generalization: some predictions from a model of Pavlovian conditioning. J Exp Psychol Anim Behav Process, 2: 88-96.

213. Ressler KJ, Paschall G, Zhou XL, Davis M (2002) Regulation of synaptic plasticity genes during consolidation of fear conditioning. J Neurosci, 22(18): 7892-7902.

214. Restivo L, Tafi E, Ammassari-Teule M, Marie H (2009) Viral-mediated expression of a constitutively active form of CREB in hippocampal neurons increases memory. Hippocampus, 19(3): 228-234.

215. Riaza Bermudo-Soriano C, Perez-Rodriguez MM, Vaquero-Lorenzo C, Baca-Garcia E (2012) New perspectives in glutamate and anxiety. Pharmacol Biochem Behav, 100(4): 752-774.

216. Riedel G, Wetzel W, Reymann KG (1996) Comparing the role of metabotropic glutamate receptors in long-term potentiation and in learning and memory. Prog Neuropsychopharmacol Biol Psychiatry, 20(5):761-789.

217. Robinson L, Platt B, Riedel G (2011) Involvement of the cholinergic system in conditioning and perceptual memory. Behav Brain Res, 221(2): 443-465.

218. Rodriguez-Ortiz CJ, Bermúdez-Rattoni F (2007) Memory Reconsolidation or Updating Consolidation? In: Bermúdez-Rattoni F (ed.) Neural Plasticity and Memory: From Genes to Brain Imaging. CRC Press: Boca Raton, chapter 11.

219. Romeo RD, Ali FS, Karatsoreos IN, Bellani R, Chhua N, Vernov M, McEwen BS. (2007) Glucocorticoid receptor mRNA expression in the hippocampal formation of male rats before and after pubertal development in response to acute or repeated stress. Neuroendocrinology, 87(3): 160-167.

220. Roozendaal B, Okuda S, Van der Zee EA, McGaugh JL (2006a) Glucocorticoid enhancement of memory requires arousal-induced noradrenergic activation in the basolateral amygdala. Proc Natl Acad Sci USA, 103: 6741-6746.

221. Roozendaal B, Hui GK, Hui IR, Berlau DJ, McGaugh JL, Weinberger NM (2006b) Basolateral amygdala noradrenergic activity mediates corticosterone-induced enhancement of auditory fear conditioning. Neurobiol Learn Mem, 86: 249-255.

222. Rosa ML, Guimarães FS, Pearson RC, Del Bel EA. (2002) Effects of single or repeated restraint stress on GluR1 and GluR2 flip and flop mRNA expression in the hippocampal formation. Brain Res Bull., 59(2): 117-124.

223. Rosen JB, Kim SY, Post RM (1994) Differential regional and time course increases in thyrotropin-releasing hormone, neuropeptide Y and enkephalin mRNAs following an amygdala kindled seizure. Brain Res Mol Brain Res, 27(1): 71-80.

224. Rotzinger S, Vaccarino FJ (2003) Cholecystokinin receptor subtypes: role in the modulation of anxiety-related and reward-related behaviours in animal models. J Psychiatry Neurosci, 28: 171-181.

225. Rudolph D, Tafuri A, Gass P, Hämmerling GJ, Arnold B, Schütz G (1998) Impaired fetal T cell development and perinatal lethality in mice lacking the cAMP response element binding protein. Proc Natl Acad Sci U S A, 95(8): 4481-4486.

226. Rudy JW, Pugh CR (1996) A comparison of contextual and generalized auditory-cue fear conditioning: evidence for similar memory processes. Behav Neurosci, 110(6): 1299-1308.

227. Rudy JW, Huff NC, Matus-Amat P (2004) Understanding contextual fear conditioning: insights from a two-process model. Neurosci Biobehav Rev, 28: 675-685.

228. Rudy JW, Matus-Amat P (2005) The ventral hippocampus supports a memory representation of context and contextual fear conditioning: implications for a unitary function of the hippocampus. Behav Neurosci 119: 154-163.

229. Sauerhöfer E, Pamplona FA, Bedenk B, Moll GH, Dawirs RR, von Hörsten S, Wotjak CT, Golub Y (2012) Generalization of contextual fear depends on associative rather than non-associative memory components. Behav Brain Res, 233(2): 483-93.

230. Schafe GE, Nader K, Blair HT, LeDoux JE (2001) Memory consolidation of Pavlovian fear conditioning: a cellular and molecular perspective. Trends Neurosci, 24(9): 540-546.

231. Scharfman HE (2007) The CA3 "backprojection" to the dentate gyrus. Prog Brain Res, 163: 627-637

232. Schettini G (1991) Brain somatostatin: receptor-coupled transducing mechanisms and role in cognitive functions. Pharmacol Res, 23: 203-215.

233. Schiller D, Monfils MH, Raio CM, Johnson DC, Ledoux JE, Phelps EA (2010) Preventing the return of fear in humans using reconsolidation update mechanisms. Nature 463: 49-53.

234. Schulz S, Siemer H, Krug M, Höllt V (1999) Direct evidence for biphasic cAMP responsive element-binding protein phosphorylation during long-term potentiation in the rat dentate gyrus in vivo. J Neurosci, 19(13): 5683-5692

235. Schwabe L, Joëls M, Roozendaal B, Wolf OT, Oitzl MS (2012) Stress effects on memory: An update and integration. Neurosci Biobehav Rev, 36(7): 1740-1749.

236. Schwartz B, Wasserman EA, Robbins SJ (2002) Psychology of learning and behavior, 5th Edition. pp. 42-53, 85, 92-94. W.W. Norton. New York

237. Seidenbecher T, Laxmi TR, Stork O, Pape HC (2003) Amygdalar and hippocampal theta rhythm synchronization during fear memory retrieval. Science, 301(5634): 846-850.

238. Sergeyev V, Fetissov S, Mathé AA, Jimenez PA, Bartfai T, Mortas P, Gaudet L, Moreau JL, Hökfelt T (2005) Neuropeptide expression in rats exposed to chronic mild stresses. Psychopharmacology (Berl), 178(2-3): 115-124.

239. Sherin JE, Nemeroff CB (2011) Post-traumatic stress disorder: the neurobiological impact of psychological trauma. Dialogues Clin Neurosci, 13(3): 263-278.

240. Shors TJ, Gallegos RA, Breindl A. (1997) Transient and persistent consequences of acute stress on long-term potentiation (LTP), synaptic efficacy, theta rhythms and bursts in area CA1 of the hippocampus. Synapse, 26(3): 209-217.

241. Siegmund A, Wotjak CT (2006) Toward an animal model of posttraumatic stress disorder. Ann N Y Acad Sci 1071: 324-334.

242. Siegmund A, Köster L, Meves AM, Plag J, Stoy M, Ströhle A (2011). Stress hormones during flooding therapy and their relationship to therapy outcome in patients with panic disorder and agoraphobia. J Psychiatr Res 45: 339-346.

243. Silva AJ, Kogan JH, Frankland PW, Kida S (1998) CREB and memory. Annu Rev Neurosci, 21: 127-148.

244. Silva AP, Carvalho AP, Carvalho CM, Malva JO (2001) Modulation of intracellular calcium changes and glutamate release by neuropeptide Y1 and Y2 receptors in the rat hippocampus: differential effects in CA1, CA3 and dentate gyrus. J Neurochem, 79(2): 286-296.

245. Silva AP, Xapelli S, Pinheiro PS, Ferreira R, Lourenço J, Cristóvão A, Grouzmann E, Cavadas C, Oliveira CR, Malva JO (2005) Up-regulation of neuropeptide Y levels and modulation of glutamate release through neuropeptide Y receptors in the hippocampus of kainate-induced epileptic rats. J Neurochem, 93(1): 163-70.

246. Skórzewska A, Bidziński A, Lehner M, Turzyńska D, Wisłowska-Stanek A, Sobolewska A, Szyndler J, Maciejak P, Taracha E, Płaźnik A (2006) The effects of acute and chronic administration of corticosterone on rat behavior in two models of fear responses, plasma corticosterone concentration, and c-Fos expression in the brain structures. Pharmacol Biochem Behav, 85(3): 522-534.

247. Sloviter RS, Zappone CA, Harvey BD, Frotscher M (2006) Kainic acid-induced recurrent mossy fiber innervation of dentate gyrus inhibitory interneurons: possible anatomical substrate of granule cell hyper-inhibition in chronically epileptic rats. J Comp Neurol, 494(6): 944-960.

248. Smiałowska M, Wierońska JM, Domin H, Zieba B (2007) The effect of intrahippocampal injection of group II and III metobotropic glutamate receptor agonists on anxiety; the role of neuropeptide Y. Neuropsychopharmacology, 32(6): 1242-1250.

249. Soares JC, Fornari RV, Oliveira MG (2006) Role of muscarinic M1 receptors in inhibitory avoidance and contextual fear conditioning. Neurobiol Learn Mem, 86(2): 188-196.

250. Soghomonian JJ, Martin DL (1998) Two isoforms of glutamate decarboxylase: why? Trends Pharmacol Sci, 19(12): 500-505.

251. Soltesz I, Bourassa J, Deschênes M (1993) The behavior of mossy cells of the rat dentate gyrus during theta oscillations in vivo. Neuroscience, 57: 555-564.

252. Soravia LM, Heinrichs M, Aerni A, Maroni C, Schelling G, Ehlert U et al (2006) Glucocorticoids reduce phobic fear in humans. Proc Natl Acad Sci U S A 103: 5585-90

253. Sørensen AT, Kanter-Schlifke I, Carli M, Balducci C, Noe F, During MJ, Vezzani A, Kokaia M (2008) NPY gene transfer in the hippocampus attenuates synaptic plasticity and learning. Hippocampus, 18(6): 564-574.

254. Sosulina L, Graebenitz S, Pape HC (2010) GABAergic interneurons in the mouse lateral amygdala: a classification study. J Neurophysiol, 104(2): 617-626.

255. Spampanato J, Polepalli J, Sah P (2011) Interneurons in the basolateral amygdala. Neuropharmacology, 60(5): 765-773.

256. Sperk G, Hamilton T, Colmers WF (2007) Neuropeptide Y in the dentate gyrus. Prog Brain Res., 163: 285-297.

257. Squire LR, Zola SM (1996) Structure and function of declarative and nondeclarative memory systems. Proc Natl Acad Sci U S A, 93(24): 13515-13522.

258. Stam R (2007) PTSD and stress sensitisation: a tale of brain and body Part 2: animal models. Neurosci Biobehav Rev, 31(4): 558-584.

259. Stanciu M, Radulovic J, Spiess J (2001) Phosphorylated cAMP response element binding protein in the mouse brain after fear conditioning: relationship to Fos production. Brain Res Mol Brain Res, 94(1-2): 15-24.

260. Stein DJ, Matsunaga H (2006) Specific phobia: a disorder of fear conditioning and extinction. CNS Spectr 11: 248-251.

261. Stone DJ, Walsh JP, Sebro R, Stevens R, Pantazopolous H, Benes FM. (2001) Effects of pre- and postnatal corticosterone exposure on the rat hippocampal GABA system. Hippocampus. 11(5): 492-507.

262. Stoppel C, Albrecht A, Pape HC, Stork O (2006) Genes and neurons: molecular insights to fear and anxiety. Gens Brain Behav. 5 Suppl 2: 34-47.

263. Stork O, Ji FY, Kaneko K, Stork S, Yoshinobu Y, Moriya T, Shibata S, Obata K (2000). Postnatal development of a GABA deficit and disturbance of neural functions in mice lacking GAD65. Brain Res., 865(1): 45-58.

264. Stork O, Yamanaka H, Stork S, Kume N, Obata K (2003) Altered conditioned fear behavior in glutamate decarboxylase 65 null mutant mice. Genes Brain Behav, 2(2): 65-70.

265. Stranahan AM, Lee K, Mattson MP (2008) Contributions of impaired hippocampal plasticity and neurodegeneration to age-related deficits in hormonal pulsatility. Ageing Res Rev 7: 164-176.

266. Ströhle A, Holsboer F (2003) Stress responsive neurohormones in depression and anxiety. Pharmacopsychiatry 3: S207-214.

267. Suzuki A, Fukushima H, Mukawa T, Toyoda H, Wu LJ, Zhao MG, Xu H, Shang Y, Endoh K, Iwamoto T, Mamiya N, Okano E, Hasegawa S, Mercaldo V, Zhang Y, Maeda R, Ohta M, Josselyn SA, Zhuo M, Kida S (2011) Upregulation of CREB-mediated transcription enhances both short- and long-term memory. J Neurosci, 31(24): 8786-8802.

268. Szinyei C, Heinbockel T, Montagne J, Pape HC (2000) Putative cortical and thalamic inputs elicit convergent excitation in a population of GABAergic interneurons of the lateral amygdala. J Neurosci, 20: 8909-8915.

269. Taniguchi H, He M, Wu P, Kim S, Paik R, Sugino K, Kvitsiani D, Fu Y, Lu J, Lin Y, Miyoshi G, Shima Y, Fishell G, Nelson SB, Huang ZJ (2011) A resource of Cre driver lines for genetic targeting of GABAergic neurons in cerebral cortex. Neuron, 71(6): 995-1013.

270. Tian N, Petersen C, Kash S, Baekkeskov S, Copenhagen D, Nicoll R. (1999) The role of the synthetic enzyme GAD65 in the control of neuronal gamma-aminobutyric acid release. Proc Natl Acad Sci U S A, 96(22): 12911- 12916.

271. Tinsley MR, Quinn JJ, Fanselow MS (2004) The role of muscarinic and nicotinic cholinergic neurotransmission in aversive conditioning: comparing pavlovian fear conditioning and inhibitory avoidance. Learn Mem, 11(1): 35-42.

272. Trifilieff P, Calandreau L, Herry C, Mons N, Micheau J (2007) Biphasic ERK1/2 activation in both the hippocampus and amygdala may reveal a system consolidation of contextual fear memory. Neurobiol Learn Mem, 88(4): 424-434.

273. Trivedi MA, Coover GD (2004) Lesions of the ventral hippocampus, but not the dorsal hippocampus, impair conditioned fear expression and inhibitory avoidance on the elevated T-maze. Neurobiol Learn Mem 81: 172-184.

274. Tronson NC, Taylor JR. (2007) Molecular mechanisms of memory reconsolidation. Nat Rev Neurosci 8(4):262-75.

275. Tsoory M, Richter-Levin G (2006) Learning under stress in the adult rat is differentially affected by 'juvenile' or 'adolescent' stress. Int J Neuropsychopharmacol., 9:713- 728

276. Tsutsumi T, Akiyoshi J, Hikichi T, Kiyota A, Kohno Y, Katsuragi S, Yamamoto Y, Isogawa K, Nagayama H (2001) Suppression of conditioned fear by administration of CCKB receptor antisense oligodeoxynucleotide into the lateral ventricle. Pharmacopsychiatry, 34: 232-237.

277. VanGuilder HD, Vrana KE, Freeman WM (2008) Twenty-five years of quantitative PCR for gene expression analysis. Biotechniques, 44: 619-626.

278. van Stegeren AH (2008) The role of the noradrenergic system in emotional memory. Acta Psychol (Amst), 127(3): 532-541.

279. Verma D, Tasan RO, Herzog H, Sperk G (2012) NPY controls fear conditioning and fear extinction by combined action on Y(1) and Y(2) receptors. Br J Pharmacol, 166(4): 1461-1473.

280. Viollet C, Vaillend C, Videau C, Bluet-Pajot MT, Ungerer A, L'Héritier A, Kopp C, Potier B, Billard J, Schaeffer J, Smith RG, Rohrer SP, Wilkinson H, Zheng H, Epelbaum J (2000) Involvement of sst2 somatostatin receptor in locomotor, exploratory activity and emotional reactivity in mice. Eur J Neurosci, 12: 3761-3770.

281. Vogt MA, Chourbaji S, Brandwein C, Dormann C, Sprengel R, Gass P (2008) Suitability of tamoxifen-induced mutagenesis for behavioral phenotyping. Exp Neurol, 211(1): 25-33.

282. von Hertzen LS, Giese KP (2005)Memory reconsolidation engages only a subset of immediate-early genes induced during consolidation. J Neurosci, 25(8): 1935-4192.

283. Vouimba RM, Richter-Levin G (2005) Physiological dissociation in hippocampal subregions in response to amygdala stimulation. Cereb Cortex, 15(11): 1815-1821.

284. Vouimba RM, Yaniv D, Richter-Levin G (2007) Glucocorticoid receptors and beta-adrenoceptors in basolateral amygdala modulate synaptic plasticity in hippocampal dentate gyrus, but not in area CA1. Neuropharmacology, 52(1): 244-252.

285. Vreeburg SA, Zitman FG, van Pelt J, Derijk RH, Verhagen JC, van Dyck R, Hoogendijk WJ, Smit JH, Penninx BW (2010) Salivary cortisol levels in persons with and without different anxiety disorders. Psychosom Med 72(4): 340-347.

286. Walker DL, Davis M (2002) The role of amygdala glutamate receptors in fear learning, fear-potentiated startle, and extinction. Pharmacol Biochem Behav, 71(3): 379-392.

287. Wallenstein GV, Vago DR (2001) Intrahippocampal scopolamine impairs both acquisition and consolidation of contextual fear conditioning. Neurobiol Learn Mem, 75(3): 245-252.

288. Wang H, Wong PT, Spiess J, Zhu YZ (2005) Cholecystokinin-2 (CCK2) receptor-mediated anxiety-like behaviors in rats. Neurosci Biobehav Rev, 29(8): 1361-1373.

289. Wang XY, Zhao M, Ghitza UE, Li YQ, Lu L (2008) Stress impairs reconsolidation of drug memory via glucocorticoid receptors in the basolateral amygdala. J Neurosci 28: 5602-5610.

290. Watson C, Paxinos G, Pelles L (2012) The mouse nervous system. 1st Edition, p. 113ff. Academic Press. Waltham, MA, USA.

291. Wefers B, Hitz C, Hölter SM, Trümbach D, Hansen J, Weber P, Pütz B, Deussing JM, de Angelis MH, Roenneberg T, Zheng F, Alzheimer C, Silva A, Wurst W, Kühn R (2012) MAPK signaling determines anxiety in the juvenile mouse brain but depression-like behavior in adults. PLoS One, 7(4): e35035.

292. Weiss EK, Krupka N, Bähner F, Both M, Draguhn A (2008) Fast effects of glucocorticoids on memory-related network oscillations in mouse hippocampus. J Neuroendocrinology 20: 549-557

293. White NM, Salinas JA (2003) Mnemonic functions of dorsal striatum and hippocampus in aversive conditioning. Behav Brain Res, 142(1-2): 99-107.

294. Whittington MA, Traub RD. (2003) Interneuron diversity series: inhibitory interneurons and network oscillations in vitro. Trends Neurosci., 26(12): 676-682.

295. Wierońska JM, Szewczyk B, Pałucha A, Brański P, Zieba B, Smiałowska M (2005) Anxiolytic action of group II and III metabotropic glutamate receptors agonists involves neuropeptide Y in the amygdala. Pharmacol Rep, 57(6): 734-743.

296. Yeckel MF, Berger TW (1990) Feedforward excitation of the hippocampus by afferents from the entorhinal cortex: Redefinition of the role of the trisynaptic pathway. Proc Natl Acad Sci U S A, 87: 5832-5836.

297. Yehuda R. (2006) Advances in understanding neuroendocrine alterations in PTSD and their therapeutic implications. Ann N Y Acad Sci 1071: 137-166.

298. Yehuda R, LeDoux J (2007) Response variation following trauma: a translational neuroscience approach to understanding PTSD. Neuron, 56(1): 19-32.

299. Yeung M, Engin E, Treit D (2011) Anxiolytic-like effects of somatostatin isoforms SST 14 and SST 28 in two animal models (Rattus norvegicus) after intra-amygdalar and intra-septal microinfusions. Psychopharmacology (Berl), 216(4): 557-567.

300. Yeung M, Treit D (2012) The anxiolytic effects of somatostatin following intra-septal and intra-amygdalar microinfusions are reversed by the selective sst2 antagonist PRL2903. Pharmacol Biochem Behav, 101(1): 88-92.

301. Zeyda T, Diehl N, Paylor R, Brennan MB, Hochgeschwender U (2001) Impairment in motor learning of somatostatin null mutant mice. Brain Res, 906(1-2): 107-114.

302. Zhang G, Asgeirsdóttir HN, Cohen SJ, Munchow AH, Barrera MP, Stackman RW Jr (2012) Stimulation of serotonin 2A receptors facilitates consolidation and extinction of fear memory in C57BL/6J mice. Neuropharmacology, 64(1): 403-413.

303. Zhu X, Han X, Blendy JA, Porter BE (2012) Decreased CREB levels suppress epilepsy. Neurobiol Dis, 45(1): 253-263.

304. Zweifel LS, Fadok JP, Argilli E, Garelick MG, Jones GL, Dickerson TM, Allen JM, Mizumori SJ, Bonci A, Palmiter RD (2011) Activation of dopamine neurons is critical for aversive conditioning and prevention of generalized anxiety. Nat Neurosci, 14(5): 620-626.

Online sources:

http://jaxmice.jax.org/strain/006417.html (21.06.12)

http://jaxmice.jax.org/strain/010708.html (13.06.12)

http://openwetware.org/wiki/Griffin:Lentivirus_Technology (13.06.12)

http://www.taconic.com/ wmspage.cfm?parm1=4247 (19.08.12)

Appendix

A.1 Chemicals

Acedic Acid	Carl Roth, Karlsruhe, Germany
Agarose	Peqlab, Erlangen, Germany
BIBP 3226	Tocris, Ellisville, Missouri, USA
Bovine serum albumine (BSA)	Carl Roth, Karlsruhe, Germany
$CaCl_2$	Sigma-Aldrich, Seelze, Germany
Cresyl violet acetate	Sigma-Aldrich, Seelze, Germany
4',6-diamidino-2-phenylindole dihydrochloride (DAPI)	Life Technologies, Darmstadt, Germany
Dental cement	Hoffmann Dental Manufaktur, Berlin, Germany
Dimethyl dicarbonat (DMDC)	Sigma-Aldrich, Seelze, Germany
DirectPCR-Tail lysis reagent	Peqlab, Erlangen, Germany
Dimethylsulfoxid (DMSO)	Finnzymes, Vantaa, Finland
di-Nucleotide-Tri-Phosphate (dNTPs)	Fermentas, St. Leon-Rot, Germany
Donkey serum	Vector laboratories, Burlingame, USA
Entellan	Merck, Darmstadt, Germany
Eosin	Merck, Darmstadt, Germany
Ethanol 100 %	Zentralapotheke Universitätsklinikum Magdeburg, Magdeburg, Germany
Ethanol 96 %	Carl Roth, Karlsruhe, Germany
Ethidium bromid	Carl Roth, Karlsruhe, Germany
Ethylendiamintetraessigsäure (EDTA)	Carl Roth, Karlsruhe, Germany
Glucose	Sigma-Aldrich, Seelze, Germany
Hematoxylin	Merck, Darmstadt, Germany
Heparine-sodium 25000 I.E.	B. Braun Melsungen AG, Melsungen, Germany
KCl	Carl Roth, Karlsruhe, Germany
Ketanest/ Xylacine	Sigma-Aldrich, Seelze, Germany
KH_2PO_4	Sigma-Aldrich, Seelze, Germany
Methylbutane	Carl Roth, Karlsruhe, Germany
Methylenblue	Sigma-Aldrich, Seelze, Germany
$MgCl_2$	Carl Roth, Karlsruhe, Germany

Mineral oil	Sigma-Aldrich, Seelze, Germany
NaCl	Carl Roth, Karlsruhe, Germany
$NaHCO_3$	Carl Roth, Karlsruhe, Germany
Na_2HPO_4	Sigma-Aldrich, Seelze, Germany
Na_2HPO_4 x $2H_2O$	Carl Roth, Karlsruhe, Germany
NaOH	Carl Roth, Karlsruhe, Germany
Oligonucleotide (dT)18 primer	Ambion/ Life Technologies, Darmstadt, Germany
Paladur resin	Heraeus Kulzer GmbH, Wehrheim, Germany
Paraformaldehyde	Carl Roth, Karlsruhe, Germany
Pentobarbital	Sigma-Aldrich, Seelze, Germany
Poly-L-Lysine 1 %	Sigma-Aldrich, Seelze, Germany
Primer for genotyping PCRs	Life Technologies, Darmstadt, Germany
Proteinase K	Carl Roth, Karlsruhe, Germany
Random decamer primer	Ambion/ Life Technologies, Darmstadt, Germany
RNAse Zap	Life Technologies, Darmstadt, Germany
Sodium Thiosulfate	Sigma-Aldrich, Seelze, Germany
ß-Mercaptoethanol	Serva, Heidelberg, Germany
Sucrose	Sigma-Aldrich, Seelze, Germany
Sunflower oil	K-Classic Kaufland, Neckarsulm, Germany
SuperaseIN	Ambion/ Life Technologies, Darmstadt, Germany
Tamoxifen	Sigma-Aldrich, Seelze, Germany
Tissue Tek O.C.T. Compound	Sakura Finetek Europe, Zoetwerwoude, Netherlands
TRIS hydrochloride	Carl Roth, Karlsruhe, Germany
Triton X	Sigma-Aldrich, Seelze, Germany
Xylene cyanol	Sigma-Aldrich, Seelze, Germany

A.2 Solutions and buffers

1 % Cresyl violet solution 1 g Cresyl violet acetate
50 ml 96 % ethanol
fill with double-destilled water to 100 ml
stir for 7 h at room temperature, protected from light
filter
store protected from light

DMDC-treatment of water: 0.1 % Dimethyldicarbonate in double-destilled water
Stir for 3 h
Autoclave

DNA loading buffer: 0.25 % bromophenol blue
0.25 % xylene cyanol FF
15 % Ficoll in H_2O

0.2 % H_2O_2 add 666.7 µl H_2O_2 30 % stock solution to 100 ml sterile double-destilled water
store protected from light

Methylene blue 10 mg Methylen blue powder
10 µl DMSO
fill up to 1 ml with 0.9 % Saline

10x Phosphate-buffered saline (PBS)
solve 11.5 g $Na_2HPO \times H_2O$
2.0 g KH_2PO_4
80.0 g NaCl
2.0 g KCl
in ca. 900 ml double-destilled water
adjust pH to 7.4
fill up to 1 l final volume with double-destilled water
- *RNAse free* *add 1 ml DMDC*

stir for 2 h
autoclave

4 % Paraformaldehyde (PFA)

solve 40 g PFA in ca. 700 ml double-destilled water,
stir on heating plate at 70 °C until solution is clear
add 500 µl NaOH (5 M) for better solving
let cool down on ice (ca. 1 h)
filtrate cooled PFA
add 100 ml 10x PBS
adjust pH to 7.4
fill up volume to 1 l with double-destilled water

- RNAse free *use DMDC-treated double destilled water and 10x PBS*
use only baked glass ware
treat plastic ware with "RNAse Zap" spray before use

Poly-L-Lysine: 1:2 dilution of Poly-L-Lysine 0.1 % in double destilled water

0.9 % Saline solve 4.5 g sodium chloride in 500 ml double-destilled water
autoclave

30 % Sucrose solve 30 g sucrose in ca. 80 ml double-destilled water
add 10 ml 10x PBS
fill up to 100 ml with double-destilled water

- RNAse free *use DMDC-treated double destilled water and 10x PBS*
use only in baked glass ware
treat plastic ware with "RNAse Zap" spray before use

50x TAE-Buffer: 242 g Tris base
57.1 ml acetic acid
100 ml 0.5 M EDTA pH 8

Tamoxifen (for i.p.-injections of 2/ 4/ 8 mg in 100 ml vehicle solution):

solve 40/ 80/ 160 mg Tamoxifen powder in 200 µl
100 % Ethanol,
Add autoclaved sunflower oil to 2 ml, vortex vigorously
Sonicate 2-3x 15 min
Prepare 500 µl aliqouts & store at -20°C

1x TE-Buffer: 1 mM EDTA pH 8
10 mM Tris/HCl pH 7.4

Tyrode buffer solve 4.000 g NaCl
0.100 g KCl
0.050 g $MgCl_2$
0.500 g $NaHCO_3$
0.100 g $CaCl_2$
0.025 g NaH_2PO_4
0.500 g Glucose
in 500 ml double-destilled water
stire until clear solution
store at 4 °C

- RNAse free *use DMDC-treated double destilled water and 10x PBS*
use only in baked glass ware
treat plastic ware with "RNAse Zap" spray before use

A.3 DNA length standard

GeneRuler™ 1kb DNA ladder	Thermo Scientific, St. Leon-Rot, Germany
GeneRuler™ 100bp DNA ladder	Thermo Scientific, St. Leon-Rot, Germany

A.4 Kits and assays

Ambion Cells-to-cDNA-Kit II	Life Technologies, Darmstadt, Germany
125I-corticosterone radio immunassay kit	MP Biomedicals Inc., New York, USA
Dream Taq polymerase	Fermentas, St. Leon-Rot, Germany
RNeasy FFPE kit	Qiagen, Hilden, Germany
RNeasy Micro Plus kit	Qiagen, Hilden, Germany
Sensiscript Reverse Transcription kit	Qiagen, Hilden, Germany
Taq Polymerase	Qiagen, Hilden, Germany

A.5 Vectors and antibodies

Vectors (purchased)

CREB Dominant-Negative Vector Set	Clontech #631925, Saint-Germain-en-Laye, France

Antibodies

HA-tag (C29F4) rabbit mAb	Cell Signaling #3724, Frankfurt am Main, Germany
Phospho-CREB (ser133)	Cell Signaling #9191, Frankfurt am Main, Germany

Secondary antibodies

Alexa Fluor 488 donkey anti-rabbit	Life Technologies #A-21206, Darmstadt, Germany
Alexa Fluor 555 donkey anti-rabbit	Life Technologies #A-31572, Darmstadt, Germany

A.6 Instruments and consumables

A.6.1 Generally used instruments and consumables

animal care

Macrolon standard cages	Ebeco, Castrop-Rauxel, Germany
Ssniff R/M-H V-1534	Ssniff Spezialdiäten, Soest, Germany
Lignocel BK 8/15	J. Rettenmaier & Söhne, Rosenberg, Germany

Plastic ware

Safe lock tubes (1.5 ml)	Eppendorf, Hamburg, Germany
Falcon tube 50 ml	Greiner Bio-one, Frickenhausen, Germany

Glass ware

glass bottles	Carl Roth, Karlsruhe, Germany
Erlenmeyer flasks	Carl Roth, Karlsruhe, Germany
Beaker	Carl Roth, Karlsruhe, Germany
graduated cylinders	Carl Roth, Karlsruhe, Germany

Pipettes

Pipettes	Brand, Wertheim, Germany
Pipette tipps	Brand, Wertheim, Germany
Pipette tips with filter	Brand, Wertheim, Germany

Freezers & Fridges

Liebherr KU 2407	Liebherr Hausgeräte, Ochsenhausen, Germany
Liebherr GU 4506	Liebherr Hausgeräte, Ochsenhausen, Germany

Sanyo Ultra Low	Ewald Innovationstechnik, Bad Nenndorf, Germany

Scales

Sartorius TE 1535	Sartorius AG, Göttingen, Germany
Sartorius TE 212	Sartorius AG, Göttingen, Germany
Sartorius TE 2101	Sartorius AG, Göttingen, Germany

Centrifuges

Centrifuge 5424	Eppendorf, Hamburg, Germany
Centrifuge 5430	Eppendorf, Hamburg, Germany
VWR Galaxy Mini	VWR International, Darmstadt, Germany

pH meter

inoLab pH720	WTW, Weilheim, Germany

Magnetic Stirrer

IKA RET basic	IKA-Werke, Staufen, Germany
magnetic stir bar	Brand, Wertheim, Germany

Rockers & vortexer

ProBlot 25 Economy Rocker	Labnet, Woodbridge, NJ, USA
IKA HS 260 basic	IKA-Werke, Staufen, Germany
VWR Lab dancer S40	VWR International, Darmstadt, Germany

Rotor incubator

Hybrid 2000	H. Saur Laborbedarf, Reutlingen, Germany

Water bath

LAUDA A103	Lauda Dr. R. Wobser, Lauda-Königshof, Germany

Sonicator

VWR symphony ultrasonic cleaner	VWR International, Darmstadt, Germany

Pumps

REGLO peristaltic pump	ISMATEC, Wertheim-Mondfeld, Germany

Autoclave

Systec DB-23	Systec Labortechnik, Wettenberg, Germany

Oven

Binder FP53	Binder, Tuttlingen, Germany

Others

Lab clock	Carl Roth, Karlsruhe, Germany
Aluminum foil	Carl Roth, Karlsruhe, Germany
Dewar transport flask Typ B	KGW Isotherm, Karlsruhe, Germany

A.6.2 PCR & gel electrophoresis

PCR Hood

Captair bio	Erlab, Köln, Germany

Plastic ware

MicroAmp Fast Reaction Tubes	Applied Biosystems, Darmstadt, Germany
MicroAmp 8-cap strip	Applied Biosystems, Darmstadt, Germany
MicroAmp Fast Optical 96-Well plate	Applied Biosystems, Darmstadt, Germany
MicroAmp Optical Adhesiv Film	Applied Biosystems, Darmstadt, Germany

Thermocycler

Veriti Thermal Cycler	Applied Biosystems, Darmstadt, Germany

Real-time-PCR

StepOne Plus Real-Time PCR system	Applied Biosystems, Darmstadt, Germany

Microwave

Clatronic MWG 746 H	Clatronic International, Kempen, Germany

Gel electrophoresis system

AGT3 & Maxi-VG	VWR International, Darmstadt, Germany

Gel documentation system

InGenius LHR	Syngene, Cambridge, UK

A.6.3 Cryosectioning and histological staining

Cryostat

CM 1950	Leica, Nussloch, Germany

Hot plate

Medite OTS 40.2530	Medite, Burgdorf, Germany

Glass & Plastic ware

staining cuvettes	Carl Roth, Karlsruhe, Germany
slide holder	Carl Roth, Karlsruhe, Germany
Object slide box	Carl Roth, Karlsruhe, Germany

A.6.4 Laser capture microdissection

Laser capture microdissection system

PALM MicroBeam	Carl Zeiss, Jena, Germany

Glass & Plastic ware

Micro tube 500 for LCM	Carl Zeiss, Jena, Germany
Adhesive cap 500 clear for LCM	Carl Zeiss, Jena, Germany
MembraneSlides 1.0 PEN	Carl Zeiss, Jena, Germany

A.6.5 Other microscopes

Leica DMI 6000 B	Leica Microsystems, Wetzlar, Germany
Nicon Eclipse E200	Nicon Instruments Europe, Amsterdam, Netherlands

A.6.6 Behavioral testing

TSE Fear Conditioning System	TSE, Bad Homburg, Germany
Open field	Stoelting Co., Wood Dale, IL, USA
Elevated plus maze	Stoelting Co., Wood Dale, IL, USA
ANYMAZE Video tracking system	Stoelting Co., Wood Dale, IL, USA

A.6.7 Stereotactic surgery

Surgery

Stereotactic frame	World precision instruments, Berlin, Germany
Surgical instruments	Carl Roth, Karlsruhe, Germany
Suture material (5-0/PS-3 Perma-Hand silk)	Ethicon GmbH, Norderstedt, Germany
Drill	World precision instruments, Berlin, Germany

Material for Injections

Ultra Micro Pump III	World precision instruments, Berlin, Germany
Microliter glass syringe (10 µl)	Hamilton Bonaduz AG, Bonaduz, Switzerland
NanoFil syringe 10 µl	World precision instruments, Berlin, Germany
NanoFil beveled injection needle 33G	World precision instruments, Berlin, Germany
Silicon tubing	World precision instruments, Berlin, Germany

Canulae

Guide canula, bilateral, 26G, 3 mm length	Plastics One, Roanoke, VA, USA
Dummy for guide canula, bilateral, 3 mm length	Plastics One, Roanoke, VA, USA
Internal canula, bilateral, 33G, 3+0.5 mm length	Plastics One, Roanoke, VA, USA
Guide canula, 26G, 5 mm length	Plastics One, Roanoke, VA, USA

Dummy for guide canula, 5 mm length	Plastics One, Roanoke, VA, USA
Internal canula, 33G, 5+0.5 mm length	Plastics One, Roanoke, VA, USA
Jeweler's screw	Plastics One, Roanoke, VA, USA

A.7 Software

SPSS	SPSS Inc., Chicago, IL, USA
Adobe Photoshop CS4 Extended	Adobe Systems, San Jose, CA, USA
EndNote	Thomson Reuters, Carlsbad, CA, USA

A.8 Provider of mouse lines used

Mouse line	**Strain name**	**Provider**
C57BL/6	C57BL/6BomTac	M&B Taconic, Berlin, Germany
NPY-GFP	B6.FVB-Tg(Npy-hrGFP)1Lowl/J	The Jackson laboratories, Bar Harbor, Maine, USA
SST-CreERT2	B6(Cg)-Ssttm1(cre/ERT2)Zjh/J	The Jackson laboratories, Bar Harbor, Maine, USA

A.9 Genotyping of different mouse lines

A.9.1 Tail biopsy

Shortly after weaning tail biopsies of 0.5 cm length were taken from the adolescent mice and individual animals were marked via ear holes. The tail tissue was stored -20 °C or processed immediately by transferring them to 200 µl DirectPCR-Tail lysis reagent.

A.9.2 Isolation of genomic DNA

To each tail cut 200 µl DirectPCR-Tail lysis reagent (Peqlab, Erlangen, Germany) and 6 µl Proteinase K (10 mg/ml; Fermentas, St. Leon-Rot, Germany) were added and incubated over night at 55 °C in a rotor incubator. The next day, the lysis was inactivated by incubation of the samples in a water bath at 85 °C for 45 min. The lysates could then be used directly for analyzing the genomic DNA of each animal via polymerase chain reaction (PCR) or they were stored at -20 °C.

A.9.3 Polymerase chain reaction (PCR) genotyping

Genotypes were determined by multiplex polymerase chain reaction on genomic DNA. In general, the polymerase chain reaction (PCR) is a widely used standard technique to amplify DNA fragments of a known sequence *in vitro* and is conducted in several cyclic repeated steps. First, during denaturation at 94 °C up to 98 °C, the DNA double strands separate into single strands. That allows for annealing of the primers, synthetic oligomers of a certain sequence. They are highly concentrated in the PCR mix and hybridize to their complementary sequence at the 3'-end of the DNA when the temperature is lowered (specific annealing temperature for each primer, depending on the primer melting temperature (T_m), usually between 55-65 °C). During extension a heat stable polymerase will elongate the primers according to the 5'- to 3'-sequence of the template DNA by adding the complementary dNTP. Since a primer pair is flanking the target DNA region repetition of these denaturation-annealing-extension cycles will increase only the number of copies from the target DNA sequence exponentially from

cycle to cycle whereas other sequences where primer pairs cannot bind remain unamplified.

The different mouse lines engaged in the studies carry different transgenes. Therefore, genotyping of each mouse line was conducted with distinct PCR protocols.

A.9.3.1 PCR protocols for genotyping of SST deficient mice

For genotyping of SST deficient mice three different primers were used in a multiplex PCR. The Primer SSTMR was primer specific for the neomycin cassette whereas the SSTWR primer was complementary to a 3'-sequence that is only present in wildtype alleles. The 5'-primer SSTUF all binds a sequence that is present in wildtype and mutated alleles.

Tab. A.9-1 Primer sequences (5' to 3') for genotyping of SST mutant mice

Primer name	**sequence**
SSTMR	GGG ACT TTC CAC ACC CTA ACT GA
SSTWR	ATA GTT TGC GCA CGT CCA TTT TCC TGT
SSTUF	GCA TGT CAG CAC TGA GTG AAG GTA

For genotyping PCR Taq DNA polymerase (Qiagen, Hilden, Germany) was used, which is derived from the thermostabile polymerase of *Thermus aquaticus.* In a 50 µl reaction tube 1 µl of the isolated genomic DNA of the individual animal was added to 11 µl of the PCR master mix consistent of the following components (for 1 reaction):

Tab. A.9-2 PCR master mix for genotyping of SST mutant mice

1.5µl	10x Cl-buffer
1.2 µl	dNTP mix (2.5 mM each)
0.75 µl	$MgCl_2$ (25 mM)
0.6 µl	Primer SSTMR (10 µM)
1.5 µl	Primer SSTWR (10 µM)
1.5 µl	Primer SSTUF (10 µM)
1.85 µl	H_2O
0.1 µl	Taq Polymerase (5 U/µl)

Next to the individual genomic DNA from animals determined for genotyping, a negative control with H_2O as a template as well as a positive control with template DNA from a $SST^{+/-}$ mouse was included.

The PCR mix was kept on ice until the thermocycler reached the denaturation temperature to prevent formation of unspecific PCR products before initial denaturation (hot start). After initial denaturation (5 min at 94 °C) gaining complete dissociation of DNA double strands, 40 cycles were conducted to amplify the specific target fragments, followed by a final extension phase (7 min at 72 °C) for terminal amplicon synthesis (Thermocycler: Verity, Applied Biosystems, Darmstadt, Germany). The PCR products were stored at 4 °C until analysis per gel electrophoresis.

Tab. A.9-3. Thermo cycler program for genotyping of SST mutant mice

Phase	duration	temperature	number of steps
Initial denaturation	5 min	94 °C	1
Denaturation	15 s	94 °C	40
Annealing	30 s	60 °C	40
Extension	60 s	72 °C	40
Final extension	7 min	72 °C	1
Storage	∞	4°C	1

A.9.3.2 PCR protocols for genotyping of NPY-GFP mice

For genotyping of NPY-GFP mice three different primers were used in a multiplex PCR, with the primer oIMR 6194 specific for the trangene, the primer oIMR 6196 specific for the wildtype allele and the primer oIMR6195 common for both alleles.

Tab. A.9-4 Primer sequences (5' to 3') for genotyping of NPY-GFP mice

Primer name	sequence
oIMR 6194	GGT GCG GTT GCC GTA CTG GA
oIMR 6195	TAT GTG GAC GGG GCA GAA GAT CCA GG
oIMR 6196	CCC AGC TCA CAT ATT TAT CTA GAG

For genotyping PCR the DREAM Taq DNA polymerase (Fermentas, St. Leon-Rot, Germany) was used. In a 50 µl reaction tube to 1 µl of the isolated genomic DNA of the individual animal 10 µl of the PCR master mix consistent of the following components (for 1 reaction) was added:

Tab. A.9-5 PCR master mix for genotyping of NPY-GFP mice

1.0 µl	10x Dream Taq Green buffer
0.8 µl	dNTP mix (2.5 mM each)
0.04 µl	$MgCl_2$ (25 mM)
2.0 µl	Q-Solution
0.25 µl	Primer oIMR 6194 (10 µM)
0.75 µl	Primer oIMR 6195 (10 µM)
1.25 µl	Primer oIMR 6196 (10 µM)
3.81 µl	H_2O
0.1 µl	DREAM Taq Polymerase (5 U/µl)

Next to the individual genomic DNA from animals determined for genotyping, a negative control with H_2O as a template as well as a positive control with template DNA from a mouse carrying the NPY-GFP transgene was included.

The PCR mix was kept on ice until the thermocycler reached the denaturation temperature to prevent formation of unspecific PCR products before initial denaturation (hot start). After initial denaturation (3 min at 94 °C) for complete dissociation of DNA double strands, 35 cycles were conducted to amplify the specific target fragments, followed by a final extension phase (7 min at 72 °C) for terminal amplicon synthesis (Thermocycler: Verity, Applied Biosystems, Darmstadt, Germany). The PCR products were stored at 4 °C until analysis per gel electrophoresis.

Tab. A.9-6 Thermo cycler program for genotyping of NPY-GFP mice

Phase	duration	temperature	number of steps
Initial denaturation	3 min	94 °C	1
Denaturation	30 s	94 °C	40
Annealing	60 s	65 °C	40
Extension	60 s	72 °C	40
Final extension	7 min	72 °C	1
Storage	∞	4 °C	1

A.9.3.3 PCR protocols for genotyping of SST-CreERT2 mice

For genotyping of SST-CreERT2 mice four different primers were used in a multiplex PCR, targeting the transgenic allele (forward and reverse primer: SomCre3 and 4) or the wildtype allele (forward and reverse primer: SomCre7 and 8).

Tab. A.9-7 Primer sequences (5' to 3') for genotyping of SST-CreERT2 mice

Primer name	sequence
SomCre3	GGC TTA AAG GCT AAC CTG ATG TG
SomCre4	GGA GCG GGA GAA ATG GAT ATG
SomCre7	CAA TGG TGC GCC TGC TGG AAG AT
SomCre8	ATG CGG AAC CGA GAT GAT GTA GC

For genotyping PCR the Taq DNA polymerase (QIAGEN, Hilden, Germany) was used. In a 50 µl reaction tube to 1 µl of the isolated genomic DNA of the individual animal 19 µl of the PCR master mix consistent of the following components (for 1 reaction) was added:

Tab. A.9-8 PCR master mix for genotyping of SST-CreERT2 mice

2.0 µl	10x Taq buffer
1.0 µl	dNTP mix (2.5 mM each)
4.0 µl	Q-Solution
0.5 µl	Primer SomCre3 (10 µM)
0.5 µl	Primer SomCre4 (10 µM)
1.0 µl	Primer SomCre7 (10 µM)
1.0 µl	Primer SomCre8 (10 µM)
8.9 µl	H_2O
0.1 µl	Taq Polymerase (5 U/µl)

Next to the individual genomic DNA from animals determined for genotyping, a negative control with H_2O as a template as well as a positive control with template DNA from a mouse carrying the SST-CreERT2 transgene was included.

The PCR mix was kept on ice until the thermocycler reached the denaturation temperature to prevent formation of unspecific PCR products before initial denaturation (hot start). After initial denaturation (3 min at 94 °C) for complete dissociation of DNA double strands, 35 cycles were conducted to amplify the specific target fragments, followed by a final extension phase (7 min at 72 °C) for terminal amplicon synthesis (Thermocycler: Verity, Applied Biosystems, Darmstadt, Germany). The PCR products were stored at 4 °C until analysis per gel electrophoresis.

Tab. A.9-9 Thermo cycler program for genotyping of SST-CreERT2 mice

Phase	**duration**	**temperature**	**number of steps**
Initial denaturation	3 min	94 °C	1
Denaturation	30 s	94 °C	35
Annealing	45 s	59 °C	35
Extension	60 s	72 °C	35
Final extension	7 min	72 °C	1
Storage	∞	4 °C	1

A.9.4 Gel electrophoresis

To analyse the DNA fragments derived from the genotyping PCRs they were separated via electrophoresis on a 1 % or 1.5 % agarose gel. For this, 1 g or 1.5 g agarose pulver was solved in 100 ml 1x TAE buffer under heating in a microwave (3 min at 600 Watt). After cooling in a water bath, 7 µl ethidium bromide (0.5 mg/ml) were added to the agarose. The fluid agarose was then poured into the gel preparation chamber and a gel comb was inserted to obtain pockets for applying DNA to the gel. After hardening, the comb was carefully pulled out of the gel and the gel was unhinged from the gel preparation chamber and transferred to the electrophoresis chamber containing TAE buffer covering the gel completely. Products from the SST mutant and SST-CreERT2 PCRs were then mixed with loading buffer (10 µl DNA + 2 µl 6x loading buffer) and transferred to an individual gel pocket. In the NPY-GFP PCR a buffer was used containing already a loading dye, hence the products were loaded on the gel directly. One of the pockets contained a DNA length standard (1 kb DNA ladder; Life Technologies, Darmstadt, Germany). Electrophoresis was performed at 120 mV for ca. 30 min. Detection and documentation of the DNA fragments was conducted with the InGenius LHR gel documentation and analysis system (Syngene, Cambridge, UK). As in other documentation systems, ultraviolet light exposure of the gel elicits a fluorescence signal of the ethidium bromide incorporated in the DNA fragments.
In the different PCR protocols engaged, different fragment sizes of the PCR product derived from the different mutant or wildtype alleles of the distinct mouse lines.

A.9.4.1 Gel electrophoresis for genotyping of SST deficient mice

On a 1 % agarose gel, DNA fragments of either 500 bp length occurred, characterizing the mutant allele, or of 900 bp length for the wildtype allele.
For $SST^{-/-}$ mice, PCR products of 500 bp and for $SST^{+/+}$ mice PCR products of 900 bp length were visible. For $SST^{+/-}$ the 500 and 900 bp fragments were detected.

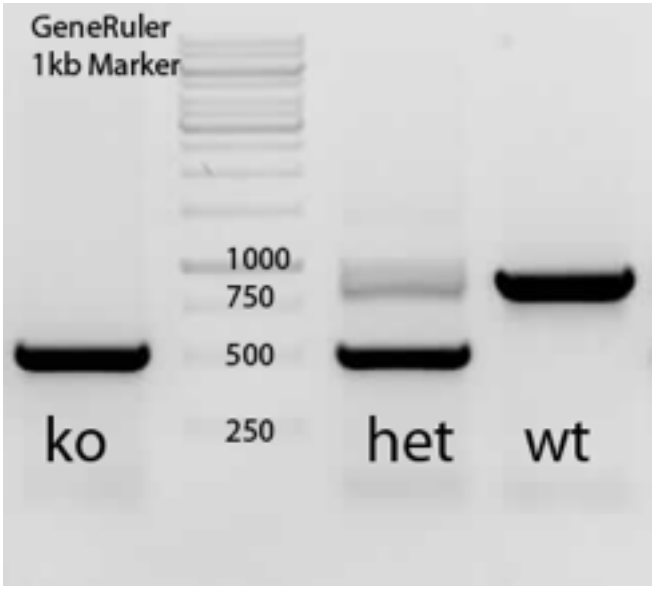

Fig. A.9-1 Gel photo of the SST mutant mice genotyping PCR products. For $SST^{-/-}$ mice (ko) a 500 bp, for $SST^{+/+}$ mice (wt) a 900 bp and for $SST^{+/-}$ mice (het) a 500 bp and 900 bp fragment was detected.

A.9.4.2 Gel electrophoresis for genotyping of NPY-GFP mice

On a 1 % agarose gel, DNA fragments of either 400 bp length were visible in mice carrying the NPY-GFP transgene, or of 500 bp length in their wildtype littermates.

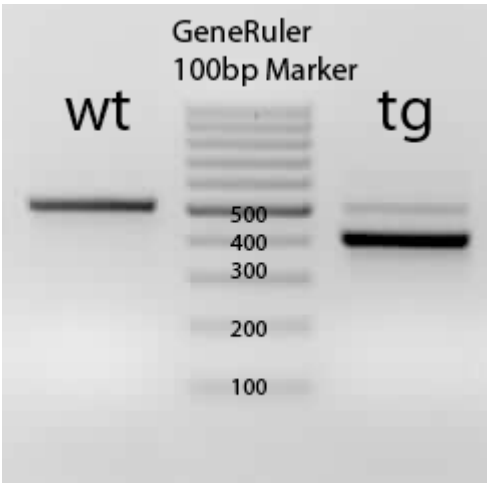

Fig. A.9-2 Gel photo of the NPY-GFP mice genotyping PCR products. For NPY-GFP transgenic mice (tg) a 400 bp, for their wildtype littermates a 500 bp fragment was detected.

A.9.4.3 Gel electrophoresis for genotyping of SST-CreERT2 mice

On a 1.5 % agarose gel, DNA fragments of either 520 bp length were visible in mice carrying the SST-CreERT2 transgene, or of 400 bp length in their wildtype littermates. Because of the wildtype x heterozygous mating scheme, only mice heterozygous for the transgene were available, giving two fragments of 520 and 400 bp length as products of the PCR.

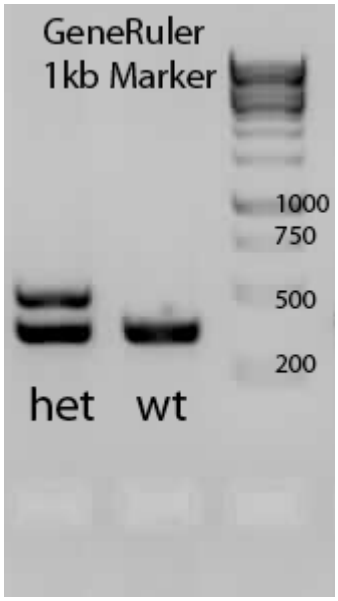

Fig. A.9-3 Gel photo of the SST-CreERT2 mice genotyping PCR products. For mice carrying the SST-CreERT2 transgene on one allele (heterozygous; het) a 520 bp and 400 bp fragment was detected. For their wildtype littermates, only the 400 bp fragment existed.

A.10 Circadian expression of somatostatin in the basolateral complex of the amygdala

To assess whether the circadian regulation of fear and anxiety is mediated by certain interneuron populations of the amygdala, first expression of the neuropeptide somatostatin (SST) and second fear and anxiety-related behavior of in mice deficient for SST was determined on two time points of the mouse active phase.

While results of the behavioral testing are presented in section 3.1.3, circadian differences in SST levels were measured by Dr. rer. nat. Bettina Müller via an Enzyme-linked Immunosorbent Assay (ELISA) in amygdala samples.

Group-housed male adult C57BL/6 mice, naive to any training or treatment except for animal care, were killed by cervical dislocation either at T1 (1 h after lights off, 8.15 to 9.15 am) or at T7 (7 h after lights off, 14.15 to 15.15 pm). Brains were removed immediately, frozen on powdered dry ice for ca. 30 s and then inserted in ice-cooled a slicer matrix (Zivic instruments, Pittsburgh, PA, USA), where 1 mm thick coronar brain slices were cut. On the sections, kept on ice, the basolateral complex of the amygdala was dissected manually with sterile 26G canulas.

Subsequently, the BLA was transferred to a lysis buffer containing tube and homogenizated. The lysis buffer consisted of 1 % DDM, 1 % NP40, 1 mM Na_3VO_4, 2 mM EDTA, 50 mM Tris-HCl (pH 8, 4°C), 150 mM NaCl, 0.5 DOC, 1 mM AEBSF, 1 µM Pepstatin A, 10 % Gycerol and, 3 tablets of Protease Inhibitor (Thermo Fisher Scientific Inc., Rockford, USA). All amygdala samples were incubation at 4 °C on a rotor platform for 20 min after lysis, centrifugated at 1000x g for 20 min at 4 °C and then stored at -80°C until determination of somatostatin peptide expression levels via ELISA (Uscn Life Science Inc., Wuhan, China).

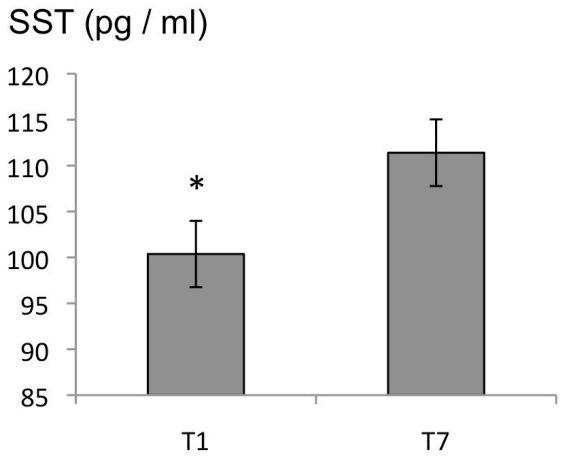

Fig. A.10-1 Circadian differences of Somatostatin expression in the amygdala. Seven hours after lights off (T7) SST peptide levels were elevated compared to T1 (one hour after lights off) in the basolateral complex of the amygdala

Analysis of SST peptide levels in the basolateral complex of the amygdala revealed a small, but significant increase in SST at T7, seven hours after lights off, compared to T1, one hour after lights off ($T(21)= -2.152$; $p=0.043$).
This difference is discussed further with respect to fear and anxiety-related behavior at T1 versus T7 in wildtype and SST deficient mice in section 3.1.3.

A.11 Long-term mRNA expression changes after JSAS: results in detail

Tab. A.11-1 Long- term mRNA expression changes after juvenile (JS), adult stress (AS) or the combintion of both (JSAS) for selected GABAergic and glutamatergic marker genes in CA1 subregions of the dorsal and ventral hippocampus including F-values (ANOVA for group) for each subregion. Changes may be driven by Mineralocorticoid *(MR)* or Glucocorticoid Receptor *(GR)* expression changes as indicated by regression analysis (see Fig. 3.2.-3). Significant increase/ decrease indicated compared to control (#) or to JSAS (*).

	DH CA1 SR	CA1 SP	CA1 SO	VH CA1 SR	CA1 SP	CA1 SO
GABAergic						
GAD 65	= F(3,20)=0.291 p=0.831	= F(3,20)=1.97 p=0.151	= F(3,20)=0.876 p=0.47	↑ JS *, ↑ AS * *(GR)* F(3,20)=3.32 p=0.041 *	= F(3,20)=1.270 p=0.312	= F(3,20)=0.334 p=0.803
GAD 67	= F(3,20)=0.303 p=0.823	= F(3,20)=2.429 p=0.095	= F(3,20)=0.147 p=0.93	= F(3,20)=0.832 p=0.492	= F(3,20)=0.411 p=0.747	= F(3,20)=0.204 p=0.892
Gabra 1	= F(3,20)=2.746 p=0.07	= F(3,20)=2.431 p=0.095	= F(3,20)=1.807 p=0.178	↓JSAS # F(3,20)=3.29 p=0.042 *	= F(3,20)=1.082 p=0.379	= F(3,20)=0.694 p=0.178
Gabra 2	= F(3,20)=1.192 p=0.338	↑ JS # F(3,20)=3.307 p=0.041 *	= F(3,20)=0.171 p=0.915	= F(3,20)=1.302 p=0.301	↑ AS # *(MR)* F(3,20)=3.908 p=0.024 *	= F(3,20)=0.302 p=0.824
NPY	= F(3,20)=0.0 p=0.999	= F(3,20)=0.258 p=0.855	= F(3,20)=0.669 p=0.581	= F(3,20)=0.67 p=0.58	↓ AS # F(3,20)=3.804 p=0.026 *	= F(3,20)=0.635 p=601
SST	= F(3,20)=1.666 p=0.206	= F(3,20)=0.366; p=0.778	= F(3,20)=0.559 p=0.648	= F(3,20)=1.76 p=0.187	= F(3,20)=0.215 p=0.885	= F(3,20)=0.288 p=0.834
Glutamatergic						
Gria 1		= F(3,12)=1.496 p=0.266			= F(3,12)=1.448 p=0.278	
Gria2		= F(3,20)=1.067 p=0.385			= F(3,20)=0.672 p=0.579	
Grin 1		= F(3,20)=0.937 p=0.441			= F(3,20)=0.746 p=0.537	
Grin 2a		= F(3,20)=0.640 p=0.598			↓ AS # F(3,20)=4.315 p=0.017 *	
Grin 2b		= F(3,20)=1.114 p=0.367			= F(3,20)=0.622 p=0.609	
Glucocorticoid receptors						
MR	= F(3,20)=1.084 p=0.379	= F(3,20)=1.973 p=0.151	= F(3,20)=1.612 p=0.218	= F(3,20)=0.205 p=0.891	= F(3,20)=1.136 p=0.359	= F(3,20)=0.266 p=0.849
GR	↑ JS #, ↑ AS * F(3,20)=3.882 p=0.024 *	= F(3,20)=1.398 p=0.272	= F(3,20)=0.927 p=0.446	= F(3,20)=2.641 p=0.077	= F(3,20)=0.692 p=0.568	= F(3,20)=0.916 p=0.451

A.12 Effect of fear reactivation on kainate-induced gamma oscillation

As described in section 3.3.2, fear conditioning induced long-lasting changes in anxiety-like behavior (see Fig. 3.3-2B), while after reactivation additional increase in baseline corticosterone level as well as increased freezing towards the background context were observed. The ventral portion of the hippocampus is closely interconnected with amygdala and entorhinal cortex (Pitkänen et al., 2000) and a target for stress and corticosterone signals (Maggio and Segal, 2009). Accordingly, the ventral hippocampus is a critical mediator of anxiety on the one hand (Bannerman et al., 2004; Kjelstrup et al., 2002), but is also involved in acquisition and expression of contextually conditioned fear on the other hand (Bannermann et al., 2004; Maren and Holt, 2004; Rudy and Matus-Amat, 2005; Trivedi and Coover, 2004). Rhythmic oscillatory activity in the gamma frequency range shape information flow in the hippocampus and interconnected limbic areas (Hajos and Paulsen, 2009). Gamma oscillations are also modulated by corticosterone (Weiss et al., 2008) and show alterations in mutant mice related to anxiety-like behavior (Dzirasa *et al*, 2011).

Therefore, long-lasting effects of fear memory formation and its reactivation on gamma oscillations in vitro were assessed in collaboration with Gürsel Caliskan, Charite, Berlin.

For this, adult male C57BL/6 animals underwent the fear conditioning and reactivation protocols in group R (N=7), NR (N=8) and CTL (N=6) as described in section 2.2.1.5 and 3.3.1 (see also Fig. 2-4). The animals were left undisturbed except for animal care in their home cage and were decapitated 30d later under deep isoflurane anesthesia. Horizontal hippocampal slices (400 µm) were cut at an angle of about 12° in the fronto-occipital direction, as described before (Liotta et al., 2011). The preparation of slices was done in ice-cold, carbogenated (5 % CO_2/ 95 % O_2) artificial cerebrospinal fluid (aCSF) containing (in mM) 129 NaCl, 21 $NaHCO_3$, 3 KCl, 1.6 $CaCl_2$, 1.8 MgCl, 1.25 NaH_2PO_4 and 10 glucose. Slices were transferred to an interface chamber perfused with aCSF at 34±0.1°C (flow rate: 1.8 ± 0.2 ml/min, pH 7.4, osmolarity ~300 mosmol/kg). Slices were incubated at least for an hour before starting recordings. Field potentials (FP) were recorded from the border of stratum lacunosum moleculare (SLM) and stratum radiatum (SR) in CA3 region of horizontal hippocampal slices. Drugs were applied via continuous bath perfusion: All drug-containing solutions were freshly prepared prior to the experiment. Kainate (100 nM) and corticosterone (1 µM) were purchased from Sigma-Aldrich, Steinheim, Germany. Microelectrodes were filled with ACSF with

resistances of 5-10 MΩ. Signals were pre-amplified using a custom-made amplifier and low-pass filtered at 3 kHz. Signals were sampled at a frequency of 5 kHz and stored on a computer hard disc for off-line analysis. Data analysis was performed off-line using Spike2 version 6 software (Cambridge Electronic Design, Cambridge, UK). The analysis of peak power (PP), total power (TP, 20-80 Hz) and peak frequency (PF) of FP oscillations in the gamma frequency band were determined for each 60 s and the average of the last 120 s of the recording was taken as the PP, TP and PF value. To investigate the development of gamma oscillations the average TP of each 10 min was calculated and plotted for 80 min. For the correlation analysis, from each recording 60 s files were extracted. An auto-correlation window of -0.05s to +0.05s was created using the function waveform correlation in Spike2 software. The value of 2nd positive peak was determined for each recording area and taken as the correlation value. Statistical data were reported as mean ± standard error of the mean (SEM). Statistical differences were determined by the Kolmogorov-Smirnov Test, One-Way ANOVA, post hoc Fisher's LSD and Dunn's method (SigmaPlot for Windows Version 11.0, 2008, Systat software).

A.12.1 Effects on gamma power

Normalized gamma power (20-80 Hz) recorded from the border of stratum lacunosum moleculare (SLM) and stratum radiatum (SR) was significantly decreased (Fig. A.12-1A, B; ANOVA for group: F(2,40)=4.42; p=0.019, Fisher's LSD post hoc) in both group NR (N=14 slices, 7 animals; 0.25±0.07, p=0.010) and group R (N=15 slices, 7 animals; 0.33±0.07, p=0.017) compared to controls (N=12 slices, 6 animals; 1.0±0.35). In parallel recordings from slices of the same animals, preapplication of 1µM corticosterone for 30min (N=10-12 slices per group) attenuated this change and somewhat increased gamma power in both NR (paired comparison: 0.25±0.07 vs. 0.77±0.31, p=0.061), but less in R (paired comparison: 0.33±0.07 vs. 0.50±0.14, p=0.31) and not in CTL (paired comparison: 1.0±0.35 vs. 0.81±0.21, p=0.95).

In a third subset of slices from the same animals (N=5-7 slices per group), continuous 80min recordings were performed to determine the development of kainate-induced gamma oscillations (Fig. 2C). Gamma power was significantly lower already after 10min of kainate wash-in (ANOVA for group: F(2,20)=4.83; p=0.022, Fisher's LSD post hoc) in both NR (0.00013±0.00005 mV^2, p=0.011) and R (0.00019±0.00010 mV^2, p=0.020) compared to CTL (0.00071±0.00027 mV^2). After 80 min, the gamma power was still

significantly diminished in NR and R (ANOVA for group: F(2,20)=3.71; p=0.046, Fisher's LSD post hoc). Slices of group NR preapplied with 1µM corticosterone showed a faster development of gamma oscillations compared to slices without corticosterone (paired comparison: after 20min, 0.00018±0.00003 vs. 0.00053±0.00007, p=0.0001; after 80min, 0.0008±0.00017 vs. 0.0030±0.00073, p=0.005). In slices from group R animals and in CTL slices corticosterone had no significant effect on gamma development (Fig. A.12-1C).

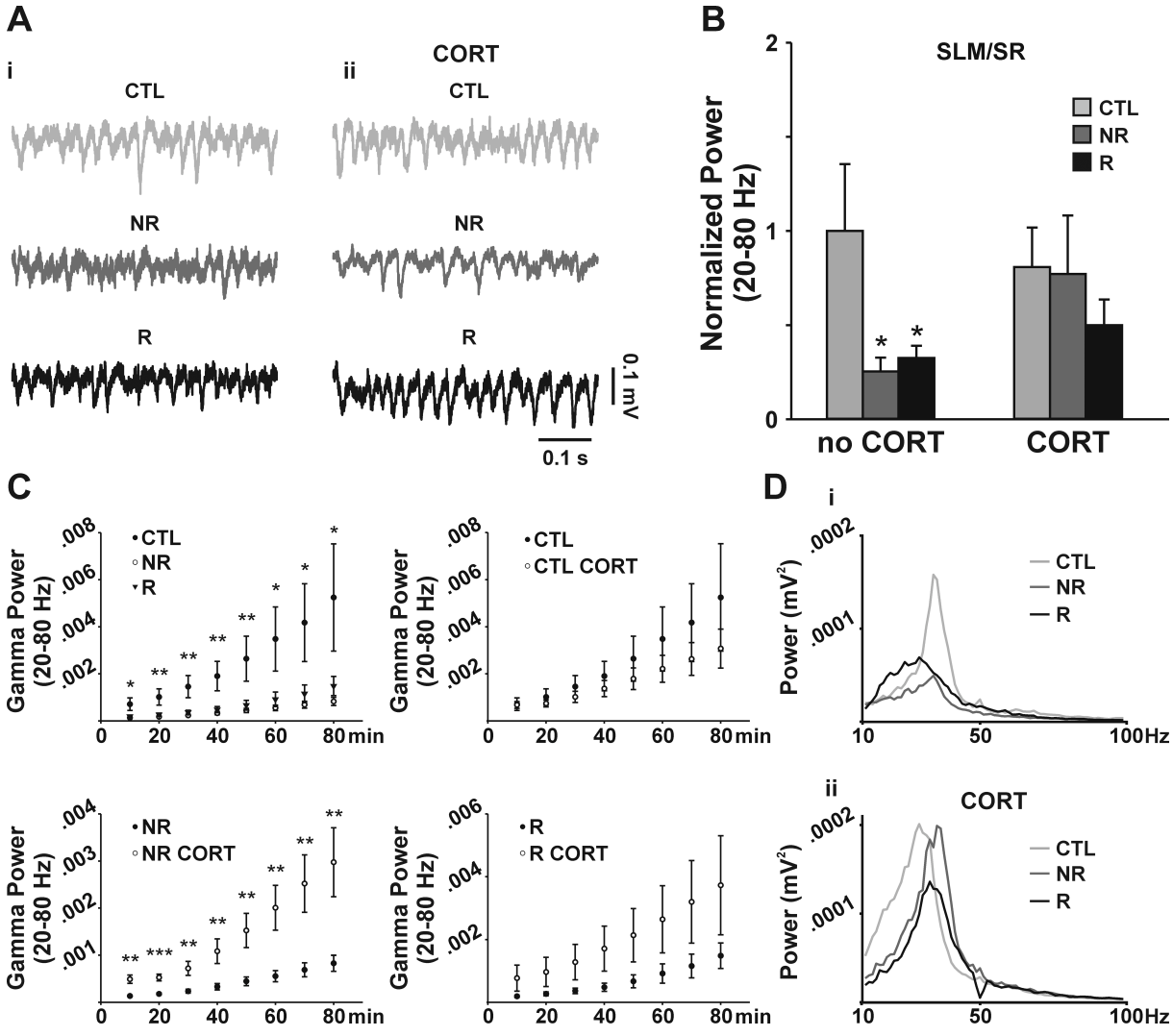

Fig. A.12-1: Fear conditioning and its reactivation reduce power of kainate-induced gamma oscillations in ventral hippocampal slices *ex vivo*. (A) Example traces of gamma oscillations from SR/SLM (i) without corticosterone (no CORT) and (ii) with corticosterone application (1µM; CORT) in unconditioned controls (CTL), non-reactivated (NR) and fear reactivated (R) animals. (B) Summary graph showing the normalized gamma power (20-80 Hz) recorded from the border of stratum radiatum (SR) and stratum lacunosum moleculare (SLM) reveals that both fear conditioning and reactivation reduce gamma power. (C) Summary graphs show the development of gamma oscillation power. Note the reduced gamma power in slices from groups NR and R compared to unconditioned controls. Preapplication of corticosterone has pronounced effect on gamma power in NR slices, but not in CTL or R slices. (D) Examples of power spectra from slices (i) without and (ii) with application of 1µM corticosterone (CORT). Values are indicated as mean ± SEM. * Significant difference between groups with * $p < 0.05$; ** $p < 0.01$; *** $p < 0.001$.

A.12.2 Effects on gamma frequency

There was no significant alteration in peak frequency of gamma oscillations in SLM/SR between groups (ANOVA for group: $F(2,40)=2.149$; $p=0.130$) or after corticosterone treatment (paired comparison: CTL: 34.8±1.0 vs. 32.6±1.1, $p=0.155$; NR: 30.5±1.8 vs. 31.5±1.4, $p=0.782$; R: 31.7±0.9 vs. 32.1±0.5, $p=0.790$).

A.12.3 Effects on gamma correlation

In SLM/SR, local gamma oscillations were significantly less correlated (Fig. A.12-2A, B; ANOVA for group: $F(2,40)=5.45$; $p=0.008$, Fisher's LSD post hoc) in both NR (N=14 slices, 7 animals; 0.10±0.03, $p=0.004$) and R (N=15 slices, 7 animals; 0.12±0.03, $p=0.009$) compared to CTL (N=12 slices, 6 animals; 0.24±0.04). Corticosterone application did not cause any significant change but an insignificant increase in NR group (paired comparison: CTL: 0.24±0.04 vs. 0.23±0.04, $p=0.818$; NR: 0.10±0.03 vs. 0.19±0.03, $p=0.059$; R: 0.12±0.03 vs. 0.14±0.03, $p=0.573$).

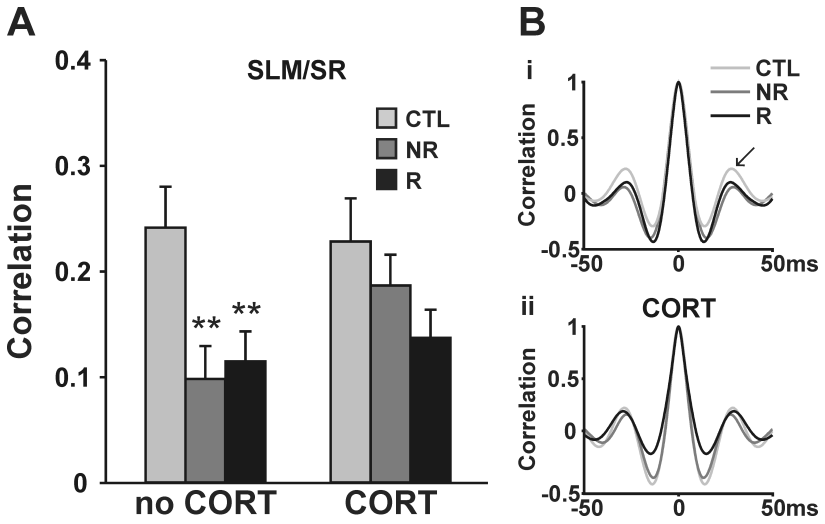

Fig. A.12-2 Fear conditioning and its re-activation decreases the correlation of kainate-induced gamma oscillations in SR/SLM in ventral hippocampal slices ex vivo**.** (A) Summary graph showing the gamma correlation in SR/SLM reveals that both fear conditioning and fear re-activation reduced gamma correlation. (B) Representative auto-correlograms for SR/SLM (i) without corticosterone (no CORT) and (ii) with 1 µM corticosterone (CORT). The 2nd positive peak was taken to quantify gamma correlation levels (indicated by arrow). CTL: Control, NR: No re-activation and R: re-activation. Values are indicated as mean ± S.E.M. * Significant difference between groups with * $p < 0.05$; ** $p < 0.01$.

The results are discussed together with behavioral, hormonal and molecular findings in section 3.3.2 and following.

Aknowledgement – *Danksagung*

Mein besonderer Dank gilt Prof. Dr. sc. nat. Oliver Stork, der mich von den ersten wissenschaftlichen Schritten als Studentin über die Dissertation zum Dr. med. bis heute exzellent betreut und gefördert hat und mir stets mit Rat und Tat zur Seite stand. Darüber hinaus möchte ich mich bei ihm auch für das entgegengebrachte Vertrauen und die Möglichkeit bedanken, dieses Thema zu bearbeiten sowie ein Teil vieler weiterer Projekte sein zu dürfen. Diese intensive Zusammenarbeit hat mir in all den Jahren so viel Freude bereitet und es überhaupt erst ermöglicht sowohl im wissenschaftlichen als auch persönlichen Bereich zu wachsen und meinen Weg zu finden.

Auch möchte ich der gesamten Arbeitsgruppe der Abteilung Genetik und Molekulare Neurobiologie des Instituts für Biologie herzlich für die gute Zusammenarbeit in anregender und freundschaftlicher Atmosphäre danken – hierbei besonders Franziska Webers, Antje Koffi von Hoff , Diana Wolter und Simone Stork für die ausgezeichnete technische Unterstützung sowie Angela Deter und Theresa Porzucek für die exzellente Tierpflege und Unterstützung bei der Tierzucht.

Ein ganz besonderer Dank gilt Dr. rer. nat. Bettina Müller sowie Dipl.-Biol. Iris Müller, die mich unermüdlich mit Korrekturen und Kommentaren beim Verfassen dieser Arbeit unterstützt haben.

Ebenso möchte ich mich bei den Kollaborationspartnern bedanken. Die Studie zu Genexpressionsveränderungen nach juvenilem und adultem Stress wurde durch die Zusammenarbeit im Rahmen des Deutsch-Israelischen Programms ermöglicht. Dank gilt dabei Prof. Gal Richter-Levin und Mitarbeitern, Universität Haifa, Israel, für die Entwicklung des juvenilen Stress Models, Prof. Menahem Segal und seinen Mitarbeitern am Weizmann Institut, Rehovot, Israel, für die Bereitstellung der Gewebeproben sowie Iris Müller aus dem Institut für Biologie für das zur Verfügung Stellen ihrer Erkenntnisse zu den Effekten juvenilen Stresses in der Furchtkonditionierung.
Die Studie zur Reaktivierung des Furchtgedächtnisses wäre ohne die Messung von Corticosteron-Plasmakonzentrationen durch Prof. Melly S. Oitzl und Mitarbeiter, Universität Leiden, Niederlande, nicht komplett. An dieser Stelle möchte ich auch Gürsel

Caliskan, M. Sc., für die Messung der Gamma Oszillationen *in vitro* danken sowie Prof. Uwe Heinemann, beide vom Institut für Physiologie der Charité-Universitätsmedizn Berlin, für die Diskussion der Ergebnisse, die die endokrinen und verhaltensbiologischen Befunde der Reaktivierungsstudie ergänzt und weiter vervollständigt haben.

Zu guter Letzt möchte ich noch all den Menschen danken, die immer für mich da waren und mich stets unterstützen – meiner Familie und meinen Freunden, ohne die dies alles nicht möglich gewesen wäre.

Statement of interest - *Selbstständigkeitserklärung*

Hiermit erkläre ich, dass ich die von mir eingereichte Dissertation zum Thema

„Molecular mechanisms of contextual fear memory generalization“

selbstständig verfasst, nicht schon als Dissertation verwendet habe und die benutzten Hilfsmittel und Quellen vollständig angegeben wurden.

Weiterhin erkläre ich, dass ich weder diese noch eine andere Arbeit zur Erlangung des akademischen Grades doctor rerum naturalium (Dr. rer. nat.) an anderen Einrichtungen eingereicht habe.

Magdeburg, den 25.09.12

Anne Albrecht

Curriculum Vitae

Personal information

Name:	Anne Albrecht
Nationality:	German
Date of birth:	31.01.1983
Place of birth:	Grimma
Marital status:	single
University address:	Department of Genetics & Neurobiology
	Institute of Biology
	Otto-von-Guericke University Magdeburg
	Leipziger Str. 44
	39120 Magdeburg, Germany
	Tel.: ++49-391-67 55 108
	Fax: ++49-391-67 55 102
	E-mail: anne.albrecht@ovgu.de
Home address:	Schäferweg 4
	04668 Grimma
	E-mail: anne.albrecht83@web.de

Education

06/2001	Abitur, High School "Johann Gottfried Seume", Grimma (grade 1.0, "very good")
10/2001 - 11/2008	Studies of human medicine at the Otto-von-Guericke University, Magdeburg
10/2003 - 03/2009	Additional studies of neuroscience within course program „Neuroscience for medicines" at the at the Otto-von-Guericke University, Magdeburg
10/2003 - 09/2004	Sabbatical for research project "Mechanisms of generalization of conditioned fear and emotional sensitization" under supervision of PD Dr. O. Stork, Institute of Physiology, Otto-von-Guericke University Magdeburg

11/2008	Degree in medicine (grade 1.5, „very good“)
11/2008	License to practice medicine
01/2009 - 06/2010	Graduate scholarship of the State Saxonia-Anhalt at the Otto-von-Guericke University Magdeburg, Institute of Biology, Department of Genetics & Molecular Neurobiology, (Prof. Dr. Oliver Stork)
11/2010	Dissertation (M.D., „Dr. med.“) „Role of the Neural Cell Adhesion Molecule (NCAM) in amygdalo-hippocampal interaction and salience coding of contextual fear memory“ under supervision of Prof. Dr. Oliver Stork, Otto-von-Guericke-University Magdeburg
09/2011	Certificate „Neuroscience for medicines“, Otto-von-Guericke-University Magdeburg
07/2010 - 08/2012	Postdoctoral fellowship at the Department of Genetics & Molecular Neurobiology, Institute of Biology, Otto-von-Guericke University Magdeburg
Since 2010	PhD research project „Mechanisms of contextual fear memory generalization“ under supervision of Prof. Dr. Oliver Stork, Otto-von-Guericke-University Magdeburg

List of publications

Albrecht A, Çalışkan G, Oitzl MS, Heinemann U, Stork O (2012): Long-lasting increase of corticosterone after fear memory reactivation: Anxiolytic effects and network activity modulation in the ventral hippocampus. Neuropsychopharmacology, 2012 Sep 12. doi: 10.1038/npp.2012.192. [Epub ahead of print]

Albrecht A, Stork O (2012): Are NCAM deficient mice an animal model for schizophrenia? Front Behav Neurosci. 6:43.

Albrecht A, Bergado-Acosta JR, Pape HC, Stork O (2010): Role of the neural cell adhesion molecule (NCAM) in amygdalo-hippocampal interactions and salience determination of contextual fear memory. Int J Neuropsychopharmacol. 13: 661-674

Stoppel C, Albrecht A, Pape HC, Stork O (2006): Genes and neurons: molecular insights to fear and anxiety. Genes Brain Behav. 5 Suppl 2:34-47.